THE UNIVERSITY
of EDINBURGH

Biogeochemical characterisation of particulate organic matter at sequential stages of transport in suspended, sinking, and benthic fractions

Laura Tulip

MRes, Ecosystem based management of marine systems, University of St. Andrews, 2012
BSc (Hons.) Marine Biology, Newcastle University, 2011

A dissertation submitted in partial fulfilment
of the requirements for the degree of
Doctor of Philosophy
of the
University of Edinburgh.

School of Geosciences

2018

Declaration

I declare that this thesis has been completed solely by myself and that it has not been submitted, in whole or in part, in any previous application for a degree. Except where states otherwise by reference or acknowledgement, the work presented is entirely my own.

Signed:

Date: 31/10/2018

Abstract

The export of particulate organic matter (POM) from the surface ocean to depth forms the basis of the biological carbon pump (BCP). It is important for modulating atmospheric carbon dioxide concentrations, amongst a range of other significant processes. Coastal zones play a significant role in organic matter cycling and burial, and have the capacity to affect a range of important biogeochemical cycles at a global scale.

Determining the source and biogeochemical composition of POM, is essential in order to determine its fate; whether POM is recycled in the water column, or exported to depth. POM is heterogeneous in nature with inputs from terrestrial, estuarine, and marine sources. Diverse sources of POM result in a wide spectrum of POM present in the water column, which can be loosely categorised into suspended particulate material (SPM) and sinking fractions. These fractions can be compositionally distinct, and contribute to carbon export to different extents. This thesis addresses key questions surrounding characterisation of POM of these different fractions, determining its origin, and reactivity. The multifaceted approach taken includes detailed microphytoplankton community dynamics, molecular-level biogeochemical analysis of POM, and reactivity (using oxygen consumption as a proxy for reactivity) measures across a seasonal cycle and is unprecedented.

An intensive sampling campaign was carried out in highly dynamic coastal waters in the Firth of Lorne, western Scotland. Microphytoplankton community composition, biochemical composition, and environmental drivers (wind speed and pycnocline depth) were found to be related to community sedimentation rates. The origin of POM was mixed as indicated by C:N ratio, δ^{13}C values, and fatty acid biomarkers. SPM had a larger terrigenous input compared to sediment trap material and sediments. A seasonal shift in SPM source from marine dominated POM in spring, to increasing terrestrial inputs into winter, which corresponded to periods of high rainfall, was observed. SPM was more labile relative to sinking and benthic fractions, and generally concentrations of organic carbon and nitrogen, amino acids, fatty acids, and carbohydrates decreased with depth. The decreasing trend in reactivity observed in SPM and sediment trap material from summer to winter, coincided with the shift in source material, with lowest reactivity occurring when terrigenous inputs were highest. Relationships were found between SPM and sediment trap reactivity, and lability parameters such as amino acids, fatty acids, and carbohydrate concentration. The BCP is complex, and a good understanding of POM characteristics and composition is essential in order to better understand POM cycling and export efficiency. This is especially important given the predicted changes to the BCP as a result of a changing climate.

Lay Summary

The biological carbon pump relocates organic-rich particles created in the surface ocean to depth. Phytoplankton cells are a key component of this organic-rich particulate material, which utilises carbon dioxide in the surface ocean and converts it into energy. The wide diversity and high biomass of phytoplankton can be key controls on the amount and quality of carbon, which is transferred from the surface ocean to greater depths. Sinking particulate material can become trapped in sediments for long timescales, therefore reducing the probability of the carbon dioxide being reintroduced back into the atmosphere. This process is very important for controlling our climate. Coastal oceans are key areas for studying the biological carbon pump due to their highly productive nature, and the additional source of organic material which is transported from the land into the ocean. There are many factors which determine the speed and efficiency of the transport of organic particles from the surface ocean to depth.

This study investigated particulate material at different stages of transport through the water column. The aim of the investigation was to determine the composition of each of these sample types over a seasonal cycle to further understanding of carbon cycling in coastal systems. Samples were taken from suspended material at the surface, sinking material which was collected at 20 m using sediment traps, and the surface sediment on the seabed. Analyses of these samples were carried out in order to determine the original source, the degradative state, and the reactivity of the particulate material.

The source of particulate material at the coastal study site was determined to be from a mixed marine and land based origin. Phytoplankton was a key component of suspended material, especially during spring when in high abundances. A seasonal transition of suspended material sourced from phytoplankton, to land derived material in winter was observed. In contrast, the sinking particulate material and sediment organic fraction predominantly originated from marine sources over the sampling season. The chemical composition of each of the sample fractions were distinct, with a higher proportion of organic-rich compounds in the suspended fraction relative to sediment trap material and sediments. This was reflected in how reactive the particulate material was for degradation with suspended particulate material being more reactive than sediment trap material. Results suggest there was inefficient transfer of organic-rich suspended particulate material to the seafloor at the study site. The high energy environment driven by wind and tidal influences favoured horizontal transport of particulate material rather than vertical transport to sediments. This has implications for feedback of carbon dioxide back into the atmosphere.

Acknowledgements

I would like to thank my supervisors David Pond and Greg Cowie for their support and encouragement. I am grateful for the time they dedicated to helping me complete this PhD. David and Greg were available for thoughtful discussions, and to provide comments on my work. Thank you to my supervisors, and to NERC, for the opportunity to be part of this project.

I would like to acknowledge the many people who have helped me at various stages of my PhD. My PhD involved extensive field work on board the RV *Seol Mara*, and I would like to thank Norman Smith and Steve Jaron for all their help. I would also like to thank Sharon McNeill, who has helped me a great deal with fieldwork, and other laboratory analyses. Thank you to Alistair James who designed and built the SETCOLs. Steve Mowbray spent a large amount of time teaching me particulate amino acid experimental techniques and data processing. I am grateful for his time, and patience explaining everything to me. Thank you to Tim Brand for his help in the laboratory with nutrient analysis, and for providing me with CTD data for the deep-water oxygen renewal event in Loch Etive. Thank you to Colin Abernethy for lithogenic trace elements analysis. To everyone else that has helped me in the laboratory, out in the field, or with writing up, thank you.

Most of all I would like to thank my family and friends. I would not have completed this without their encouragement. The support of my parents Alison and Alan, who have always taught me to believe in myself, has definitely helped me through the many periods of doubt. My brother Christoph has always been at the other end of the phone full of jokes. Thank you Jack for the love, support, and understanding you have given me over the past 4 years. Chester and Rooster, my two favourite boys, were always there to put a smile on my face. Last but not least, to all my friends at home and those I have made along the way, your help, support, and fun times will never be forgotten.

Contents

List of Tables

List of Figures

List of acronyms and abbreviations

AA	Amino acid
AA-N	Amino acid contribution to total nitrogen
AA-OC	Amino acid contribution to total organic carbon
ANOSIM	Analysis of similarity
BCP	Biological carbon pump
CHO	Carbohydrate
CHO-OC	Carbohydrate contribution to total organic carbon
C:N	Carbon-to-nitrogen ratio
CT	Controlled temperature room
CTD	Conductivity, temperature, depth sensor
δ^{13}**C**	Delta carbon 13; stable isotope of carbon
DI	Degradation index as described by Dauwe and Middelburg (1998)
DOC	Dissolved organic carbon
F1	Positively buoyant fraction of settlement columns
F2	Neutrally buoyant fraction of settlement columns
F3	Negatively buoyant fraction of settlement columns
FAMES	Fatty acid methyl esters
GC	Gas chromatography
HPLC	High performance liquid chromatography
MPA	Marine protected area
MUFA	Monounsaturated fatty acids
nMDS	Non-metric multidimensional scaling
OC	Organic carbon
PCA	Principle component analysis
PM	Particulate material; includes both organic and inorganic particulate material
POM	Particulate organic material
PRIMER	Plymouth Routines In Multivariate Ecological Research statistical package
PUFA	Polyunsaturated fatty acids
S	Sediment
SFA	Saturated fatty acids
SAC	Special area of conservation
SAMS	Scottish Association of Marine Science

SD	Standard deviation
SETCOL	Settlement column
SIMPER	Similarity percentage analysis
SPM	Suspended particulate material; includes organic and inorganic material suspended in the water column at time of sampling
SPM A	Suspended particulate material sampled from above the pycnocline
SPM B	Suspended particulate material sampled from below the pycnocline
ST	Sediment trap
TC	Total carbon; includes both organic and inorganic carbon
TEP	Transparent exopolymer particles
TFA	Total fatty acid
TFA-OC	Total fatty acids contribution to total organic carbon
TLC	Thin layer chromatography
TN	Total nitrogen
TOC	Total organic carbon; organic fraction of carbon
UV	Ultraviolet

Chapter 1

Introduction

1.1 The biological carbon pump

The oceans play a central role in the global carbon cycle, which regulates climate and acts as a sink for carbon dioxide (CO_2; Falkowski et al., 2003). CO_2 from the atmosphere is drawn into the surface oceans via the solubility pump, where is it then converted from dissolved to particulate material via primary production (Volk and Hoffert, 1985). The biological carbon pump (BCP) drives the cycling of photosynthetically produced organic carbon from the surface to depth via sinking particles, advection, or vertical mixing (Figure 1.1; Turner, 2015). This particulate organic carbon (POC) is either consumed, exported to depth, and/ or sequestered into the deep sea and sediments. Approximately 10 GT of carbon per year are exported into the deep ocean, and without this export atmospheric CO_2 would be approximately double current concentrations (Le Moigne et al., 2012; Mayor et al., 2014; Sanders et al., 2014). This export is important to the biological and chemical functioning of the ocean, supporting food webs, and elemental distributions throughout the water column (Burd et al., 2016). Remineralisation (conversion of POC to inorganic carbon via respiration) of POC in the upper pelagic zone provides nutrients for surface production, while material exported to depths greater than 1000 m is considered to be sequestered and out of contact with the atmosphere for centuries or longer (Lampitt et al., 2008; Passow and Carlson, 2012; Burd et al., 2016).

The focus of this study is the coastal BCP (Figure 1.1). Coastal seas are a component of the continental shelf and are dynamic environments which represent approximately 10 % of the global ocean area, yet they are responsible for 10 to 30 % of global marine primary production (Bauer et al., 2013). Additionally, continental shelves and coastal seas are also key areas for terrestrial, estuarine, and marine carbon cycling with an estimated 80 % of global organic carbon burial in continental margin sediments (Berner, 1989). Approximately 50 % of organic carbon in the deep ocean is supplied from continental shelves (Wakeham and Lee, 1989; Bauer et al., 2013). This demonstrates that coastal seas and the continental shelf are disproportionately important to carbon cycling, and have the capacity to affect a range of important biogeochemical cycles at a global scale.

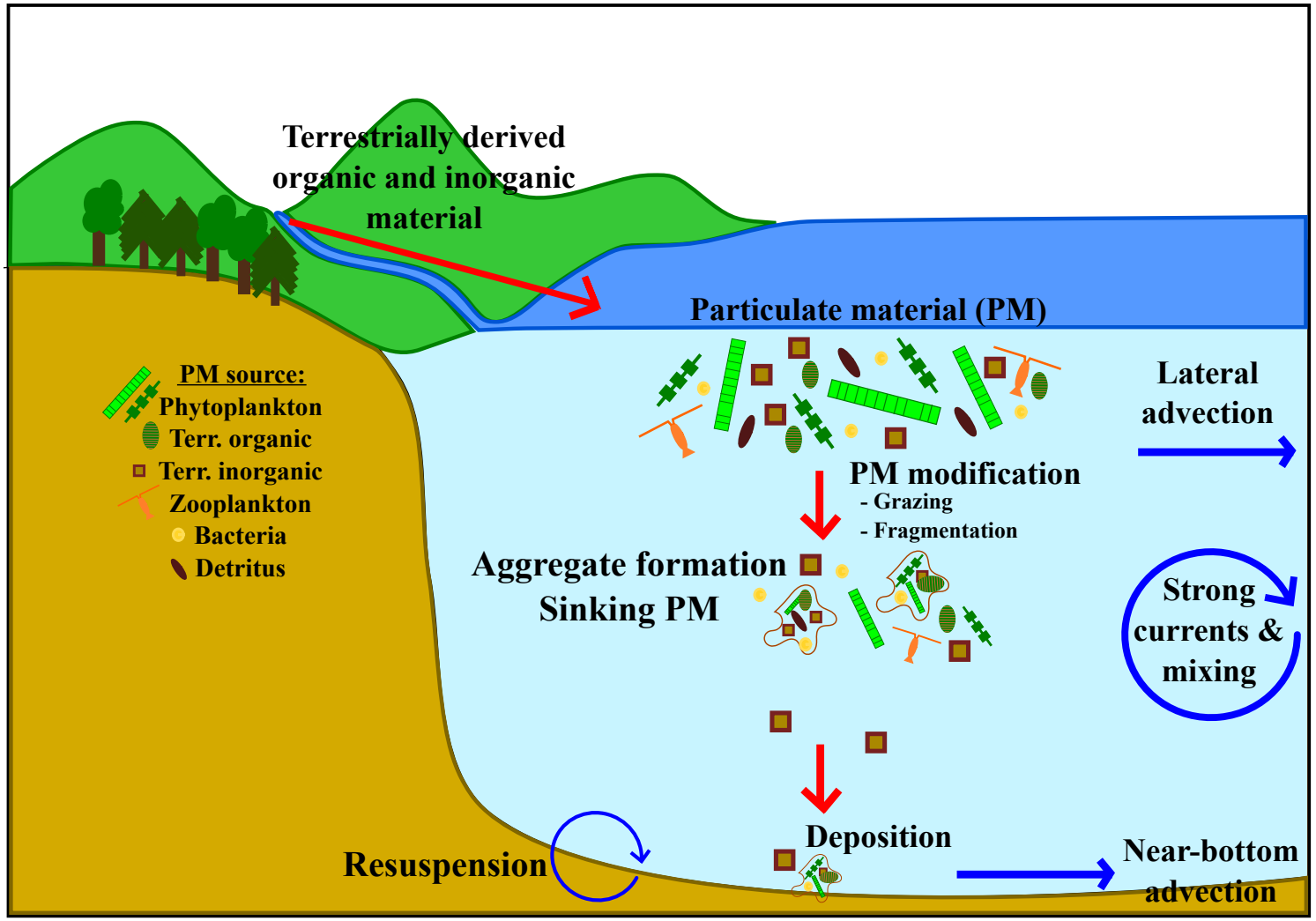

Figure 1.1: Schematic of the biological carbon pump in a coastal setting

The BCP is driven by phytoplankton, which convert inorganic carbon into organic carbon via photosynthesis, fuelled by light and nutrients (Falkowski et al., 2003). A range of nutrients are required for phytoplankton growth, including essential macro-nutrients such as nitrate, phosphate, silicate, and iron the micro-nutrient (Reynolds, 2006). Redfield (1934) stated that a 16:1 ratio of nitrate-to-phosphate was the optimal stoichiometry for photosynthesis to occur, however other studies highlight that this ratio is dependent on growth rate and can be species-specific (Tett et al., 1985; Arrigo, 2005). Availability and concentration of macro-/ micro-nutrients in the water column can limit primary production (Hecky and Kilham, 1988). These nutrients are replenished in the surface ocean by physical mixing, land run off, and upwelling regions (Guinder et al., 2015). Temperate coastal waters typically have a spring and autumn phytoplankton bloom (e.g. Townsend et al., 1994; Daniels et al., 2015; Guinder et al., 2015). Strong winds and water column turbulence result in a well mixed environment, with reduced growth resulting from low light levels during winter. With progression into spring, light levels increase, and a threshold is reached were nutrient, temperature, light intensity, and water column turbulence is optimal for phytoplankton to bloom (Townsend et al., 1994). As phytoplankton abundance increases, the availability of nutrients decreases resulting in a decline in phytoplankton biomass. As the water column becomes stratified during summer, generally there is a further decline of nutrients which limits phytoplankton growth. Stronger and more frequent winds in autumn, increase turbulence in the water column mixing nutrients to the surface, which results in a second smaller phytoplankton bloom in autumn. A proportion of the biomass produced during phytoplankton bloom periods is grazed upon, respiring some of the organic carbon into dissolved inorganic carbon (Smetacek, 1985; Turner, 2015). A further fraction of the biomass escapes and sinks out of the euphotic zone and is exported to depth. Seasonal phytoplankton blooms have been linked to periodic formation of aggregates and particulate organic material (POM) flux that reaches the seafloor (Billett et al., 1983; Conte et al., 2001; Kiriakoulakis et al., 2001). However, not all phytoplankton blooms end in aggregation and sedimentation, as this depends on species present, environmental conditions, and production of "sticky" polysaccharide exudates e.g. transparent exopolymer particles (TEP; Passow, 2002; Guo et al., 2016). Additionally, it is important to consider that POM is heterogeneous in nature, and terrestrial POM also makes a significant contribution to aggregate composition in coastal environments (Hedges et al., 1997; Loh et al., 2002), and will be discussed in later chapters.

This exported organic and inorganic carbon can have a number of interchangeable terms including particulate material (PM), POM, marine aggregates, or marine snow aggregates. These terms can include a suite of organic and inorganic components from a range of sources. Additionally, PM can refer to one phytoplankton cell or a whole host of components, whereas aggregates are generally classified as being composed of more than one particle, and as being 0.5 mm or larger in diameter (e.g. MacIntyre et al., 1995; Riley et al., 2012; Passow, 2016). Aggregates can be formed from many components, including individual phytoplankton cells, faecal pellets, other detritus, inorganic material, TEP, and host dense bacterial communities (Conte et al., 2001; Herndl and Reinthaler, 2013). To clarify, the terms PM and aggregates, meaning organic and inorganic particles of either single cells or numerous components aggregated together, are both used in this thesis.

The BCP can be relatively inefficient, as the majority of POC fixed into phytoplankton cells via photosynthesis, is remineralised in the epipelagic (upper 100 to 200 m) or upper layers of the mesopelagic (200 to 1000 m; Hedges, 1992; De La Rocha and Passow, 2007; Turner, 2015). It is generally agreed that 5 to 25 % of net primary production is exported from the euphotic zone depending on location (De La Rocha and Passow, 2007). In central ocean gyres, export from the euphotic zone is usually <10 % (Neuer et al., 2002), in contrast to polar waters, which can range from 30 to 100 % (Buesseler, 1998). At bathypelagic depths (>1000 m), generally <3 % of net primary production has survived export from the surface ocean (De La Rocha and Passow, 2007; Turner, 2015). However, in shallow coastal zones with high productivity, 30 to 40 % of the annual water column production can be transported to the seafloor (Lee and Cronin, 1984).

Atmospheric CO_2 concentrations have increased by 40 % since pre-industrial times as a result of fossil fuel emissions and net land use change emissions, and are predicted to rise further (IPCC, 2013). The ocean has the capacity to store approximately 48 times more inorganic carbon relative to the atmosphere (Sabine et al., 2004). Theoretically, increasing atmospheric CO_2 concentration increases the potential at which CO_2 can diffuse into surface waters. However, changes to physical oceanic conditions such as circulation and stratification, and to biological processes such as export production and calcification, in response to climate change can affect the BCP. Small changes to the ocean environment could potentially affect its capacity to store CO_2, and therefore have significant impact on atmospheric CO_2 concentrations. On a time scale of several thousand years, 90 % of the anthropogenic CO_2 emissions are predicted to end up in the ocean (Sabine et al., 2004). On a decadal timescale, the ocean may become a less efficient sink for anthropogenic CO_2 (Sabine et al., 2004); this could be the result of a combination of factors including the changing physical (e.g. temperature, acidification, upwelling) and biological (e.g. shift towards dominance of smaller phytoplankton) environment (Passow and Carlson, 2012).

Many of the complex and interrelated processes affecting the composition, quantity, and spatial distribution of PM export are poorly understood or constrained (Burd et al., 2016). A better understanding of the present day BCP is essential in order to predict the effects of climate change on PM export and recycling (Passow and Carlson, 2012; Turner, 2015). With this in mind, the focus of this thesis is on enhancing understanding of the biogeochemical composition of suspended, sinking, and benthic fractions of PM in a coastal setting. In this thesis attention is paid to microphytoplankton community dynamics, and factors that affect their suspension and sinking in the water column, and linking biogeochemical composition of PM to reactivity. The remainder of this chapter provides a general review of microphytoplankton dynamics in the suspended fraction, and factors affecting PM composition and sedimentation.

1.2 Controls on the suspension and sinking of phytoplankton

The suspension and sinking of phytoplankton controls the residence time of marine POM in the surface ocean, which in turn determines the proportions of POM which are remineralised at the surface or exported to depth, and ultimately the efficiency of the BCP. Another factor that controls

the prevalence of phytoplankton is zooplankton grazing (Kiørboe et al., 1996). Marine phytoplankton are disproportionally important for global net primary production; phytoplankton represent less than 1 % of the Earth's photosynthetic biomass yet are responsible for >45 % of global net primary production (Field et al., 1998; Simon et al., 2009). Phytoplankton generate energy via photosynthesis, and therefore live in the sun-lit surface ocean down to 200 m (Simon et al., 2009). There are estimated to be between 4000 to 5000 marine species, of which most are unicellular microscopic organisms (microphytoplankton), ranging between 20 to 200 μm (Simon et al., 2009). Diatoms, dinoflagellates, and haptophytes dominate phytoplankton communities on continental shelves, and are responsible for seasonal blooms in temperate and polar waters (Simon et al., 2009). They are the main marine planktonic primary producers within the nano- (2 to 20 μm) and microphytoplankton size classes. Diatoms represent approximately 40 % of all known marine phytoplankton species and are of significant importance from both ecological and biogeochemical standpoints, especially in nutrient-rich systems (Falkowski et al., 2004). Dinoflagellates are heterotrophs, with less than half the group able to photosynthesize (Simon et al., 2009). They usually have two flagella and thick cellulose plates (Simon et al., 2009). In temperate environments, dinoflagellates tend to dominate when diatoms do not during quiescent conditions (Falkowski et al., 2004). Phytoplankton community dynamics, which can vary substantially over a seasonal cycle in response to nutrient availability and other environmental conditions, play a central role in the BCP due to varying contributions to carbon fixation and export fluxes (as sinking cells and as aggregates; Durkin et al., 2016). The vast diversity of phytoplankton and seasonal differences in community structure is responsible for a large degree of the variability in the export flux (e.g. Guidi et al., 2009; Lomas et al., 2010; Henson et al., 2012; Turner, 2015; Guo et al., 2016). Detailed phytoplankton community structure is often lacking in carbon export studies. Its inclusion would provide valuable information on how community structure might affect carbon export.

Mobility and sedimentation rates are two factors that control the position of phytoplankton in the water column. Successful growth and survival of phytoplankton depends on phytoplankton residence time in the euphotic zone, to permit net photosynthesis, in surplus to total daily respiration and organic secretion losses (Smayda, 1970). Some species are able to swim or regulate their buoyancy, however populations are still controlled by the physical environment, advection, and turbulence (Margalef, 1978; Smayda, 1970). Unlike diatoms, dinoflagellates are motile, and the velocity at which they can swim is dependent on size (Kamykowski et al., 1992). Swimming velocities are generally around 1.3 m h^{-1}, with ranges of 0.03 to 6.5 m h^{-1} reported (Kamykowski et al., 1992). Smayda (1970) made observations on "natural sea water samples [that] soon after collection show[ed] that many phytoplankters sink to the container bottom; others remain suspended and some may even ascend to the surface". This highlights a range of sedimentation responses by different phytoplankton species. Buoyancy and sedimentation of microphytoplankton are important processes to understand, as they affect cell water column positioning and therefore the efficiency and rate of primary production (Smayda, 1970; Richardson and Cullen, 1995). Additionally, understanding the sinking rate of individual, chain forming, and aggregated cells is essential for enhancing understanding of carbon export from the euphotic zone. There are a suite of interacting factors that affect microphytoplankton sedimentation rates, which can broadly be

split into three categories; morphological, physiological, and physical factors.

1.2.1 Morphological controls on sedimentation rates

Firstly, morphological features that affect sedimentation rate include cell size, shape, presence of chitin fibres forming spines and ridges, and colony formation (Lannergren, 1979; Reynolds, 2006; Smayda, 2010). In theory, larger cells should sink faster (e.g. Smayda, 1970; Riebesell, 1989; Waite et al., 1997), which explains the dominance of microphytoplankton (over larger phytoplankton cells) in stratified waters with low turbulence (Margalef, 1978). However, other studies have found no relationship between sedimentation rates and cell size (Bienfang et al., 1982; Peperzak et al., 2003), which suggests other factors need to be considered. Chain formation is a mechanism which effects cell size and is common in non-motile organisms such as diatoms, however it also occurs in motile dinoflagellate species such as *Alexandrium* spp. (BjÆrke et al., 2015). The ecological rationale for chain formation is not well understood; it has been suggested as an adaptive response for diatoms, whereby they adjust their chain length to minimise losses to grazers (BjÆrke et al., 2015). For example, *Skeletonema marinoi* was shown to suppress chain formation in response to copepod chemical cues (Bergkvist et al., 2012). A further study found turbulence and nutrient availabilities were key factors controlling chain length (Dell'aquila et al., 2017). Silica-shelled frustules are a typical characteristic of diatoms, which can form extensive blooms and contribute around 50 % of POC export to depth (Dugdale and Wilkerson, 1998; Falkowski et al., 2004). Other studies suggest that sinking velocities of single diatom cells or chains are species-specific and not systematically linked to size (e.g. Smayda, 1970; Bienfang, 1980; Smayda and Bienfang, 1983). This is also shown by the varying results from studies, which have found chain length to have differing impacts on sinking rate depending on species, combination of species, or natural assemblages used (e.g. Smayda, 1970; Peperzak et al., 2003; Reynolds, 2006; Landeira et al., 2014). In two studies that used natural microphytoplankton assemblages, one found no correlation between chain length and sinking rate (Waite et al., 1992a), and the other found shorter chains sank faster than long chains (Peperzak et al., 2003). Peperzak et al. (2003) hypothesized that the spiral chains of some chain forming species retained water around their chains which would reduce overall chain density and therefore sedimentation rates. Experiments which removed the chitin fibres of *Thalassiosira fluviatilis* found they sank more than 1.7 times faster in comparison to intact cells (Walsby and Xypolyta, 1977). Conversely, extruding fibres and spines are said to give rise to mechanical sticking or entangling of particles which could enhance sinking rates (Kiørboe et al., 1990; Peperzak et al., 2003). Therefore, morphological features of phytoplankton have the potential to influence sedimentation rates and formation of aggregates. Species-specific morphological traits, coupled with continuously varying physiological mechanisms, are responsible for explaining sedimentation rate differences between species.

1.2.2 Physiological controls on sedimentation rates

Secondly, physiological mechanisms influencing cell sedimentation rate include modifying cell density via a range of processes such as cell biochemical composition, internal ionic composition, and numbers or size of intracellular vacuoles (e.g. Margalef, 1978; Lannergren, 1979; Richardson

and Cullen, 1995; Reynolds, 2006; Smayda, 2010). Generally, phytoplankton have a higher density than seawater, with cell walls composed of silica (2.6 x 10^3 kg m^{-3}), calcium carbonate (3.0 x 10^3 kg m^{-3}), and cellulose (1.5 x 10^3 kg m^{-3}), all of which are denser than sea water (1.025 x 10^3 kg m^{-3}; Vogel, 1983). During different growth phases microphytoplankton can utilise and store different proportions of proteins, carbohydrates and lipids, which will affect their buoyancy (Ríos et al., 1998). Experiments have shown that cells have the capacity to recover from unbalanced growth and regulate their buoyancy, when placed under nutrient-replete conditions (Richardson and Cullen, 1995). For example, the sinking rate of *Thalassiosira weissflogii* increased during nutrient-depleted conditions, due to an accumulation of carbohydrates as a result of unbalanced growth (Richardson and Cullen, 1995). Senescent populations of microphytoplankton have been connected to higher sinking rates (Smayda, 1970) despite the senescent phase being linked to high lipid synthesis in some microphytoplankton species (Diekmann et al., 2009). Lipids have a specific gravity less than seawater, so synthesis and storage of lipids during this phase would suggest increased buoyancy of cells, and not higher sinking rates. Additionally, studies on newly formed sinking aggregates have shown them to be dominated by lipids, which are derived from microphytoplankton (Balzano et al., 2011). Therefore, over the course of a spring bloom, microphytoplankton biochemical composition can change, and in turn affect cell density and therefore buoyancy, and position in the water column. Vacuoles are suggested as a further mechanism for regulating cell density. Diatoms contain vacuoles which can occupy approximately 40 % of their cell volume, are used for nutrient storage, and are predicted to play a significant role in buoyancy regulation (Falkowski et al., 2004; Erga et al., 2010). Ion regulation of cell sap has also been suggested as a plausible mechanism to regulate cell density (Reynolds, 2006). Gemmell et al. (2016) found that *Coscinodiscus wailesii* were able to change their sinking rate from slow, to fast, and then transition back to slow again; only a 1.5 % change in cell density via ion regulation would be required to achieve these changes in sinking rate. In addition to morphological features which can affect sedimentation rate, physiological mechanisms are shown as a further regulation of cell buoyancy and sinking.

1.2.3 Environmental controls on sedimentation rates

Thirdly, physical environmental factors that affect microphytoplankton sedimentation rate include water column turbulence, stratification, light, and nutrient availability (Bienfang et al., 1982; Johnson and Smith, 1986; Smayda, 1997). Turbulent motion in the water column has been suggested to re-disperse microphytoplankton that are passively sinking back to the surface (Huisman et al., 2002). However, there is a fine balance between excessive turbulence which translocates cells to depth, and low turbulence which allows cells to sink to depth (Huisman et al., 2002). Cell buoyancy has been linked to cell age, light availability, and nutrient status of the cell (Johnson and Smith, 1986). Microphytoplankton have been shown to have higher sinking rates when nutrients are depleted (e.g. Bienfang et al., 1982; Waite et al., 1992a; Peperzak et al., 2003), which is suggested to be an adaptive response, to permit sinking out of unfavourable conditions (Smetacek, 1985; Richardson and Cullen, 1995). Under well-stratified, nutrient-replete conditions, *T. weissflogii* maintained almost neutral buoyancy in contrast to nitrate-depleted conditions in which cells

were shown to sink (Richardson and Cullen, 1995). Another study, using a number of microphytoplankton species, found that nutrient depletion was not necessarily linked to higher sinking rates, and sedimentation rates were dependent on species and nutrient dynamics (Bienfang and Harrison, 1984). Low levels of irradiance have been shown to coincide with high cell sinking rates (e.g. Johnson and Smith, 1986; Riebesell, 1989; Waite et al., 1992b). Despite the dynamic environment microphytoplankton inhabit, the prevailing sinking rate of diatom species can be quickly altered in response to changing environmental conditions (Riebesell, 1989; Gemmell et al., 2016). It is likely to be a complex interaction between morphological, physiological, and physical environment factors that regulate the position of phytoplankton in the water column.

The suspension and sinking of phytoplankton has been investigated using a range of methods including high-resolution optical techniques (Gemmell et al., 2016), fluorometry (Szyper and Karl, 1991), and settlement columns (SETCOL; e.g. Bienfang, 1981b; Bienfang et al., 1983; Bienfang and Harrison, 1984; Pitcher et al., 1989; Kiørboe et al., 1996; Waite and Nodder, 2001; Peperzak et al., 2003; Guo et al., 2016). These studies have investigated phytoplankton sedimentation in response to nutrient enrichment (e.g. Bienfang, 1981b; Bienfang and Harrison, 1984; Richardson and Cullen, 1995), carbohydrate ballast (Richardson and Cullen, 1995), light intensity (Bienfang et al., 1983), taxonomic properties of phytoplankton assemblage (Pitcher et al., 1989; Guo et al., 2016), cell size (Peperzak et al., 2003), environmental conditions (Guo et al., 2016), or a combination of factors. None of these studies have investigated the combined effects of the three main macromolecular compounds protein, lipid, and carbohydrate (which vary with growth phase and season) on phytoplankton sedimentation rates. Seasonal changes to phytoplankton community structure, and biochemical composition, have the potential to influence the quality and quantity of POM available for export and its sedimentation rates. Given the significant role that phytoplankton play in carbon export, it is important to determine key factors, and specific environmental conditions, which affect their sedimentation.

1.3 Factors affecting the composition and sedimentation of PM

1.3.1 Sources of PM

In addition to autochthonous sourced phytoplankton POM, allochthonous inputs from terrestrial origins represent a substantial fraction of organic and inorganic material entering the coastal marine environment (Figure 1.1; Hedges et al., 1988a; Loh et al., 2002; Davis et al., 2018). Terrestrial organic material contributes approximately 0.4 to 0.5 x10^{15} g C yr^{-1} of organic carbon to the marine environment (Hedges et al., 1997; Benner, 2004). Terrigenous organic carbon is generally composed of vascular plant debris, soil, and older fossil organic carbon derived from carbonate rock erosion (e.g. Bianchi, 2011). Soils receive debris from vascular plants, which then undergo extensive microbial attack before entry into the marine environment (Hedges and Keil, 1995; Hedges and Oades, 1997). The surviving organic fraction of the terrestrial material is likely to be adsorbed onto mineral surfaces which physically protects it from microbial attack (Hedges and Oades, 1997). Additionally, high concentrations of refractory, largely nitrogen-free biomacromolecules including lignin, tanin, suberin and cutin, characterise the presence of terrestrial PM

(Hedges et al., 1997). The typical composition of terrestrially derived material contains a minor fraction of organic material, with geopolymers and mineral material predominating (Hedges, 1992). The entry of terrestrial organic carbon into the marine environment depends on riverine transport, land use, drainage, and weather (Hedges et al., 1997; Bianchi, 2011). In addition to terrestrially derived POM, marine POM forms the second main source of POM in coastal systems. PM is heterogeneous in nature meaning it is derived from a mixture of sources and usually contains fresh, labile material as well as older, more refractory components, and inorganic material (e.g. Cowie and Hedges, 1994). Planktonic organic material can be more fresh and labile in comparison to the more refractory, degraded terrestrial input (Hedges and Keil, 1995; Loh et al., 2002; Burdige, 2005). Additionally, interactions between mineral material and organic material (both marine and terrestrial) are major controls of organic material dynamics.

The majority of POM in the surface ocean is remineralised in the water column and escapes export the sea floor (Buesseler, 1998; De Haas et al., 2002; Passow and Carlson, 2012). However, this is location-specific, as in shallow, highly productive coastal areas, up to 30 % of the annual water column production is transported to the sea floor (Davies, 1975). The biochemical composition of POM is determined by its source, and in turn this will affect its fate in the water column.

1.3.2 Particle characterisation

Spatial and temporal variations of particle types, concentrations, and aggregate composition in the water column lead to an array of PM with different characteristics. These different characteristics can affect POM fate in the water column, the amount of carbon exported, the distribution of associated elements, and can also control the amount of light able to penetrate the surface (Burd and Jackson, 2009).

The size and sinking rate are two key characteristics of PM which can determine its classification (Figure 1.2). Larger particles sink faster according to Stokes' Law (McDonnell and Buesseler, 2010; Durkin et al., 2015). The velocity at which aggregates sink from the surface, affects the strength and efficiency of the BCP (McDonnell and Buesseler, 2010). At the lower end of the sedimentation scale, sinking rates of individual diatom cells generally range from 0.1 to 10 m d^{-1} (Smayda, 1970). The sedimentation rate of aggregates is typically difficult to measure due to their fragile nature, and have been estimated in laboratory settling columns and *in situ*, ranging from 5 to 2500 m d^{-1} (Sanders et al., 2014). Observations of diatoms on the seafloor of deep-sea systems weeks after a surface bloom, suggests fast vertical transport and repackaging of cells into aggregates with faster sinking rates (Beaulieu, 2002; Burd and Jackson, 2009). However, it has been shown that sinking of intact phytoplankton cells can also represent a substantial contribution to carbon export (Durkin et al., 2016).

Aggregates formed can be loosely classified into fast-sinking (>20 m d^{-1}), slow-sinking (<20 m d^{-1}) and suspended particulate material (SPM; Riley et al., 2012). Slow-sinking PM is thought to originate from nano- and picophytoplankton (Baker et al., 2017), or from the physical (Stemmann et al., 2008) or biological fragmentation of larger particles (Giering et al., 2014). Recent studies have highlighted the abundance and importance of small, slow-sinking particles which are often

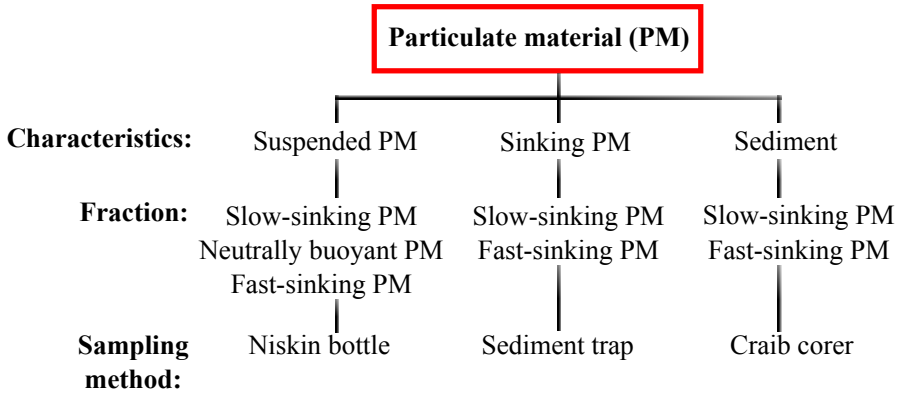

Figure 1.2: Summary of fractions of particulate material (PM) classified in this study and their sampling method

under-sampled using sediment trap deployments (Alonso-Gonzalez et al., 2010; Riley et al., 2012; Baker et al., 2017; Cavan et al., 2017). *In situ* sampling of smaller, slow-sinking SPM in parallel to larger particles is difficult, as the entire spectrum of particles present in the water column cannot be measured by one single instrument (Stemmann et al., 2008). This study uses three different methods to sample PM at different stages in the water column and seafloor (Figure 1.2). These are loosely categorised into SPM, sinking PM, and sediments. However, it is recognised that there is overlap between particle categories in this study. For example, as the SPM was collected using a Niskin bottle, this fraction could potentially collect both slow-sinking, neutrally buoyant, and fast-sinking PM. A number of studies have shown that the majority of PM was present as suspended, slow-sinking particles (e.g. Alonso-Gonzalez et al., 2010; Riley et al., 2012; Cavan et al., 2017). Alonso-Gonzalez et al. (2010) found that 60 % of total PM was represented as slowly sinking particles (sinking rates 0.7 to 11 m d^{-1}). Similarly, Riley et al. (2012) found that 63 % of the carbon flux in the North Atlantic was transported as small or slowly sinking particles. However, this contribution was likely to decrease with depth as the majority of small or slowly sinking particles were remineralised (Riley et al., 2012). A further study has shown that the long residence time of slow-sinking PM, results in its minor contribution to the overall mass flux (Wakeham and Lee, 1993). Goutx et al. (2007) showed that slower sinking particulates were degraded more quickly when compared to faster sinking particulates, which maintained their original biological signal to a certain extent. These studies focused on open-ocean sites where the composition of PM is likely to be different in comparison to coastal sites, which is the focus of this study. Terrigenous inputs into open-ocean sites would be negligible in comparison to the coastal site focused on in this study. Therefore, this compositional difference between open ocean and coastal sites may greatly affect the proportions of PM in the slow versus fast sinking fractions.

High density is a further key characteristic of fast-sinking PM. The incorporation of biogenic (e.g. silica, calcite, opal) and lithogenic minerals into PM can increase the density of PM, and act as a ballast for higher sinking velocities (Klaas and Archer, 2002; Sanders et al., 2010; Passow et al., 2014). The association between inorganic minerals and PM has been referred to as the 'ballast effect' due to the protection of PM by inorganic matrices, and added excess density which increases sinking velocity (Klaas and Archer, 2002; Passow et al., 2014). Fast sinking rates of PM from

the euphotic zone to the deep ocean have been reported to occur with the presence of inorganic minerals (Klaas and Archer, 2002; Sanders et al., 2010; Riley et al., 2012). Laboratory experiments investigating aggregate formation with the addition of clay have found that the total volume of aggregates is related to the amount of clay (Passow et al., 2014). This could have implications for the size and density of PM which in turn would affect its sedimentation rate. The addition of clay to laboratory-formed aggregates produced more numerous, denser, and smaller aggregates (approximately 1.6 mm) when compared to aggregates with no clay addition (approximately 5.0 mm; Passow et al., 2014). The coagulation of PM and minerals modifies the aggregate size, shape and porosity, all of which are important factors affecting their sedimentation and reactivity in the water column.

Focusing on a coastal study site with terrestrial/ marine organic and mineral inputs has implications for PM characterisation, which in turn determines its remineralisation efficiency or export. The composition of PM can physically effect its size and density, and chemistry. Linking PM characteristics to the biochemical composition and reactivity has the potential to determine its fate in the water column.

1.3.3 Biochemical composition

A range of organic biomarkers have previously been used to identify the source and degradative state of organic material in the water column (e.g. Wakeham et al., 1997a; Budge et al., 2001; Parrish et al., 2005). Biomarkers are able to provide information on organic material source and the type of planktonic source (e.g.diatom, dinoflagellate, zooplankton, bacterial; Wakeham et al., 2009). Additionally, they can also be used to distinguish between material that is fresh and likely to be readily utilised, versus refractory material that is likely to be preserved. The use of individual biomarkers does have limitations, as a result of non-uniform distributions in organic material from different sources, and degradation pathways that can be compound-specific (Dauwe and Middelburg, 1998). However, the focus of this study uses universal biopolymers, amino acids, fatty acids, and carbohydrates, which together represent important fractions of analytically recognisable organic material in marine and terrestrial organisms (Dauwe and Middelburg, 1998).

Amino acids are important structural components of proteins and represent the largest organic nitrogen reserve in most organisms (Lee and Cronin, 1982). Amino acids are generally labile in comparison to bulk carbon and nitrogen, and the reactivity of individual amino acids is dependent on whether they are protein versus non-protein, and whether they are structural cell wall associated or intracellular (Cowie and Hedges, 1992b; Wakeham and Lee, 1993). Concentrations and relative abundances of individual amino acids, through preferential consumption of labile compounds and preservation of refractory compounds, are able to provide information on the degradative state of organic matter (e.g. Cowie and Hedges, 1994). For example, the progressive enrichment of diatom cell wall amino acids (e.g. serine, glycine, threonine), which are physically protected by the siliceous test, is an indicator of diagenesis (e.g. Hecky et al., 1973; Cowie and Hedges, 1992b). Conversely, intracellular amino acids (e.g. glutamic acid, phenylalanine, tyrosine) are among the most labile compounds in living plankton and are preferentially degraded (e.g. Cowie

and Hedges, 1992b; Wakeham and Lee, 1993; Dauwe et al., 1999). Consistent trends between amino acid composition and degradation was used to produce a quantitative degradation index (DI; Dauwe and Middelburg, 1998; Dauwe et al., 1999), which has been used in many studies (e.g. Sheridan et al., 2002; Ingalls et al., 2003; Arnarson and Keil, 2005, 2007; Ingalls et al., 2006; Alonso-González et al., 2010; Wakeham et al., 2009; Carr et al., 2016). Further studies have used individual amino acid composition in SPM, sinking material, and sediments to investigate diagenetic alteration (e.g. Ittekkot et al., 1984; Lee and Cronin, 1984; Cowie and Hedges, 1994; Dauwe and Middelburg, 1998; Lee et al., 2000). Studies investigating the diagenetic state of POM in sinking versus sediment fractions have found a decrease in amino acid contribution to total organic carbon and nitrogen, and an increase in diagenetic parameters (e.g. increase in mole percentages of non-protein amino acids β-alanine and γ-aminobutyric acid) in sediments relative to water-column particulates (Cowie and Hedges, 1992b, 1994). Amino acids serve as useful indicators of organic matter transformation in coastal systems with mixed marine and terrigenous inputs (e.g. Cowie and Hedges, 1992b).

Lipids serve a variety of functions in all living organisms, including membrane structure, energy storage, and regulation of metabolic processes (Sargent, 1976; Wakeham et al., 1993). They are carbon-rich compounds with certain components being essential nutrients for animals (e.g. polyunsaturated fatty acids, PUFAs; Sargent, 1976; Pond et al., 1996; Parrish et al., 2005). Many lipids are reactive relative to bulk organic material, and fatty acid biomarkers are well established as indicators of the biological community in surface waters (Wakeham and Lee, 1993; Wakeham et al., 1997a); fatty acids were the focus of lipid analysis for this thesis. Additionally, proportions of PUFA, monounsaturated (MUFA), and saturated (SFA) fatty acids can be used to assess the degradative state of organic material (e.g. Fileman et al., 1998; Najdek et al., 2002). For example, diatom cells are rich in PUFAs, and these are labile and readily utilised from the water column SPM (Li et al., 2014). With increasing degradative state, the relative contribution of PUFA to total fatty acid composition generally decreases whilst SFA increase (e.g. Conte et al., 2001; Najdek et al., 2002; Wolff et al., 2011). A further study found fatty acid diagenetic trends from surface water samples, which were composed of plankton-derived PUFAs, to deep-water sediment traps that were rich in MUFAs and SFA, typical of zooplankton (Wakeham et al., 1997a). Also, diatom (16:4(n-1)) and dinoflagellate (18:4(n-3) and 22:6(n-3)) fatty acids are established source biomarkers (e.g. Wakeham et al., 1997a; Cripps and Clarke, 1998; Fileman et al., 1998; Budge et al., 2001; Najdek et al., 2002; Goutx et al., 2007). However, is has been recently shown that bacteria and invertebrates are capable of synthesising PUFA (Kabeya et al., 2018). Utilising these fatty acids biomarkers with other biochemical parameters indicative of source will aid determination of POM origin. Generally total fatty acid concentrations have been found to decrease with increasing depth (Fileman et al., 1998; Parrish et al., 2005), and between sinking and benthic fractions (Budge and Parrish, 1998). Additionally, relative proportions of individual fatty acids were shown to vary with POM fraction (Budge and Parrish, 1998). Bacterial and terrestrial fatty acid biomarkers dominated sediment composition relative to SPM, which had greater relative proportions of marine biomarkers. The use of fatty acid biomarkers and relative proportions of groups of fatty acids can provide useful information on sources and degradative states of POM.

Carbohydrates are abundant biochemicals and common structural and storage compounds in marine organisms (Cowie and Hedges, 1984; Ríos et al., 1998). High carbohydrate and low amino acid contents are characteristic of terrigenous source material (Haake et al., 1993). A key role of carbohydrates in vascular plants is structural, and they account for approximately 75 weight % (Hamilton and Hedges, 1988). In comparison, less than half of bulk carbohydrates in plankton are structural and they comprise 20 to 40 weight % (Hamilton and Hedges, 1988). This range of carbohydrate contribution to plankton mass is dependent on environmental conditions such as nutrient and light availability (Richardson and Cullen, 1995). Glucose is a common storage sugar and has been shown to be susceptible to degradation in SPM (Ittekkot et al., 1982), sediment trap materials (Cowie and Hedges, 1984), and sediments (Hamilton and Hedges, 1988). Seasonal trends in the relative proportion of terrigenous polysaccharides have been observed in sediment traps and sediments (Cowie and Hedges, 1984). Carbohydrate sourced from the marine environment dominated sediment trap and sediment composition, with an increase of terrestrial sourced carbohydrate in winter. Another study showed weight percentages of bulk carbohydrate increased with depth from plankton source to over 3000 m (Hedges et al., 2001). In comparison, shallower coastal sites (210 m, Saanich Inlet) have found glucose contributions to total carbohydrate to decrease with increasing sediment trap depth, and lower contributions in sediments relative to sediment trap materials (Hamilton and Hedges, 1988). Carbohydrates form an important component of both marine and terrestrial organisms. Additionally, they play an key role in phytoplankton buoyancy regulation via carbohydrate ballast (Richardson and Cullen, 1995). Therefore, carbohydrates are an substantial component of organic material, and are important to characterise.

1.3.4 Reactivity of POM

The relative proportions of the three major biochemical classes discussed (amino acids, fatty acids, and carbohydrates) influences the reactivity of POM. Amino acids, fatty acids, and carbohydrates are more reactive to degradation relative to bulk organic material (Cowie and Hedges, 1992b, 1994; Wakeham et al., 1997b). Phytoplankton are a major source of POM in surface waters and are rich in these three main macromolecules (Ríos et al., 1998). Terrigenous material forms an additional main source of POM in coastal zones, and the chemical composition of this material can be very different to marine sources (Hedges and Keil, 1995; Hedges et al., 1997). However, POM composed primarily of marine derived organic material is generally more reactive than terrestrial material, due to the heavily altered nature of terrestrial material, which occurs during soil formation and during its transport (Hedges and Keil, 1995; Loh et al., 2002; Burdige, 2005). Additionally, the high mineral loading of terrestrial material can physically protect the organic fraction from degradation.

Sorption of minerals can protect organic material making it less bioavailable (Keil et al., 1994; Hedges and Keil, 1999). Sorptive preservation has the potential to protect organic material from remineralisation, and it has been shown that organic matter in sediments can be protected by minerals for up to 500 years (Keil et al., 1994; Arnarson and Keil, 2005). Once the organic material was desorbed from the minerals, remineralisation of the organic material occurred within days (Keil et al., 1994). This demonstrates how minerals can protect organic material from degradation, and

this is especially important in coastal regions where there is a high mineral load. Mineral incorporation into aggregates can protect PM from bacterial degradation by reducing their bioavailability on a timescale of weeks (Arnarson and Keil, 2005). This implies that POM with mineral protection in coastal settings could transition to the seafloor without extensive degradation. Other studies have shown that the biochemical structure of POM containing inorganic matrices can undergo minimal changes due to their protection from bacterial degradation (Hedges et al., 2001; Arnarson and Keil, 2005). A study using the addition of clay, found organic-mineral aggregates to be less bioavailable than organic aggregates without clay addition (Arnarson and Keil, 2005). Carbonate and opal are natural ballasting components of marine POM and do not have the same sorptive properties as clays and other terrestrially derived minerals. Studies have found carbon-specific respiration rates in ballasted aggregates versus non-ballasted aggregates were similar, which suggests incorporation of carbonate and opal did not provide labile POM protection from bacterial remineralisation (Ploug et al., 2008a; Iversen et al., 2010).

As discussed, biochemical composition is important in determining the lability of POM. Additionally, the bio-availability of POM has been linked to POM characteristics. For example fast-sinking POM contained less labile material in comparison to slow-sinking which contained more labile material (Goutx et al., 2007). This fast sinking material could potentially include mineral ballast, which increases its sedimentation rate, and decreases its bio-availability. Further studies have shown that addition of minerals can decrease the amount of POC in aggregates (Passow et al., 2014; Schmidt et al., 2014). These studies did not investigate the reactivity of the aggregates created, but decreased relative proportions of POC and the addition of mineral material which can physically protect the organic material; suggesting the created aggregates would have a lower reactivity relative to those without mineral addition. A further study has shown the respiration rate of bacteria which colonise aggregates is proportional to POC content (Ploug and Grossart, 2000). Other factors which affect the reactivity of POM include modification processes by zooplankton and bacteria. Both zooplankton and bacteria able to transform the biochemical composition of POM into less reactive by-products, through the selective consumption of labile compounds (Cowie and Hedges, 1996). Additionally, zooplankton are able to fragment aggregates thereby affecting sedimentation rates, residence times in the water column, and potentially reactivity (Mayor et al., 2014). There are many factors which affect the reactivity of POM, which ultimately determines its fate in the water column; whether the material is remineralised at the surface, or exported to depth. Linking biochemical composition to POM reactivity will provide information on which key components determine the speed of remineralisation of POM.

1.3.5 Physical processes

There are a number of physical processes that affect the formation, composition, and sedimentation of PM in a coastal environment (Figure 1.1). Coastal regions are generally hydrographically dynamic environments with strong currents and mixing in a relatively shallow, highly advective water column (Hedges et al., 1988a). This results in lateral advection and sediment focusing of PM, which in turn supplies oceanic environments with PM that originates from coastal regions (Wakeham and Lee, 1989; Bauer et al., 2013). Advection of PM affects the sedimentation of PM

from the surface (from a marine or terrigenous origin), which rarely has a straightforward vertical journey to the seafloor. Therefore, distribution of PM in coastal zones is suggested to be driven by the hydrodynamic sorting of PM in the water column (Keil and Hedges, 1993).

Resuspension of sediments is a further process which determines the re-distribution of PM, and occurs via wave or tidal mixing (Cowie and Hedges, 1992b). It is a typical process that occurs in most coastal zones, and involves the re-distribution of relatively old planktonic remains back into the water column (Hedges and Keil, 1995). An increase in mass flux with depth is a key indicator for lateral advection and resuspension processes (e.g. Sancetta and Calvert, 1988; Cowie and Hedges, 1992b).

Physical processes affecting the distribution of PM are important to consider as they have the potential to translocate PM from its source, so it has the potential to be under-sampled from the study site. Alternatively, these processes have the potential to re-introduce PM, which has already be deposited and undergone benthic degradation processes, back into the water column. This would affect the material collected in sediment traps as the biochemical composition of sedimenting PM compared to resuspended PM would be different.

1.4 Summary

There have been many open-ocean studies examining the spatial and temporal flux of PM into deep sea environments (e.g. Wakeham et al., 1997a; Lee et al., 2000; Hedges et al., 2001; Ingalls et al., 2006; Lampitt et al., 2008; Steinberg et al., 2008; Wilson et al., 2008; Wakeham et al., 2009; Wilson et al., 2013). Further studies in coastal settings have investigated PM flux, and composition in plankton, suspended PM, sinking PM and/ or sediment fractions (e.g. Cowie and Hedges, 1984; Hedges et al., 1988b; Sancetta and Calvert, 1988; Cowie and Hedges, 1992b; Budge and Parrish, 1998; Dauwe et al., 1999; Budge et al., 2001; Parrish et al., 2005). The organic biogeochemical composition of PM is a significant factor in determining the efficiency of the BCP because it can affect POM characteristics such as size, shape, and density, sinking velocities, lability and remineralisation rates. A number of these highlighted studies have used biochemical components such as lipids (e.g. Wakeham et al., 1997a; Parrish et al., 2005), amino acids (e.g. Cowie and Hedges, 1992b; Ingalls et al., 2006), carbohydrates (Cowie and Hedges, 1984), pigments, or a combination of biochemicals (e.g. Lee et al., 2000; Hedges et al., 2001; Wakeham et al., 2009), as markers of POM source and diagenetic status. These studies have enhanced understanding of how PM biogeochemical composition varies with source material, PM depth in the water column, and in response to modification processes. Coastal studies have observed a shift from POM of a marine predominance, to a relatively higher proportion of terrestrially derived POM during winter (Cowie and Hedges, 1984; Hedges et al., 1988b). Additionally, relative proportions of key biochemical compounds (carbohydrate, amino acids, and fatty acids) were generally found to decrease with depth, and during transition into the sediment interface (e.g. Hamilton and Hedges, 1988; Cowie and Hedges, 1992b; Budge and Parrish, 1998; Fileman et al., 1998; Parrish et al., 2005). This study investigates plankton dynamics, PM composition, and sedimentation rates in a complex near-shore environment, in which terrigenous inputs play a critical role in organic matter cycling.

The magnitude of the BCP, and complex interrelated processes, which vary across spatial and temporal scales, have resulted in constrained understanding of certain aspects of the BCP. For example, the composition and physiological state of phytoplankton are recognised as key drivers in producing aggregates (e.g. Wakeham et al., 2009; Herndl and Reinthaler, 2013; Guo et al., 2016). However, few studies investigating carbon export simultaneously analyse the overlying phytoplankton community structure. Seasonal variations to community structure linked to phytoplankton biochemical composition (which can provide physiological status of cells), could provide valuable information on key species or community structures which have the highest contribution to carbon export, and provide information on the biochemical quality of the POM.

An additional area in which understanding could be furthered, and was identified as a key research area at a recent BCP workshop, included enhanced characterisation of PM, with the aim of linking PM characteristics to function, behaviour, and fate in the water column (Burd et al., 2016). The large particle size spectrum of PM and complex interrelated processes modifying particles during their sedimentation, can make characterising PM challenging. The episodic pulsing nature of the BCP, driven by blooming organisms and periods of high terrestrial run-off for example, and PM size spectra makes it difficult to representatively sample PM using discrete time points and one instrument. Recent studies have highlighted the importance of the contribution of slow-sinking, suspended particles to carbon export, which were previously thought to be remineralised at shallower depths (Riley et al., 2012; Durkin et al., 2015; Baker et al., 2017; Cavan et al., 2017). The origin of slow-sinking suspended material, and whether is it generated at the surface or as a result of larger particles fragmenting, is a key question to be addressed, especially in a coastal setting. Using a suite of biogeochemical indicators has the potential to aid understanding of why, and how, certain types of PM (including slow and fast sinking particles) are either labile or refractory to degradation. Studies have previously investigated remineralisation of POM (e.g. Boyd et al., 2015; McDonnell et al., 2015), but rarely simultaneously measured biogeochemical composition. The coupling of these two approaches would provide valuable information on key compounds driving reactivity and determining the fate of POM in the water column. These are important areas to address as the origin and biogeochemical composition of PM are key factors in controlling PM sinking velocities and degradation, thereby affecting the efficiency of the BCP (De La Rocha and Passow, 2007). Enhancing understanding of composition, reactivities, and fate in the water column of different PM fractions could lead to accurate representation in carbon budgets and biogeochemical models.

The effect of climate change on the BCP is expected to be complex (Passow and Carlson, 2012; Boyd, 2015). Phytoplankton community structure is predicted to change with global replacement of diatoms by smaller phytoplankton cells (Henson et al., 2013; Boyd, 2015). This shift is induced by a predicted increase in stratification and nutrient depletion as climate changes (Gattuso et al., 2015). With this scenario, the higher relative proportions of small versus large particles, could lead to slower sinking velocities of PM, and a reduction in the amount of carbon exported. Additionally, it has been suggested that over the last 20 years, the amount of organic carbon in the marine environment has doubled as a result of increases in run-off (Callaway et al., 2012). Shifts in phytoplankton community structure, and potential increases in the relative proportions

of terrestrial material in the marine environment as a result of increased run-off, could result in PM with a very different biogeochemical composition to those observed in present studies. This would affect a range of oceanic scale biogeochemical cycles, the distribution of elements in the water column, and the food source available to both pelagic and benthic fauna.

1.5 Thesis motivation and research questions

The first motive for this study was to enhance understanding of microphytoplankton community dynamics and associated sedimentation rates. Examining how the dominant species and/or community structure affects sedimentation rates over a seasonal cycle, could further understanding of which microphytoplankton species are key contributors to carbon export. Recent studies have shown the importance of individual phytoplankton cells in contributing to carbon export (Dall'Olmo and Mork, 2014; Durkin et al., 2015, 2016). Additionally, previous studies have linked post-bloom phytoplankton populations to higher sedimentation rates (Smayda and Boleyn, 1966; Passow, 1991), despite higher lipid synthesis in some species during this period (Diekmann et al., 2009). This seems counter-intuitive, as lipids are less dense than seawater, and should increase buoyancy. However, this is also dependant on the other biogeochemical components, which could potentially counter act the higher lipid content. A clearer understanding of how microphytoplankton community composition, linked to biochemical composition and environmental conditions, can affect sedimentation mechanisms which drive the BCP is needed.

A second motivation focused on the need to characterise PM of different fractions with respect to their seasonally varying biogeochemical composition and flux. Molecular-level analysis of key biogeochemical compounds, can provide detailed information on origin, and degradation state of POM, that routine bulk analyses cannot. Suspended and sinking fractions of PM could potentially be sourced from different origins, have different sedimentation mechanisms, and therefore varying contributions to carbon export. The dynamic nature of coastal environments, and diverse sources of PM drives the coastal BCP, which also plays a major role in oceanic and global carbon budgets. Accurate characterisation across a spectrum of PM is needed to achieve a clearer idea of the function, behaviour, and fate of PM in a coastal setting.

The final motive was to determine how the chemical composition of different fractions of POM effected reactivity. Many studies have investigated biogeochemical composition of POM (e.g. Cowie and Hedges, 1992b; Lee et al., 2000; Parrish et al., 2005; Wakeham et al., 2009) and remineralisation rates (e.g. Boyd et al., 2015; McDonnell et al., 2015; Cavan et al., 2017) individually, and have rarely addressed both simultaneously (Goutx et al., 2007). This coupling will add an extra dimension to understanding which key biogeochemical components, or combinations, drive the remineralisation rates of different fractions of POM.

These motives take a holistic approach to enhancing understanding of the BCP; from microphytoplankton community dynamics, which underpin the BCP, to determining the biogeochemical composition and reactivity of POM, which affects POM fate and cycling in the water column and seafloor. These motivations have lead to the following research questions which will be addressed

in this thesis:

1. What is the role of biochemical and environmental parameters in determining microphytoplankton sedimentation rate?
2. How does the biogeochemical composition of particulate material vary at sequential stages of transport from the surface to the seafloor?
3. What is the relationship between the biogeochemical composition and reactivity of suspended and sinking fractions of particulate material?

1.6 Thesis outline

The remainder of this thesis is composed of five chapters which are briefly described below:

- Chapter 2 characterises the biological, chemical and physical environment at site LY1 in the Firth of Lorne. Site LY1 was selected as a coastal environment representative of the west coast of Scotland and has been historically sampled. Field work studies were carried out at site LY1 between March 2015 to November 2016. This chapter investigates seasonal changes in the physical (temperature, salinity, density, cline depths, stratification index), chemical (inorganic nutrient concentrations), and biological (chlorophyll-a concentrations, microphytoplankton community composition) environment. The physical environment of an additional study site, RE5 in Loch Etive, is also contrasted to the main site LY1. This environmental characterisation chapter is used as a benchmark for the other experimental chapters, which utilise samples collected from LY1 and RE5.
- Chapter 3 investigates sedimentation rates of the suspended fraction of POM with a particular focus on microphytoplankton. Settlement columns (SETCOLs, designed by Bienfang et al. (1983)) were used to calculate the sedimentation rate of microphytoplankton community, collected above and below a density discontinuity, in relation to environment and biochemical composition drivers. The results are discussed in the context of how microphytoplankton community structure, seasonal changes in the physical environment, and biochemical composition have the potential to influence sedimentation rates.
- Chapter 4 describes the biogeochemical composition of suspended, sinking, and benthic fractions of PM collected from site LY1 over a seasonal cycle. A range of source and degradation indicators were used to investigate PM composition during periodic sampling "snap shots" down the water column. A range of diagenetic indicators, molecular-level analysis (amino acids and fatty acids), and lithogenic tracer elements, were used to determine the source and degradation state of POM at sequential stages of transport. The results are discussed in the context of biogeochemical differences between PM fractions, and the role of seasonality affecting PM source material.
- Chapter 5 describes the use of oxygen consumption rates as a proxy for PM reactivity. Both SPM collected from above and below the pycnocline, and sinking sediment trap material,

were analysed for seasonal reactivity differences. Reactivity is defined as the rate at which PM is respired and broken down into organic and inorganic material. During PM degradation, oxygen is consumed directly or indirectly and is therefore a good tracer for biological activity. SPM and sediment trap material was incubated for short periods (up to 5 hours) and oxygen consumption rates were measured using oxygen optode sensor spots (PyroScience Sensor Technology). The relationship between PM reactivity and biogeochemical composition was investigated. The results are discussed in the context of PM of different fractions having different remineralisation efficiencies, which will ultimately impact their contribution to carbon export.

- Chapter 6 aims to provide a overview of the overall results and findings of the previous four chapters. Suggestions for future areas of research, and final conclusions are also made.

Chapter 2

Environmental characterisation of a western Scotland coastal site

2.1 Introduction

The coastline of west Scotland has a complex morphology in which glaciation has produced many islands, peninsulas, and glacially deepened sea lochs (or fjords; Edwards and Sharples, 1985). Hydrography is influenced by the north east Atlantic Ocean and the Scottish Coastal Current which is driven from south to north by the Irish and Clyde Seas (Figure 2.1; Ellet and Edwards, 1983). The complex coastal morphology, abundance of topographic features, and convoluted bathymetry result in locally fast flowing, turbulent, and well mixed upper water column (Ellet and Edwards, 1983). Stratification of coastal waters varies and is determined by salinity changes from freshwater input, and the degree of wind and tidal mixing (Ellet and Edwards, 1983). The focus of this study is the north east end of the Firth of Lorne, where several other bodies of water converge (Loch Linnhe, Loch Creran, Loch Etive, and the Sound of Mull).

Located in the Firth of Lorne, site LY1 was selected as a seasonal sampling station with the aim of: 1) collecting periodic snap shots of microphytoplankton community composition and sedimentation (Chapter 3), 2) determining biogeochemistry of water column suspended, sinking, and benthic particulate material (Chapter 4), and 3) determine the reactivity of organic matter (Chapter 5). Site RE5 in Loch Etive was used as an additional study site, with a vastly different physical environment, to compare to data from LY1.

2.1.1 Firth of Lorne and study site LY1

Site LY1 (56°28.9 'N, 5°30.1 'W, 52 m depth) is a site representative of western Scottish coastal waters (Figure 2.2; Fehling et al., 2006). Site LY1 is part of a transect of stations along the Firth of Lorne into Loch Creran, and historical data sets from the 1970s, 1980s and 2000s provide background information on the area. These historical data sets include phytoplankton abundance, inorganic nutrient analysis, and particulate carbon and nitrogen analysis. Additionally, the Firth of Lorne is a Special Area of Conservation (SAC) due to the presence of inshore rocky reef habitats, and in 2014 a network of Marine Protected Areas (MPA) were designated in this area and formally

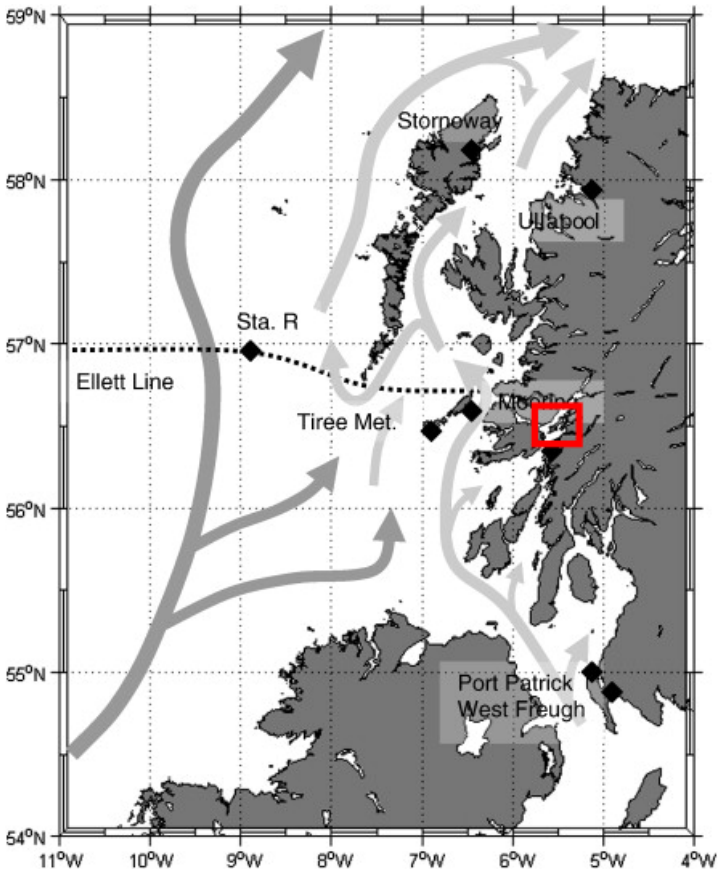

Figure 2.1: Current flow on the west coast of Scotland and area of study highlighted in red box. Modified from Inall et al. (2009)

protected since 2016.

Located north east of the Greag Isles and on the east coast of the Isle of Lismore, LY1 receives an outflow from the fjordic sea lochs Etive, Creran and Linnhe, and an inflow from the open sea. Loch Linnhe is one of the largest sea lochs on the west coast of Scotland, and receives considerable freshwater inflow. Circulation in the Firth of Lorne is influenced by freshwater input in the upper and central sections, sourced from lochs Linnhe, Creran, and Etive. The lower seaward section is heavily influenced by Atlantic and Irish sea origin waters (Figure 2.1; Berx et al., 2015). Additionally, the Corryvreckan whirlpool, driven by tidal forcing between the islands of Scarba and Jura, is located further south from LY1. Recorded maximum water speeds of 4.5 m s^{-1} affect sediment dynamics within the surrounding area of the whirlpool (Howe et al., 2015). These strong tidal flows extend out into the Firth of Lorne (Dale et al., 2011). Additionally, there is a wide variation in bathymetry and currents within the Firth of Lorne, that drives the turbulent flow of seawater making the area a highly dispersive environment (Dale et al., 2011). This high energy environment results in the suspension of sediments, which are controlled by tide and wind driven currents (Dale et al., 2011). The composition of the suspended sediment determines whether it is likely to sink or undergo lateral advection (Perry, 2010). Inshore, shallow water (<50m) sediment is composed of thick accumulations of mud, in addition to fine-grained, organic-rich sediment which is supplied via riverine input from Lochs Etive and Linnhe (Howe et al., 2015). Considering

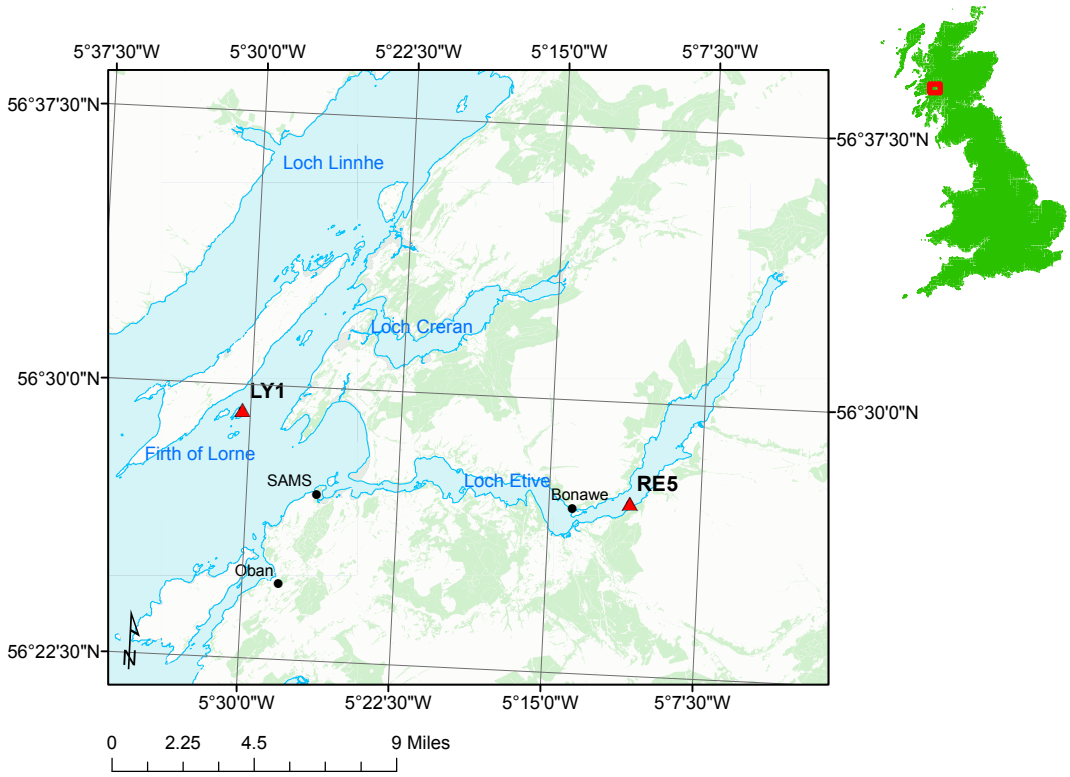

Figure 2.2: Site LY1 in the Firth of Lorn and RE5 in Loch Etive (OS Maps). SAMS: Scottish Association of Marine Science

the dynamic environment of LY1 is essential for interpreting the quantity and quality of particulate material collected during sampling.

2.1.2 Loch Etive and study site RE5

Loch Etive is a sea loch situated north of Oban along the fjordic coastline of the west coast of Scotland (Figure 2.2; Gage, 1972). The loch is approximately 30 km in length and is composed of a series of shallower lower basins oriented east to west, and a main upper basin oriented north east to south west (Figure 2.3; Howe et al., 2002). Fjordic systems are characterised by the presence of sills, which restrict exchange of water between the open sea and the fjord basin (Stashchuk et al., 2007). Loch Etive contains six sills, the largest of which is the Bonawe sill (13 m below mean high water (Nørgaard-Pedersen et al., 2006), which separates the lower basin (maximum depth of 68 m) from the upper basin, which stretches from the Bonawe sill to the head of the loch at Glen Etive (Edwards and Sharples, 1985). The upper basin reaches a maximum depth of 153 m at the Bonawe deep (RE5; Figure 2.3).

Loch Etive is connected to the Firth of Lorne through a narrow (200 m) and shallow sill which creates strong tidal flows at the Falls of Lora (Edwards and Sharples, 1985). Tidal forcing is predominantly semi-diurnal, with a neap range of 1.1 m and a spring range of 1.8 m (Austin and

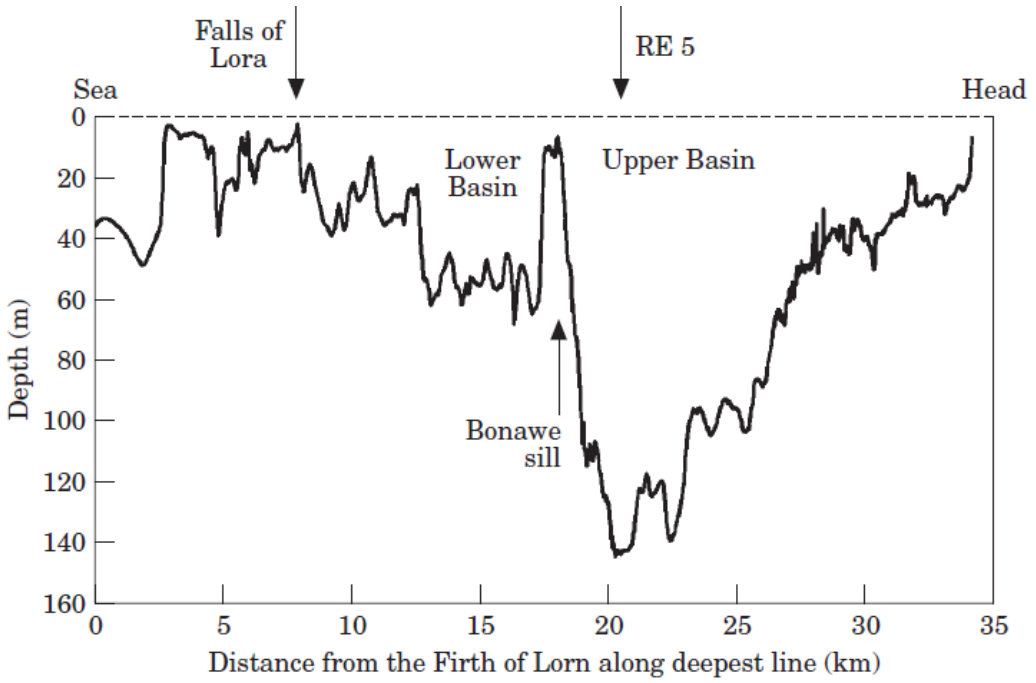

Figure 2.3: Bathymetry of Loch Etive taken from Overnell et al. (2002)

Inall, 2002). These tidal streams create a turbulent, dispersive environment with maximum surface currents recorded of 4 m^{-1} s^{-1} (Hicks et al., 2016). Attenuation at the Falls of Lora reduces the tidal range inside the loch to 2 m compared to an external range of 4 m (Wood et al., 1973). The rivers Awe (which enters laterally adjacent to Bonawe sill), Etive and Kinglass are major contributors to freshwater inputs into Loch Etive. The total river catchment area is larger than any other Scottish fjord, and is approximately 1400 km^2 (Edwards and Edelsten, 1977; Howe et al., 2002).

The upper basin and site RE5 (56°27 'N, 5°11 'W) has been widely studied because it is an excellent example of restricted exchange dynamics. High freshwater input and the restricted exchange with the Firth of Lorne limits deep water renewal events occurring. Renewal events occur on average every 16 months when freshwater inputs are reduced, and surface water temperatures decreases (Edwards and Edelsten, 1977). Surface density reaches a critical value where it is able to circulate deep within the upper basin and replenish the old water. Additionally, wind conditions are important for driving these renewal events through the creation of internal waves (Hicks et al., 2016). Deep water currents are considerably smaller (0.5 m^{-1} s^{-1}) than those observed at the turbulent tidal stream of the Falls of Lora (Howe et al., 2002). Renewal events can vastly change deep water properties; for example, a renewal event in May 2000 resulted in dissolved oxygen concentrations increasing from 0.9 mg L^{-1} to 9.5 mg L^{-1} (Austin and Inall, 2002).

2.1.3 Research objectives

This chapter aims to provide a descriptive characterisation of the physical, chemical, and biological environment at site LY1 over two sampling seasons (2015 and 2016). In addition, this study aims to describe the environment at RE5 and compare parameters to similar dates visited at LY1. Research questions specific to this Chapter include:

1. How do the environmental parameters differ seasonally and between the two sample years (2015 and 2016) at LY1?
2. What are the environmental differences between sites LY1 and RE5?

2.2 Methods

2.2.1 Study site

LY1 was easily accessible from the Scottish Association for Marine Science (SAMS) based at Dunstaffnage with a short journey time of 20 minutes on RV *Seol Mara*. Site LY1 was periodically sampled from March to November in 2015 (Table 2.1) and 2016 (Table 2.2). Dates were categorised into seasons based on the meteorological calender which defines spring (March, April, May), summer (June, July, August) and winter dates (September to February; autumn and winter were grouped into winter seasons due to the low number of sampled dates; UK Meterological Office, 2019). Loch Etive RE5 was sampled on 13th June 2016 during a collaborative trip with Doctor Greg Cowie and undergraduate students from the University of Edinburgh.

2.2.2 Sample collection

A conductivity, temperature and depth (CTD) profiler (Seabird SBE 19, Sea-Bird Electronics) was used to determine physical parameters of the water column, including the position of the pycnocline which was important for sampling. Samples were taken from above and below the pycnocline and were of interest to investigate how microphytoplankton sedimentation rate changed across a density discontinuity (Chapter 3). The CTD was lowered by a winch cable over the stern of the boat and kept submerged at the surface for one minute to allow the sensors to equilibrate. The CTD was then lowered to approximately 5 metres from the seabed whilst measuring temperature, conductivity, density, dissolved oxygen concentrations, and fluorescence profiles of the water column. Water column profiles were examined on-board using SeaTerm programme to determine water sampling depths. On return to the laboratory, raw CTD data were processed using SBE data processing software.

A range of water column samples were taken during the 2015 sampling campaign from depths above and below the pycnocline (Table 2.1). The quantity and type of samples collected was increased during the 2016 field work. Water column samples were taken with Niskin bottles from above and below the pycnocline, 20 m (depth at which sediment traps were deployed) and 45 m (close to the seafloor where cores were taken; Table 2.2).

Table 2.1: Details of water column samples collected during 2015 sampling campaigns including date, season, sample depth (m) above (A) and below (B) the pycnocline, and sample analyses

Date	Day in year	Season	Sample depth (m)	Pycnocline	Analyses
20/03/2015	79	Spring	5	A	Inorganic nutrients; Chlorophyll; Phytoplankton community composition; SETCOL experiments
			10	B	
07/04/2015	97	Spring	5	A	
			10	B	
15/04/2015	105	Spring	3	A	
			15	B	
05/05/2015	125	Spring	3	A	
			10	B	
13/05/2015	133	Spring	2	A	
			10	B	
11/06/2015	162	Spring	6	A	
			10	B	
06/07/2015	187	Summer	5	A	
			10	B	
18/08/2015	230	Summer	3	A	
			8	B	
27/10/2015	300	Winter	3	A	
			10	B	

Table 2.2: Details of water column samples collected during 2016 sampling campaigns including date, season, sample depth (m) above (A) and below (B) the pycnocline, and sample analyses

Date	Day in year	Season	Sample depth (m)	Pycnocline	Analyses
03/03/2016	90	Spring	4	A	Inorganic nutrients (all depths)
			10	B	
06/04/2016	97	Spring	5	A	
			10	B	
			20	-	Chlorophyll (all depths)
			32	-	
16/05/2016	137	Spring	5	A	
			10	B	Phytoplankton community composition (A & B only)
			20	-	
			45	-	
01/06/2016	153	Spring	3	A	
			10	B	
			20	-	SETCOL experiments (A &B only)
			45	-	
05/07/2016	187	Summer	3	A	
			10	B	
			20	-	
			45	-	
01/08/2016	214	Summer	3	A	
			10	B	

Table 2.2: continued

Date	Day in year	Season	Sample depth (m)	Pycnocline	Analyses
			20	-	
			45	-	
15/08/2016	228	Summer	3	A	
			10	B	
			20	-	
			45	-	
13/09/2016	257	Summer	5	A	
			10	B	
			20	-	
			45	-	
10/10/2016	284	Winter	3	A	
			10	B	
			20	-	
			45	-	
07/11/2016	312	Winter	3	A	
			10	B	
			20	-	
			45	-	

2.2.3 Environmental characterisation

Cline depths (thermocline, halocline and pycnocline) were calculated using the two-box method of Planque et al. (2006), in which the water column is formed by two homogeneous layers separated by a sharp cline. The mixed layer depth (Z_x) is calculated as shown in equation 2.1.

$$Z_x = Z_1 \frac{\rho_m - \rho_1}{\rho_0 - \rho_1} \tag{2.1}$$

where Z_1 is the water column total height, ρ_m is the mean of the hydrological variable, ρ_1 is the bottom water hydrological variable, and ρ_0 is the surface water hydrological variable

Stratification index ($\hat{S}$) was used as a measure of stratification and was calculated by integrating the mean density (sigma-theta) differences down the water column profile (Fortier and Legget, 1982) obtained by the CTD as shown in equation 2.2.

$$\hat{S} = \frac{\sum_{i=1}^{i=n} \Delta\sigma_{ti}.\Delta_{Zi}}{n} \tag{2.2}$$

where n is the number of pairs of adjacent measurements, $\Delta\sigma_{ti}$ the difference in water density

between the *i*th pair of measurements and Δ_{Zi} the depth interval between the *i*th pair of measurements fixed at 1 m. When the difference in density was greater than 0.1, the water column was considered to be stratified (Fortier and Legget, 1982).

Wind speed and rainfall data from the Dunstaffnage weather station (56° 'N, 5°26.3 'W) were obtained for the period January 2015 to December 2016 from the UK Meteorological Office Historic station data (UK Meterological Office, 2017). Dunstaffnage weather station is a historic station which has been collecting data since 1972.

2.2.4 Inorganic nutrient concentrations

Water samples (50 ml) from above and below the pycnocline were filtered through 25 mm glass fibre filters (Whatman GF/F) and the filtrate was collected into 50 ml plastic centrifuge tubes (2015 sampling). In addition to samples from above and below the pycnocline, nutrient samples were taken from 20 m (sediment trap depth) and approximately 45 m (near seafloor sample) for 2016 sampling. Tubes were labelled and frozen at -20°C until analysis. Determination of inorganic nutrient concentration (silicate, nitrate, and phosphate) was carried out using colorimetric analysis (Grasshoff et al., 2009) with an auto-analyser (Lachat QuickChem 8500) using a standard flow injection method.

Batches of samples were removed from the freezer and defrosted overnight before analysis. For each batch, standard stock solutions of nutrients were prepared in DI H_2O from which a mixed working solution of nitrate, phosphate and silicate standards was used. Each calibration was conducted with five dilutions at 20, 25, 33.3, 50 and 100 times and a blank run with low nutrient seawater (OSIL nutrients <1 μM per litre). For natural seawater concentrations the following ranges were chosen: PO_4 0 - 2.5 μM, SiO_3 0 - 10.0 μM, NO_3 0 - 10.0 μM. Calibration coefficients were obtained using first or second order polynomial regression (Omnion software, Lachat Instruments, USA).

Triplicate aliquots (8 ml) from samples were used for analysis. The times 33.3 dilution standards were run in triplicate at the beginning and the end of each batch in order to obtain a drift correction. Incremental drift correction, calculated from the average difference of the drifts, was applied to samples. The limits of detection (LOD) for the instrument was calculated for each nutrient by sampling low nutrient seawater in triplicate and then multiplying the standard deviation by three (LOD PO_4 0.13 μM, SiO_3 0.05 μM, and NO_3 0.27 μM). Method precision was calculated by dividing the standard deviation of the replicates by the mean and multiplying by 100. The method precision for PO_4, SiO_3, and NO_3 was $\leq$ 7.5 %, 28.26 %, and 24.3 % respectively.

2.2.5 Chlorophyll-a

Chlorophyll-a samples collected during 2015 from the depths specified in Table 2.1 were measured by filtering 500 ml through 25 mm glass fibre filters (Whatman GF/F; NB: 2016 chlorophyll samples not yet processed). Samples were frozen at -20 °C until analysis. Pigments were extracted in 10 ml of 90 % acetone, which was placed in a 15 ml centrifuge tube while the filter was still

frozen. The centrifuge tubes were kept in the dark at 4 °C for a minimum of 18 hours. Tubes were placed on ice in the dark, individually sonicated for 1 minute, and then centrifuged for 6 minutes at 4 °C at 4000 rpm.

The fluorometer (Turner TD 700 Laboratory fluorometer, Turner Designs) was set up using a pre-stored calibration using 25 mm glass test tubes (Tett, 1987). Before every sample was measured, test tubes were rinsed thoroughly first with DI H_2O and then with 90 % acetone. Samples were then placed in to the test tube and wiped clean before placing in the fluorometer. A second measurement of each sample for pheophytin concentrations was taken using fresh sample with the addition of 50 μL of 2 N 8 % hydrochloric acid which was gently mixed.

2.2.6 Microphytoplankton community composition

Microphytoplankton community composition was investigated (Table 2.1 and 2.2) using 55 ml samples preserved in Lugol's solution. Samples were carefully homogenised and placed into a 50 ml settlement chamber (Hydrobios) for 24 hours. Once settled, samples were analysed using an Axio S100 or S200 inverted microscope fitted with 10x, 20x and 40x magnification objectives and x10 eyepieces (use of two microscopes due to logistical limitations on microscope use). Each chamber underwent an initial scan to estimate dominant species present and determine count method. Full chamber counts were carried out at 200x magnification. During blooms of species such as *Skeletonema*, *Chaetoceros* and *Pseudo-nitzscha* spp., half chamber or transect cell counts were used along with full chamber counts for everything else. Chain lengths of all chain forming species were recorded. Guides used for phytoplankton ID included Identifying marine phytoplankton (Tomas, 1997), Phytoplankton of Norwegian Coastal Waters (Throndsen et al., 2007), Marine Phytoplankton (Hoppenrath et al., 2009), and Coastal Phytoplankton (Kraberg et al., 2010).

2.2.7 Statistical analysis

Principle component analysis (PCA) is a multivariate tool that allows a large number of variables to be reduced into a few principle components. A correlation matrix was used to perform PCA to investigate the dissimilarity in the chemical and physical parameters between sample dates and depths for both of the sample years (spring sample dates 2015 n = 6, summer sample dates 2015 n = 2, winter sample dates 2015 n = 1, spring sample dates 2016 n = 4, summer sample dates 2016 n = 5, winter sample dates 2016 n = 2). Environmental data was log transformed to account for the high degree of variation between environmental parameters. This PCA analysis was carried out using Minitab 17.

Further multivariate statistical analyses were used to identify differences in microphytoplankton community composition over the sampling days. Microphytoplankton cell counts were fourth root transformed to account for both absent and highly abundant species. Seasonal similarities between the microphytoplankton communities in 2015 and 2016 were represented with non-metric multidimensional scaling (nMDS) plots. A Bray Curtis similarity matrix was used. The spatial orientation of samples on nMDS plots indicates the similarity of microphytoplankton communities between sample dates. Statistical differences between the seasonal composition of microphytoplankton

communities were analysed using one way permutation based analysis of similarity (ANOSIM). Similarity percentage (SIMPER) analysis was used to identify the most important microphytoplankton taxa contributing to the similarities. A 90 % cut off for low contributions was applied to the SIMPER analysis. Analyses were carried out using PRIMER v.6 software.

2.3 Results and discussion

2.3.1 Site LY1

2.3.1.1 Environmental characterisation

CTD casts show temporal variability in upper 20 m water column structure between 2015 (Figure 2.4) and 2016 (Figure 2.5; full water column profiles Figure A.1). Water temperature down the water column was relatively uniform between March and November during both years ranging from 5.99 to 13.78°C in 2015, and 7.62 to 14.36°C in 2016. The top 5 m of the water column was generally warmer than deeper depths for the majority of 2015 and 2016 until winter when the water column was warmer below 5 m than the surface layers. There was a more pronounced thermocline especially during summer and winter sampling dates in 2016 (Figure 2.5) when compared to 2015 (Figure 2.4).

Salinity ranged from 22.74 psu to 33.21 psu during 2015, and was highly variable within the superficial layer over the year (Figure 2.4). Surface salinity was lowest during spring and winter, with higher surface salinity during summer months. Differences between salinities in the surface layers and deeper layers were larger earlier in the year. Surface salinity was low during the initial sampling days in 2016, but then increased substantially during spring and early summer (Figure 2.5), in contrast to the lower surface salinities during this period in 2015. Surface salinity decreased in the following months and was at its lowest mid-August at 25.50 psu (Figure 2.5).

Salinity determined seawater density at LY1 as temperature was found to be relatively uniform down the water column (except in winter 2016). Density ranged from 17.89 to 25.54 kg m^3 during 2015, and from 18.81 to 26.08 kg m^3 during 2016. Within the top 5 m density was highly variable in comparison to deeper layers, which had a lower range of densities over both the years. There were larger differences in density down the water column at the beginning of the year in 2015, where surface seawater density was less dense than later in the year (Figure 2.4). This was in contrast to 2016, where at the beginning of the year surface density was at its highest and began to decrease later in the year from day 175 (Figure 2.5).

The extent of stratification at LY1 varied over 2015 and 2016 (Figure 2.6). Following the first few sampling days where the water column was stratified, vertical stratification fluctuated above and below the 0.1 threshold (Fortier and Legget, 1982) until day 150 when stratification peaked again. Subsequently stratification decreased for the remainder of 2015 except for an increase on the last sampling date. This trend of higher stratification earlier in 2015 corresponds to the period when surface density was at its lowest relative to deeper layers and later sampling dates (Figure 2.4). This trend was reversed in 2016 when, apart from initial sampling dates where surface density

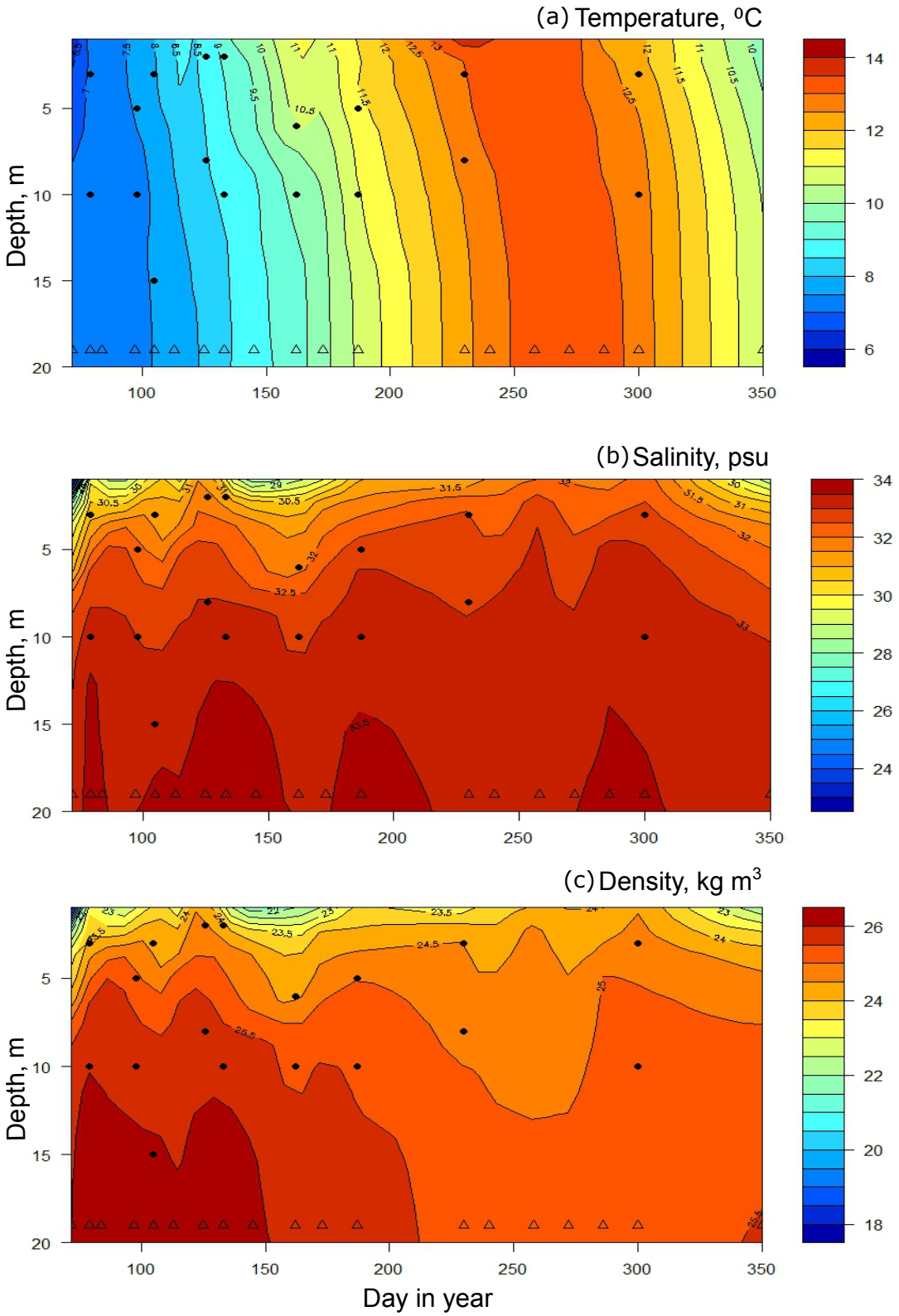

Figure 2.4: 2015 water column profiles of (a) temperature (°C), (b) salinity (psu), and (c) density (kg m^3) at LY1. Circle = SETCOL experiment depths, triangles = CTD sampling events

was low resulting in higher stratification, there was a low degree of stratification during early 2016 (Figure 2.6). Stratification increased later in 2016 when surface waters were less saline and dense

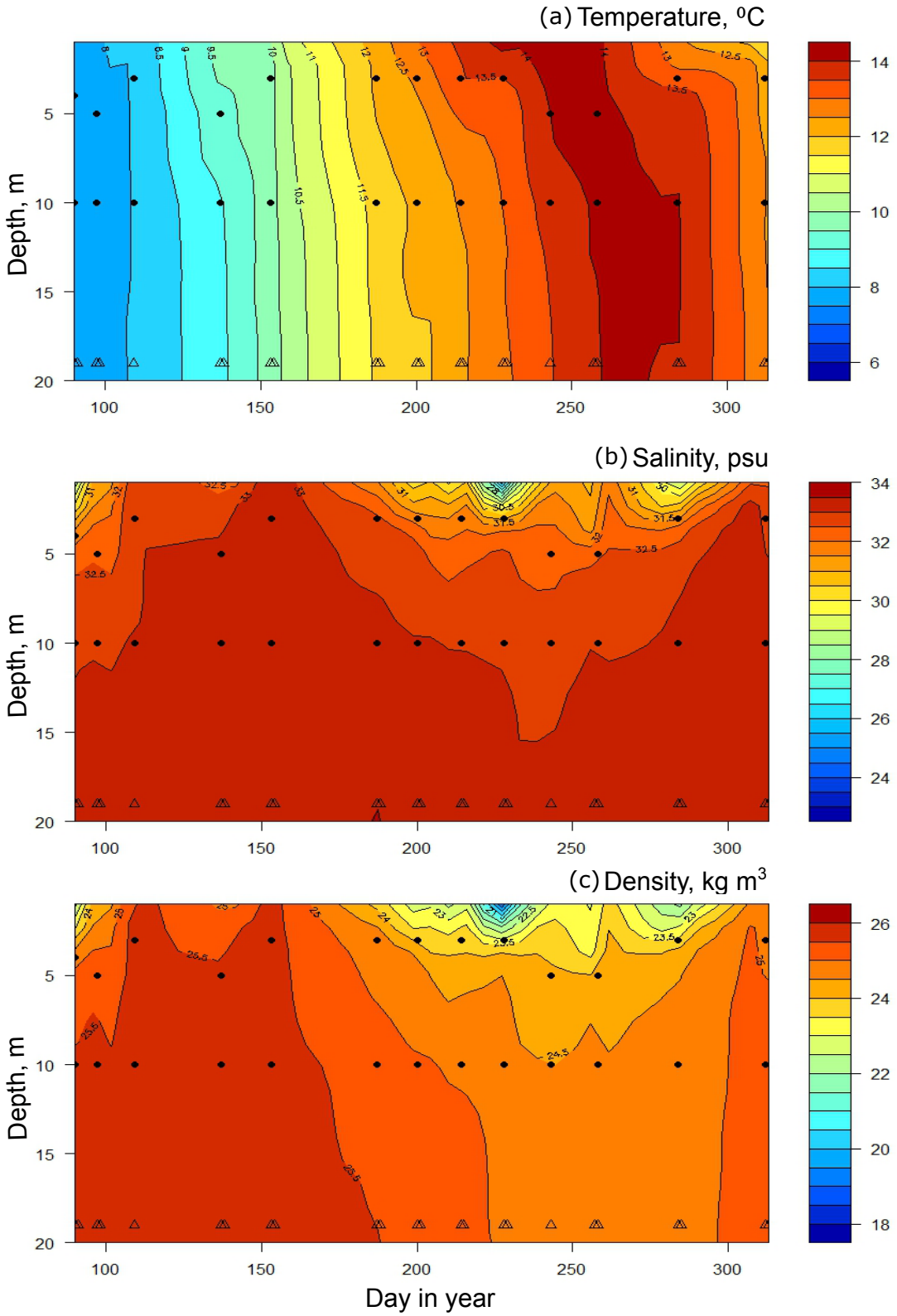

Figure 2.5: 2016 water column profiles of (a) temperature (°C), (b) salinity (psu), and (c) density (kg m^3) at LY1 Circle = SETCOL experiment depths, triangles = CTD sampling events.

relative to under lying waters (Figure 2.5). Generally, there was a higher degree of stratification in 2015 than 2016 (Figure 2.6).

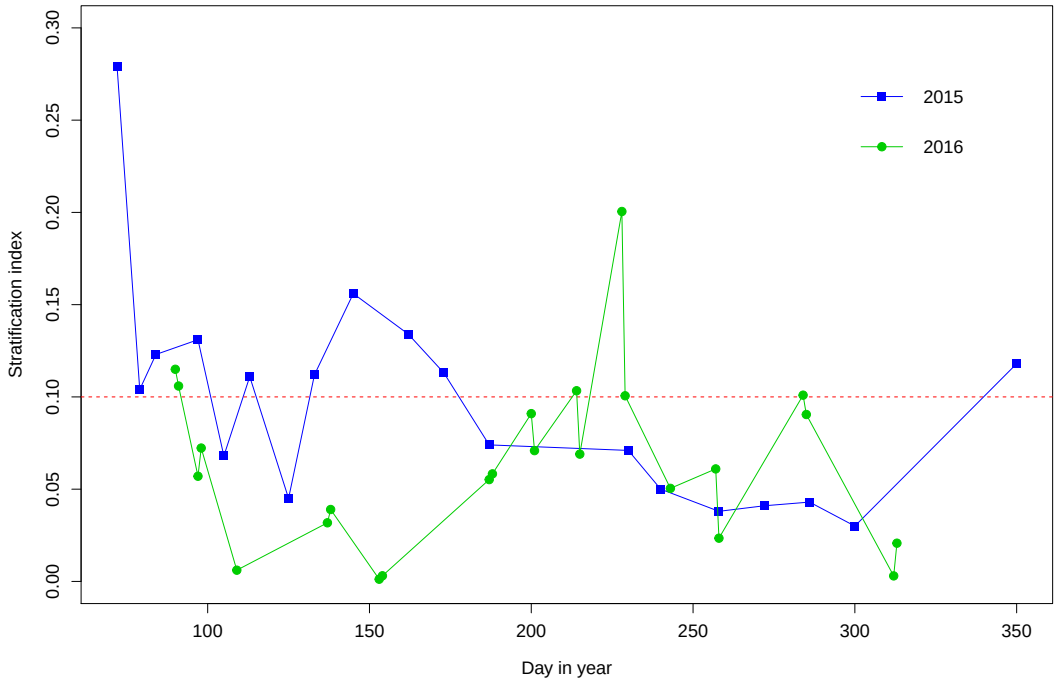

Figure 2.6: Stratification index at LY1 during 2015 and 2016 with 0.1 stratification threshold (red line)

Seasonal changes to physical and chemical parameters are evident at site LY1. A PCA analysis was carried out to determine dissimilarity in the chemical and physical parameters between sample dates and depth for both years. Increasing distance between sample dates indicated a higher dissimilarity in environmental parameters between sample date and depth (Figure 2.7a). In 2015, PC1 explained 34.8 % of the variance in the data, while component 2 accounted for 21.8 %, giving a total of 56.7 % explained variation from these two axes alone. Figure 2.7a shows grouping of points based on sample day with spring dates (represented in green, 79 to 162) being highly variable but more similar to each other than sample dates in summer and winter (represented in orange and grey, day 187 to 300). The large spread between sample day and depth above and below the pycnocline during spring dates (Figure 2.7), shows the variability of the chemical and physical environment earlier in the year and variability with depth (Figure 2.4). Summer and winter sampling days were similar to each other in terms of environmental characteristics, and were also similar for samples from the same date taken from above and below the pycnocline. Temperature, wind speed, and phosphate were important for explaining the spread of PC1 (Figure 2.7b). Higher temperatures during summer and winter dates compared to lower temperatures during spring explained the separation. Higher concentrations of nitrate, phosphate (Figure 2.10) and wind speed (Figure 2.9) during spring resulted in the dissimilarity of these dates to summer and winter where they were lower. Day in year, stratification index, and silicate were responsible for the ordination of PC2. There was a higher degree of stratification in spring 2015 than in summer or winter (Figure 2.6).

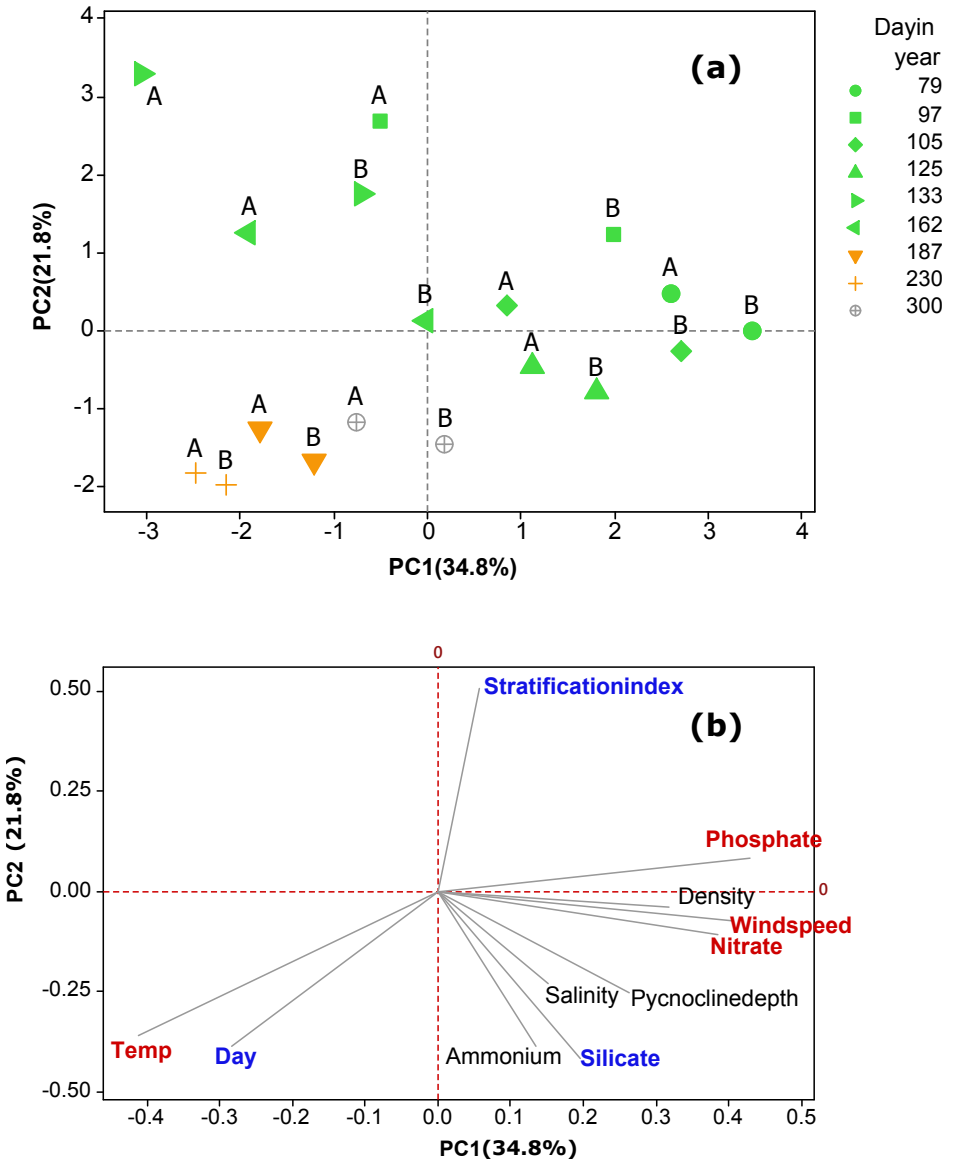

Figure 2.7: (a) Principle component analysis (PCA) ordination of log transformed environmental data for each sample day in 2015 above (A) and below (B) the pycnocline. Green= spring dates, orange= summer dates, grey= winter dates (b) Loading plot of environmental variables indicating the relation between sample day and depth with environmental variables. Red font highlights factors important in explaining the spread of sample days on PC1 and blue on PC2

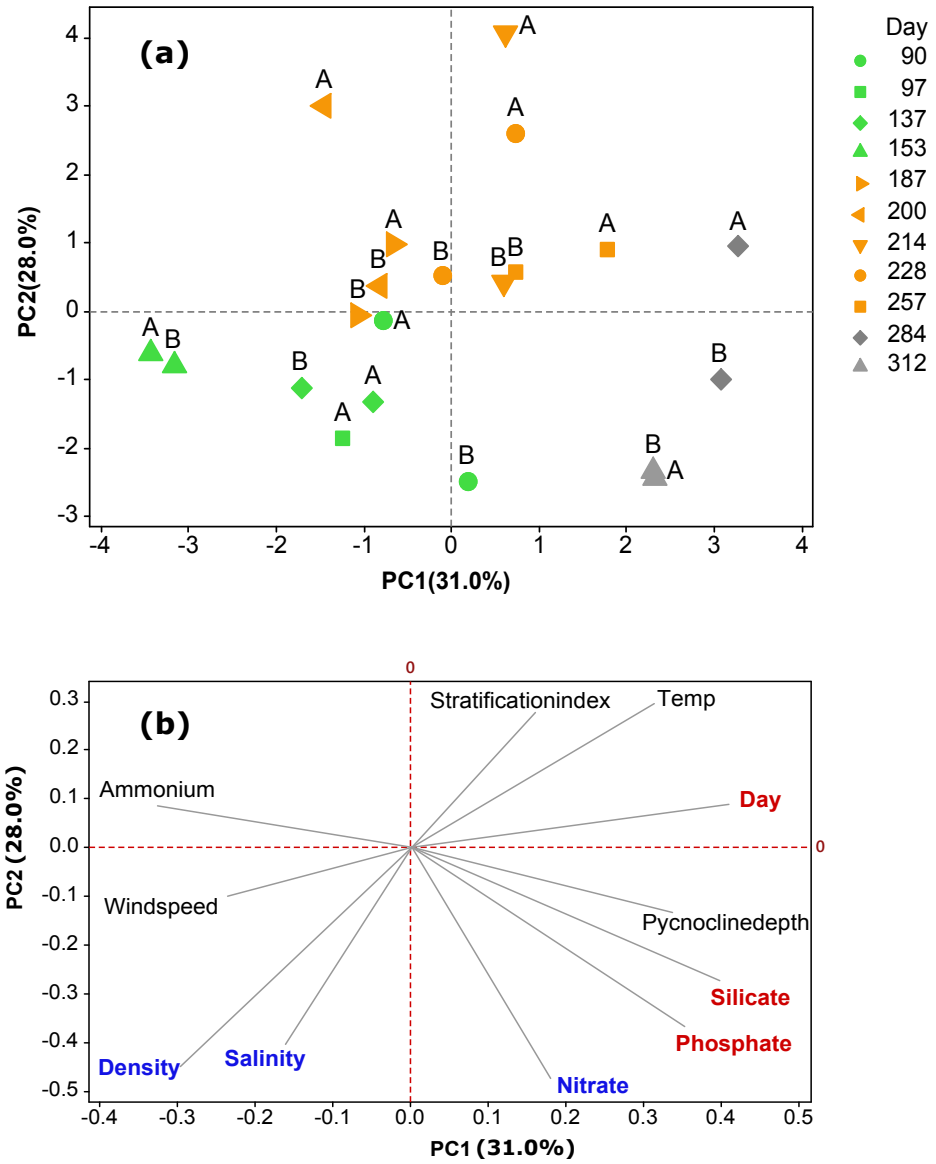

Figure 2.8: (a) Principle component analysis (PCA) ordination of log transformed environmental data for each sample day in 2016 above (A) and below (B) the pycnocline. Green= spring dates, orange= summer dates, grey= winter dates. (b) Loading plot of environmental variables indicating the relation between sample day and depth with environmental variables. Red font highlights factors important in explaining the spread of sample days on PC1 and blue on PC2

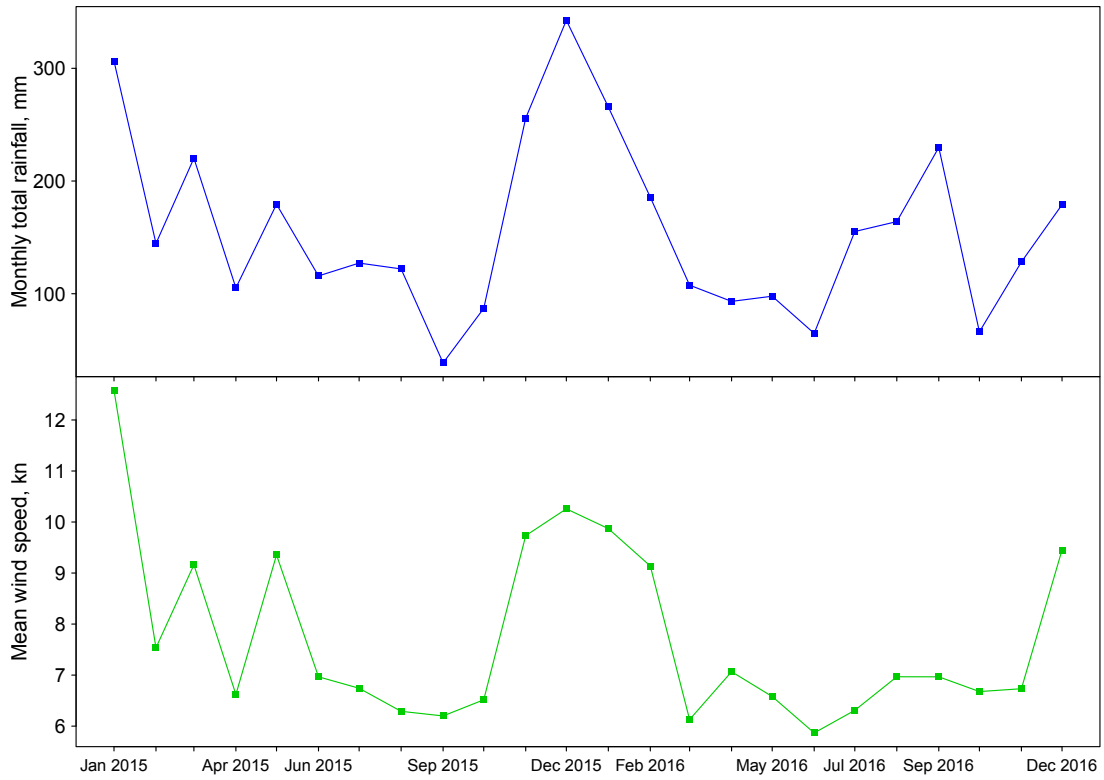

Figure 2.9: Monthly total rainfall (mm), and monthly mean wind speed (kn) at Dunstaffnage weather station from 2015 to 2017

In 2016, PC1 explained 31.0 % of the variance in the data, while component 2 accounted for 28.0 %, giving a total of 59.0 % explained variation. A number of spring and summer sample dates were in close proximity indicating similar environmental characteristics (Figure 2.8a). The largest differences between above and below the pycnocline depths sampled on the same date were the first sample date in spring (day 90), the majority of summer dates, and the first winter date (284; Figure 2.8a). This coincides with the water column being relative well mixed during spring (Figure 2.5) with stratification increasing during summer and winter (Figure 2.6). Sample day and higher silicate and phosphate concentrations during winter (Figure 2.11), were responsible for explaining the dissimilarity of winter dates to summer and spring (Figure 2.8b). Spring surface waters had high salinities and densities relative to summer and winter periods, which caused environmental dissimilarities between these seasons (Figure 2.8b). Additionally, higher nitrate concentrations in the spring and late winter were responsible for the difference between low concentrations in summer sampling dates. The sample day of the year, high silicate and phosphate concentrations in winter resulted in the dissimilarity of winter to spring and summer sampling dates.

Environmental data including total rainfall and mean wind speed from Dunstaffnage station were analysed. Peaks in rainfall in March and May corresponded to low surface salinities during that period (Figure 2.4). The highest monthly rainfall for both years occurred in December 2015 and January 2016 with 342.6 mm, and 265.7 mm of rain respectively (Figure 2.9). Other periods of high rainfall occurred during summer months in 2016, which resulted in less saline surface waters (Figure 2.5) during the summer as opposed to spring in 2015. Wind speed was more variable in

spring 2015 than 2016, with highest speeds of 12.6 kn in January 2015, and 9.9 kn in February 2016 (Figure 2.9).

2.3.1.2 Inorganic nutrient concentrations

Dissolved inorganic phosphate, silicate, and nitrate concentrations were higher in early spring and lowest in summer and winter (Figure 2.10). Phosphate, silicate, and nitrate concentrations were variable above versus below the pycnocline over the sampling period.

Initial phosphate concentrations were substantially higher below (3.4 μM) than above (1.7 μM) the pycnocline and remained higher for the majority of 2015 (Figure 2.10). Silicate concentrations were high and relatively similar at both depths for the first few sample dates, after which concentrations decreased and were variable between depths. Nitrate concentrations were highest below the pycnocline in early spring (9.2 μM) after which they subsequently decreased at both depths and to a minimum of 0.3 μM above the pycnocline.

Concentrations of phosphate, silicate, and nitrate in 2016 followed a similar trend to 2015. Concentrations were higher during spring and increased down the water column until summer; after which, surface concentrations decreased relative to deeper concentrations (phosphate and silicate). However, there were lower concentrations down the entire water column relative to spring for nitrate (Figure 2.11). During winter, concentrations of phosphate, silicate and nitrate increased. Phosphate concentration was highest (0.6 μM) above the pycnocline at the end of the year (day 312) and lowest (0.1 μM) in surface waters during the summer (day 214). Silicate concentrations were highest towards the end of the year (5.2 μM) and down the entire water column. Nitrate concentrations were highest below the pycnocline at the beginning (6.5 μM) and end (4.4 μM) of the year with low concentrations during the intermediate dates.

2.3.1.3 Microphytoplankton community composition

Microphytoplankton abundance was generally higher above than below the pycnocline during 2015, reaching a maximum of 43 x 10^5 and 20 x 10^5 cells L^{-1} respectively. The initial peak in microphytoplankton abundance above the pycnocline (day 98) corresponded with maximum chlorophyll concentrations (5.5 μg L^{-1}; Figure 2.12a). Following this chlorophyll maximum, concentrations slightly decreased and there was a large decrease in cell abundance (Figure 2.12a). The secondary peak in microphytoplankton abundance (day 162) above the pycnocline was mirrored with an increase in chlorophyll concentration. Below the pycnocline, chlorophyll concentration gradually increased to a maximum of 7.1 μg L^{-1} (Figure 2.12b). During this period of high chlorophyll concentrations, microphytoplankton abundance peaked and then declined. However, also during this period, there was also a decrease in the number of cells when chlorophyll concentration was at its highest.

LY1 demonstrated a classic temperate microphytoplankton cycle, with a spring bloom dominated by diatoms and driven by high nutrient availability (Figure 2.10 and 2.13). Diatom abundance peaked on day 98 in 2015 (Figure 2.13a), and day 90 in 2016 (Figure 2.13c) above the pycnocline,

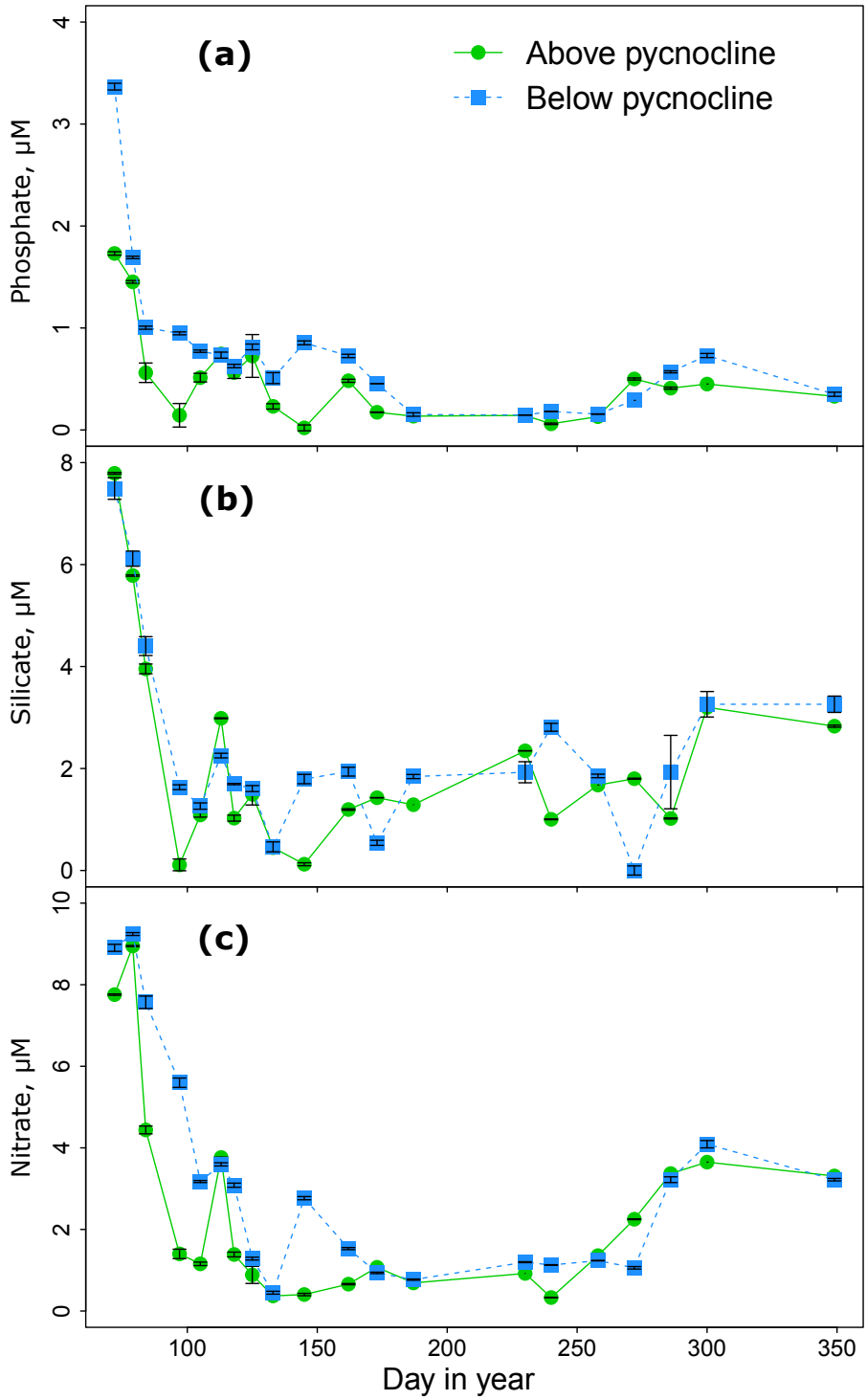

Figure 2.10: Dissolved inorganic phosphate (a), silicate (b), and nitrate (c) concentrations (μM) at LY1 during 2015. Error bars show the method error represented as standard deviation (n=3).

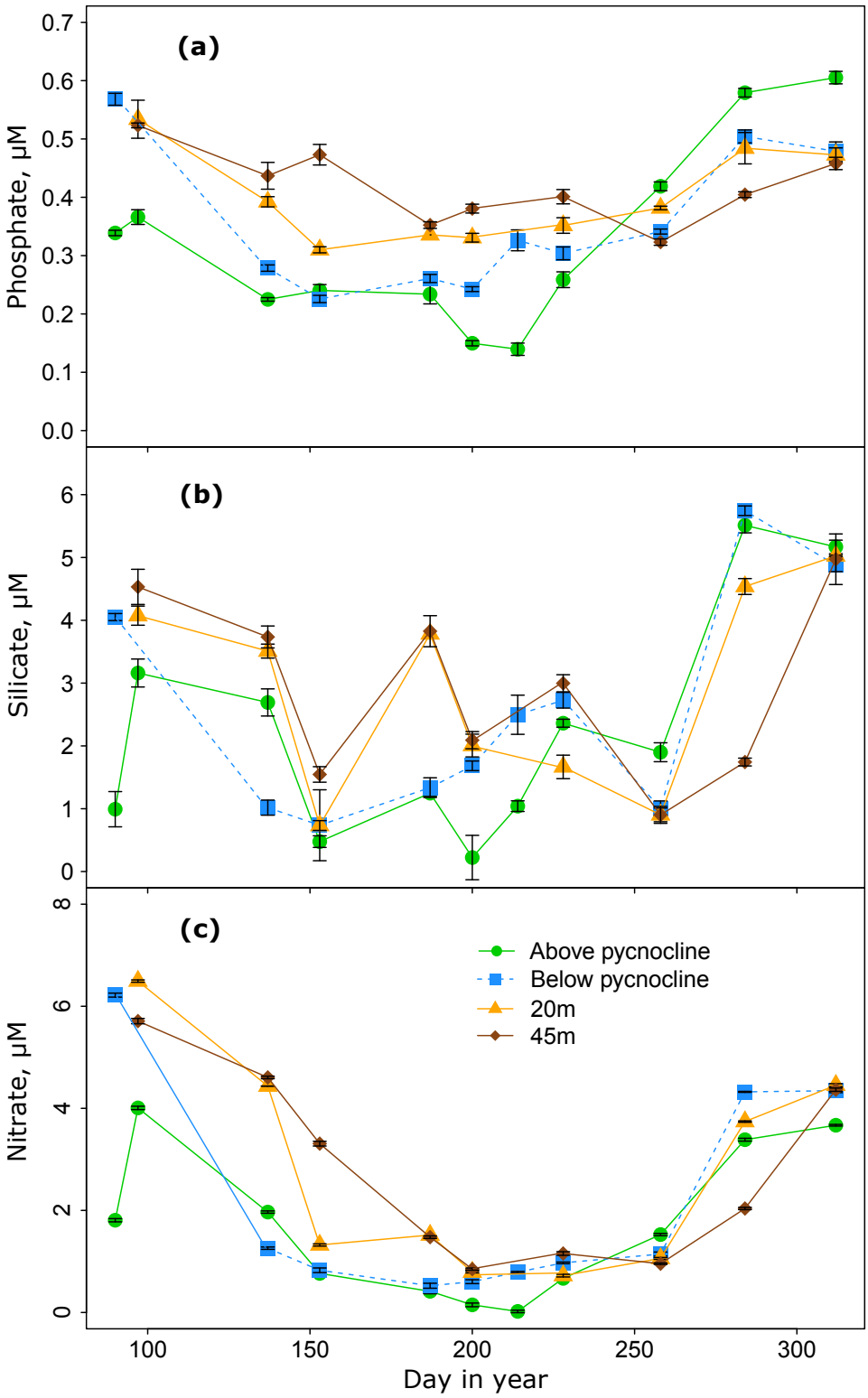

Figure 2.11: Dissolved inorganic phosphate (a), silicate (b), and nitrate (c) concentrations (μM) at LY1 during 2016. Error bars show the method error represented as standard deviation (n=3).

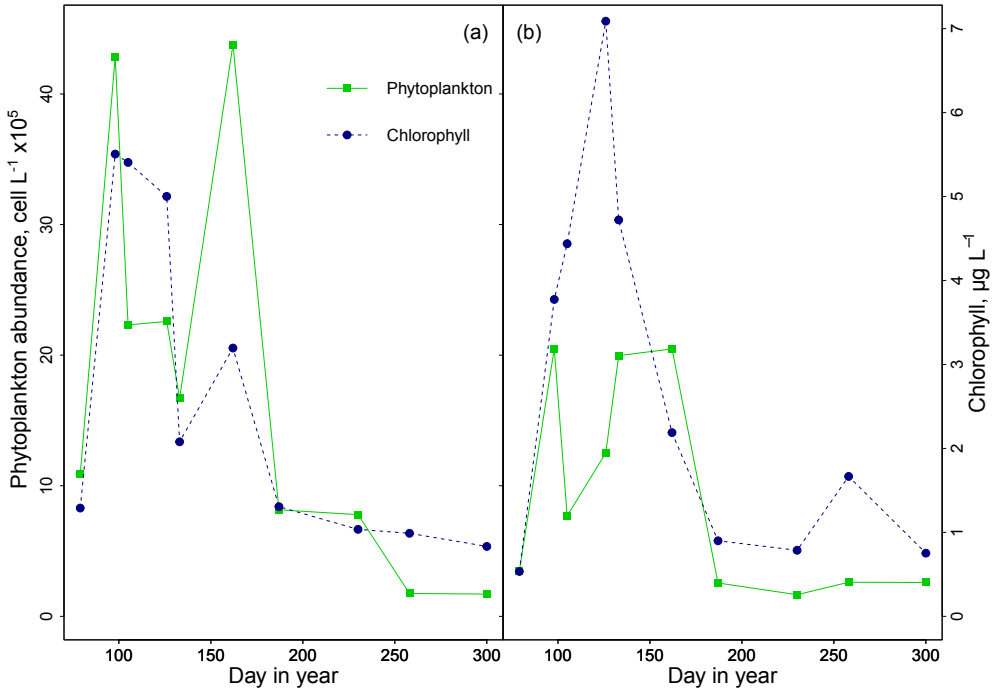

Figure 2.12: Seasonal microphytoplankton abundance (cells L^{-1} x10^5) and chlorophyll concentration (μg L^{-1}) above (a) and below (b) the pycnocline at site LY1 during 2015

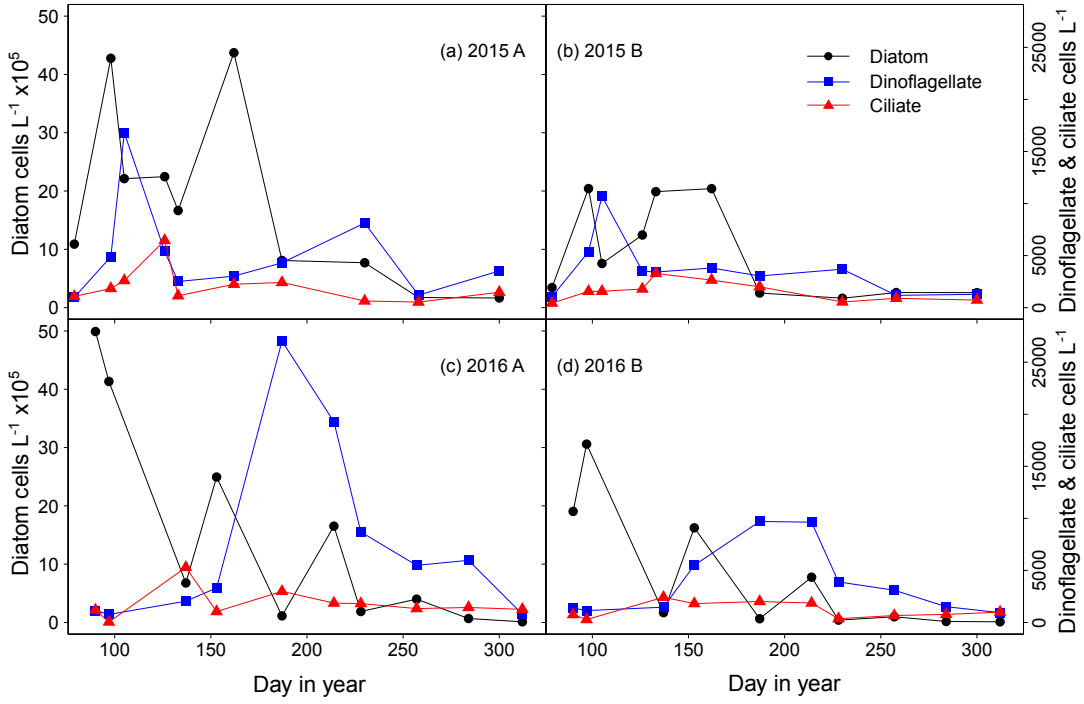

Figure 2.13: Diatom (cells L^{-1} x10^5), dinoflagellate and ciliate (cells L^{-1}) abundance at LY1 above (A) and below (B) the pycnocline during 2015 (a) 2015 A, (b) 2015 B, and 2016 (c) 2016 A, (d) 2016 B

and subsequently decreased as nutrient availability decreased. There was a secondary bloom of diatoms on day 162 in 2015, in which cell abundances were at comparable levels to the primary bloom. The 2016 secondary bloom occurred on day 153 but was of a lower abundance compared to the primary bloom. Abundances of dinoflagellates were highest in spring 2015 (0.17 x 10^5 cells L^{-1}), and then decreased until late summer (Figure 2.13a). In 2016 dinoflagellate abundance was almost double than observed in 2015 and highest in summer (0.27 x 10^5 cells L^{-1}; Figure 2.13c). Ciliate abundance was less variable throughout the years when compared to diatoms and dinoflagellates with peaks in abundance in spring of both years. The seasonal cycle below the pycnocline was similar to above in the respective years, but with lower cell abundances (Figure 2.13b and c).

Diatoms were the dominant group of microphytoplankton above and below the pycnocline during 2015 and 2016. The most abundant diatom genus was *Skeletonema* spp. which accounted for between 0.4 to 96.9 % and 0.6 to 97.5 % of all cells enumerated in 2015 and 2016, and reached a maximum of 41 x 10^5 cells L^{-1} in 2015 (Figure 2.14) and 48 x 10^5 cells L^{-1} in 2016 (Figure 2.15). Other abundant diatom groups were *Chaetoceros* spp. (coastal), *Thalassiosira* spp., and *Pseudo-nitzschia delicatissima*. These four highly abundant diatoms were present throughout the entire year of 2015 (Table A.1) and 2016 (Table A.2). *Skeletonema* spp. was the dominant diatom on the majority of the sample dates in 2015 followed by *Chaetoceros* spp. (coastal), and then *P. delicatissima* (Table A.1). In 2016 *Skeletonema* spp. was again the predominant diatom, followed by *Chaetoceros* spp. and then *P. seriata* (Table A.2). There were many other less abundant diatoms enumerated whose presence, and maximum abundance varied seasonally, and key taxa are mentioned in Table A.1 and A.2.

The predominant dinoflagellate taxa in 2015 was *Katodinium* spp. with a maximum cell abundance of 0.1 x 10^5 cells L^{-1} (Table A.1). *Scripsiella* spp. and *Gymnodinium* spp. were the next predominant taxa. In 2016, *Scripsiella* spp. was the most abundant dinoflagellate (0.2 x 10^5 cells L^{-1}), dominating the majority of the 2016 sampling dates (Table A.2). *Katodinium* spp. was less abundant in 2016 (0.1 x 10^5 cells L^{-1}) than 2015, being the second dominant dinoflagellate taxa observed.

Patterns in abundance of diatoms and dinoflagellates varied seasonally and between 2015 and 2016 (Figure 2.14 and Figure 2.15 respectively). With a focus on diatoms, *Skeletonema* spp. had the highest percent contribution to total cell abundance peaking in spring and winter 2015. Trends were relatively similar above and below the pycnocline, however on day 258 *Skeletonema* spp. abundances declined below the pycnocline. As the percentage contribution of *Skeletonema* spp. decreased during spring/summer, the percent contribution of *Chaetoceros* spp. (coastal) gradually increased to a point in which it became the predominant taxa on day 162. *Thalassiosira* spp. generally had a low percentage contribution to total cell abundance, which peaked in spring and *P. delicatissima* spp. peaked in late summer/winter. Dinoflagellates contributed a much lower percentage to total cell abundance than diatoms. The highest contribution of the predominant *Katodinium* spp. was 0.99 % and occurred in spring and late summer, being higher below the pycnocline than above. *Scripsiella* spp., had a higher contribution from summer onwards.

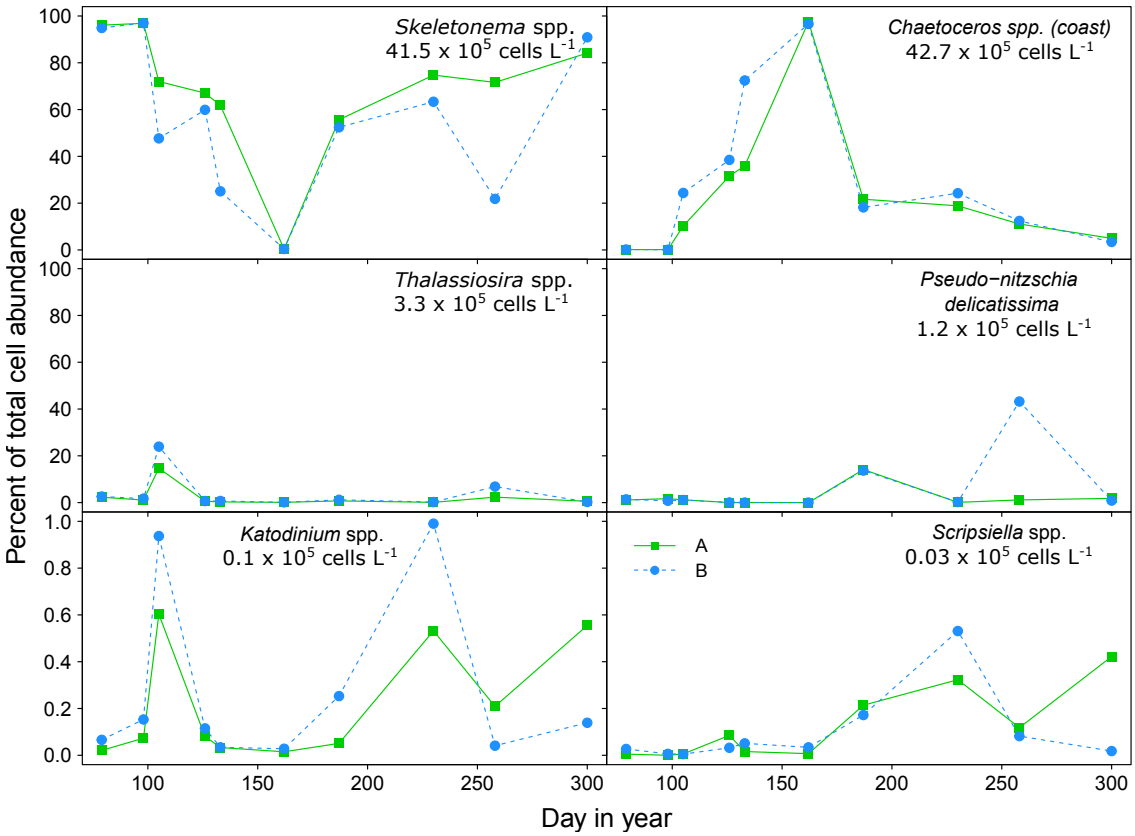

Figure 2.14: Seasonal percentage contribution to total microphytoplankton cell abundance during 2015 for the six most abundant diatoms and dinoflagellates above (A) and below (B) the pycnocline. Maximum recorded abundance is shown for each diatom and dinoflagellate (x 10^5 cells L^{-1})

In 2016, *Skeletonema* spp. dominated the spring bloom and with two other periods of high abundances following later in the sampling period (Figure 2.15). When *Skeletonema* spp. was not dominating the community composition, *Chaetoceros* spp. (coastal) was. However, the maximum abundance of *Chaetoceros* spp. (coastal) was substantially lower in 2016 (23.5 x 10^5 cells L^{-1}) compared to 2015 (42.7 x 10^5 cells L^{-1}). Both *Thalassiosira* spp. and *P. delicatissima* had a low percent contribution to total cell abundance, which was highest in winter, and had lower maximum cell abundances in comparison to 2015. In contrast to 2015, *Scripsiella* spp. had a higher contribution to total cell abundance than *Katodinium* spp.. For both dinoflagellates peak contributions were in spring and summer with the contribution of *Scripsiella* spp. increasing in winter. The percent contribution of *Katodinium* spp. was highest below the pycnocline whilst *Scripsiella* spp. was highest above.

Spring, summer, and winter microphytoplankton community composition was significantly different between sample dates in 2015 (ANOSIM, Global R= 0.407, P= 0.1 %; Figure 2.16i). Pairwise tests show significant differences in community composition between spring and summer (ANOSIM, Global R= 0.405, P= 0.5 %), and spring and winter (ANOSIM, Global R= 0.435, P= 2.2 %). There was no significant difference between summer and winter 2015 (ANOSIM, Global R= 0.5, P= 13.3 %).

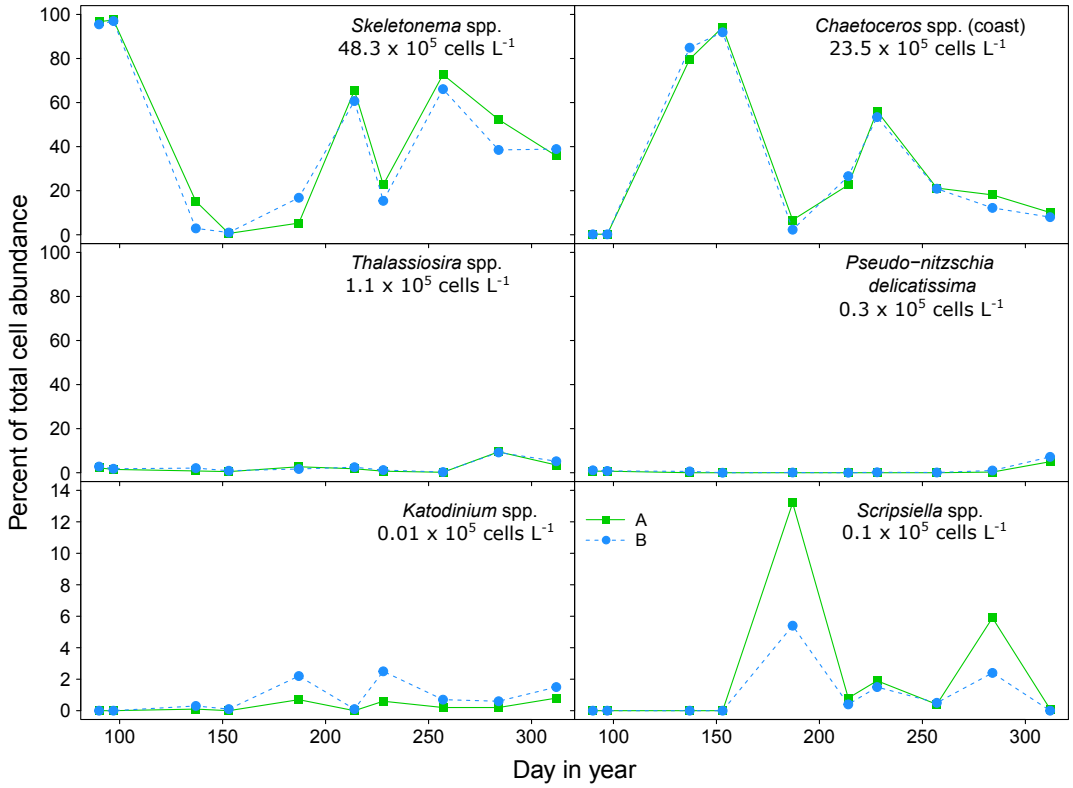

Figure 2.15: Seasonal percentage contribution to total microphytoplankton cell abundance during 2016 for the six most abundant diatoms and dinoflagellates above (A) and below (B) the pycnocline. Maximum recorded abundance is shown for each diatom and dinoflagellate (x 10^5 cells L^{-1})

Table 2.3: Summary of the most important taxa contributing to the similarity of community composition in spring, summer, and winter 2015 and 2016 (SIMPER)

	Spring	Summer	Winter
2015	*Skeletonema*	*Skeletonema*	*Skeletonema*
	Chaetoceros spp.	*Chaetoceros* spp.	*Chaetoceros* spp.
	Thalassiosira spp.	*L. danicus*	*P. delictissima*
	P. delictissima	*P. delictissima*	*Cylindrothecae*
2016	*Skeletonema*	*Skeletonema*	*Skeletonema*
	Chaetoceros spp.	*Chaetoceros* spp.	*Cylindrothecae*
	Thalassiosira spp.	*Cylindrothecae*	*Chaetoceros* spp.
	Cylindrothecae	*L. minimus*	*Skeletonema*

SIMPER analysis highlighted *Skeletonema* spp. and *Chaetoceros* (coastal) spp. were the most important taxa contributing to the similarity of community compositions across the sample seasons in 2015 (Table 2.3). Spring and winter community composition was the most dissimilar (34.92

%), closely followed by spring and summer (34.14 %), and lastly summer and winter (31.48 %) were the least dissimilar (SIMPER).

Microphytoplankton community composition was not significantly different between spring, summer, and winter seasons in 2016 (ANOSIM, Global R= 0.165, P= 7.3 %; Figure 2.16ii). There were significant differences in community composition between paired seasons spring and winter (ANOSIM, Global R= 0.405, P= 2.2 %), and summer and winter (ANOSIM, Global R= 0.677, P= 3.6 %). There was no significant difference in community composition between spring and summer 2016 (ANOSIM, Global R= 0.075, P= 17.2 %). Due to the low number of sample dates in winter, there is low confidence in the statistical tests.

SIMPER analysis highlighted *Skeletonema* spp., *Chaetoceros* (coastal) spp. and *Cylindrothecae* spp. were the most important taxa contributing to the similarity of community compositions across the sample seasons in 2016 (Table 2.3) Spring and winter had the most dissimilar community composition (38.74 %), closely followed by spring and summer (30.83 %), and lastly summer and winter (28.10 %) were the least dissimilar (SIMPER).

2.3.2 Site RE5

2.3.2.1 Environmental characterisation

Density and salinity were initially higher at the immediate surface, after which they then decreased to approximately 5 m, and subsequently increased with depth (Figure 2.17). The halocline and pycnocline were situated at 23 m and 26 m respectively. Temperature initially decreased from the surface until approximately 18 m, where it then generally increased with increasing depth. Deeper waters were warmer than those at the surface. Dissolved oxygen concentrations were highest in the upper 20 m, and decreased slowly with depth. Oxygen concentration was considerably lower at depths greater than 120 m, in the isolated bottom waters of RE5, falling to less than 3.0 mg L^{-1}. The fluorescence profile followed a similar trend to oxygen concentration and generally decreased with depth. PAR was highest in the upper 20 m after which there was a large increase in attenuation with depth.

A deep water renewal event during June 2016 was observed at RE5 (data supplied by Tim Brand; Figure 2.18). Prior to this study, on 03/06/2016 deep water (>60 m) dissolved oxygen concentrations were low (approximately 0.8 to 1.2 mg L^{-1}) relative to shallower depths. An increase in surface salinity and density observed on 13/06/2016 and 16/06/2016 was sufficiently dense to flush out and replace older deep water with surface water. By 16/06/2016 there had been a partial renewal of deep water as shown by increasing dissolved oxygen concentrations relative to 03/06/2016. By 24/06/2016 there had been a full renewal of older deep water with surface water, and dissolved oxygen concentrations near the sea floor were relatively similar to surface concentrations (approximately 4.0 mg L^{-1}).

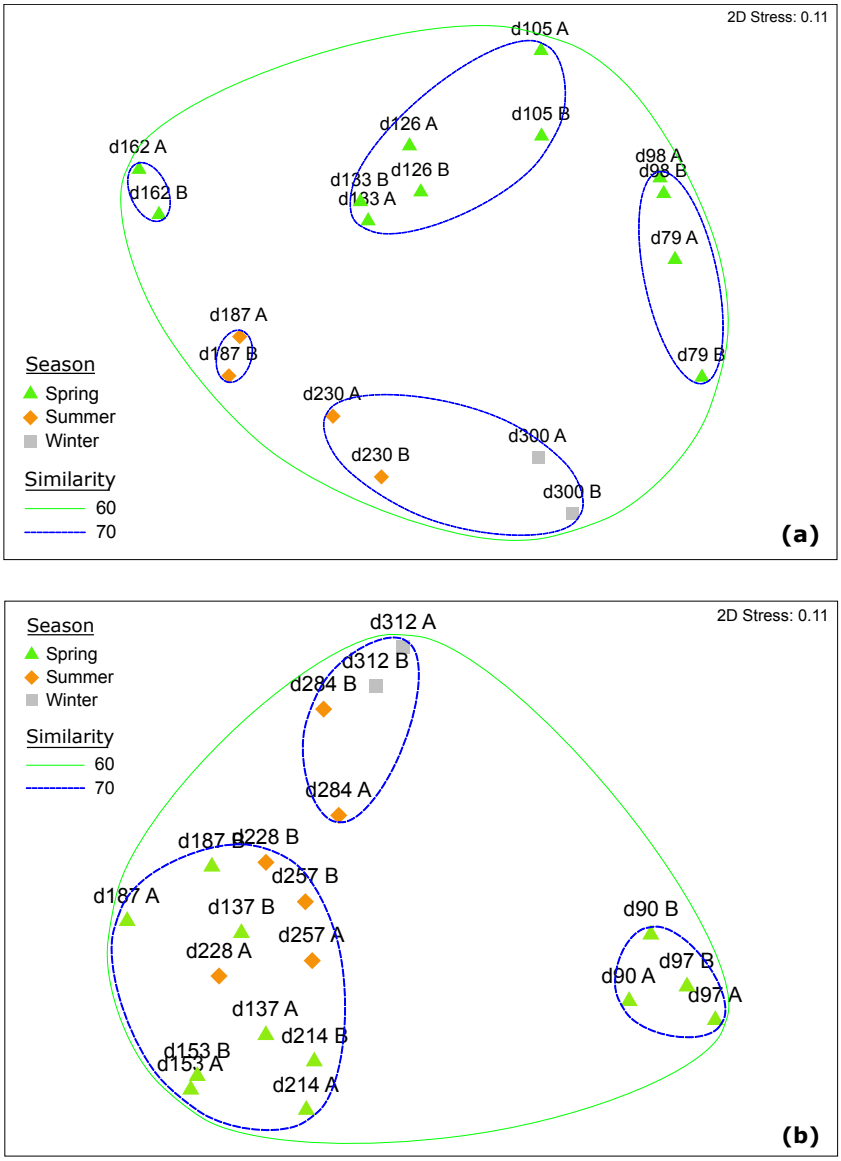

Figure 2.16: Non-metric multidimensional scaling (nMDS) plot of fourth root transformed 2015 (a) and 2016 (b) microphytoplankton taxa. Ordination based on season (spring, summer and winter). Labels are sample day of year and depth above (A) and below (B) pycnocline. 2D stress is 0.1 which indicates a fair representation of the data

2.3.2.2 Inorganic nutrient concentrations

Phosphate concentrations increased with depth and accumulated in deep water (Figure 2.19). Silicate and nitrate concentrations were relatively similar between the chlorophyll maximum and 25 m and after which accumulated with depth.

2.3.2.3 Microphytoplankton community composition

Total cell abundance at the chlorophyll maximum was 2.1 x 10^5 cells L^{-1}, and 0.1 x 10^5 cells L^{-1} at 25 m. Diatoms dominated the community composition at 5 m and 25 m, contributing to 96.2 % and 84.6 % of the community composition respectively (Figure 2.20). Dinoflagellates and ciliates

had a higher contribution to community composition at 25 m (9.8 % and 5.6 % respectively), in comparison to 5 m (1.7 % and 2.1 % respectively). Diatoms with the highest contribution to community composition at 5 m included: *Skeletonema* spp. 90.49 %, and *Chaetoceros* spp. (coastal) 5.11 % (Table 2.4). The two most dominant dinoflagellates at 5 m were *Scrippsiella* spp. (0.71 %) and *Heterocapsa* spp. (0.49 %).

At 25 m depth *Skeletonema* spp. (81.17 %), *L. minimus* (1.28 %), *Cylindrothecae* spp. (0.62 %) were the three diatoms which contributed the most to total cell abundance. *Katodinuim* spp. was the dominant dinoflagellate at 25 m contributing 4.18 % followed by *Gymnodinium* spp. (2.80 %), *Heterocapsa* spp. (1.47 %), and *Protoperidinium* spp. (1.40 %).

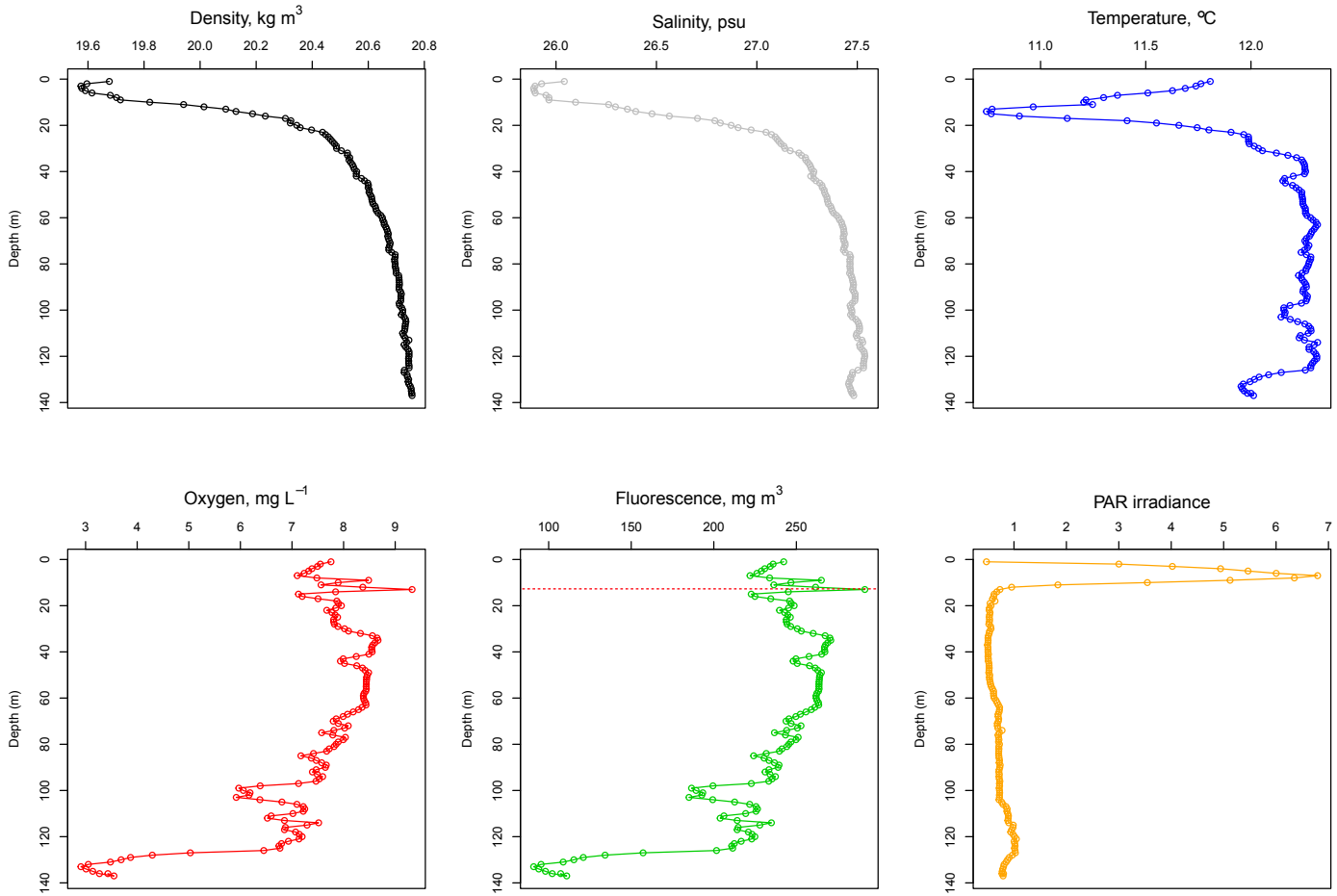

Figure 2.17: Water column profiles of density (kg m^3), salinity (psu), temperature (°C), dissolved oxygen (mg L^{-1}), fluorescence (mg m^3), and PAR irradiance at RE5 on 13th June 2016. Red dashed line on the fluorescence profile indicates the chlorophyll maximum (13 m)

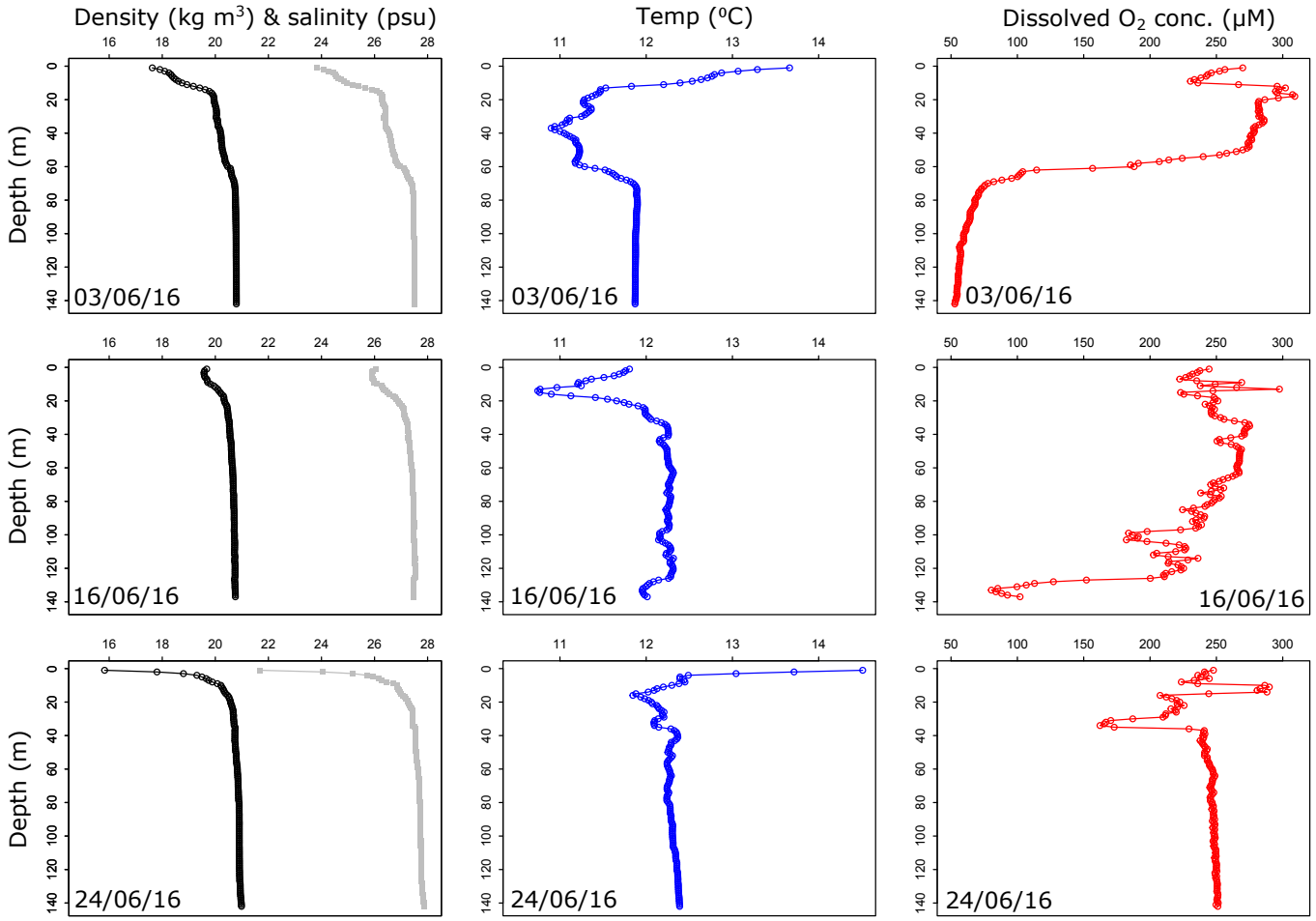

Figure 2.18: Water column profiles of density (kg m^3; black line), salinity (psu) (grey line), temperature (°C),and dissolved oxygen (μM) at RE5 on three sample dates in June during the occurrence of a deep water renewal event (data supplied by Tim Brand)

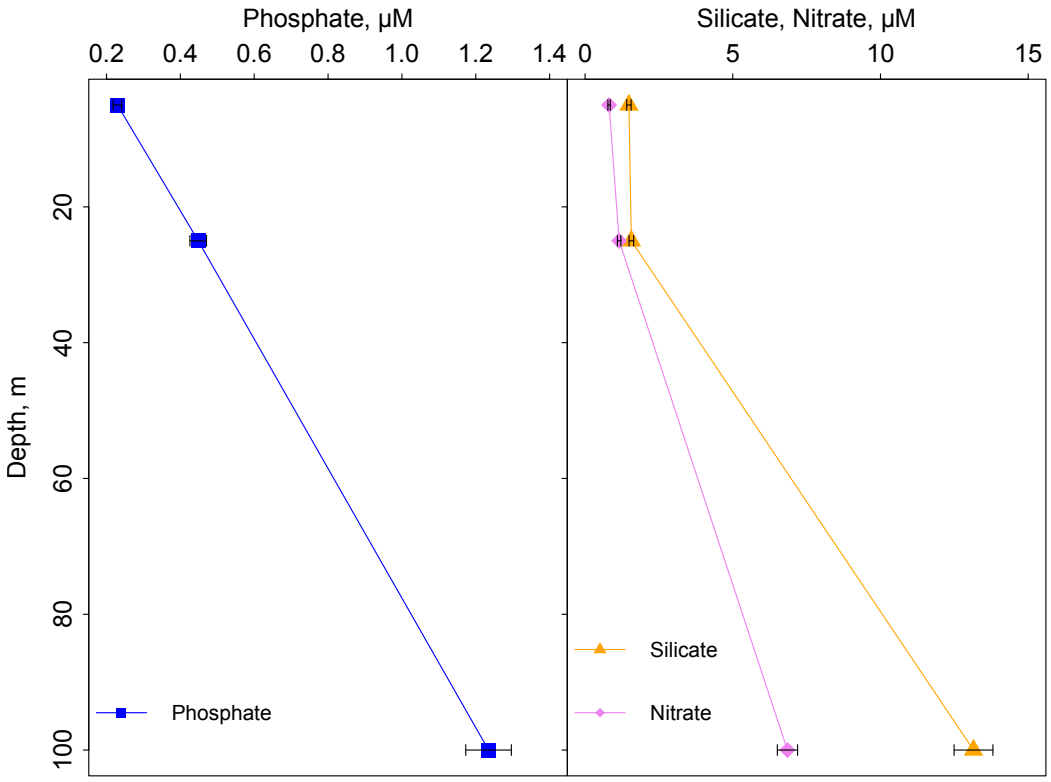

Figure 2.19: Water column profiles of dissolved inorganic phosphate, silicate, and nitrate concentrations (μM) at RE5 on 16th June 2016. Error bars show the method error represented as standard deviation (n=3).

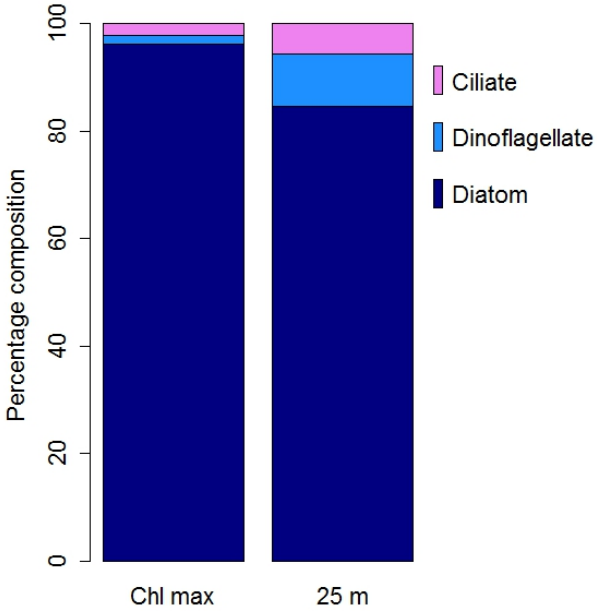

Figure 2.20: Percentage composition of diatoms, dinoflagellates, and ciliates to microphytoplankton community composition at RE5 at the chlorophyll maximum and 25 m depth on 13th June 2016 at RE5

Table 2.4: Key microphytoplankton taxa sampled on 13/06/16 at RE5 at the chlorophyll max (5 m) and 25 m. Percentage contribution of key taxa to total cell abundance as well as maximum cells L^{-1}

	% contribution of total cells		Max.cells L^{-1}	
	5 m	25 m	5 m	25 m
Diatoms				
Skeletonema spp.	90.49	81.17	190,124	11,406
Chaetoceros spp. (Coast)	5.11	0.00	10,727	0
Thalassiosira spp.	0.19	0.47	400	67
L. minimus	0.04	1.28	80	180
L. danicus	0.00	0.01	0	13
Certulina spp.	0.00	0.10	0	13
Paralia spp.	0.00	0.33	0	47
P. delictissima	0.00	0.10	7	13
P. seriata	0.04	0.05	87	7
Cylindrothecae spp.	0.04	0.62	80	87
Dinoflagellates				
Katodinium spp.	0.07	4.18	146	587
Scripsiella spp.	0.71	0.10	1,493	13
Gyrodinium spp.	0.00	0.05	0	6
Heterocapsa spp.	0.49	1.47	1,027	207
Gymnodinium spp.	0.31	2.80	640	393
Prorocentrum spp.	0.01	0.05	20	6
Protoperidinium spp.	0.12	1.40	253	160

2.3.3 Seasonal variability in hydrographic conditions and inorganic nutrient concentrations at site LY1

Seasonal differences in hydrography between 2015 and 2016 were observed at site LY1. The density structure of the water column differed between the years due to variation in the timing of fresh water input (Figure 2.9). High rainfall in spring and winter 2015 resulted in a less dense superficial layer, and a higher degree of stratification during these periods. Conversely, the main period of rainfall and stratification in 2016 was summer and winter. During spring 2016 surface salinity was at a maximum which extended down the water column. Additionally, there was a more pronounced thermocline during summer/winter 2016 than 2015 (Figure 2.5 and Figure 2.4 respectively). These differences in water column structure which occurred seasonally and between the two sample years have the potential to affect chemical and biological parameters.

Inter annual variations in inorganic nutrient concentrations were observed with maximum concentrations in spring 2015 (phosphate 1.73 μM, silicate 7.79 μM, nitrate 9.24 μM; Figure 2.10) and winter 2016 (phosphate 0.61 μM, silicate 5.74 μM, nitrate 6.21 μM; Figure 2.11). Concentrations

of all nutrients were higher in 2015 than 2016. However, both years displayed typical nutrient dynamics with higher concentrations in spring before the start of the microphytoplankton bloom. With the initiation of the bloom and higher microphytoplankton cell densities, concentrations of phosphate, nitrate, and silicate decreased as nutrient uptake increased (Brito et al., 2015). Inorganic nutrient concentrations were low above the pycnocline on day 150 when there was a high microphytoplankton abundance, and when the water column was more stratified than previous dates (Figure 2.6). On day 150 below the pycnocline, concentrations increased when compared to previous and subsequent days, which corresponded to a higher degree of stratification (Figure 2.6). The stratified nature of the water column and low total number of microphytoplankton cells, when compared to water sampled above the pycnocline, resulted in higher concentrations of nutrients as was a lower abundance of microphytoplankton to utilise them. Inorganic nutrient concentrations gradually increased towards the end of 2015 and 2016 in line with lower microphytoplankton abundances and a higher degree of mixing to replenish nutrient concentrations from depth. Fehling et al. (2006) found maximum late winter concentrations of 0.5 to 0.7 μM phosphate and 6 to 8 μM nitrate (2000 to 2003) which were in more of a similar range to 2016 than 2015 concentrations. Fehling et al. (2006) concluded that with nutrients within this range, the origin of the water body was from the main basin of the Firth of Lorne transported from the Scottish Coastal Current.

Differences in the environmental parameters for each sampling date in 2015 and 2016 were of interest as linking environmental drivers to microphytoplankton sedimentation was investigated in Chapter 3. PCA analysis for both years showed clear separation between sample dates in different seasons. Key environmental drivers for explaining the differences between sample dates included factors controlling the physical structure of the water column (salinity, density, and stratification index) and inorganic nutrient concentration (phosphate, silicate, and nitrate). The water column was more stratified in 2015 than 2016 and with spring 2015 being the period of highest stratification. Salinity and density were key drivers in explaining the dissimilarity between sample dates in 2016, with more saline and dense waters found in summer. The stratification index was not a key driver in explaining the differences between sample dates and this could be due to the lower number of dates the index reached over the 0.10 threshold (in contrast to 2015).

The short period of time in which weather conditions (e.g. wind speed and direction, precipitation) and tide can change, results in water column modification and nutrient redistribution (Brito et al., 2015). This is especially true at a shallow water site, such as LY1, with strong tidal flows (Dale et al., 2011). In turn, this can affect the abundance and diversity of the phytoplankton community.

2.3.4 Seasonal variability in microphytoplankton composition

At LY1 there were similar trends of seasonal microphytoplankton bloom dynamics in 2015 and 2016, but differences in community structure. Diatoms dominated at LY1 and were more abundant when nutrient concentrations were highest in spring. *Skeletonema* and *Chaetoceros* spp. were the dominant diatom species at LY1 in both years. Diatoms are known to be a highly diverse and ecologically important group, which at latitudes are found in high abundances in nutrient rich coastal systems (Malviya et al., 2016). Other studies have found these taxa to be abundant at LY1

and decrease in abundance further offshore (Brito et al., 2015). This study found cell abundances varied seasonally and between years, with *Skeletonema* and *Chaetoceros* spp. alternating in their dominance. Modifications to the physical environment including degree of stratification, light intensity, and amount of mixing can affect microphytoplankton community structure (Margalef, 1978). Typically diatoms will dominate the phytoplankton community composition during periods of increased turbulence and nutrient availability (r-strategy), in contrast to dinoflagellates which favour stratified and oligotrophic environments (k-strategy; Margalef, 1978). When the water column was more stratified (e.g. day 150 in 2015), concentrations of nutrients above the pycnocline were lower and cell abundance higher, in contrast to below the pycnocline where nutrient concentrations were higher and cell abundance lower. The dominant species at LY1, *Skeletonema* spp., is said to thrive when nutrient availability is high and the water column is slightly mixed (Reynolds, 2006). Dynamic changes to the environment affects abundance and dominance of microphytoplankton taxa.

A dinoflagellate bloom occurred in spring 2015 dominated by *Katodinium* spp. and was followed by a smaller secondary bloom later in the year. There was a large dinoflagellate bloom in summer 2016 above the pycnocline, which reached higher cell abundances than the bloom in 2015 and was dominated by *Scripsiella* spp.. This 2016 bloom coincided with the period of highest stratification and low concentrations of phosphate, silicate, and nitrate. Dinoflagellates are known to dominate during quiescent conditions (Falkowski et al., 2004), and successively bloom following a decrease in diatom cell abundances.

At RE5, the structure of the microphytoplankton community changed with increasing depth. Diatoms dominated the community composition at 5 and 25 m (96.2 and 84.7 % respectively). Dinoflagellates and ciliates had a higher contribution to total cell abundance at 25 m. *Skeletonema* spp. dominated composition at both sample depths, which is a typical feature of Loch Etive microphytoplankton community structure (Wood et al., 1973). Other dominant taxa have been found to include *Chaetoceros* spp. which accounted for 5.11 % of total cells at 5 m, yet was not present at 25 m. Wood et al. (1973) found *Skeletonema* spp. inter-annual June abundances to range from 0.5 x 10^5 to 38 x 10^5 cells L^{-1} (1970 to 1971). This study found *Skeletonema* spp. abundance in June 2016 at RE5 was 1.9 x 10^5 cells L^{-1}, which falls into this historic range. In contrast, *Skeletonema* spp. abundances measured at site LY1 in June 2016 were substantially lower (0.2 x 10^5 cells L^{-1}) as *Chaetoceros* spp. (coastal) was the dominant taxa on that sample date. *Scripsiella*, *Heterocapsa*, and *Prorocentrum* spp. have been observed as key dinoflagellate taxa found in Loch Etive (Wood et al., 1973). This is in agreement with this study, as *Scripsiella* and *Heterocapsa* spp. were the most abundant in addition to *Katodinium* and *Gymnodinium* spp. (Table 2.4). However, the contribution of dinoflagellates to total microphytoplankton composition were higher in the 1970 to 1971 study (0.4 to 16.1 %; Wood et al., 1973), relative to contributions between 0.01 to 4.18 % found in this study which depended on species and depth.

2.3.5 Contrasting study sites LY1 and RE5

Site RE5 located in Loch Etive had contrasting environmental characteristics when compared to the coastal site LY1. Firstly, RE5 is an example of a restricted exchange environment, which is land locked and has limited exchange to the Firth of Lorne via a narrow and shallow sill. The restricted nature of the study site is shown by the residence time of deep water at RE5 of approximately 16 months (Edwards and Edelsten, 1977). Deep water renewal, driven by surface water density, occurred over the course of this study period in June 2016. This renewal event substantially modified dissolved oxygen concentrations of deep water from approximately 20 μM pre-flush to 250 μM post-flush. LY1 is a very dynamic environment, which is generally well mixed, turbulent coastal site with inputs from a number of lochs and the sea. Water column temperature at RE5 ranged between 10.74 to 12.32°C, which is at the upper end of the temperature range found at LY1 in June 2015 and 2016 (9.21 to 11.31°C). Salinity (25.89 to 27.54 psu) and density (19.57 to 20.76 kg m^3) increased with depth at RE5 and the range was notably lower than at LY1 in June (salinity 28.87 to 33.57 psu, density 21.95-25.96 kg m^3). Despite lower densities at RE5, both LY1 and RE5 had similar stratification indices on 02/06/2016 ($\hat{S}$= 0.003) and 13/06/2016 ($\hat{S}$= 0.001). Availability of inorganic nutrients varied between the two sample sites. Concentrations of nitrate were similar at comparable water column depths, and silicate concentrations were lower at LY1 than RE5. Higher silicate uptake as a result of a higher abundance of diatoms at LY1, in comparison to RE5, could explain this. In surface waters (approximately 5 m) phosphate concentrations were similar in comparison to deeper samples (20 m) concentrations were higher in Loch Etive.

Microphytoplankton cell abundance in Loch Etive (2.1 x 10^5 cells L^{-1} 13th June 2016) was lower than than abundances observed at LY1 on a similar sample date (25 x 10^5 cells L^{-1} 1st June 2016). *Skeletonema* spp. dominated the microphytoplankton community at both study sites but at vastly different abundances (Table A.2 & 2.4). This could be a result of the different nutrient and environmental dynamics observed between the sites.

2.4 Conclusions

Understanding how environmental dynamics at site LY1 varied over the course of the two year sampling period, is a fundamental building block to aid understanding of more complex interactions (e.g. microphytoplankton sedimentation rate in relation to environmental variation). Key conclusions from the environment characterisations of study sites LY1 and RE5 over 2015 and 2016 include:

1. PCA analysis showed that there was seasonal variation between the sampling dates, which were driven by differences in the measured parameters including; stratification index, temperature, inorganic nutrient concentration. There was a large degree of variation between spring sample dates in 2015, which was driven by nutrient concentrations (nitrate, phosphate, and silicate). Differences between spring and summer/ winter in 2015 were a result of water column temperature and stratification index. The large variability between spring and summer sample dates in 2016 was caused by higher seawater densities and stratification

in summer as opposed to spring.

2. Seasonal differences in water column stratification were observed between 2015 and 2016 at LY1. Higher stratification was observed in spring 2015 than spring 2016, and summer 2016 versus summer 2015. This was driven by higher rainfall during spring 2015 relative to spring 2016, and higher rainfall in summer 2016 in comparison to spring 2015.

3. Microphytoplankton community composition was similar over the course of 2015 and 2016. The diatom *Skeletonema* spp. dominated the community composition for the majority of both years and when it's abundance declined, *Chaetoceros* spp. dominated. Dinoflagellates were generally more abundant in 2016 in comparison to 2015.

4. LY1 is a more dynamic, open, well mixed system compared to RE5. In contrast, site RE5 is a land-locked, restricted exchange environment. Both sites were sampled during the same time of year (June 2016), and environmental characteristics of the two sites differed with lower salinities and densities observed at RE5, in comparison to the coastal site LY1. Nutrient, temperature, salinity and density dynamics varied between the sites which likely influenced microphytoplankton abundances and composition.

Chapter 3

Seasonal microphytoplankton community sedimentation linked to environmental and biochemical drivers

3.1 Introduction

The sinking of intact microphytoplankton cells, and aggregated cells, are a major contributor to carbon export from the euphotic zone (e.g. Buesseler, 1998; Durkin et al., 2016). In particular, high cell densities and senescent populations of microphytoplankton have been shown to be key contributors to the export of organic material (Buesseler et al., 2007). However, not all microphytoplankton blooms contribute significantly to particulate organic material (POM) sedimentation (Passow, 1991). For example, fluxes of microphytoplankton are dependent upon functional groups; diatom blooms have been shown to have a higher contribution to carbon export relative to dinoflagellate blooms (Durkin et al., 2016; Guo et al., 2016). Additionally, microphytoplankton community composition is a key factor in determining sedimentation rates, and for formation of aggregates, which have the potential to accelerate particulate material export from the surface (Smayda and Bienfang, 1983; Herndl and Reinthaler, 2013; Guo et al., 2016). Furthermore, morphological and physiological variations between species and assemblage structure in response to environmental conditions, adds a further complexity to understanding microphytoplankton sedimentation and contribution to carbon export. Despite the importance of the role of microphytoplankton in the export of organic material, detailed analysis of community structure is often missing from studies. Given the range of factors affecting microphytoplankton sedimentation, and the large amount of variability in community composition within and between seasonal cycles, the study of microphytoplankton community structure is critical for the fundamental understanding of the mechanisms of carbon sedimentation and the biological carbon pump. Ultimately, understanding these processes is essential for determining the magnitude and efficiency of global biogeochemical cycles.

There have previously been many studies investigating the sedimentation rates of microphytoplankton using a range of methods, including high resolution optical techniques for individual based diatom sinking rate observations (Gemmell et al., 2016), mesocosm experiments (Riebesell, 1989), and settlement columns (SETCOL) designed by Bienfang (1981a) (e.g. Johnson and Smith,

1986; Pitcher et al., 1989; Waite et al., 1992a; Fisher and Harrison, 1996; Peperzak et al., 2003; Guo et al., 2016; Cavan et al., 2017). Additionally, Stokes Law (Stokes, 1851) is often used to calculate microphytoplankton sedimentation rates (e.g. Smayda, 1970; Vogel, 1983; Richardson and Cullen, 1995). However Stokes Law use has been debated as one questions the assumptions that microphytoplankton are typically spherical which, in the presence of chitin fibres and hairs, they are not (Peperzak et al., 2003; Reynolds, 2006). Secondly, continuous modification of cell density which microphytoplankton can achieve through various mechanisms (e.g. cell biochemical composition, internal ionic composition, number or size of intracellular vacuoles), and during different growth phases, is not accounted for with Stokes Law (Peperzak et al., 2003). Comparisons between laboratory studies is difficult due to different experimental set ups which differ in pre-conditioning treatments, microphytoplankton species or assemblages used, cultured versus natural microphytoplankton samples used, and growth phase of laboratory samples used. As a result, there are a wide range of microphytoplankton sedimentation rates recorded with an overall average of approximately 1 m d^{-1} or less for intact cells (Smayda, 1970; Bienfang, 1980; Riebesell, 1989), and up to 100 m d^{-1} for diatom flocs (Smetacek, 1985). There is increasing evidence that small particles in the size range of microphytoplankton, are a substantial component of sinking carbon in the water column, in addition to larger aggregates of POM and inorganic material (e.g Dall'Olmo and Mork, 2014; Durkin et al., 2015; Puigcorbé et al., 2015; Durkin et al., 2016). Typically, this proportion of small particulates is often under-sampled with sediment trap deployments due to its slow sinking nature (Stemmann et al., 2008). Using the SETCOL method enables water column samples, which will contain both buoyant, slow and fast-sinking POM, to be split based on their size, density, and sedimentation rates. This will allow classification of which types of microphytoplankton are substantial contributors to the export flux.

The SETCOL method is relatively simple, and involves taking an initially homogeneously mixed sample, leaving it for a settlement period, and after which samples have split into positively, neutrally, and negatively buoyant fractions (Figure 3.1; Bienfang, 1981a). SETCOL results have been described as realistic when they are carried out at near *in situ* irradiance and temperature (Peperzak et al., 2003). There have been many studies investigating the sinking rate of cultured (e.g Bienfang et al., 1982; Waite et al., 1992a; Richardson and Cullen, 1995; Fisher and Harrison, 1996) and natural microphytoplankton populations using SETCOL (e.g Bienfang, 1981a; Johnson and Smith, 1986; Bienfang and Harrison, 1984; Pitcher et al., 1989; Waite et al., 1992a; Peperzak et al., 2003; Guo et al., 2016). Few studies have investigated biochemical composition (e.g. carbohydrates (Richardson and Cullen, 1995)) as an important driver in cell density modification and explaining natural microphytoplankton community sinking rates. Analysis of the three main macromolecules contributing to microphytoplankton organic carbon content (protein, carbohydrate, and lipid; Boëchat and Giani, 2000), and their affect on sedimentations rates, has not been addressed over a seasonal cycle. Investigating this will provide valuable information on how biochemical composition, which varies seasonally with growth phase, affects the sedimentation of cells. The coupling of biochemical composition and environmental factors, in addition to analysis of microphytoplankton community structure, has the potential to enhance understanding of the key drivers of sedimentation.

3.1.1 Research objectives

Microphytoplankton represent a substantial proportion of carbon export from the euphotic zone. Microphytoplankton communities were sampled from above and below the pycnocline to investigate how changes in seawater density and other environmental and biochemical parameters affect sedimentation rates of cells. Microphytoplankton communities were placed in SETCOLs, and community and species-specific sedimentation rates were calculated. The aim was to identify key microphytoplankton types that contribute to export of organic material. Additionally, carbon analysis of each SETCOL fraction enabled the sedimentation rate of particulate carbon to be calculated. The relationship between calculated sedimentation rates, water column biochemistry, and physical parameters were investigated. Research questions specific to this Chapter include:

1. How does the sedimentation rate of microphytoplankton change seasonally above versus below the pycnocline?

2. How does changes to the microphytoplankton community composition affect sedimentation rates?

3. What are the key environmental drivers for explaining microphytoplankton sedimentation rate?

4. What are the key biochemical drivers for explaining microphytoplankton sedimentation rate?

3.2 Methods

3.2.1 Sample site and field work

Investigations were carried out at site LY1 (Chapter 2, Figure 2.2) with frequent sampling trips in 2015 and 2016 (Chapter 2, Table 2.1 & 2.2).

Water samples were collected from depths above and below the pycnocline, which were selected based on CTD data. Niskin bottles (5 L) were used to collect samples at the desired depth by lowering them on the winch at the stern of the boat. Niskins were fired by a messenger at the required depth. The Niskins containing the sample seawater were used to rinse pre-labelled Nalgene containers first before filling. Nalgene containers were stored in a cool box to control temperature changes to water collected for laboratory analysis of microphytoplankton community composition and SETCOL experiments. These samples were used for microphytoplankton community composition and sedimentation rate measurements from SETCOL experiments, water biochemistry in terms of total lipids, carbohydrates, and protein, inorganic nutrient concentrations (Chapter 2, Section 2.2.4), and chlorophyll-a analysis (Chapter 2, Section 2.2.5).

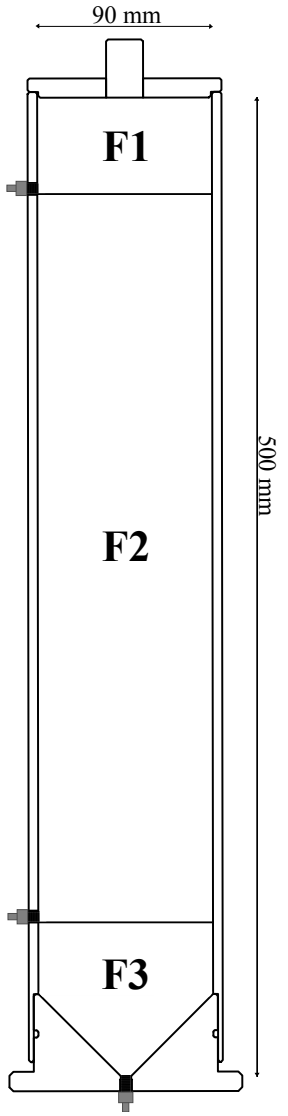

Figure 3.1: SETCOL designed by Bienfang (1981a) showing three fractions and ports; F_1 positively buoyant, F_2 neutrally buoyant, F_3 negatively buoyant. Diagram modified from original, which was drawn by Alistair James (Scottish Association of Marine Science)

3.2.2 SETCOL experiments

In the laboratory, water samples stored in the Nalgene containers were carefully inverted to homogenise, and placed into two SETCOLs (3.06 L) for each of the two depths above and below the pycnocline (Figure 3.1 and Figure B.1). Samples were left for approximately 6 h in a constant temperature (CT) room at 10°C (which was the yearly average water column temperature). Six hours was chosen as the settlement period recommended by other studies (e.g. Bienfang et al., 1983; Johnson and Smith, 1986; Pitcher et al., 1989; Szyper and Karl, 1991; Waite et al., 1992a). After the settlement period, each of the three fractions (Figure 3.1) were carefully drained (total volumes; F1 318 ml, F2 2390 ml, F3 350 ml) to minimise movement of particles between each fraction in the column.

From each fraction, 55 ml was taken and stored in amber Nalgene bottles containing 0.55 ml of 10 % acidified Lugols iodine solution to preserve at 10°C and stain the microphytoplankton for later analysis. Microphytoplankton cells were counted for each fraction as detailed in Chapter 2, Section 2.2.6.

3.2.2.1 Sedimentation rate calculations

Sedimentation rates were calculated using microphytoplankton cell abundance accumulated in F3, relative to the initial homogeneous abundance of cells in the entire SETCOL using Bienfang (1981a) equation. Sedimentation rate (ψ) equalled the fraction of initial biomass that sank to F3 (fs) multiplied by the length of the column (l), and divided by settling interval (t).

$$\psi = \frac{f_s l}{t} \tag{3.1}$$

Sedimentation rates were calculated for the entire microphytoplankton community, and individual taxa that were most abundant (e.g. *Skeletonema* spp., *Chaetoceros* spp. (coastal)), and also were present for the majority of the sampling year (e.g *Cylindrothecae* spp., *Gyrodinium* spp.). Rates were calculated for individual microphytoplankton cells, and also chain lengths of chain forming diatom species. Cells which had a sedimentation rate of 0 m d^{-1} were classified as neutrally buoyant.

3.2.3 Biochemical composition of particulate organic material

Following settlement experiments in SETCOL the concentration of total particulate carbon, total protein, carbohydrate, and lipid in each of the three fractions was analysed to determine the relationship between biochemistry and sedimentation rates. Sub-samples were taken from each fraction (F1 45 ml, F2 300 ml and F3 55 ml) and single samples were filtered for total protein, carbohydrate and lipid analysis on pre-ashed (450°C, 6 h) 25 mm glass fibre filters (Whatman GF/F). Only one sample for total particulate carbon analysis was taken due to the limit on sample volume per fraction. Samples were stored at -80°C until analysis.

3.2.3.1 Particulate carbon analysis

Single samples from each SETCOL fraction were filtered through pre-ashed (450°C, 6 h) 25 mm glass fibre filters (Whatman GF/F) for particulate total carbon (TC) analysis. Filters were then dried overnight at 60°C and then folded into tin disks. Samples were analysed with an ANCA NT prep system coupled with a 20-20 Stable Isotope Analyser (PDZ Europa Scientific Instruments, Northwich, UK). Calibration was performed using a solution of isoleucine (L-Isoleucinie, Europa STD) at concentrations of 1 μg N and 5.14 μg C. Standards were placed in tin caps (with Chromosorb W, PDZ Europa Ltd.) and oven dried at 60°C overnight. Calibrations were performed with a series of isoleucine standard concentrations ranging from 5 to 100 μg N (25.7- 514 μg C) run at the beginning of each batch. Two reference samples (40 μg isoleucine) were analysed after every 8 samples to check the instrument precision (mean C instrument precision 99 % $\pm$ 0.06 SD

and mean N instrument precision 99 % ± 0.02 SD) and a drift correction applied. All samples were blank corrected. The limit of detection ranged from 0.02 to 0.1 μg N and 0.1 to 2.1 μg C.

3.2.3.2 Total lipid

Total lipid from each SETCOL fraction was analysed using spectrophotometric methods following an extraction stage (Folch et al., 1957). Pre-filtered samples on GF/F filters were placed in 15 ml glass centrifuge tubes with a conical bottom and PTFE lined screw caps. Then, 4 ml chloroform: methanol (2:1 *v/v*) was added to the test tubes and vortexed. Filters were left overnight to allow lipid extraction. After which the test tubes were vortexed and then filters were removed from the test tube using clean tweezers. Then, 1 ml of 0.88% (*w/v*) potassium chloride was added to the test tubes (to encourage phase separation) which were then vortexed. Tubes were then centrifuged at 1500 rpm for 10 minutes. The top part of the soluble mixture was removed and discarded. The remaining mixture of chloroform and lipids was dried under nitrogen for approximately 20 minutes. Dry tubes were then placed into a desiccator fitted with a vacuum pump, which was left to run for approximately 20 minutes. Samples were left in the desiccator in the dark for 24 hours.

Lipids were measured following carbonisation by the method of Marsh and Weinstein (1966), which was selected due to its ability to detect a large range of lipid classes. Dried samples were removed from the desiccator, and 2 ml concentrated H_2SO_4 (reagent grade 95.5%) was added to the test tubes which were carefully agitated. Test tubes were then heated to 200°C ± 2°C for 15 minutes in a heat block. After 15 minutes the tubes were quickly cooled to room temperature in a water bath for 15 seconds, and then placed in an ice bath for 5 minutes. After cooling, 2 ml H_2SO_4 was added and heated to 200°C for 15 minutes, then quickly cooled in a water bath. Then, 3 ml DI H_2O was added slowly and samples carefully mixed before placing in an ice bath for approximately 10 minutes. For each batch of samples triplicate blank precombusted GF/F filters were analysed as a control. Absorbance was measured at 375 nm (Nicolet Evolution 300 spectrophotometer, Thermo Electron Corporation, Madison, WI) using VisonProTM software (Thermo Electron Corporation) in quartz cuvettes using glyceryl tripalmitate in chloroform (1 mg ml^{-1}) as a standard. Method precision was calculated by dividing the standard deviation of the calibration replicates by the mean and multiplying by 100. The method precision was $\leq$ 7.3 %. The limit of detection for total lipid was 0.02 μg ml^{-1}.

3.2.3.3 Total carbohydrate

Total carbohydrate was analysed using spectrophotometric methods following the phenol-sulphuric acid method (Dubois et al., 1956). Pre-filtered samples on 25 mm GF/F filters were placed into 15 ml polypropylene tubes with 1 ml DI H_2O, and 1 ml 5% phenol solution, and vortexed. Samples were kept at room temperature for 40 minutes before slowly adding 5 ml H_2SO_4 (concentrated 95.5%), carefully mixed, and left for a further 10 minutes. Samples were then centrifuged for 5 minutes at 3500 rpm. The supernatant was transferred into a quartz cuvette, and the absorbance was measured at 490 nm (Nicolet Evolution 300 spectrophotometer, Thermo Electron Corporation, Madison, WI) using VisonProTM software (Thermo Electron Corporation). For each

batch of samples triplicate blank precombusted GF/F filters were analysed as a control. D-glucose was used as a standard (1 mg ml^{-1}). Method precision was calculated by dividing the standard deviation of the calibration replicates by the mean and multiplying by 100. The method precision was ≤ 7.7 %. The limit of detection for total carbohydrate was 0.06 μg ml^{-1}.

3.2.3.4 Total protein

Total protein was analysed using the Lowry method (Lowry et al., 1951). Reagent D was made daily using a 48:1:1 ratio of Lowry reagents A (2% *w/v* Na_2CO_3 in 0.1 N NaOH), B (1% *w/v* NaK Tartrate tetrahydrate in DI H_2O), and C (0.5% *w/v* $CuSO_4.5H_2O$ in DI H_2O). Stock solutions of Reagents A, B, and C were kept at room temperature. Pre-filtered samples on GF/F filters were placed in 15 ml polypropylene centrifuge tubes with 1 ml DI H_2O, and 5 ml alkaline copper solution (Reagent D), vortexed, and left for 10 minutes at room temperature. During this time, Reagent E was prepared with 2 N Folin-Ciocalteu phenol reagent (FCR) in an amber stock bottle (1:1 *v/v* DI H_2O). Following 10 minutes at room temperature, samples were vortexed and 0.5 ml Reagent E was added. Samples were vortexed immediately after FCR was added, placed in the dark, and incubated for 1.5 hours at room temperature with occasional mixing. Samples were then centrifuged at 3000 rpm for 10 minutes. For each batch of samples triplicate blank precombusted GF/F filters were analysed as a control. The absorbance of each sample was read at 600 nm (Nicolet Evolution 300 spectrophotometer, Thermo Electron Corporation, Madison, WI) using VisonProTM software (Thermo Electron Corporation). Calibration curves were prepared for each batch of samples with a bovine serum albumin (BSA) stock solution (1 mg ml^{-1}; Sigma P5396). Method precision was calculated by dividing the standard deviation of the calibration replicates by the mean and multiplying by 100. The method precision was ≤ 2.1 %. The limit of detection for total protein was 0.005 μg^{-1}.

3.2.4 Statistical analyses

Pearson's correlation analysis was used to examine the relationship between environmental variables, biochemical composition (protein, carbohydrate, and lipid concentration per cell), chain length, and microphytoplankton community sedimentation rate. Regression analysis was carried out using linear and non-linear (quadratic and cubic polynomials) methods where appropriate. Correlation and regression analyses were carried out in R Studio.

3.3 Results

3.3.1 Microphytoplankton community composition

A detailed analysis of the microphytoplankton community composition was carried out in Chapter 2, Section 2.3.1.3. In summary, community composition varied seasonally and between the 2015 and 2016 sample years (Figure 3.2). Cell abundances were highest above the pycnocline and in spring in both sample years. *Skeletonema* and *Chaetoceros* spp. dominated the community composition and a minor proportion of total cell abundance was contributed by other taxa.

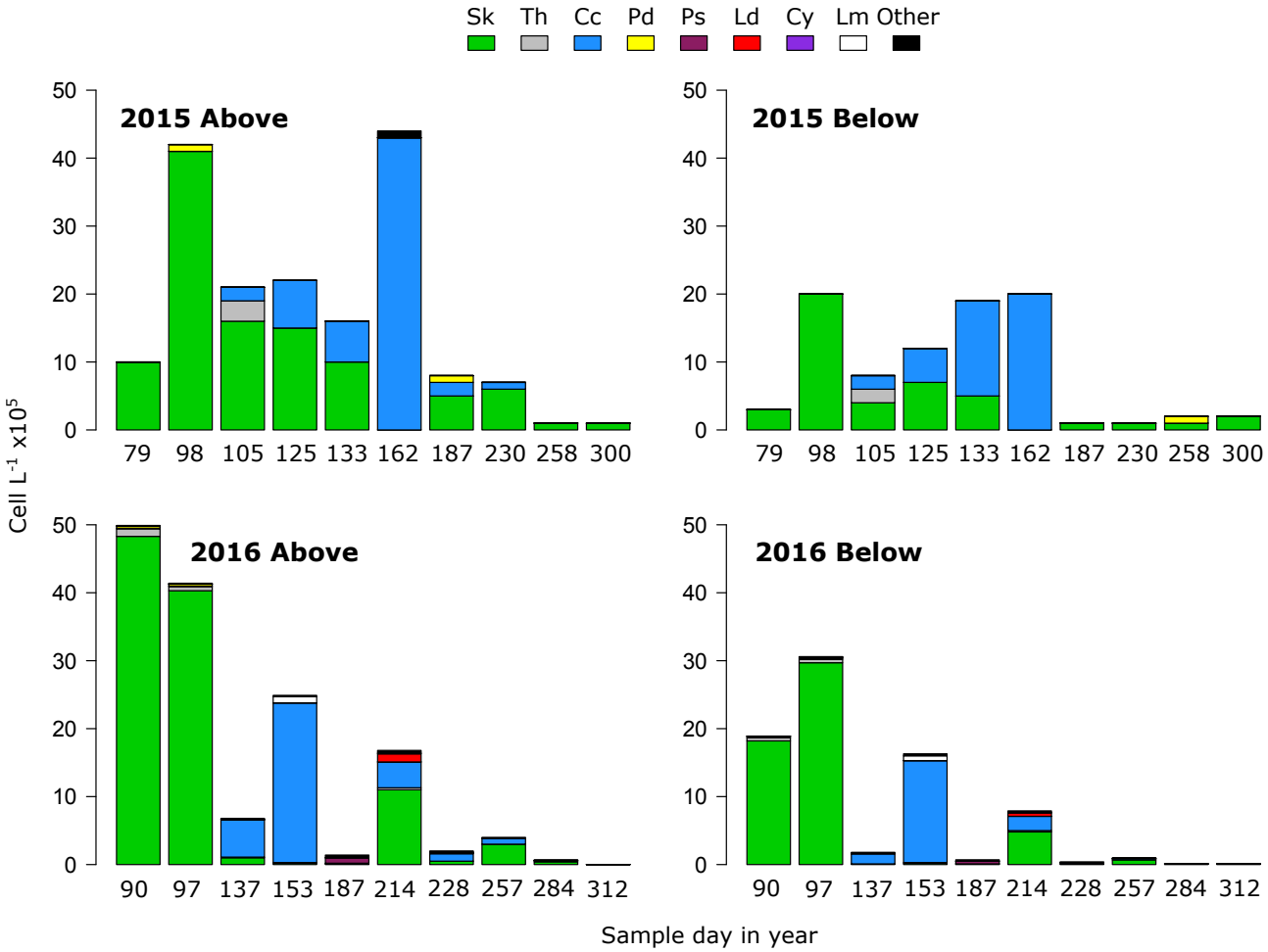

Figure 3.2: Seasonal total microphytoplankton cell abundance (cells L^{-1} x10^5) and species composition on sample dates in 2015 and 2016 from samples above and below the pycnocline. Sk: *Skeletonema* spp., Th: *Thalassiosira* spp., Cc: *Chaetoceros* spp. coastal, Pd: *Pseudo-nitzschia delicatissima*, Ps: *P. seriata*, Ld: *Leptocylindricus danicus*, Cy: *Cylindrothecae* spp., Lm: *L. minimus*, and other species.

3.3.2 Sedimentation rates

3.3.2.1 Microphytoplankton community

Above the pycnocline sedimentation rates ranged from 0.59 m d^{-1} (day 98) to 0.89 m d^{-1} (day 126) in 2015 (Figure 3.3a). In 2016 the range above the pycnocline was much greater than in 2015, with maximum and minimum sedimentation rates of 1.42 (day 153) and 0.72 (day 228) m d^{-1} respectively (Figure 3.3b). Below the pycnocline maximum community sedimentation rate in 2015 was 1.24 m d^{-1} (day 105) and minimum 0.70 m d^{-1} (day 133). This range was smaller and less variable in 2016 ranging from 0.70 (day 312) to 1.02 m d^{-1} (day 137). There was no significant difference in microphytoplankton community sedimentation rates between spring, summer, and winter seasons in 2015 and 2016 (Kruskal-Wallis, H_{2015} = 4.18, H_{2016} = 1.48, df = 2, P_{2015} = 0.12, P_{2016} = 0.48). Regardless of season, there was no significant difference between median sedimentation rate of total microphytoplankton community and depth above and below the pycnocline in either year (Mann Whitney U-test, U_{2015}= 84.0, U_{2016}=101.0, n_{2015}= 9, n_{2016}=10, P_{2015}= 0.9, P_{2016}= 0.8).

The difference between community sedimentation rates above and below the pycnocline in 2015 was higher in spring when differences in environmental parameters were larger (e.g. salinity, temperature, and density; Chapter 2, Figure 2.4) when compared to sample dates later in the year. In 2016 sedimentation rates were less variable below the pycnocline than above.

Microphytoplankton categorised into phyletic groups of diatoms, dinoflagellates, and ciliates were shown to have significantly different sedimentation rates between groups (not between sample years or depth above and below pycnocline; Figure 3.4). Dinoflagellates had the highest median sinking rate (median 1.25 $\pm$ 0.03 S.E. m d^{-1}), followed by diatoms (median 0.83 $\pm$ 0.03 S.E. m d^{-1}), and then ciliates (median 0.78 $\pm$ 0.04 S.E. m d^{-1}; Kruskal-Wallis, H = 53.00, df = 2, P = 0.000).

Investigating the relationship between seasonal microphytoplankton community composition changes and sedimentation rate was difficult due to variability in community composition. A nMDS ordination carried out in Chapter 2, Section 2.3.1.3 showed that sample dates in spring 2015 (day 79, 98, 105, 133, 125), despite variability between dates, were more similar in composition (dominated by *Skeletonema* spp.) when compared to other seasons (Figure 2.16i & Figure 3.2). Spring 2015 was also the period where sedimentation rates were most variable in comparison to later seasons (Figure 3.3a). The decrease in sedimentation rate on day 98 in 2015 above the pycnocline corresponded to a peak in total cell abundance for the entire season which was dominated by *Skeletonema* spp. (96.86 %; Figure 3.2). Peaks in sedimentation rate below the pycnocline in 2015 (day 105 and 125) corresponded to a mixed community composition of mainly *Skeletonema* spp., *Thalassiosira* spp., and *Chaetoceros* (coastal) spp. (Figure 3.2).

In 2016, sedimentation rates were relatively similar on days 90 and 97 (Figure 3.3b), which had similar microphytoplankton community compositions (Figure 2.16ii & 3.2) and were dominated by *Skeletonema* spp. Peak sedimentation rate occurred above the pycnocline on days 153 and

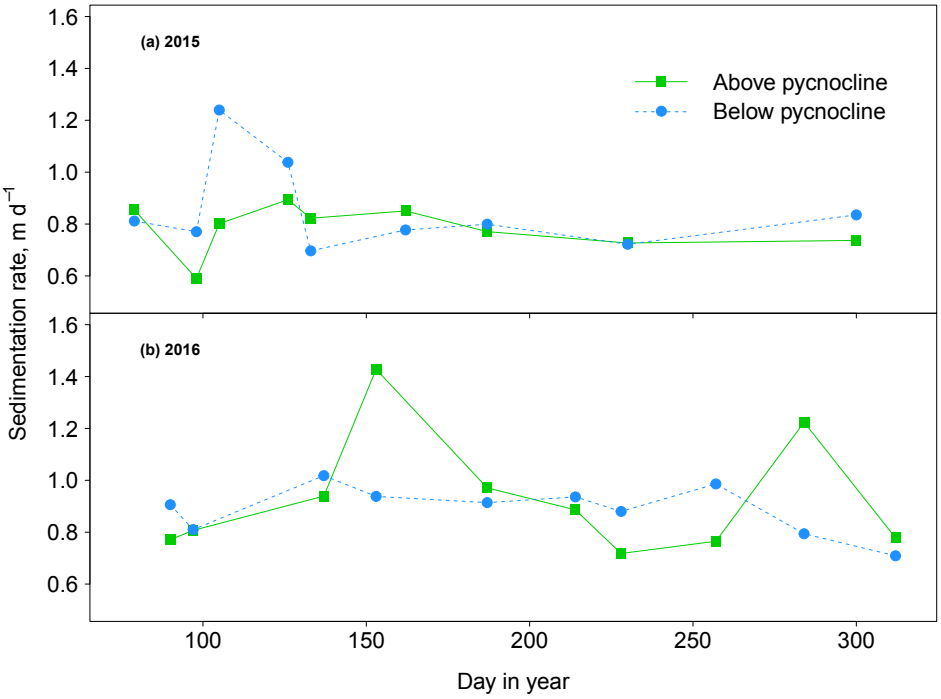

Figure 3.3: Seasonal sedimentation rate (m d^{-1}) of total microphytoplankton community sampled from above and below the pycnocline in 2015 (a) and 2016 (b)

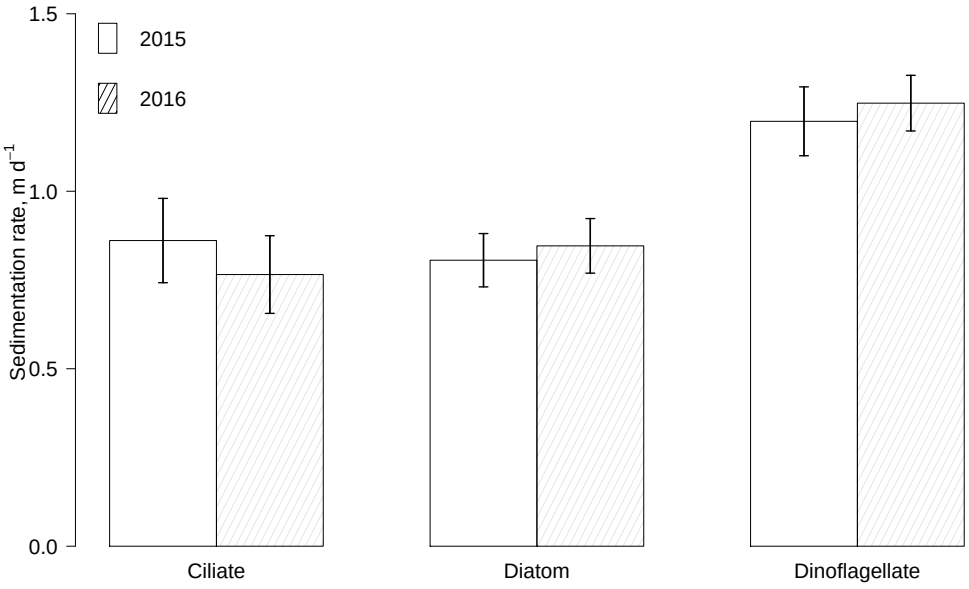

Figure 3.4: Median dinoflagellate (n= 91), diatom (n= 181), and ciliate (n= 27) sedimentation rate $\pm$ SE (m d^{-1}) from 2015 and 2016

284 (Figure 3.3ii). *Chaetoceros* spp. (coastal) reached its maximum abundance (94.2 %) for the year and dominated the microphytoplankton community on day 153. The secondary peak in sedimentation rates occurred when there was a mixed species composition and lower cell abundances (Figure 3.2).

Sedimentation rates in 2015 were higher when there was a mixed community composition (e.g. day 105 and 125 below; mixed community composition of *Skeletonema*, *Chaetoceros* and *Thalassiosira* spp.) and lower when one taxa was dominant and at maximum abundance (e.g. day 98 above and below; *Skeletonema* dominant and, 162 below; *Chaetoceros* dominant). However this depended on which taxa of microphytoplankton was dominant, as dominance and maximum abundance of *Skeletonema* spp. had a lower sedimentation rate (0.59 m d^{-1}) in 2015 compared to dominance and maximum abundance of *Chaetoceros* spp. (coastal), which had higher sedimentation rates (1.42 m d^{-1}) in 2016. Despite *Skeletonema* spp. having a lower sedimentation rate at maximum abundance when compared to *Chaetoceros* spp. (coastal), it had substantially higher cell densities of 4.1 x 10 ^{5} cells L^{-1} in comparison to 2.4 x 10 ^{5} cells L^{-1} of *Chaetoceros* spp. (coastal).

3.3.2.2 Species-specific

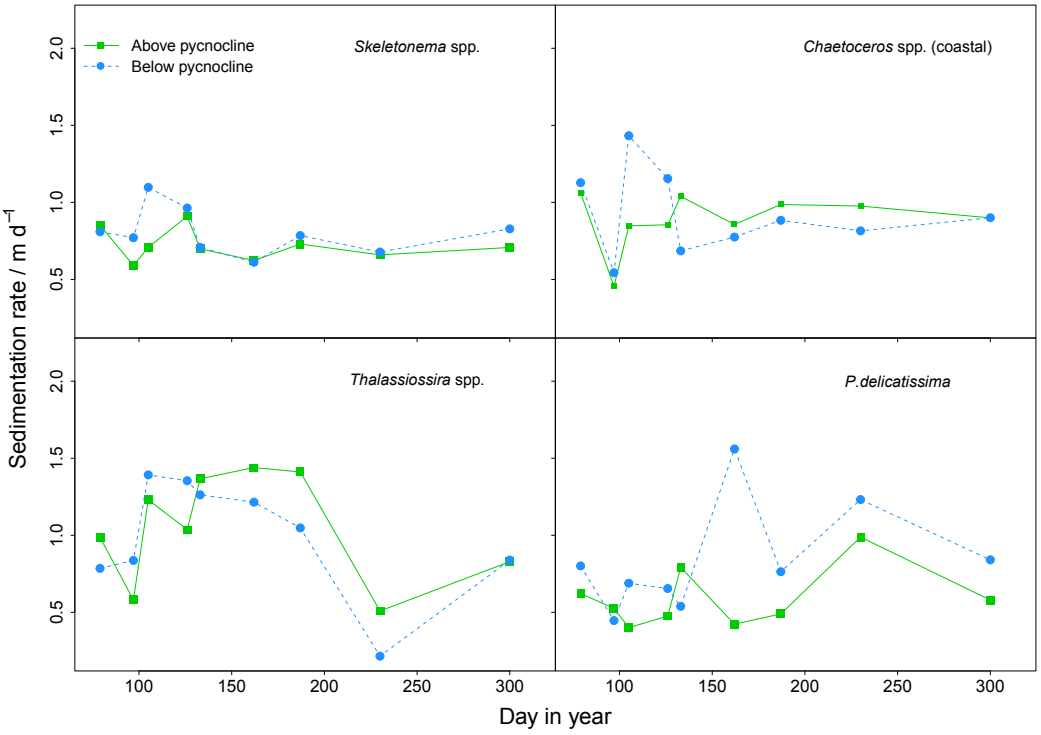

Figure 3.5: Sedimentation rates (m d^{-1}) of diatoms *Skeletonema* spp., coastal *Chaetoceros* spp. (coastal), *Thalassiosira* spp., and *P. delicatissima* during 2015 above and below the pycnocline

Sedimentation rates of the four most abundant diatom species varied greatly between species in 2015 (Figure 3.5), and 2016 (Figure 3.6). Both *Skeletonema* spp. and *Chaetoceros* spp. (coastal)

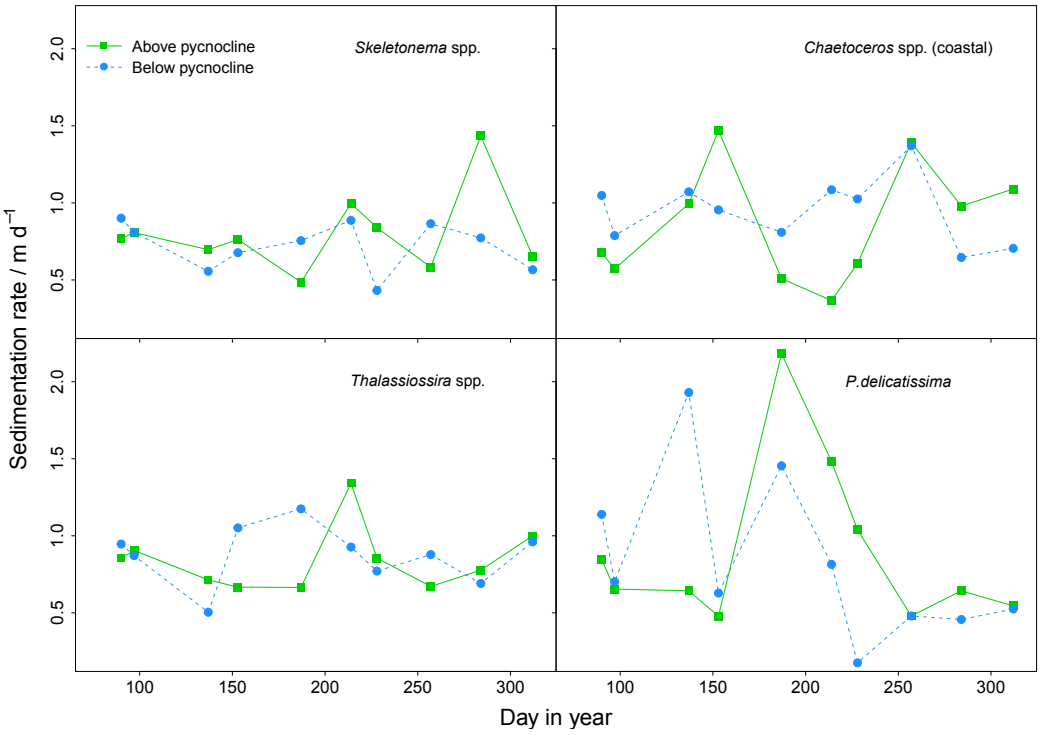

Figure 3.6: Sedimentation rates (m d^{-1}) of diatoms *Skeletonema* spp., coastal *Chaetoceros* spp. (coastal), *Thalassiosira* spp., and *P. delicatissima* during 2016 above and below the pycnocline

seasonal sedimentation rates above and below the pycnocline (Figure 3.5) followed a relatively similar trend to microphytoplankton community sedimentation rate (2015; Figure 3.3). This was a result of both species dominating the community composition at various times of the year (Chapter 2, Figure 2.14). Sedimentation rate of *Thalassiosira* spp. was highest in spring, coinciding with maximum abundance and had the highest contribution to community composition (SIMPER analysis). *P. delicatissima* sedimentation rate was generally higher below the pycnocline than above (Figure 3.5).

Skeletonema spp. and *Chaetoceros* spp. (coastal) were responsible for driving the microphytoplankton community sedimentation rate in 2016. This is shown by the similar trends of species-specific sedimentation rates (Figure 3.6) when compared to community sedimentation rates (Figure 3.3b). Peaks in sedimentation rate of *Skeletonema* spp. and *Chaetoceros* spp. (coastal) corresponded to peaks in community sedimentation rate. *Thalassiosira* spp. sedimentation rates were lower during spring 2016 than 2015, and after which the seasonal range of sedimentation was similar between the years. Sedimentation rates of *P.delicatissima* were highly variable above and below the pycnocline in 2016, ranging from 0.18 to 2.18 m d^{-1}.

Sedimentation rates of solitary cells of *Cylindrothecea* spp. were generally lower above the pycnocline than below during spring 2015, and subsequently switched to higher sinking rates above the pycnocline than below later in the year (Figure 3.7). There was less seasonal variation in sedimentation rates of *Cylindrothecae* spp. in 2016. *Pleurosigma* spp. sedimentation rates were highly

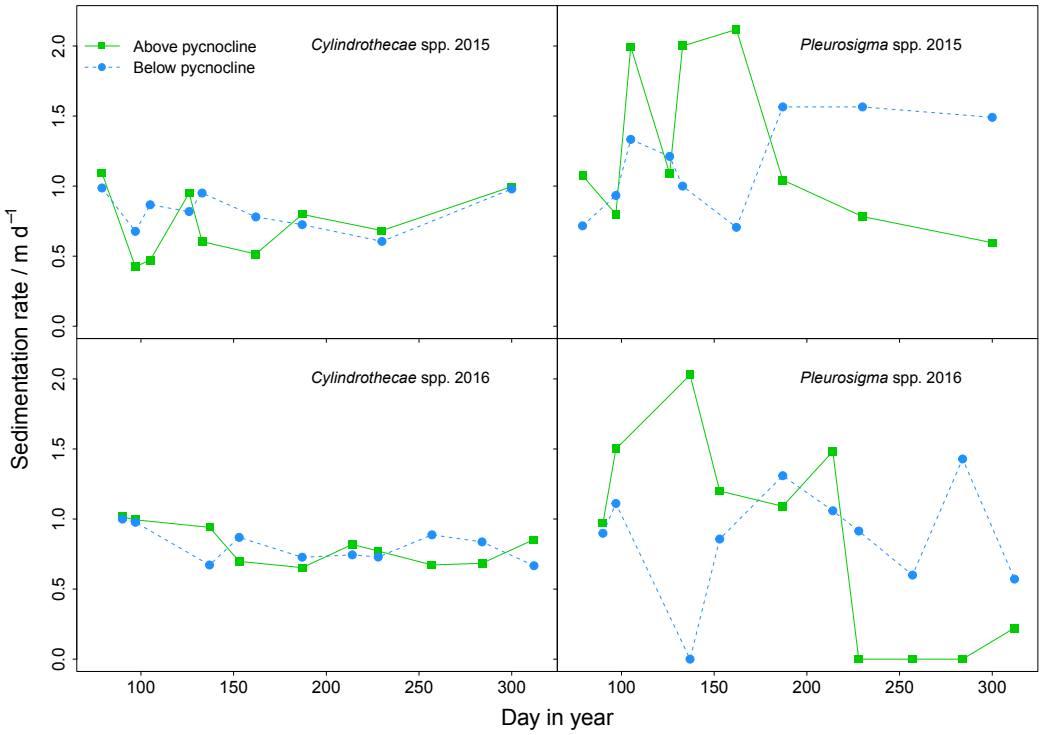

Figure 3.7: Sedimentation rates (m d^{-1}) of solitary diatoms *Cylindrothecae* spp. and *Pleurosigma* spp. during 2015 and 2016 above and below the pycnocline

variable at both depths in 2015 and 2016. Sedimentation rates ranged from neutral buoyancy to 2.12 m d^{-1}.

Sedimentation rates of key dinoflagellate taxa were highly variable (Figure 3.8), and often higher than diatoms (Figure 3.5 and 3.6). *Katodinium* spp. were the most abundant dinoflagellate in 2015 and seasonal sedimentation rates were similar both above and below the pycnocline (Figure 3.8). Sedimentation rates were initially higher above the pycnocline, and then decreased to similar rates found below the pycnocline in early spring. At both depths sedimentation rate increased up to mid-year, then decreased to a rate similar to early spring, and then increased to a higher rate below the pycnocline than above. Trends in *Katodinium* spp. sedimentation rate in 2016 were similar to 2015 with the exception of a decrease in sedimentation rate above the pycnocline between day 150 to 200.

Sedimentation rates of *Scripsiella* spp. were generally higher than *Katodinum* spp. and *Gyrodinium* spp. (Figure 3.8). *Scripsiella* spp. sedimentation rate was initially high above and below the pycnocline and steadily decreased above the pycnocline over the year until day 187 when rates increased to values observed in spring. Below the pycnocline, sedimentation rates were variable until day 230 when *Scripsiella* spp. sedimentation rate decreased to 0.30 m d^{-1}. In 2016 *Scripsiella* spp. sedimentation rate peaked in spring, mid-year and winter. On the last sample date (day 312), *Scripsiella* spp. was neutrally buoyant above the pycnocline and absent from samples below the pycnocline.

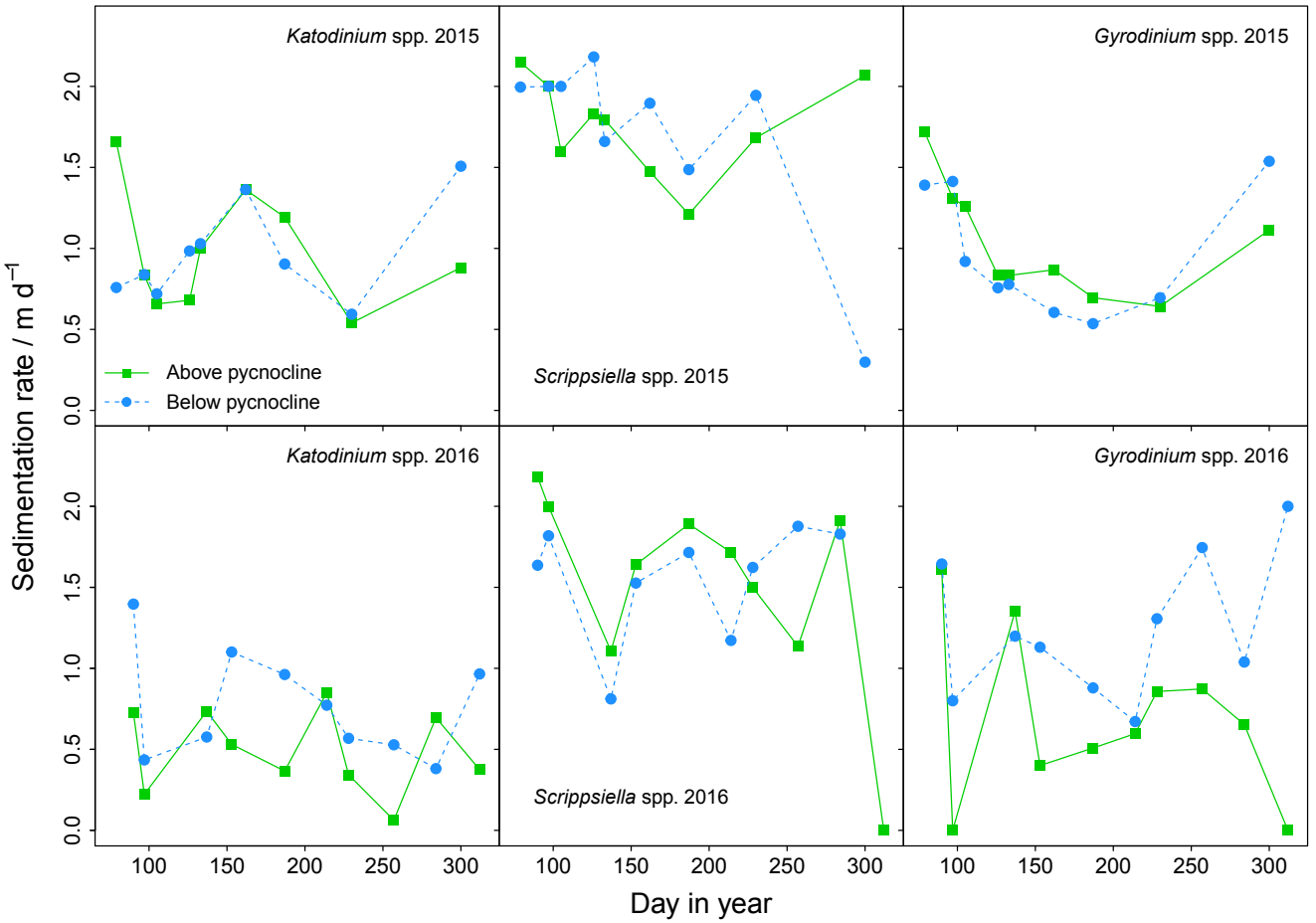

Figure 3.8: Sedimentation rates (m d^{-1}) of key dinoflagellates *Katodinium* spp., *Scrippsiella* spp., and *Gyrodinium* spp. during 2015 and 2016 above and below the pycnocline

Gyrodinium spp. sedimentation rate above and below the pycnocline followed similar trends with higher sinking rates during spring 2015, which decreased mid-year, and increased in winter (Figure 3.8). Sedimentation rates were much more variable and did not mirror trends above versus below the pycnocline in 2016. Neutral buoyancy occurred above the pycnocline during spring and winter, and sedimentation rates were generally higher below the pycnocline than above in 2016.

3.3.2.3 Chain length

The yearly median cells per chain above and below the pycnocline in 2015 was 4 (Figure 3.9i), and 5 in 2016 (Figure 3.9ii). Median cells per chain varied seasonally in both years, with similar trends observed above and below the pycnocline within their respective years. The number of cells per chain increased above the yearly 2015 median mid-spring (April) above the pycnocline, and later spring (May) below the pycnocline (Figure 3.9i). During summer months (July and August), median cells per chain decreased both above and below the pycnocline, and there was a higher density distribution of chains around 2 and 3 cells in length. There was a relatively even density distribution for chain lengths 1 to 10, and an increase in median cells per chain in October 2015 above the pycnocline. Below the pycnocline in October 2015, there was high density distribution of longer chain lengths. Median cells per chain decreased over the course of spring 2016, and then increased in early summer (July and August; Figure 3.9ii). There was a higher density distribution of shorter chain lengths towards the end of summer and into winter. Similarly to 2015, on the last sample day in November 2016, the density distribution of cells per chain was more evenly distributed between shorter to longer chains than previous months. Especially during summer and winter, there was a lower frequency of longer chains in 2016 when compared to 2015.

Chain length frequency data were further investigated to include species composition (Figures 3.10 & 3.12). There were 18 microphytoplankton taxa which were included as chain forming diatom species, in which *Skeletonema* and *Chaetoceros* coastal spp. dominated. The abundance of chain lengths and species contribution to chain length abundance varied seasonally. There was a relationship (either linear or quadratic) between diatom cells per chain and sedimentation rate sampled above the pycnocline for the majority of sampling dates in 2015 (no relationship between sedimentation rate and chain length on days 79 and 300; Figure 3.11). Day 97 was dominated by *Skeletonema* spp. (except for high abundances of *P. delicatissima* of one chain length; Figure 3.10), and the only sample date to have a negative relationship with lower sinking rates observed for longer chain lengths (Figure 3.11). The subsequent four sampling dates (day 105, 125, 133, and 162) all had differing species compositions (which were either a mixed assemblage of *Skeletonema*, *Chaetoceros* coastal, *Thalassiosira*, *P. delicatissima*, or dominated by *Chaetoceros* coastal spp. on day 187), but the same general trend of higher sedimentation rates when chain lengths were longer. Low abundances of chain forming diatoms were observed on days 187, 230, and 300 (Figure 3.10). The quadratic relationship on day 187 showed shorter chain lengths having similar sedimentation rates to longer chain lengths (Figure 3.11). The shorter chains were dominated by *P. delicatissima* in contrast to the longer chains which were predominantly *Skeletonema* and *Chaetoceros* (coastal) spp. On the subsequent sampling day (230), the relationship between sedimentation rate and chain length was linear with increasing rates with increasing chain lengths

(Figure 3.11). Therefore shorter chain lengths on day 230, had slower sedimentation rates than the shorter chain lengths on day 187. The species composition of the shorter chain lengths was different between the two dates, with *P. delicatissima* present on day 187 when sedimentation rates were higher, and absent on day 230 when rates were lower.

The species composition of chain forming diatoms was similar below the pycnocline to above (Figure 3.12), but at lower chain length abundances when compared to above the pycnocline (Figure 3.10). There were more sample dates below the pycnocline that did not have a relationship between chain length and sedimentation rate (days 79, 97, 133, and 187). Other sample dates followed the same trend in community composition and relationship between increasing chain length resulting in higher sedimentation rates (days 125, 162, and 230). There was a difference between chain length and sedimentation rate on day 105, with increasing sedimentation rates with longer chain lengths above the pycnocline, and the converse relationship below the pycnocline. The community composition was relatively similar between the two depths but at lower abundances below the pycnocline (Chapter 2, Section 2.3.1.3).

Poor relationships between chain length and sedimentation rates were observed in 2016 both above and below the pycnocline. On sample dates where there were relationships found, r^2 was low (<0.5) on all but two dates (Figure B.2 & B.3).

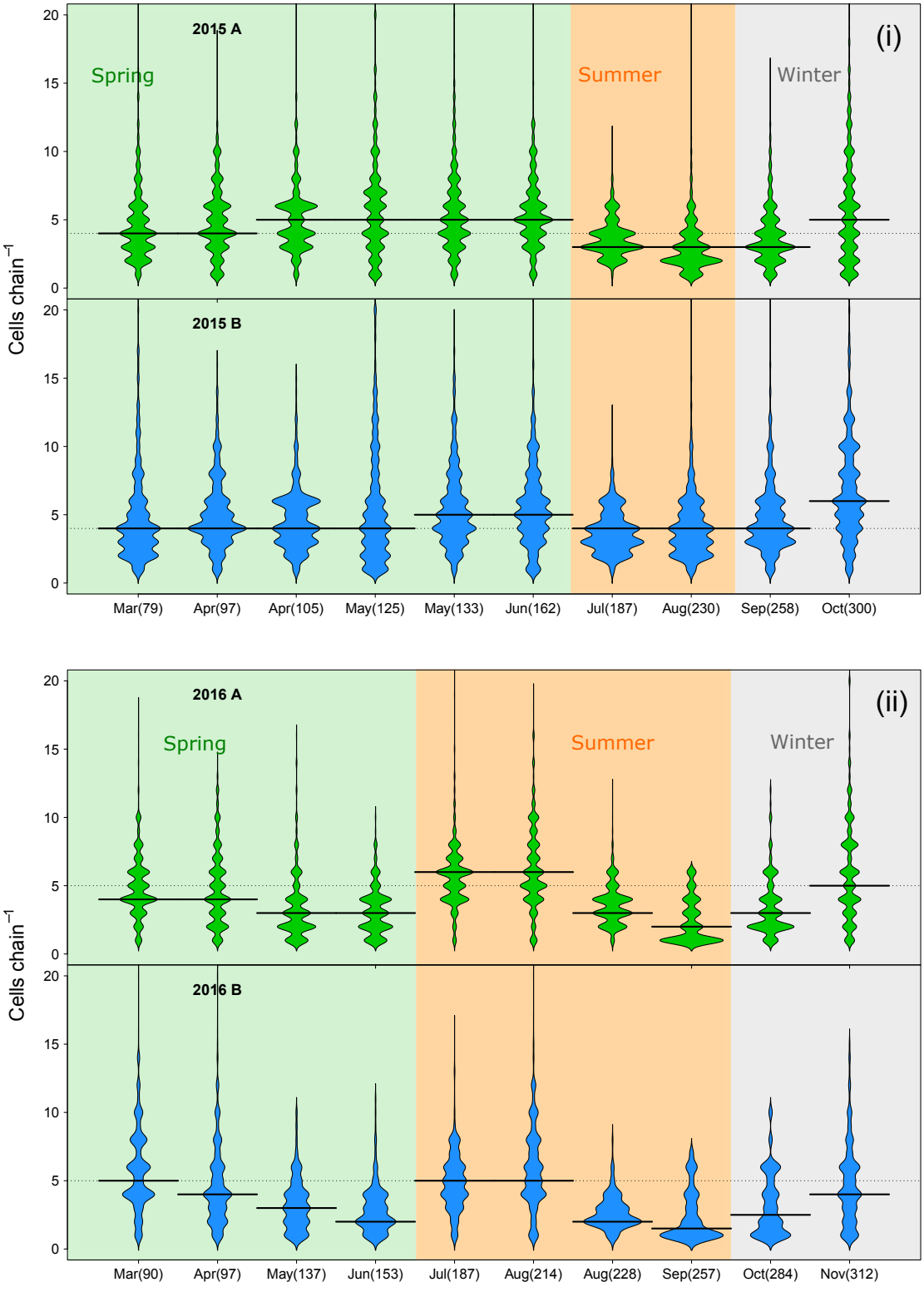

Figure 3.9: Frequency distribution of number of cells per chain from all chain forming diatoms sampled over 2015 (i) and 2016 (ii) above (A) and below (B) the pycnocline. Thick horizontal lines are median cells per chain per sample date and the thickness of the beanplot shows density distribution of chain length. The dashed line is the overall median over the year

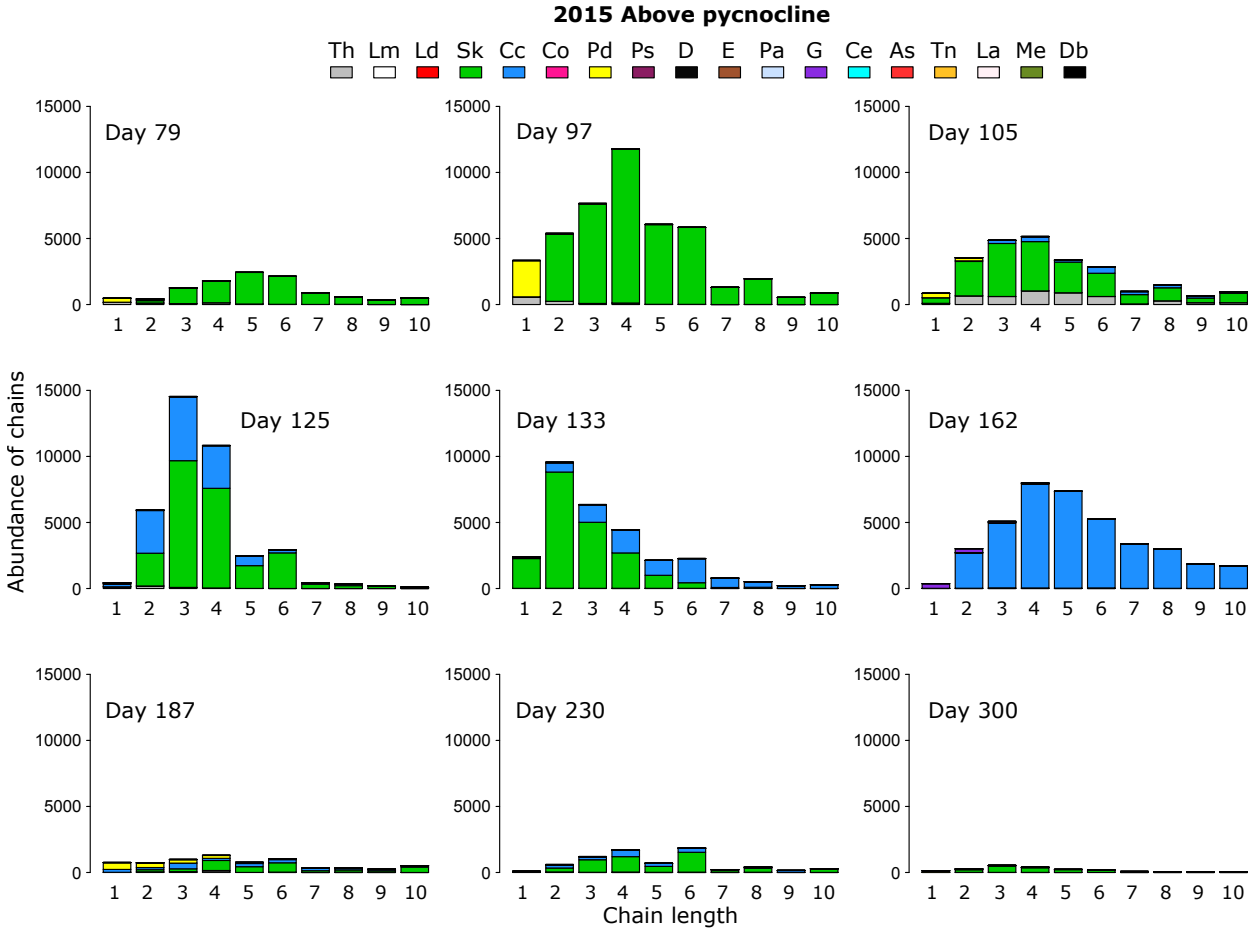

Figure 3.10: Chain length abundance and species contribution of all chain forming diatoms in samples from above the pycnocline taken over nine sample dates in 2015. Th: *Thalassiosira* spp., Lm: *Leptocylindricus minimus*, Ld: *L. danicus*, Sk: *Skeletonema* spp., Cc: *Chaetoceros* spp. (coastal), Co: *Chaetoceros* spp. oceanic, Pd: *Pseudo-nitzschia delicatissima*, Ps: *P. seriata*, D: *Dactyliosolen* spp., E: *Eucampia* spp., Pa: *Paralia* spp., G: *Guardinia* spp., Ce: *Ceratium* spp., As: *Asterionellopsis* spp., Tn: *Thalassionema* spp., La: *Lauderia* spp., Me: *Meuniera* spp., Db: *D. blavyanus*

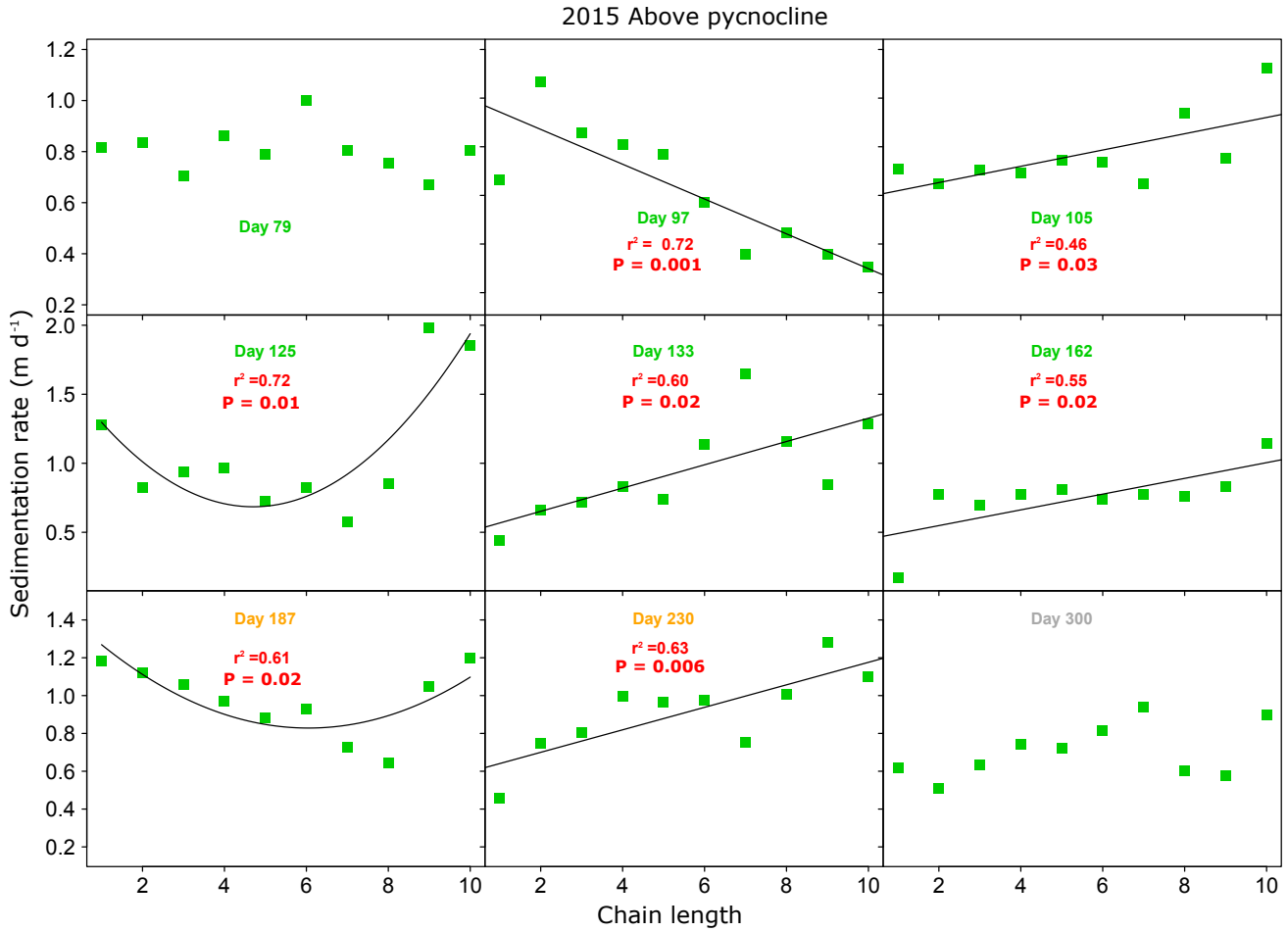

Figure 3.11: Chain length and sedimentation rate (m d^{-1}) over each sampling date in spring (green; days 79, 97, 105, 125, 133, 162), summer (orange; days 187, 230), and winter (grey; day 300) 2015 from samples taken above the pycnocline. On each plot are lines of best fit (linear and quadratic) and regression statistics (r^2)

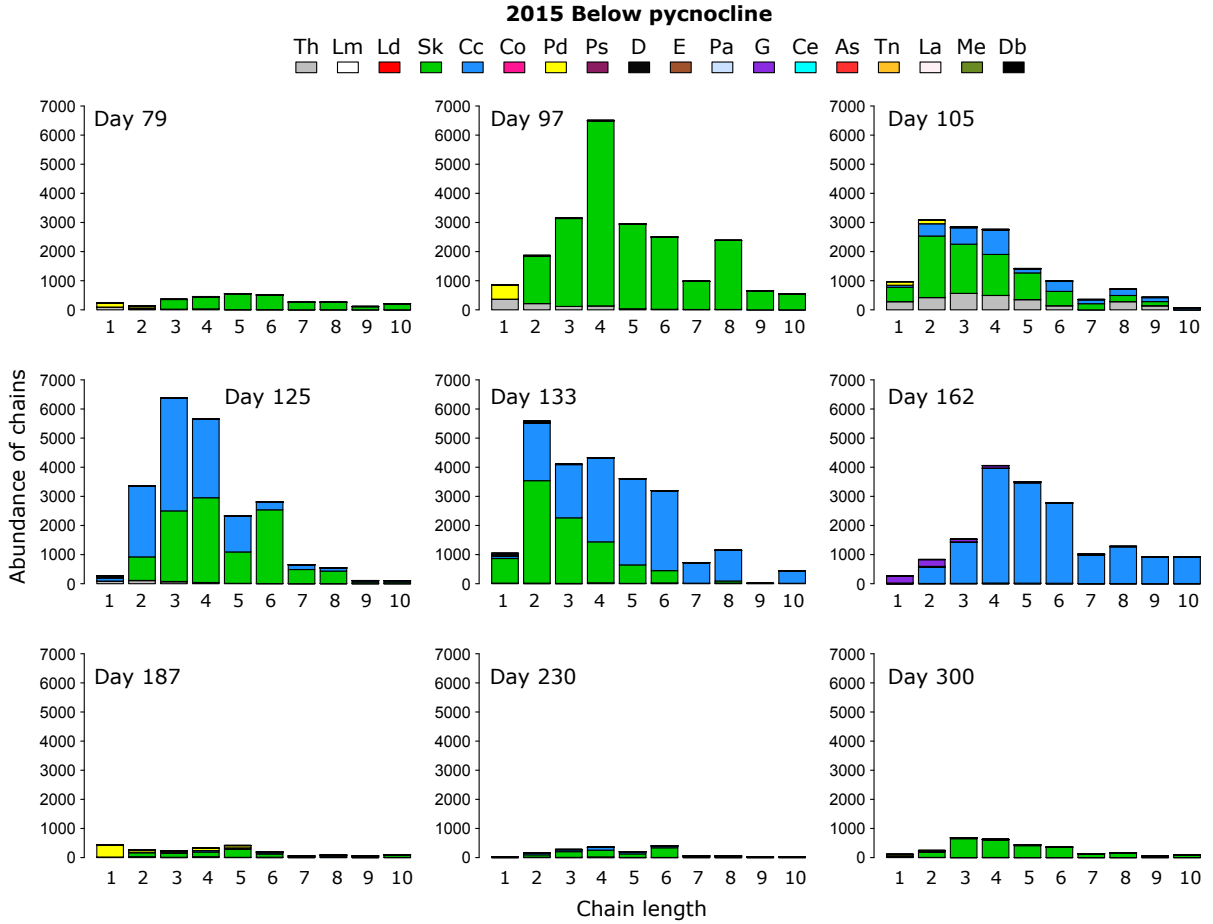

Figure 3.12: Chain length abundance and species contribution of all chain forming diatoms in samples from below the pycnocline taken over nine sample dates in 2015. Th: *Thalassiosira* spp., Lm: *Leptocylindricus minimus*, Ld: *L. danicus*, Sk: *Skeletonema* spp., Cc: *Chaetoceros* spp. coastal, Co: *Chaetoceros* spp. oceanic, Pd: *Pseudo-nitzschia delicatissima*, Ps: *P. seriata*, D: *Dactyliosolen* spp., E: *Eucampia* spp., Pa: *Paralia* spp., G: *Guardinia* spp., Ce: *Ceratium* spp., As: *Asterionellopsis* spp., Tn: *Thalassionema* spp., La: *Lauderia* spp., Me: *Meuniera* spp., Db: *D. blavyanus*

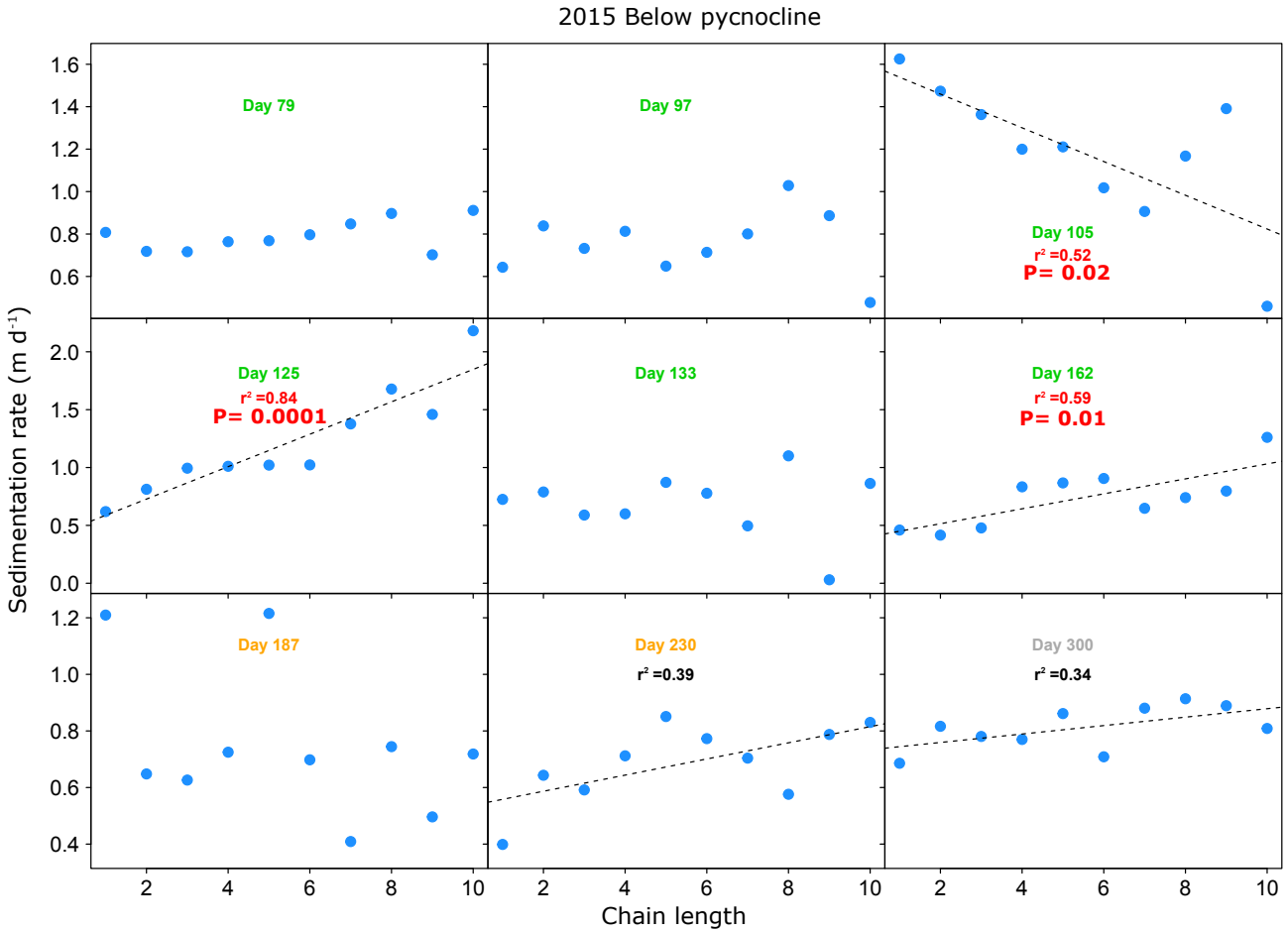

Figure 3.13: Chain length and sedimentation rate (m d^{-1}) over each sampling date in spring (green; days 79, 97, 105, 125, 133, 162), summer (orange; days 187, 230), and winter (grey; day 300) 2015 from samples taken below the pycnocline. On each plot are lines of best fit (linear) and regression statistics (r^2)

3.3.2.4 Carbon

Sedimentation rates of total particulate carbon from 2016 SETCOL samples varied over the year, and with depth above versus below the pycnocline (Figure 3.14). Initial sedimentation rates (day 90 and 97) were similar between the two sample depths, which coincided with the spring microphytoplankton bloom, with slightly higher carbon sedimentation rates below the pycnocline. During spring and summer there were higher carbon sedimentation rates above the pycnocline (1.17 μg C m d^{-1}) and lower sedimentation rates below (0.52 μg C m d^{-1}) on day 109, and lower carbon sedimentation rates above the pycnocline (0.45 μg C m d^{-1}) when sedimentation rates were higher below (0.95 μg C m d^{-1}) on day 153. Peaks in carbon sedimentation rate occurred on day 187 in samples from above the pycnocline (1.64 μg C m d^{-1}). Following this maximum and from day 214 onwards, carbon sedimentation rates were more similar above and below the pycnocline relative to earlier dates.

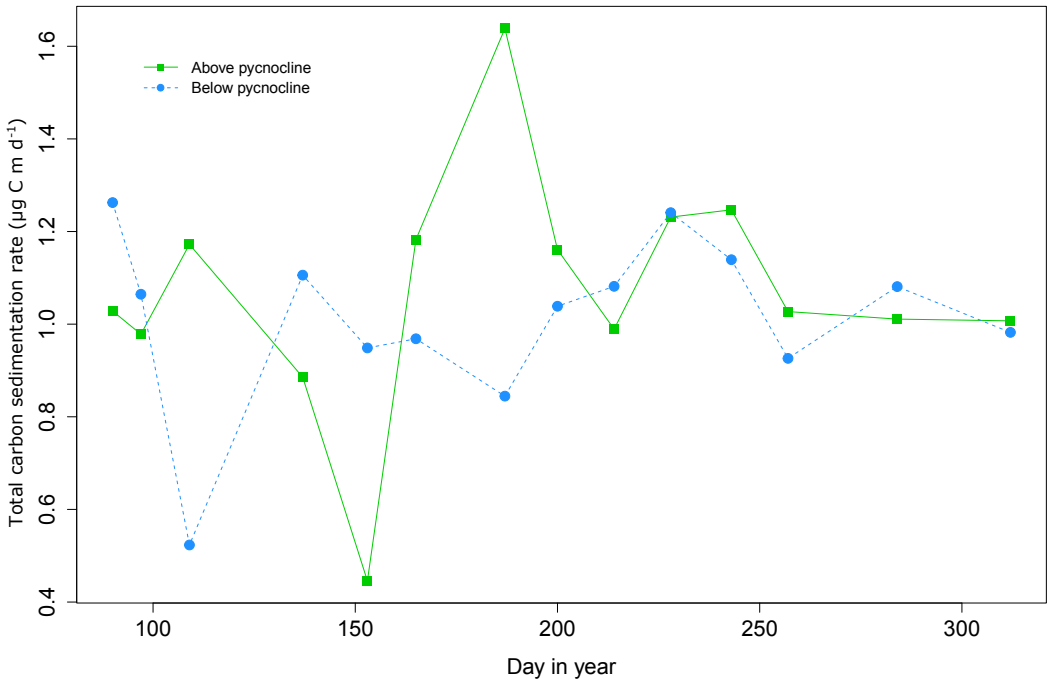

Figure 3.14: Sedimentation rate (μg C m d^{-1}) of total particulate carbon sampled from above and below the pycnocline, calculated from 2016 SETCOL experiments

3.3.3 Biochemical composition of microphytoplankton

The biochemical composition of microphytoplankton was relatively similar above and below the pycnocline in 2015 (Figure 3.15). From day 187 onwards there was a higher proportion of carbohydrates below the pycnocline when compared to above the pycnocline. The percentage contribution of lipid per cell was relatively consistent from the first sample date, and over spring/ early summer in 2015 (mean 28.0 % $\pm$ 1.9 SD). Late summer (day 230, 36.9 % lipid per cell) and winter (day 300, 43.0 % lipid per cell) the percentage of lipid per cell increased relative to earlier sampling dates.

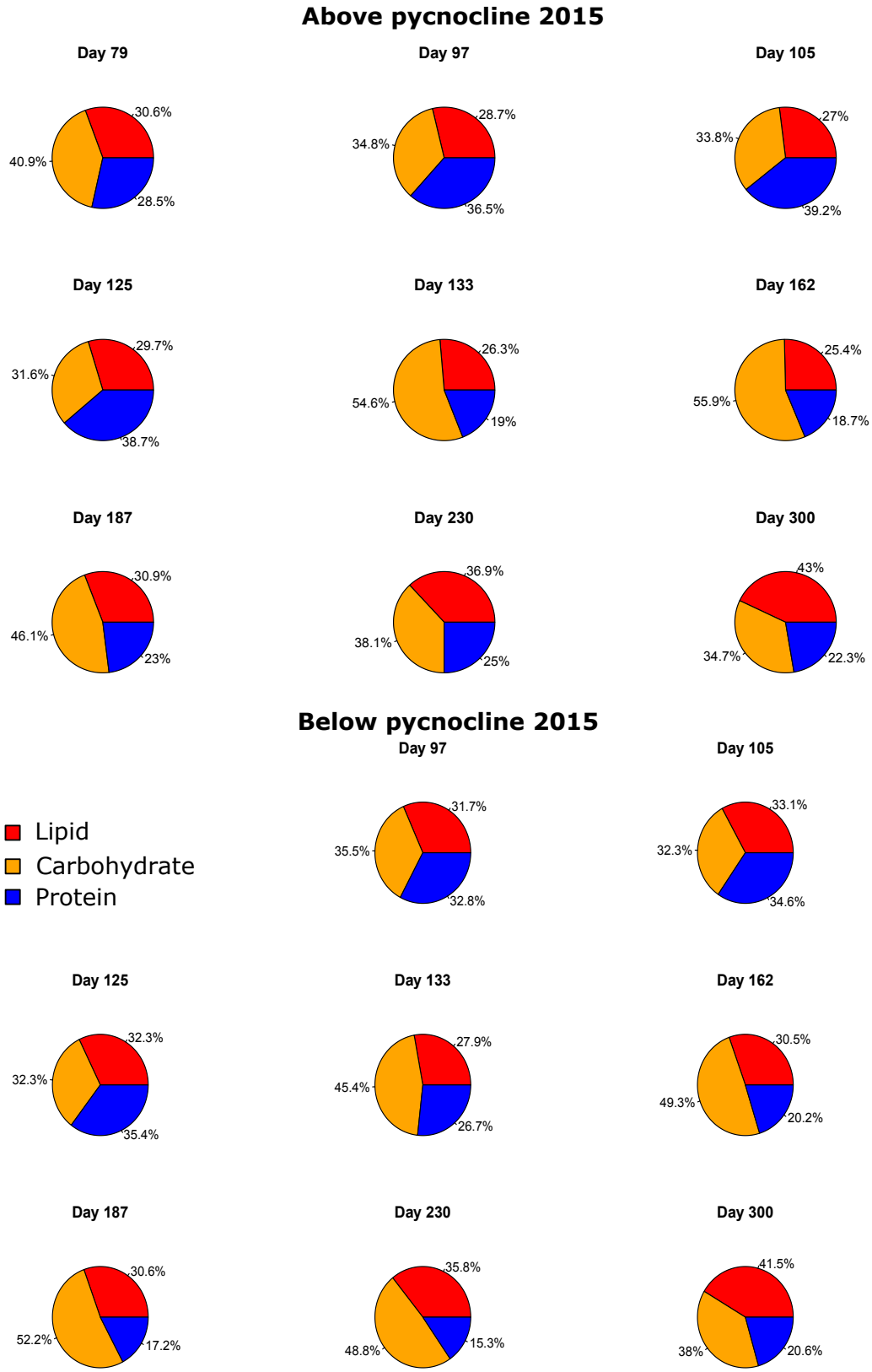

Figure 3.15: Percentage composition of lipid, carbohydrate, and protein per microphytoplankton cell sampled over 2015 from above and below the pycnocline.

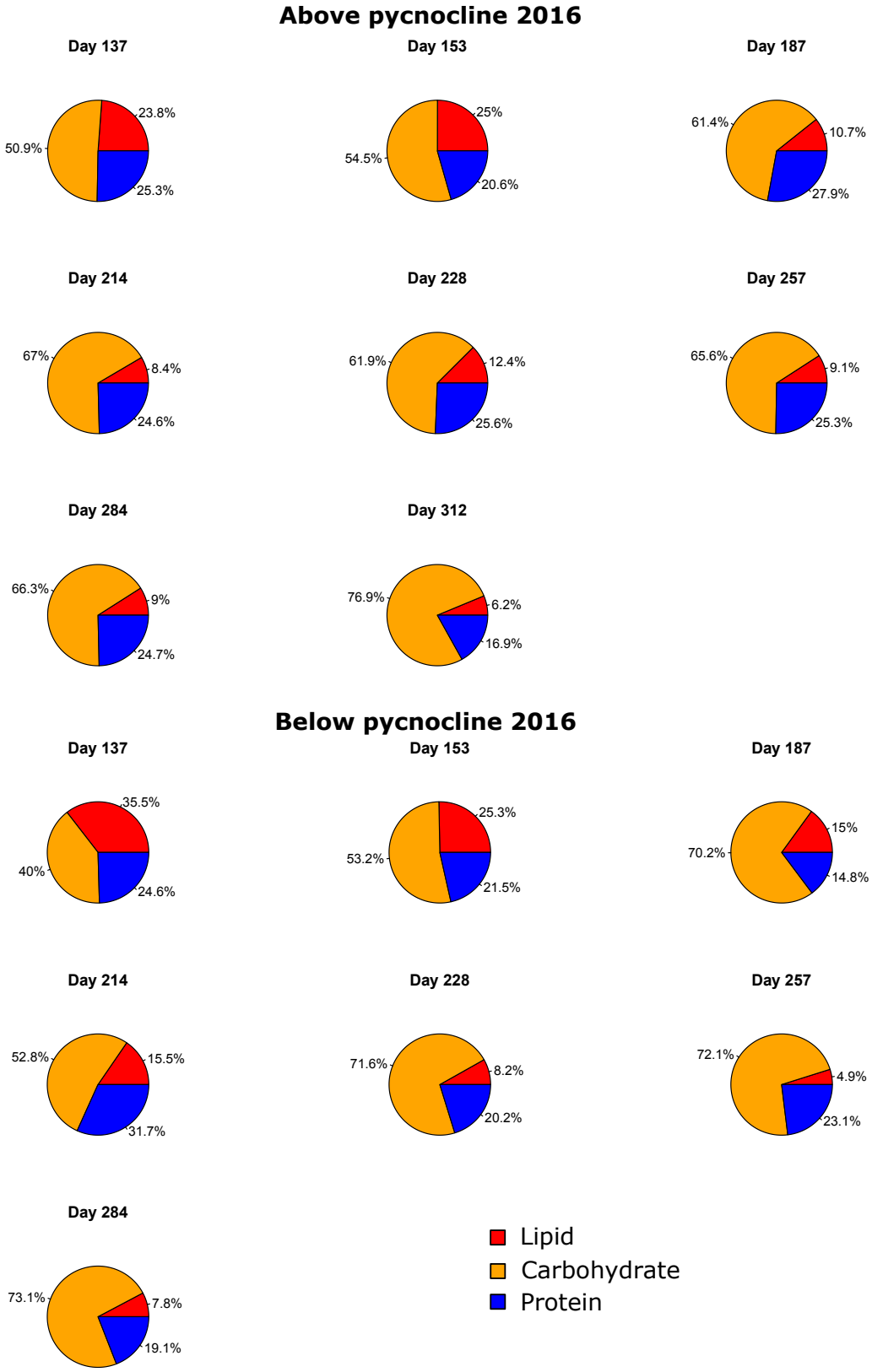

Figure 3.16: Percentage composition of lipid, carbohydrate, and protein per microphytoplankton cell sampled over 2016 from above and below the pycnocline.

Table 3.1: Pearsons correlation analysis (R value) between microphytoplankton community sedimentation rate and environmental and chemical parameters from samples above and below the pycnocline in 2015 and 2016

	2015				2016			
	Above		Below		Above		Below	
	R	P	R	P	R	P	R	P
Inorganic nutrients								
PO_4^{3-}	**0.69**	**0.04**	0.30	0.44	-0.07	0.84	-0.60	0.09
SiO_3^{2-}	0.56	0.12	-0.01	0.98	-0.33	0.36	**-0.79**	**0.01**
NO_3^{-}	-0.05	0.89	0.22	0.57	-0.02	0.62	-0.59	0.09
Environmental								
Day	-0.20	0.61	-0.28	0.46	-0.02	0.96	-0.41	0.24
Salinity	-0.38	0.32	0.37	0.32	0.20	0.58	-0.07	0.84
Temperature	-0.04	0.92	-0.38	0.31	-0.04	0.92	-0.15	0.69
Density	-0.34	0.37	0.48	0.19	0.19	0.61	0.13	0.73
Stratification index	-0.18	0.65	-0.19	0.62	-0.51	0.14	0.17	0.63
Wind speed	0.22	0.58	**0.75**	**0.02**	-0.02	0.97	-0.25	0.49
Pycnocline depth	0.36	0.34	**0.86**	**0.003**	**-0.67**	**0.04**	-0.43	0.21
Biochemical								
Protein	-0.64	0.06	**-0.73**	**0.03**	**-0.87**	**0.005**	0.54	0.57
Carbohydrate	-0.47	0.21	-0.47	0.20	**-0.87**	**0.005**	-0.63	0.10
Lipid	**-0.74**	**0.02**	**-0.73**	**0.04**	-0.49	0.22	0.54	0.12

Carbohydrates had a higher percentage composition in samples from above and below the pycnocline in 2016 when compared to 2015 (Figure 3.16). In contrast to 2015, the percentage contribution of lipid per cell was higher in 2016 spring sample dates and then decreased on subsequent dates.

3.3.4 Environmental and biochemical controls on microphytoplankton sedimentation rate

The relationships between inorganic nutrients, environmental parameters, biochemical composition and microphytoplankton community sedimentation rates depended on depth in water column above versus below the pycnocline, and the sampling year (Table 3.1). Phosphate concentration had a significant positive correlation with microphytoplankton community sedimentation rate above the pycnocline in 2015. Sedimentation rate increased as phosphate concentration increased. Below the pycnocline the rate of sedimentation increased as silicate concentration decreased. Environmental parameters wind speed and pycnocline depth were significantly related to sedimentation rate below the pycnocline in 2015. As wind speed and pycnocline depth increased, so did sedimentation rate. Additionally, pycnocline depth was the environmental parameter in relating increased sedimentation rate with increasing depth above the pycnocline in 2016.

Correlation analysis between the sedimentation rate of protein, carbohydrate and lipid concentration per cell and total community sedimentation was carried out. Lipid was an important biochemical component linked to the sedimentation rate of microphytoplankton community in 2015 above and below the pycnocline. Sedimentation rates were lower when there were higher concentrations of lipid. Similarly, sedimentation rates decreased when protein concentration was higher. In 2016 the relationship between protein and carbohydrate concentration with community sedimentation rate was significant.

3.4 Discussion

3.4.1 Microphytoplankton community dynamics and sedimentation rate

Diatoms dominated the microphytoplankton community at LY1 in 2015 and 2016. *Skeletonema* spp. and *Chaetoceros* coastal spp. were the dominant taxa responsible for explaining seasonal variation in microphytoplankton community composition in 2015 and 2016. Microphytoplankton community composition was significantly different between spring, summer and winter. Shifts in microphytoplankton community composition from *Skeletonema* spp. dominated, to *Chaetoceros* coastal spp. dominated, to mixed species communities were observed (Figure 3.2). The extent and timings of these shifts were different between 2015 and 2016 (Figure 3.2). These shifts in community structure and cell abundance are likely to occur in response to changes in environmental conditions such as temperature and ocean chemistry (Jo et al., 2017). A further study by Fragoso et al. (2016) found that phytoplankton community structure between spring and summer varied depending on hydrographic characteristics such as temperature, salinity, and nutrient concentrations. The highest abundances of *Skeletonema* spp. occurred in early spring, when the water column was cooler and more stratified, relative to summer (Chapter 2). Higher abundances of *Skeletonema* spp. were observed during spring and also early summer in 2015, in comparison to the high abundances of *Skeletonema* spp. which were only observed in spring 2016. The lower degree of stratification during late spring and early summer months and higher temperatures observed in 2016 could be responsible for this. When the water column was warmer and with varying degrees of stratification, *Chaetoceros* coastal spp. dominated with a mixed assemblage of other species. These two dominating taxa have different morphological traits. Both are chain forming species with *Skeletonema* spp. forming long straight chains, and *Chaetoceros* coastal spp. produces protuberances in the form of chitin spines. *Chaetoceros* coastal spp. can also form long straight chains, and chains of varying spatial orientations including spirals. These morphological differences are likely to have an affect on sedimentation rate, discussed later. Dinoflagellates were abundant in spring and late summer in 2015 and *Katodinium* spp. were dominant (Chapter 2, Section 2.3.1.3). In 2016, peak abundances of dinoflagellates were observed in summer and *Scripsiella* spp. were dominant (Chapter 2, Table A.2). Generally, ciliates were less abundant than dinoflagellates, and peaked following the spring bloom of diatoms in both sample years (Chapter 2, 2.13). Shifts in microphytoplankton community composition affect the size distribution of cells, and morphology of the assemblage, which in turn affects sedimentation rate (e.g. Bienfang, 1981b; Pitcher et al.,

1989; Finkel et al., 2010; Burd et al., 2016). Analysis of microphytoplankton community composition within and between the two sample years highlights the extent of which the community can vary. This is important to consider when assessing sedimentation rates.

Microphytoplankton community sedimentation ranged seasonally from 0.59 to 1.24 m d^{-1} with maximum sedimentation rates observed in spring (day 105) in 2015, and ranged from 0.71 to 1.43 m d^{-1} with maximum sedimentation rates observed in spring (day 153) in 2016. There was no significant difference in sedimentation rate between spring, summer, and winter seasons, or depths above and below the pycnocline, in either of the sample years. This lack of significance could be a result of the number of samples per season, as other studies have found significant differences between seasons, but not necessarily with sample depth (Peperzak et al., 2003; Guo et al., 2016). Guo et al. (2016) used four replicates per sample date, three of which were used for community sedimentation rate calculations. Peaks in microphytoplankton community sedimentation rate occurred when the community assemblage was mixed (e.g. day 105 & 126 in 2015 below the pycnocline; Figure 3.2 & 3.3). A mixed community with different cell sizes, shapes, and morphologies has the potential to enhance sedimentation rates through interactions between cells that may contain protuberances (spines or arms), which encourages aggregation and potentially sedimentation (Bravo and Figueroa, 2014). However, this was not the case all the time, and other interacting factors were certainly important in further explaining this relationship. In 2015 and the majority of 2016, when there was dominance of the community composition by one species, sedimentation rates seemed less variable when compared to dates where the composition was mixed. Assessing community sedimentation is important as there is likely to be interaction between cells which influences sedimentation. However, genus-specific sedimentation rates further enhance understanding of which key species could be driving overall community sedimentation rates.

Genus-specific sedimentation rates demonstrate clearly that *Skeletonema* spp. and *Chaetoceros* spp. (Figure 3.5 and 3.6) were driving the community sedimentation rate in both years (Figure 3.3), because they dominated the community composition (Figure 3.17). Sedimentation rates of *Skeletonema* spp. range from 0.43 m d^{-1} (Peperzak et al., 2003) to 1.28 m d^{-1} (Guo et al., 2016), using natural microphytoplankton assemblages in SETCOLs. This study found mean sedimentation rates of *Skeletonema* spp. to be within this reported range; 0.80 m $d^{-1} \pm 0.16$ SD in 2015 and 0.76 m $d^{-1} \pm 0.22$ SD in 2016. *Chaetoceros* spp. mean sedimentation rate was very similar between 2015 (0.92 m $d^{-1} \pm 0.22$ SD) and 2016 (0.91 m $d^{-1} \pm 0.30$ SD), and high in comparison to maximum rates of 0.20 m d^{-1} observed by Peperzak et al. (2003). However, this difference could be due to the sedimentation rate of *Chaetoceros* in this study were composed of a number of different species, whereas Peperzak et al. (2003) reported sedimentation rate was specifically for *Chaetoceros radicans*. Diatom sedimentation rates are known to be highly species-specific (e.g. Smayda and Bienfang, 1983; Waite et al., 1992a). This is also shown in this study when comparing seasonal sedimentaton rates of the key species (Figure 3.5 & 3.7). *Pleurosigma* spp. were found to have a much wider range (0.60 to 2.12 m d^{-1}) of seasonal sedimentation rates when compared to *Cylindrothecae* spp. (range 0.42 to 1.29 m d^{-1}). The morphology of these taxa are different, *Cylindrothecae* spp. has a typical body length of 6 to 50 μm with long extended needle like edges, and *Pleurosigma* spp. is typically wider with a length range of 65 to 75 μm (Kraberg et al., 2010).

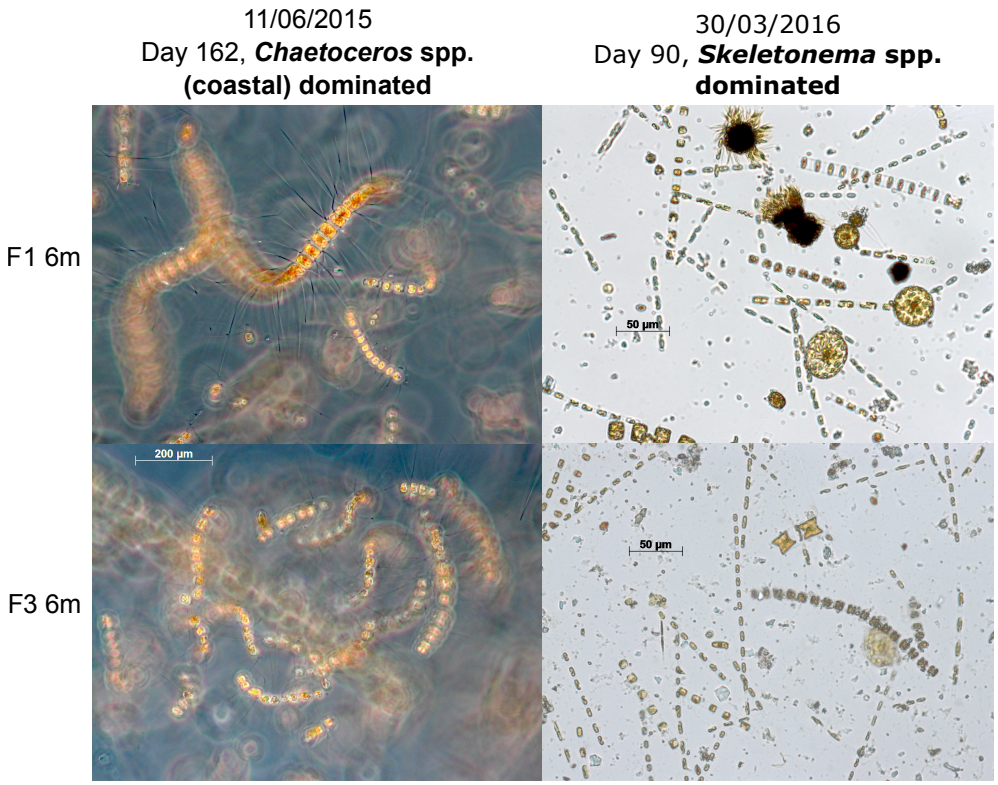

Figure 3.17: Examples of microscope field of views dominated by *Chaetoceros* spp. (coastal) and *Skeletonema* spp. from 11/06/2015 SETCOL fractions F1 and F3 (samples from 6 m depth), and 30/03/2016 SETCOL fractions F1 and F3 (samples from 3 m depth)

This is a key demonstration of how morphological differences between species could be an important factor (in addition to physiological and environmental factors) in explaining sedimentation rates.

Dinoflagellates were found to have a significantly higher sedimentation rates relative to diatoms and ciliates (Figure 3.4). This is in line with other studies that have found variable sedimentation rates between dinoflagellate taxa, which are generally higher than those of diatoms (Smayda and Bienfang, 1983; Kamykowski et al., 1992). Dinoflagellates are composed of thick cellulose plates which are denser (1.5 x 10^3 kg m^{-3}) than seawater (Vogel, 1983; Simon et al., 2009). Despite their excess density, dinoflagellates are able to swim using their flagella to seek light and nutrients or evade predation (Smayda, 1997). Swimming speeds of some species have been reported to be between 26 to 52 m d^{-1} (Lewis et al., 2006; Guo et al., 2016), which was significantly faster than their average sedimentation rate calculated in this study 1.25 m d^{-1} $\pm$ 0.03 SE. However, reported swimming velocities of the key taxa in this study, *Scripsiella* and *Gyrodinium* spp., were lower than the previous range reported at 13.20 and 26.30 m d^{-1} respectively (Table 3.2). Additionally, other records of *Scripsiella* and *Gyrodinium* spp. sedimentation rates fell within the range observed in this study (e.g. Kamykowski et al., 1992; Peperzak et al., 2003). Despite their higher sedimentation rate, dinoflagellate dominated microphytoplankton communities have a lower contribution to carbon flux relative to diatoms, as they generally disintegrate in the water column (Guo et al., 2016). However, cyst formation is a key component of many dinoflagellates life cycle, in which

Table 3.2: Key dinoflagellate swimming velocities, shape, equivalent spherical diameter (ESD), sedimentation rates, and density. Images of *Katodinium* spp. from King County (2017), *Scripsiella* spp. from The University of British Columbia (2012), and *Gyrodinium* spp. from Swedish Meterological and Hydrological Institute (2018). All information from Kamykowski et al. (1992) except [1] Cohen (1985), [2,3] Smayda (2000), [4] Peperzak et al. (2003)

Dinoflagellate		Swimming velocity m d^{-1}	Size ESD	Sedimentation rate m d^{-1}	Density g cm^{-3}
Katodinium spp.	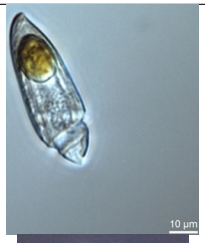	7.5[1] to 32.8[2]	-	0.43[3]	-
Scripsiella spp.	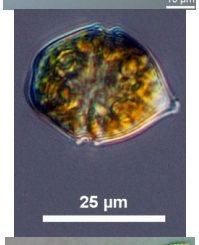	13.20	21.60	0.77	1.08
Gyrodinium spp.	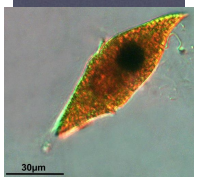	26.30	33.20	1.71[4] to 3.70	1.09

they can induce a resting phase until optimal environmental conditions occur (Bravo and Figueroa, 2014). Therefore, not all dinoflagellates may disintegrate in the water column as many can form benthic resting cysts, which are later re-dispersed into the water column. At LY1 dinoflagellates made up a low proportion of the total microphytoplankton community composition, contributing <3 %, and <20 % in 2015 and 2016 respectively. Diatoms dominated the microphytoplankton community composition at LY1, but dinoflagellates had significantly higher sedimentation rates than diatoms. High sedimentation rates and the fact that dinoflagellates form cysts as part of their life cycle, suggests less abundant taxa still form an important component of carbon export.

Ciliates formed between <2 %, and <10 % of the total microphytoplankton community composition in 2015 and 2016 respectively. They are important grazers of planktonic bacteria (alongside heterotrophic dinoflagellates and mesozooplankton) and ciliates can graze more than 59 % of primary production in coastal environments (Calbet and Landry, 2004; Ichinotsuka et al., 2006). Grazing is selective with rates depending on the size, shape, and biochemical composition of the food (Verity and Smetacek, 1996; Ichinotsuka et al., 2006). Additionally, ciliates are able to swim in response to light, and a range of chemical and mechanical cues (Fenchel and Jonsson, 1988). Ciliates (0.81 m d^{-1} $\pm$ 0.07 SD) had similar sedimentation rates to diatoms (0.83 m d^{-1} $\pm$ 0.03 SD) possibly as an adaptive response to sediment in line with their food source.

Chain formation was found to influence diatom sedimentation rates. For a number of sample dates,

as chain length increased sedimentation rates increased (Figure 3.11 & 3.13). This is in agreement with other studies e.g. Smayda (1970); Reynolds (2006); Landeira et al. (2014). However this trend was not universally found on all of the sample dates which is in agreement with other studies which have found that sedimentation rates are not systematically linked to chain length (e.g. Smayda and Bienfang, 1983; Waite et al., 1992b). There were exceptions to this trend including two sample dates (day 97 above, and 105 below the pycnocline in 2015) when sedimentation rates decreased as chain length increased. *Skeletonema* spp. dominated the chain forming taxa on day 97 above the pycnocline when this inverse relationship with sedimentation occurred. Other studies have also found an inverse relation between *Skeletonema* spp. chain length and sedimentation rate (Smayda and Boleyn, 1966; Smayda, 1970; Waite et al., 1992a). When *Skeletonema* spp. and *Chaetoceros* coastal spp. dominated the community composition at similar cell densities (Figure 3.2), community sedimentation rates of *Skeletonema* spp. dominated day 98 were lower (0.59 m d^{-1}) than *Chaetoceros* spp. dominated day 162 (0.85 m d^{-1}). This could be due to a range of factors such as differences in time of sampling dates and environmental conditions, morphological or physiological differences between the two taxa, and the species make-up of the remaining community composition. Differences in chain length abundances may also be a factor with a higher abundance of longer chain *Chaetoceros* spp. on day 162 relative to *Skeletonema* spp. on day 98 (Figure 3.10). Lower abundance of longer chain lengths of *Skeletonema* spp. resulted in a lower community sedimentation rate when compared to day 162 where there was a higher abundance of longer chained *Chaetoceros* coastal spp. which sank faster. The variation between species chain length and sedimentation rate could be an adaptive response to modify sinking rates based on the environmental conditions. For example, chain formation and higher sedimentation rates have been suggested to be advantageous to microphytoplankton through increased access to nutrients (Smayda, 1970). However, this advantage depends on local nutrient conditions and turbulence (BjÆrke et al., 2015; Dell'aquila et al., 2017). Small scale turbulence may replenish nutrients but it also has the ability to translocate grazers, which have the ability to fragment chains as a response to chemical cues (BjÆrke et al., 2015). Dead and metabolically stressed chains of cells sink faster than solitary cells, and in some cases there is find no clear relationship between cell size or shape, which suggests the physiological/ biochemical status of a cell is more important than morphological factors for determining sedimentation rates (Waite et al., 1997; Peperzak et al., 2003; BjÆrke et al., 2015).

Total particulate carbon sedimentation rates calculated from SETCOL experiments, provide valuable information on the transport of carbon from the surface waters. There was large variation in total carbon sedimentation rates observed above and below the pycnocline in spring and early summer, which could be a driven by two factors (Figure 6.1). Firstly, there was a large degree of variation in microphytoplankton cell abundance and composition. In comparison to late summer/ winter, when cell abundance was relatively low, carbon sedimentation rates were similar between these dates when compared to spring. There was no correlation observed between microphytoplankton community sedimentation rates and total carbon sedimentation rate. Peaks in microphytoplankton community sedimentation did not coincide with higher total carbon sedimentation. Therefore, higher sedimentation rates of microphytoplankton community does not

necessarily translate into higher total carbon sedimentation rates. The peak in microphytoplankton community sedimentation on day 153, was driven by *Chaetoceros* spp. and occurred on the same sampling day as the minimum total carbon sedimentation rates in samples from above the pycnocline (0.45 μg C m d^{-1}). This means that despite the high sedimentation rate of *Chaetoceros* spp., the carbon content of the suspended fraction in SETCOL was higher than the sinking *Chaetoceros* spp. fraction. Although diatoms dominated the microphytoplankton community at LY1, dinoflagellates had significantly faster sedimentation rates relative to diatoms and ciliates (Figure 3.4). During this period of low carbon sedimentation rates on day 153, sedimentation rates of dinoflagellates were also low (0.94 m d^{-1}). The maximum carbon sedimentation rate occurred above the pycnocline on day 188 (1.64 μg C m d^{-1}) when microphytoplankton community sedimentation rates were low, cell abundance was relatively low, and dominated by *P. seriata*. However, sedimentation rates of dinoflagellates were high (1.51 m d^{-1}) on this day relative to previous days. Microphytoplankton community sedimentation rate is a poor indicator of total carbon sedimentation rate, and it is important to consider microphytoplankton groups and individual taxon sedimentation rate. Additionally, there are sources other than microphytoplankton that need to be considered when accounting for total particulate carbon sedimentation rates. In a coastal environment, terrigenous organic and inorganic material will form an important contribution to the carbon budget, which is not analysed in these SETCOL experiments, and is discussed in Chapter 4.

Microphytoplankton community structure is a key determinant in influencing total community sedimentation behaviour, aggregate formation, and export (Riebesell, 1989; Turner, 2015; Bach et al., 2016; Guo et al., 2016). Shifts in microphytoplankton community composition in response to changing environmental conditions, have been observed to affect community sedimentation rates at LY1. Community composition at LY1 was dominated by diatoms which, relative to other microphytoplankton groups in other studies, are major contributors to export flux (Guo et al., 2016; Bannon and Campbell, 2017). However, high dinoflagellate sedimentation rates and the lack of a relationship been microphytoplankton community sedimentation rates and total carbon sedimentations rates, suggests other groups of microphytoplankton and other particulate material is important in addition to diatoms in explaining carbon sedimentation at LY1 (e.g. TEP, bacteria, inorganic material). Additionally, the lack of relationship between microphytoplankton community sedimentation rates and total carbon sedimentations rates could be a result of a time lag in response to environmental factors.

3.4.2 Environmental and biochemical controls on sedimentation rate

The effect of inorganic nutrient concentration, environmental, and biochemical parameters on microphytoplankton sedimentation rates depended on sample year, and depth above versus below the pycnocline. Phosphate depletion above the pycnocline in 2015 related to lower sedimentation rates, which was not expected as higher sedimentation rates have been linked to nutrient depletion (Table 3.1). Bienfang et al. (1982) found low phosphate concentrations were related to lower sedimentation rates with laboratory cultured unialgae diatom species. However, in studies using natural microphytoplankton assemblages have found increased sedimentation during phosphate

depletion (Bienfang and Harrison, 1984; Waite et al., 1992a), whilst others have found no correlation (Bienfang, 1981b; Culver and Smith, 1989; Johnson and Smith, 1986; Guo et al., 2016). This could be due to differences in the microphytoplankton community composition used and subsequent differences in nutrient uptake rates. Silicate depletion was related to sedimentation rate increases below the pycnocline in 2016. Bienfang et al. (1982) found that silicate depletion elicited the largest increase in sedimentation rates out of phosphate and nitrate in all four laboratory cultured test species. Silicate is an essential nutrient for diatom growth and therefore silicate limitation could have elicited increased sedimentation rates at LY1. In this study, nitrate had no significant relationship to community sedimentation rate for either year or depth. There are conflicting results in the literature regarding the effect of nutrient status on sedimentation rates. Results are dependent on what type of microphytoplankton are cultured (unialgal or mixed assemblages), natural assemblages, methodology of estimating sedimentation rates, and experimental design. Despite differences in the relationship between nutrient availability and sedimentation rates, it is generally accepted that there are genus specific differences in sedimentation response to nutrient declines (Waite et al., 1992a). For example, *Skeletonema* spp. is suggested to be less sensitive to nutrient depletion than *Chaetoceros* spp. (Waite et al., 1992a). This means when *Skeletonema* spp. dominated, nutrient fluctuation could have a lesser effect on sedimentation rates when compared to *Chaetoceros* spp. dominated dates. When investigating community sedimentation rates of a mixed assemblage of species, with mixed requirements for certain nutrients, it is hard to distinguish the relationship between nutrient concentration and community sedimentation rates because of these different requirements.

Wind speed and pycnocline depth were the two significant factors related to microphytoplankton community sedimentation rate. Increased wind speed and pycnocline depth were related to higher sedimentation rates below the pycnocline in 2015 (Table 3.1). Increased wind speed effects water column turbulence and physical mixing, which could lead to higher sedimentation rates of stressed cells as they are uniformly mixed and receive insufficient light (Huisman et al., 2002). Additionally, water column stratification is a key process in determining the resources available for phytoplankton growth (Van De Poll et al., 2013). A deeper pycnocline could entrain microphytoplankton out of photic zone, which could further induce physiological stress, and increased sedimentation rates. Conversely, shallower pycnocline depths corresponded to higher sedimentation rates above the pycnocline in 2016. These shallower pycnocline depths could create sub-optimal conditions for microphytoplankton (e.g. light intensity) resulting in physiological stress and induce higher sedimentation rates. The remaining physical environmental parameters were generally poorly correlated to community sedimentation rates in 2015 and 2016 both above and below the pycnocline (Table 3.1). Other studies have also found poor correlation with environmental or physical parameters, and suggested it to be a result of delays between environmental conditions and the associated physiological responses (Bienfang, 1981b; Pitcher et al., 1989; Guo et al., 2016). The time frame of ecological responses to continuously changing environmental conditions is suggested to be controlled by the generation time of the shortest lived species (Reynolds, 2006). This time delay is a plausible explanation for the lack of correlation observed in this study,

in addition to the suggestion that biological factors play a more important role in explaining sedimentation rates (Johnson and Smith, 1986; Peperzak et al., 2003; Guo et al., 2016).

Altering cell biochemistry in response to various environmental factors, is one mechanism in which microphytoplankton can regulate cell density, and therefore sedimentation rates (e.g. Jo et al., 2017). Regulation of cell density to modify cell buoyancy has been suggested to be more important than particle size (e.g. Waite et al., 1997; Peperzak et al., 2003; Erga et al., 2010; BjÆrke et al., 2015). However, studies focusing on the relationship between all three of the main macromolecular components of microphytoplankton (protein, carbohydrate, and lipids), which determine buoyancy and therefore sedimentation, are lacking. Previous studies have focused on bulk carbon measurements (e.g. Johnson and Smith, 1986; Pitcher et al., 1989; Szyper and Karl, 1991), or one macromolecular component (Richardson and Cullen, 1995). Synthesis and storage of protein, carbohydrate and lipid during different growth phases is likely to affect cell buoyancy (e.g. Diekmann et al., 2009; Erga et al., 2015; Bannon and Campbell, 2017). The typical biochemical composition of natural microphytoplankton populations is on average 40 $\pm$ 7, 26 $\pm$ 14, and 15 $\pm$ 8 % protein, carbohydrate, and lipid respectively (Emerson and Hedges, 1988; Ríos et al., 1998). The lipid fraction (920 kg m^{-3}) is the less dense compared to protein (1300 kg m^{-3}), and carbohydrate (1500 kg m^{-3}), and accumulation of lipid has been linked to the senescent phase (Smayda, 1970; Reynolds, 2006). This suggests that senescent microphytoplankton following the end of a bloom, should have lower sedimentation rates (Smayda, 1970), which contradicts the theory that post bloom microphytoplankton communities are significant contributors to carbon export (Guo et al., 2016). The percentage contribution of lipid per cell was observed to increase from spring to winter sample dates (Figure 3.15). Sedimentation rate of lipid was inversely related to microphytoplankton community sedimentation rate (Table 3.1). Therefore, at higher lipid concentrations, which occurred in late summer/ winter, microphytoplankton community sedimentation rates were lower as expected (Figure 3.3). Carbohydrate and protein dominated microphytoplankton biochemical composition in 2016, and were negatively correlated with community sedimentation rates above the pycnocline (Figure 3.16). Other studies using cultures of *T. weissflogii* and *Ditylum brightwellii* have found no correlation between carbohydrate content and sedimentation rates (Fisher and Harrison, 1996), and increased sedimentation rates with an increase of carbohydrate (Richardson and Cullen, 1995). This study, and others, suggest that cell biochemistry is an important factor in determining cell sedimentation rates. This is important information in terms of further understanding sedimentation mechanisms, but also in terms the quality and composition of organic matter being exported.

3.4.3 Evaluation of methodology

Generally, the use of SETCOLs to investigate sedimentation rates of plankton is well accepted and widely used (e.g. Pitcher et al., 1989; Kiørboe et al., 1996; Waite and Nodder, 2001; Peperzak et al., 2003; Guo et al., 2016; Cavan et al., 2017). Peperzak et al. (2003) has summarised the disadvantages of the use of SETCOL, and causes for errors in sedimentation rate calculations, which include wall effects of the measuring device imposed onto the sinking particle, presence of high cell densities, non-linearity between incubation time and settled fraction, and incubation

conditions that differ from *in situ* temperature and irradiance.

To minimise sedimentation rate calculation errors in this study, a review of SETCOL methodology in the literature was undertaken. Incubation period for this study was selected following a literature search of other studies using natural phytoplankton assemblages (e.g. Bienfang et al., 1983; Johnson and Smith, 1986; Pitcher et al., 1989; Szyper and Karl, 1991; Waite et al., 1992a). SETCOLs containing samples from above and below the pycnocline were incubated at the same temperature, despite differences between depths in *in situ* temperature, because both SETCOLs were mounted on the same stand (Figure B.1). However, temperature differences between above and below the pycnocline sample depths were small (<0.6°C) with only one occasion where the difference was 1°C. Other studies using SETCOL methods have also carried out incubations of samples from two different depths in identical experimental conditions (Johnson and Smith, 1986). Additionally, SETCOLs would have been incubated at exactly *in situ* temperature which was not possible in this study due to equipment failure. Incubations were carried out in the light because the aim of this experiment was to take a "snap shot" of the microphytoplankton community in a parcel of water, transfer it to SETCOLs with similar environmental conditions and study sedimentation rates. Other studies investigating microphytoplankton community sedimentation rates have also been carried out in light (e.g. Johnson and Smith, 1986; Pitcher et al., 1989; Riebesell, 1989; Peperzak et al., 2003). It has been shown that physiologically stressed phytoplankton cells have higher sedimentation rates compared to non-stressed cells (Eppley et al., 1967; Peperzak et al., 2003). The agreement between sedimentation rates observed in this study with other studies, suggests SETCOL incubation conditions had a negligible affect on calculated microphytoplankton sedimentation rates.

3.5 Conclusions

The aim of this study was to investigate community composition, environmental, and biochemical drivers on seasonal microphytoplankton community sedimentation rates. Key conclusions include:

1. Diatoms specifically *Skeletonema* and *Chaetoceros* spp., dominated the microphytoplankton community composition at LY1 during 2015 and 2016. There were community composition shifts between seasons in response to environmental changes. For example, *Skeletonema* was present at maximum abundances during spring, and when abundances of *Skeletonema* decreased, *Chaetoceros* spp. abundance increased. The microphytoplankton community composition was composed of a variety of taxa throughout the sample season. Community composition analysis was important for determining sedimentation rates. Microphytoplankton community sedimentation rate was observed to change when there was a shift in community structure.

2. The abundance and chain length of chain forming diatoms varied seasonally and with species. Abundances of longer chain lengths (>5) were higher in spring and summer. Sedimentation rates increased with increasing chain length but this relationship had a number of caveats including sample day, depth above versus below the pycnocline, sample year, and

community composition. However, chain formation and high sedimentation rates of long chains of diatoms are important for transporting carbon from the surface. Further evidence of the importance of long diatom chains (e.g. *Skeletonema* spp., *Thalassiosira* spp., *Guardinia* spp.) to the sinking flux of POM includes observations in sediment trap deployments at 20 m at LY1 (Chapter 4, Figure 4.24).

3. Dinoflagellates had significantly faster sedimentation rates relative to diatoms and ciliates. However, sedimentation rate was species-specific and varied seasonally. It is likely that this was driven by morphological and physiological differences between species. Microphytoplankton community sedimentation rate was not correlated with total particulate carbon sedimentation rate. Diatoms dominated community composition at LY1 and community sedimentation rates. However, dinoflagellates were also important in explaining total particulate carbon sedimentation rates. This highlights the importance of minor components of microphytoplankton community composition, and other sources of carbon, role in explaining total particulate carbon sedimentation rates.

4. Higher wind speeds and deeper pycnocline depths were significantly correlated with higher microphytoplankton community sedimentation rates. No correlations were observed between other environmental variables with microphytoplankton community sedimentation rates. This could be due to species-specific responses and the time-lag between continual environmental changes and physiological responses.

5. There was a negative relationship between lipid concentration per cell sedimentation rates, and microphytoplankton community sedimentation rates in 2015. Cells contained a higher proportion of lipid towards the end of summer and winter, relative to earlier sampling dates, which coincided with lower community sedimentation rates relative to spring. Protein and carbohydrate dominated cell biochemical composition in 2016, and were inversely correlated with microphytoplankton community sedimentation rates. The lack of a consistent trend between biochemical composition and community sedimentation rates could be a result of other simultaneous factors affecting sedimentation rates.

It is difficult to isolate the individual effects of factors influencing sedimentation rate when it is likely to be a suite of interacting and interchangeable factors controlling sedimentation. Due to the complex dynamics between microphytoplankton ecology, continuously changing environmental conditions, and associated sedimentation rates, many studies often focus in detail on one trait as the driving cause for sedimentation. Given the complexity of the processes controlling sedimentation, and its importance in global biogeochemical cycles, it is a key area for further research.

Chapter 4

Seasonal biogeochemical composition of particulate material at sequential stages of transport in the marine environment

4.1 Introduction

Coastal environments represent significant areas for both organic carbon production, preservation, and remineralisation (Cowie and Hedges, 1992b). The sources and processes that control the transport of particulate material (PM) through the water column to marine sediments, can have substantial implications for global biogeochemical cycles (Wakeham and McNichol, 2014). Decomposition of the organic component of particulate material (POM) results in its biochemical transformation, and nutrient regeneration (or remineralisation; Loh, 2005). Degradation, decomposition, and remineralisation all refer to biologically catalysed reduction, which usually results in the conversion of organic carbon, nitrogen, phosphorous and sulphur into inorganic products (Loh et al., 2008a). The extent of these processes depend on POM properties, such as size, shape and residency time in the water column, and biogeochemical composition (Cripps and Clarke, 1998). The composition of PM is heterogeneous in nature and in coastal environments, both marine and terrestrial derived PM play an important role in carbon export and cycling (Hedges et al., 1997). However, it is generally accepted that marine POM is more reactive than terrestrial POM (Cowie and Hedges, 1984; Wakeham et al., 1997b). Additionally, the organic component of PM in coastal systems is likely to be minor relative to inorganic material. The complex biogeochemical composition of PM as a result of source inputs, and continuous modification processes in the water column, results in the selective preservation of more stable molecular compounds, and in the loss of labile compounds (Cowie and Hedges, 1994; Wakeham et al., 1997b; Dauwe et al., 1999). This selective degradation and preservation of compounds can have important implications on the fate of POM in terms of whether it is remineralised or exported.

A further key factor affecting POM fate in the water column includes its classification into suspended or sinking fractions. There are a wide spectrum of particles present in the water column with diverse properties, and at different stages of transport. Generally, they are simplified into small (<20 μm) slow-sinking, and large (>20 μm) fast-sinking particles (Wakeham and Lee, 1989,

1993). Suspended particulate material (SPM) can be composed of small particles dominated by microphytoplankton cells, bacteria, clay minerals, and detritus (Lampitt et al., 1993; Wakeham and Lee, 1993). Typically SPM has long residence times in the water column and is collected via filtration methods (Rontani et al., 2011). Larger, faster sinking particles commonly consist of zooplankton faecal pellets, large phytoplankton cells, and aggregated material (Sanders et al., 2014; Turner, 2015). A number of studies have shown that the majority of PM was present as suspended, slow-sinking particles (e.g. Alonso-Gonzalez et al., 2010; Riley et al., 2012; Cavan et al., 2017). However, SPM is predicted to be a minor contributor to overall mass flux relative to larger, faster sinking PM, as a result of slow sinking speeds and long residency times (Wakeham and Lee, 1993; Turner, 2015). The majority of studies to date have focused on open-ocean sites, with few studies focusing on coastal systems. Size, shape, and biogeochemical composition of PM will have an effect on the fate of PM during its transition through the water column.

A suite of biogeochemical tools have been used to characterise the source and diagenetic state of POM in the water column and sediments. The coupling of elemental compositions and ratios with stable carbon isotopes (δ^{13}C), have been used to determine carbon sources (e.g. Hedges et al., 1988b; Cowie et al., 1992; Loh et al., 2008b). Additionally, molecular-level analysis, and the use of organic biomarkers, provides information about source and diagenetic status of POM in the water column and sediments (e.g. Cowie and Hedges, 1992b; Wakeham et al., 1997b; Kiriakoulakis et al., 2001; Sheridan et al., 2002). Molecular-level analysis can provide information that would be excluded from routine bulk elemental analysis. For example, studies have found extensive degradation accompanied by minimal changes in bulk organic matter parameters (Hedges et al., 2001; Armstrong et al., 2002). Highly labile amino acids and lipids relative to bulk POM, provide information on the degradative state and relative proportions of phytoplankton groups contributing to POM (Wakeham et al., 1997a; Ingalls et al., 2006). Studies have used biochemical components such as lipids (Wakeham et al., 1997a; Parrish et al., 2005), amino acids (Cowie and Hedges, 1992b; Ingalls et al., 2006), carbohydrates (Cowie and Hedges, 1984), pigments, or a combination of biochemicals (Lee et al., 2000; Hedges et al., 2001; Wakeham et al., 2009), as markers of POM source and diagenetic status. These studies have enhanced understanding of how PM biogeochemical composition varies with source material, PM depth in the water column, and in response to modification processes. Coastal studies have observed a shift from POM of a marine predominance, to a relatively higher proportion of terrestrially derived POM during winter (Cowie and Hedges, 1984; Hedges et al., 1988b). Additionally, relative proportions of key biochemical compounds (carbohydrate, amino acids and fatty acids) were generally found to decrease with depth, and during transition through the water column into the sediment interface (Hamilton and Hedges, 1988; Cowie and Hedges, 1992b; Budge and Parrish, 1998; Fileman et al., 1998; Parrish et al., 2005).

Insights into seasonal shifts in PM source and biogeochemical composition are important for understanding temporal differences in composition of PM as particles sink. A recent study investigated the bulk biochemistry of suspended, slow, and sinking fractions of particulate and dissolved material collected over a seasonal cycle (Davis et al., 2018). However, few studies have included a molecular-level compositional comparison of SPM, sinking, and sediment samples at the same

time, depth, and location over a seasonal cycle (from March to November). This investigation, coupled with detailed microphytoplankton community composition and sedimentation rates calculated in Chapter 3, will provide a greater understanding of organic carbon source, biochemical composition, and transfer down the water column to sediments in a coastal setting. The analysis of multiple biochemicals will give an insight into the origin, transformation, and cycling of POM at a western Scotland coastal site.

4.1.1 Research objectives

The aim of this chapter was to investigate the seasonal biogeochemical composition of PM at different stages of diagenetic alteration: SPM, sinking material, and sediment. SPM was sampled from above and below the pycnocline to investigate compositional differences across a density discontinuity, where environmental, chemical, and biological parameters were different. Elemental, isotopic, and biochemical composition of different particulate fractions were collected and analysed from site LY1 in the Firth of Lorne. Molecular-level analysis of amino acids and fatty acids (together with bulk carbohydrate analysis) were selected as these biochemicals represented a large proportion of organic carbon, and they are well recognised source and degradation indicators. A selected range of amino acids and fatty acid biomarkers were used to determine the source and degradative state of organic material at respective stages of transport through the water column. This study aims to enhance understanding of the quantity and quality of organic material at sequential stages of transport in a coastal setting. Defining the biogeochemical composition of these particulate fractions was then used to determine the relative reactivity of SPM and sinking particulates described in Chapter 5. Research questions specific to this Chapter include:

1. How does the source of organic material change between suspended, sinking and benthic fractions?

2. What are the seasonal diagenetic trends in suspended, sinking and benthic fractions?

3. How do seasonal diagenetic trends change with sequential stages of transport from suspended, sinking and benthic fractions?

4.2 Methods

4.2.1 Sample collection

Samples were collected from the suspended, sinking and benthic fractions (Figure 4.1) on board the RV *Seol Mara* at site LY1 (Chapter 2, Figure 2.2) from March to November 2016 (Table 4.1). Suspended particulate material and sediment cores were taken on the first day of fieldwork. Sediment traps were also deployed on this day. On subsequent fieldwork days the sediment traps were collected after approximately 24 hours of deployment.

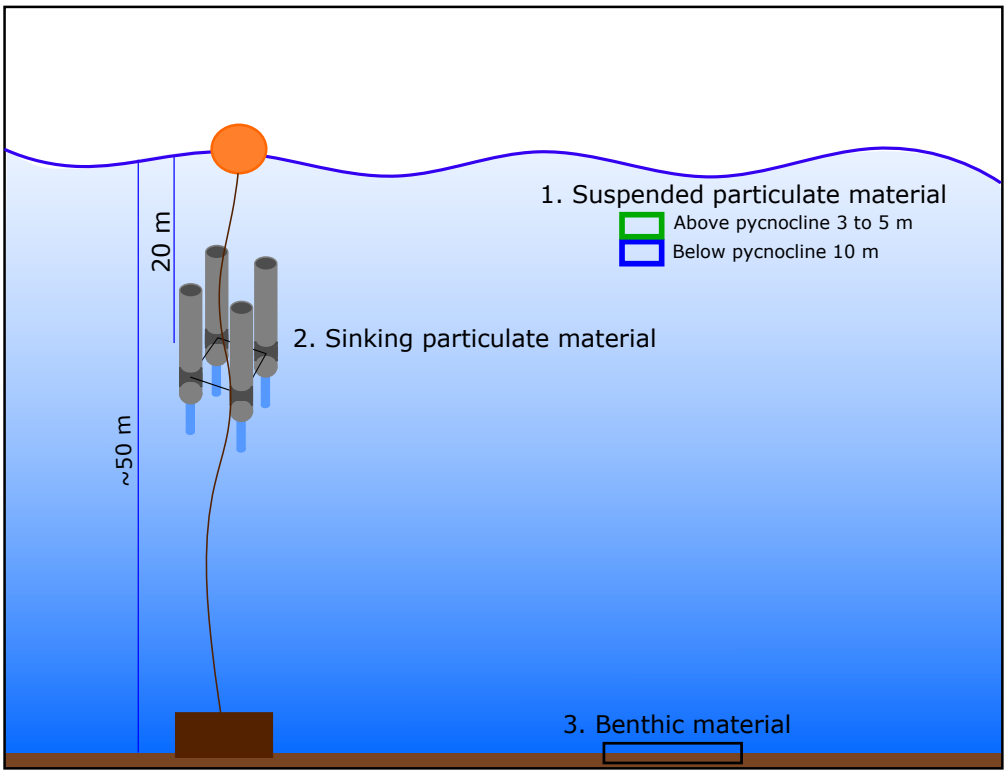

Figure 4.1: Schematic of suspended particulate material (SPM) collected from above and below the pycnocline, sinking particulate material using a sediment trap deployed to 20 m, and benthic material using a Craib corer from LY1 (approximately 50 m depth)

4.2.1.1 Suspended particulate material

A CTD (Seabird SBE 19, Sea-Bird Electronics) was deployed to determine the position of the pycnocline. Approximately 25 L of seawater was collected using 5 L Niskin bottles from two depths above and below the pycnocline (Table 4.1). Water from each of the sample depths was pooled into Nalgene containers and stored in a cool box until samples were returned to the laboratory and processed.

4.2.1.2 Sediment trap particulate material

Two moored sediment traps were suspended at a depth of 20 m below the surface to collect sedimenting PM (Figure 4.2). Each sediment trap consisted of four grey tubes (110 cm height x 11 cm diameter) with removable clear plastic collecting tubes. Two traps were deployed in order to obtain larger samples of sedimenting material. They were deployed at LY1 on separate moorings as close as logistically possible to each other. A high salinity solution (100 g L^{-1}) was placed in two of the four collecting cups, in a diagonal arrangement, prior to deployment to reduce resuspension losses and microbial degradation. Two collecting cups were left without the high salinity treatment, as these samples were used for reactivity experiments (Chapter 5). Sediment traps were deployed for approximately 24 hours. Upon retrieval of the traps, the collection cups were removed and pooled into two Nalgene containers, one for salinity treated and one for no treatment. Nalgene containers were placed into cool boxes and processed on returning to the laboratory.

Table 4.1: Sample collection dates for suspended particulate material (SPM) taken from above and below the pycnocline, sediment traps deployed to 20 m depth, and sediment cores take from approximately 50 m

Date	Day in year	Suspended particulate material	Sediment trap at 20 m	Sediment $\sim$ 50 m
30/03/2016	90	4 & 10 m	Deployed	-
31/03/2016	91	-	Collected	-
06/04/2016	97	5 & 10 m	Deployed	3 cores
07/04/2016	98	-	Collected	-
16/05/2016	137	5 & 10 m	Deployed	3 cores
17/05/2016	138	-	Collected	-
01/06/2016	153	3&10 m	Deployed	3 cores
02/06/2016	154	-	Collected	-
05/07/2016	187	3 &10 m	Deployed	3 cores
06/07/2016	188	-	Collected	-
01/08/2016	214	3 & 10 m	Deployed	3 cores
02/08/2016	215	-	Collected	-
15/08/2016	228	3 & 10 m	Deployed	3 cores
16/08/2016	229	-	Collected	-
13/09/2016	257	5 & 10 m	Deployed	3 cores
14/09/2016	258	-	Collected	-
10/10/2016	284	3 & 10 m	Deployed	3 cores
11/10/2016	285	-	Collected	-
07/11/2016	312	3 &10 m	Deployed	3 cores
08/11/2016	313	-	Collected	-

4.2.1.3 Benthic material

Three sediment cores were taken using a hydraulically dampened Craib corer lined with an acrylic core tube (24 cm height x 5.9 cm diameter; Figure 4.3). The corer was attached to the winch and lowered to the sediment surface to collect sediment cores with undisturbed water-sediment surface layer. Triplicate cores were obtained which were then sliced for the top 1 cm of sediment. Coring was repeated if the surface of the sediment was found to be disturbed. The sediment slice was placed in a pre-labelled zip lock bag, wet weight was taken, and then the sample was frozen at -20°C (carbon and nitrogen, and carbohydrate samples) or -80°C (fatty acid, amino acid, and pigment samples).

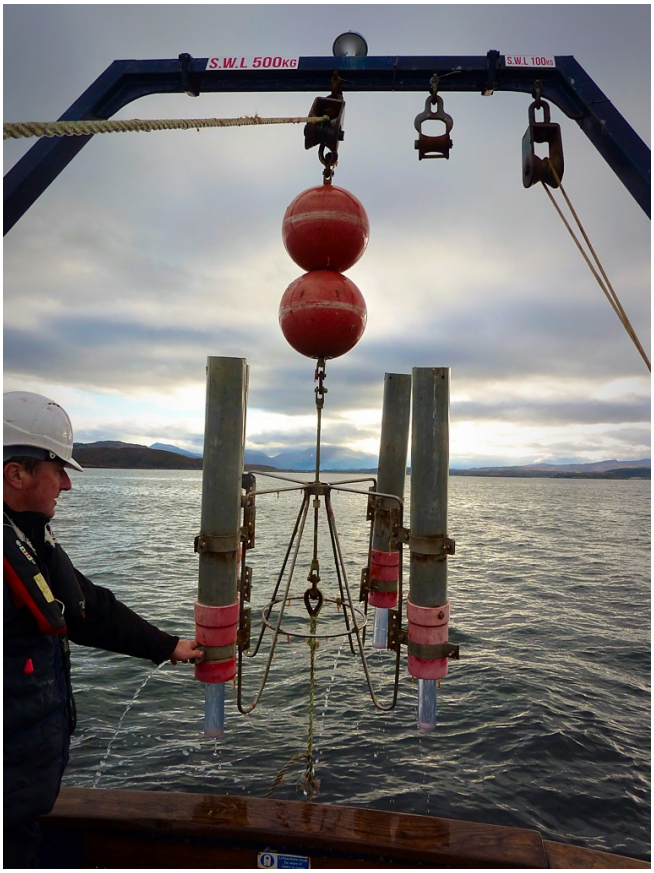

Figure 4.2: Sediment trap designed by Leftley and MacDougal (1991)

4.2.2 Sample processing

4.2.2.1 Suspended particulate material

SPM collected from above and below the pycnocline was filtered onto pre-weighed glass fibre (Whatman GF/F) and cellulose nitrate (Whatman) filters for a suite of biogeochemical analysis (all GF/F filters ashed at 450°C for 6 hours; Table 4.2) and the remaining fraction was used in SETCOL experiments (Chapter 3).

4.2.2.2 Sediment trap particulate material

In the laboratory pooled sediment trap material was sieved (mesh size 850 μm) to remove zooplankton. Due to the large volume of seawater the sediment slurry was collected in (Figure 4.4), sediment trap material was carefully homogenised in the Nalgene container and then split by volume into the desired number of fractions for analysis. Fractions were filtered in triplicate for the analyses listed in Table 4.3. Filters were washed with filtered seawater of a known salinity to remove excess salt and stored until analysis. The salinity of the filtered seawater could then be used to salt correct filter weights.

One fraction was used to calculate total dry mass of sediment trap material collected. This fraction

Figure 4.3: Fired Craib corer returning to the surface

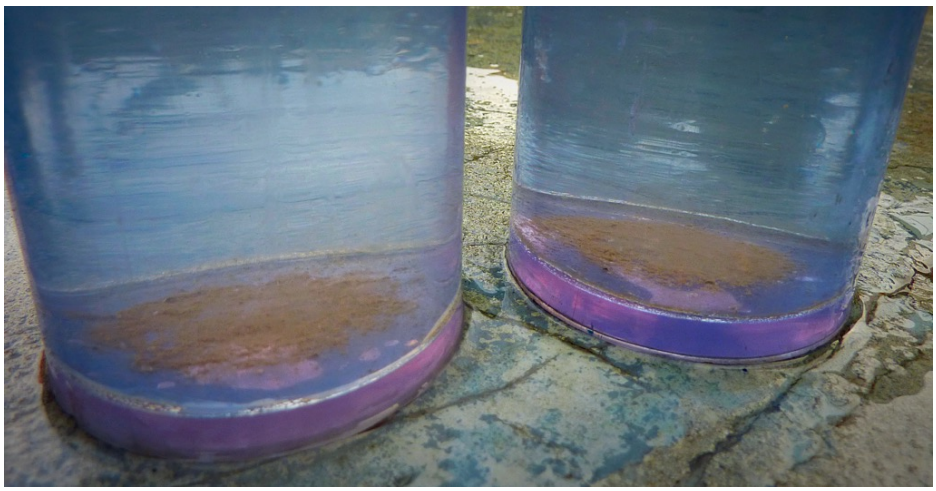

Figure 4.4: Collecting cups from sediment trap deployed for 24 hours containing sedimented particulate material

Table 4.2: Volumes of seawater filtered for analysis completed on suspended particulate material (SPM)

Analyses	Volume filtered (ml)	Filter type	Sample storage
Carbon & nitrogen	300	25 mm GF/F	-20°C
Organic carbon	300	25 mm GF/F	-20°C
Amino acids	1000	25 mm GF/F	-80°C
Fatty acids	1000	25 mm GF/F	-80°C
Carbohydrates	1000	25 mm GF/F	-80°C
Pigments	1000	47 mm GF/F	-80°C
Lithogenic elements	1000	25 mm Cellulose nitrate	Oven dried
Inorganic nutrients	50	25 mm GF/F	Filtrate -20°C

was filtered onto pre-weighed GF/F filters (450°C, 6 h) and the wet and dry weight was taken.

A fraction of the pooled sediment trap material that contained no salt was used in reactivity experiments (Chapter 5).

Table 4.3: Details of sediment trap material sample splits

Analyses	Fraction of split	Filter type	Sample storage
Carbon & nitrogen	1/8	25 mm GF/F	-20°C
Amino acids	1/8	47 mm GF/F	-80°C
Fatty acids	1/8	47 mm GF/F	-80°C
Carbohydrates	1/8	47 mm GF/F	-80°C
Pigments	1/8	47 mm GF/F	-80°C
Lithogenic elements	1/8	47 mm Cellulose nitrate	Oven dried
Total dry mass	1/8	47 mm GF/F	Oven dried

4.2.2.3 Benthic material

Sediment cores for fatty acids and pigment analysis were immediately stored in the dark and frozen at -80°C until analysis. The remaining cores were stored at -20°C, freeze-dried, and homogenised using an agate mortar at 350 rpm for 7 min. Samples were then placed back into the freezer until analysis (amino acid and carbohydrate analysis), or stored at room temperature (particulate carbon and nitrogen, and lithogenic tracer element analysis).

4.2.3 Biogeochemical analytical methods

4.2.3.1 Particulate carbon and nitrogen analysis

Particulate total carbon (TC), organic carbon (OC) and total nitrogen (TN) samples from SPM were taken by filtering 300 ml of seawater from above and below the pycnocline through pre-ashed (450°C, 6 h) 25 mm glass fibre filters (Whatman GF/F). A 1/8th fraction split of sediment

trap material was split into replicates and filtered (Table 4.3), and approximately 20 mg of freeze-dried sediment was used. For all sample types half of the replicates were used for TC and TN analysis, and the other half was acid treated for OC.

Filters for OC analysis were fumed (SPM and sediment trap filters) for 4 h in HCl saturated air to remove inorganic carbon. Filters (both acid treated and non-acid treated for TC/TN) were then dried overnight at 60°C and then folded into tin disks. Sediment samples for OC analysis were weighed into glass vials in which 1 ml sulphurous acid was added. Vials were placed into a vacuum desiccator overnight. Acid treated and untreated sediment samples were then weighed into tin disks. Samples were analysed with an ANCA NT prep system coupled with a 20-20 Stable Isotope Analyser (PDZ Europa Scientific Instruments, Northwich, UK). Calibration was performed using a solution of isoleucine (L-Isoleucinie, Europa STD) at concentrations of 1 μg N and 5.14 μg C. Standards were placed in tin caps (with Chromosorb W, PDZ Europa Ltd.) and oven dried at 60°C overnight. Calibrations were performed with series of isoleucine standard concentrations ranging from 5 to 100 μg N (25.7- 514 μg C) run at the beginning of each batch. Two reference samples (40 μg isoleucine) were analysed after every 8 samples to check the instrument precision (mean C instrument precision 99 % $\pm$ 0.06 SD and mean N instrument precision 99 % $\pm$ 0.02 SD) and a drift correction was applied. Separate samples from the same time point were run in duplicate (to test method precision), and all samples were blank corrected. The standard deviation (SD) of δ^{13}C values for a certain range of carbon (25.7- 514 μg C) were checked and data were used if SD was <0.5. The limit of detection ranged from 0.02 to 0.1 μg N and 0.1 to 2.1 μg C. Overall method precision varied between fraction type; precision in SPM above the pycnocline ranged from 0.1 to 22.6 %, in SPM below the pycnocline from 2.2 to 94.4 %, sediment trap material from 0.7 to 101.5 %, and in sediments from 0.9 to 39.1 % (Table C.1 % C.2).

4.2.3.2 Total hydrolysable amino acid analysis

Figure 4.5: Vials containing water column samples on 25 mm GF/F filters (samples 1 to 10) and sediment trap samples on 47 mm GF/F filters (samples 11 to 19) after addition of the internal standard

Total hydrolysable amino acids were analysed according to Cowie and Hedges (1992a). Freeze-dried GF/F filters were carefully placed in pre-labelled 7 ml glass vials with tweezers that had been rinsed in methanol and dichloromethane. Double distilled 6 N HCl was bubbled with N_2 for 10 minutes in a ultrasonic bath. Vials were flushed with argon gas for two minutes before adding 2 ml DD 6 N HCl (for 25 mm GF/F, 3 ml for 47 mm GF/F) whilst still flushing. Immediately after vials were removed from flushing, filters were submerged in the acid and homogenised, and

the vials were flamed shut. Vials were placed in a heat block at 155°C for 70 minutes. Whilst the vials cooled, the internal standard mixture was made with a ratio of *v/v* 1:1:1 α-Aminoadipic acid: ρ-Fluorophenylalanine: δ-Hydroxylysine, and between 50 to 500 μL added to samples depending on sample type and amount of material present on filters. Vials were opened, the internal standard mixture was added, and the vials were vortexed (Figure 4.5). Vials were placed in a centrifugal evaporator overnight. The residue was redissolved in 2 ml DI H_2O (for 25 mm GF/F, 3 ml DI H_2O for 47 mm GF/F), vortexed and placed in a ultrasonic bath for approximately 30 minutes. Samples were vortexed and then centrifuged (5 mins at 3000 rpm). Samples were filtered through glass fiber filters (Gelman A/E, 0.7 μm, 13 mm), pH adjusted with HCl and KOH to a range of between 9.5 to 10.5, placed into 2 ml high-performance liquid chromatography (HPLC) autosampler vials, and capped with a Teflon-lined septa.

Freeze dried sediment samples were pre-weighed (approximately 30 mg) into 7 ml glass vials and 1 ml DD 2 N HCl was added to remove any calcium carbonate present. Samples were then placed in the centrifuge-evaporator overnight. Analysis of sediment samples then followed the same procedure as the SPM on 25 mm GF/F samples as detailed above.

The high performance liquid chromatography (HPLC) equipment (Agilent) used for amino acid analysis consisted of a quaternary pump (1050 series), vacuum degasser (1050 series), temperature controlled ALS (1100 series), a fluorescence detector (1046A series), and a C_{18} column (Supleco, 150 mm length, 4.6 mm i.d., 4 μm particle size) maintained at 40°C. Fluorescent derivatives of primary amines were formed by reaction with a solution of 25 mg *o*-phthaldialdehyde (OPA, Sigma), 50 μL mercaptoethanol (Sigma), 50 μL Brij 23 solution (Sigma), 0.5 ml methanol, and 4 ml 1 M borate buffer. The OPA derivatives were detected using an excitation wavelength of 325 nm and monitoring emission wavelength of $\geq$ 465 nm. The sample was mixed 50:50 with reagent in an autosampler loop. Solvent A consisted of methanol, and solvent B consisted of 40 mM and 5 % tetrahydrofuran (pH 6.3 although exact conditions were adjusted to optimise separation). The initial solvent composition and gradient (10 to 70 % solvent A) were occasionally altered to optimise resolution.

Chromatograms were analysed using ChromPerfect software (Justice Laboratories) and degradation indices (DI) were calculated for each sampling date following Dauwe and Middelburg (1998); Dauwe et al. (1999). Loses were accounted for by the addition of the internal standard. Separate samples from the same time point were run in duplicate where possible. Overall method precision for SPM above the pycnocline samples ranged from 0.79 to 19.57 %, SPM below the pycnocline from 5.41 to 20.32 %, sediment trap material from 9.96 to 114.06 %, and in sediments from 2.69 to 27.58 % (Table C.3 & C.4)

4.2.3.3 Fatty acid analysis

SPM and sediment trap filters

Filters were placed into 7 ml vials with 5 ml 2:1 chloroform: methanol. Samples were spiked with 5 μL of fatty acid methyl ester internal standard (23:0) using a Hamilton syringe. Samples were

vortexed and stored at -20°C until analysis. Samples were removed from the freezer, vortexed, and filters were removed from the vials using clean tweezers. Samples were extracted following the Folch et al. (1957) procedure where a quarter volume of 0.88 % (*w/v*) potassium chloride was added to the vials, vortexed and centrifuged at 1500 rpm for 2 minutes. The top layer was removed using a glass pasteur pipette and the bottom layer remaining in the vial was dried under nitrogen. Dry samples were placed in a vacuum desiccator in the dark overnight. Samples were removed from the desiccator and redissolved in approximately 0.5 ml chloroform after being vortexed. The lipid solution was transferred into pre-weighed 2 ml vials using glass pasteur pipettes. The original 7 ml vials were rinsed with chloroform for a second time which was then added to the 2 ml vial. Vials were then placed under nitrogen to dry before being placed in a vacuum desiccator in the dark. Vials were weighed for total lipid amounts before adding 100 μL chloroform for storage.

For fatty acid analysis, samples were transferred into 7 ml vials, dried under N_2, and 0.5 ml toluene and 1 ml 1 % methanol sulphuric acid methylation reagent was added (Christie, 1982). Samples were vortexed, purged with N_2, and placed in a heat block at 50°C for 16 hours. Once cooled, 2 ml DI H_2O and 2 ml hexane: diethyl ether (1:1 *v/v*) was added. Samples were vortexed and centrifuged at 1500 rpm for 2 minutes. The upper organic layer was transferred into new 7 ml vial. A further 2 ml hexane: diethyl ether was added to the original 7 ml vial which was then vortexed, centrifuged and the upper organic layer added to the second vial. Then, 1 ml $NaHCO_3$ (2 % *w/v*) was added to the second vial which was then vortexed, centrifuged, and placed in the -20°C freezer to freeze the bottom layer. Once frozen, the top layer was poured into a new 7 ml vial, dried under N_2 and placed in a vacuum desiccator in the dark. Samples were removed from the desiccator and dissolved in $\sim$ 50 to 100 μL hexane. Samples were applied to the base of a thin layer chromatography (TLC) plate (10 x 10 cm). The TLC plate was developed in a hexane: diethyl ether: acetic acid (90:10:1) solvent system until solvent was within the top 2 cm of plate.

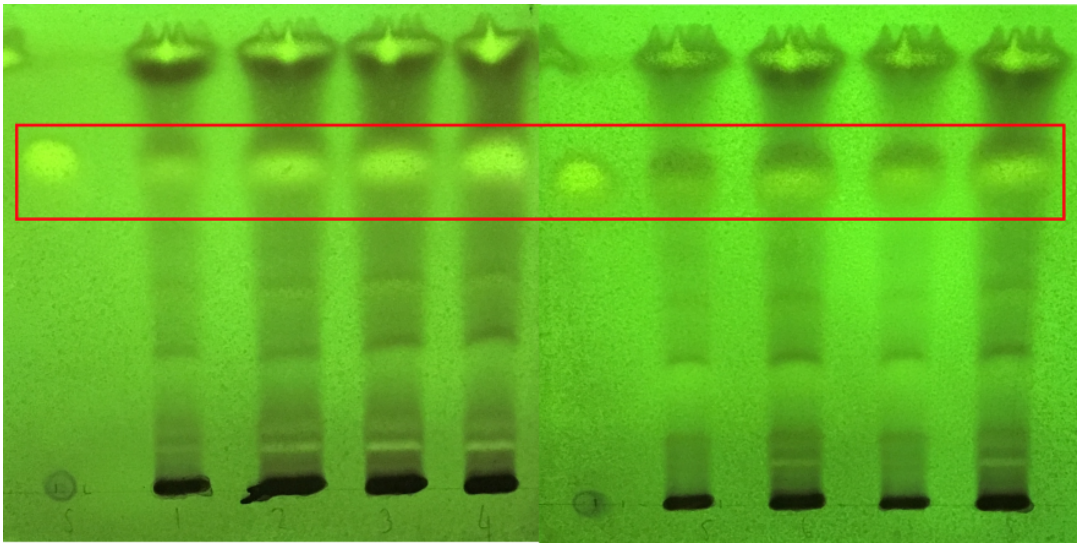

Figure 4.6: TLC plates showing separation of lipid classes of benthic sediment samples with FAMES identified using a FAME standard (FAMES highlighted in red box)

The TLC plate was removed from the tank, the solvents were allowed to evaporate and the plate

was sprayed with dichlorofluorescien stain. Fatty acid methyl ethers (FAMES) were visualised under UV light and marked with pencil (Figure 4.6). FAMES were then scraped off the TLC plate and placed into a 7 ml vial. Then, 2 ml hexane: diethyl and 1 ml $NaHCO_3$ (2 % *w/v*) was added, vortexed, and centrifuged. Vials were placed in freezer to freeze bottom layer. The top layer was poured into a new 7 ml vial and dried under N_2. Samples were redissolved in $\sim$ 200 μL hexane and transferred into 2 ml vials for storage in -20°C freezer until analysis.

Sediments

Freeze dried sediment samples were weighed into 40 ml vials and 20 ml 2:1 chloroform: methanol was added, vortexed and stored at -20°C. Clean 40 ml vials were placed into a holder with a glass funnel and 90 mm filter paper (Whatman). The funnel, filter paper, and vial were washed with 2:1 chloroform: methanol which was then disguarded. Sediment samples were poured through the filtering apparatus. An additional 10 ml was added to the original sediment samples, vortexed, and poured through the filtering apparatus. Samples were extracted using the Folch et al. (1957) method, and then processed using the same method as for SPM and sediment trap filters.

Fatty acid methyl esters were analysed by gas chromatography (GC) on a Trace 2000 GC fitted with a Restek, Stabil-wax column (30 m x 0.32 mm i.d.) using hydrogen as the carrier gas. The oven programme started at 50°C for 1 minute and then increased by 4°C per minute up to 190°C. Then there was a 1.5°C increase per minute up to 230°C which was held for 8 minutes. Fatty acids in samples were quantified using 23:0 recoveries and relative response factors. Fatty acids were identified based on the example chromatogram in Figure C.1.

Separate samples from the same time point were run in duplicate except for sediments which were only ran once (to test method precision). Loses were accounted for by the addition of the internal standard. Overall method precision for SPM above the pycnocline samples ranged from 0.70 to 38.84 %, SPM below the pycnocline from 2.70 to 38.14 %, and sediment trap material from 3.53 to 72.08 % (Table C.5 & C.6).

4.2.3.4 Carbohydrate analysis

SPM and sediment trap material filtered onto GF/F filters, were analysed for total carbohydrates using the Dubois et al. (1956) method as detailed in Chapter 3, Section 3.2.3.3. The same method was used for sediment samples using approximately 20 mg of sediment, and precombusted sediment from LY1 (500°, 4 h) was used as blanks.

4.2.3.5 Lithogenic tracer element analysis

Sample dissolution of SPM and sediment trap filters

SPM and sediment trap material filters (Cellulose nitrate, Whatman; Figure 4.7) were placed into acid cleaned Teflon beakers and digested using high purity acids (SpA grade, ROMIL Ltd., Convent Drive, Waterbeach, Cambridge, UK). To remove oxidisable organic matter, 2 ml Nitric acid (HNO_3, 69%) was added to the beakers and heated. Once cooled, 2 ml Perchloric acid ($HClO_4$,

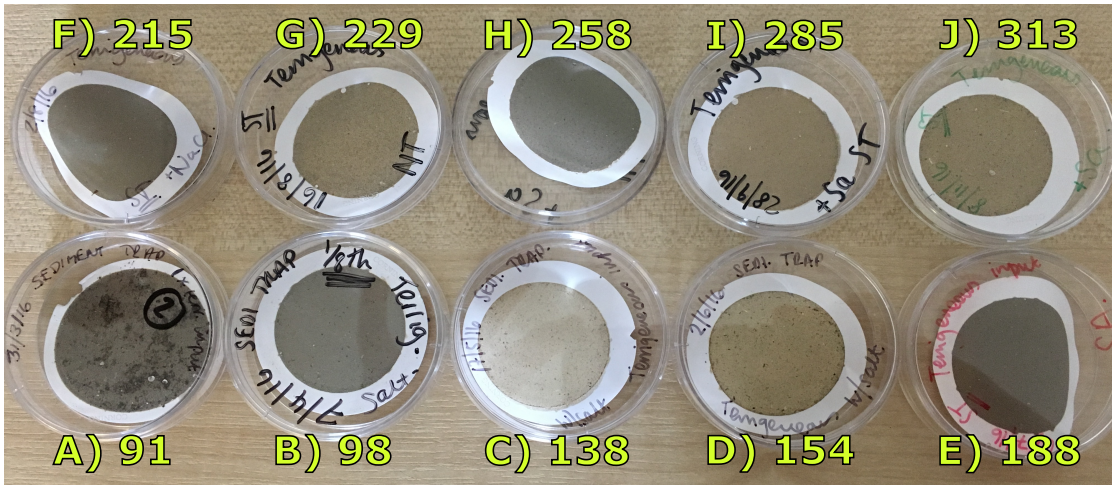

Figure 4.7: Sediment trap bulk particulate material filtered onto cellulose nitrate filters from sample days in year (A) 91 (31/03/2016), (B) 98 (07/04/2016), (C) 138 (17/05/2016), (D) 154 (02/06/2016), (E) 188 (06/07/2016), (F) 215 (02/08/2016), (G) 229 (16/08/2016), (H) 258 (14/09/2016), (I) 285 (11/10/2016), and (J) 313 (08/11/2016)

70%) was added and heated for 8 hours to remove any remaining organic material. Once cooled, the lids of the beakers were removed to allow the samples to evaporate. To the dry residue and to digest any silicate present, 3 ml HNO_3 (69 %), 1 ml Hydrofluoric acid (HF, 40 %), and 1 ml Hydrochloric acid (HCl, 35 %) was added, gently mixed, and heated to approximately 170 °C. Samples were refluxed for 8 hours after which samples were allowed to evaporate to remove chlorine and acid residues. The remaining dry residue was dissolved with DI H_2O, and transferred into acid cleaned 25 ml volumetric flasks. This solution had a final concentration of 5 % HNO_3 and was transferred into acid cleaned 30 ml HDPE storage bottles. In conjunction with every batch of unknown samples, a marine sediment reference material (GBW07315), and a reagent blank (blank cellulose nitrate filter and empty beaker) were digested and processed.

Sample digestion of benthic sediment

Benthic sediment samples were pre-weighed (approximately 10 mg) into acid cleaned Teflon beakers. For complete dissolution of the sample, 3 ml HNO_3 (69 %), 1 ml HF (40 %) and 1 ml HCl (35 %) was added and gently mixed. Samples were left to stand for 15 minutes, covered with caps and then heated to ∼170°C to reflux for 8 hours. Samples were then allowed to evaporate and made up to a final concentration of 5 % HNO_3 following the same method as the filter material.

Major element analysis (Al, Ba, Ca, Fe, Mg, Mn) was performed on a Perkin Elmer Optima DV4300 ICP-OES equipped with an AS93plus auto-sampler, a Scott-type spray chamber and GemTip cross-flow nebulizer. Single samples were ran and blank data were passed within an acceptable tolerance for the method. The limit of detection for Al, Ba, Ca, Fe, Mg, Mn were 0.003, 0.001, 0.011, 0.002, 0.001, 0.00001 mg g^{-1} respectively.

4.2.4 Statistical analysis

Principle component analysis (PCA) is a multivariate tool that allows a large number of variables to be reduced into a few principle components. A correlation matrix was used to perform PCA to investigate compositional trends between samples at different diagenetic stages down the water column (SPM above (n=10) and below (n=11) the pycnocline, sediment trap (n=10), and sediment (n=11) samples; samples collected between March to November 2016). Amino acid (mole %) (n=19) and fatty acid (% composition) (n=21) data were standardised by subtracting values from the overall mean and dividing by standard deviation to mean centre and account for mixed units. This PCA analysis and other statistical tests were carried out using Minitab 17 and R Studio.

4.3 Results

4.3.1 Relative contribution of major compound groups to organic material

The amount of total organic carbon (TOC) identified as carbon derived from amino acids, carbohydrates and fatty acids varied seasonally and generally decreased down the water column from SPM above the pycnocline, to SPM below the pycnocline, to sediment trap material (Figure 4.8). Amino acids, carbohydrates and fatty acids relative to OC were highest in SPM above the pycnocline, and ranged from 36.1 to 58.7 %, followed by SPM from below the pycnocline (20.8 to 48.7 %). The three major groups of compounds accounted for between 18.5 to 38.4 % and 27.4 to 36.9 % in sediment trap and sediments respectively. Carbohydrates and amino acids dominated the measurable fraction of TOC in all samples with amino acids accounting for 21.9 to 36.0 % in SPM above the pycnocline, 12.4 to 33.4 % in SPM below the pycnocline, 5.2 to 19.8 % in sediment trap material, and 11.5 to 17.1 % in sediment material. Carbohydrate accounted for 9.4 to 22.0 % of TOC in SPM above the pycnocline, 6.1 to 17.7 % in SPM below the pycnocline, 7.2 to 15.0 % in sediment trap material, and 15.8 to 20.3 % in sediment material. Fatty acids had the lowest contribution to TOC in all sample types, which ranged from 4.0 to 8.3 % SPM above the pycnocline, 2.3 to 9.3 % SPM below the pycnocline, 1.2 to 12.0 % sediment trap material, and 0.1 to 0.3 % in sediment material. The percentage contribution of amino acids, carbohydrates, and fatty acid carbon generally decreased between SPM and sediment trap samples. Percent amino acid carbon contribution in sediments was either similar to or higher than in sediment trap material but lower than in SPM samples. Fatty acid carbon accounted for a minute proportion of TOC in sediments, which ranged from 0.1 to 0.3 %.

Values of δ^{13}C were most enriched in SPM above and below the pycnocline during spring, when phytoplankton abundance was at a maximum, and most depleted during winter when cell abundances were low (Figure 4.9A). The seasonal range in δ^{13}C of SPM was very similar above and below the pycnocline between -20.7 to -25.3 ‰, and -20.1 to -25.5 ‰ respectively (Figure 4.9A). There were periods where δ^{13}C values were similar between SPM, sediment trap, and sediment fractions (days 90, 97, 153). Sediment trap samples were the most enriched sample type over the summer period reaching -19.3 ‰ and a minimum of -23.7 ‰ δ^{13}C. There was a relatively homogeneous seasonal distribution of δ^{13}C in sediment samples which ranged from -20.8 to -21.5

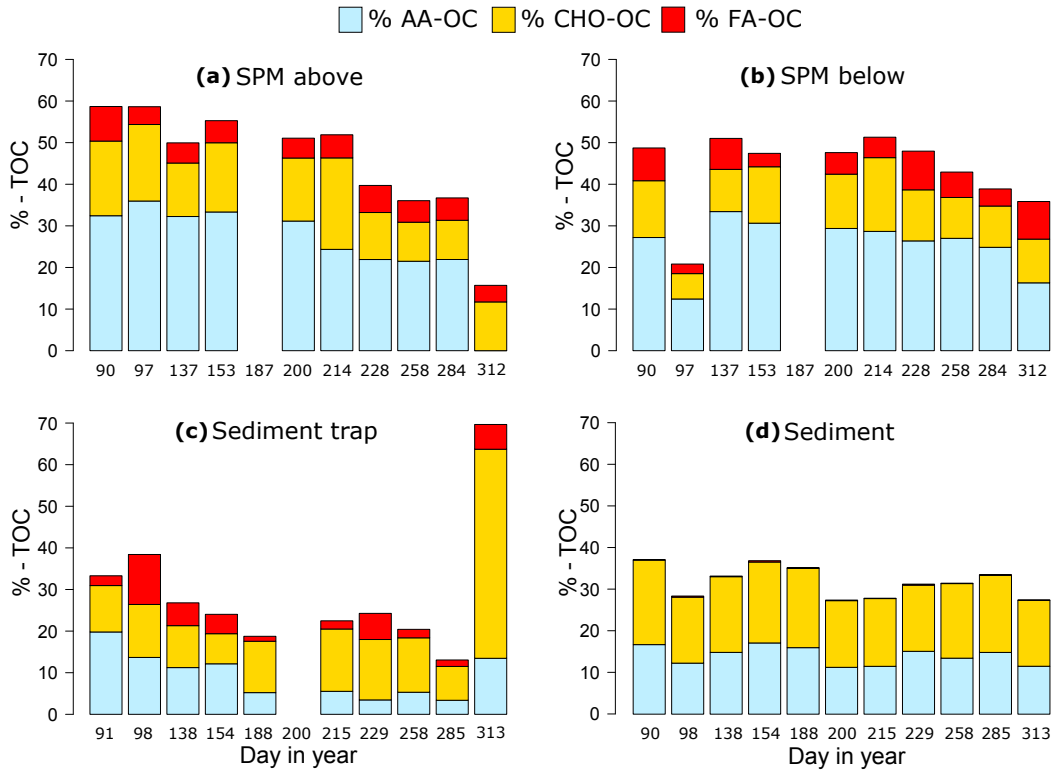

Figure 4.8: Relative contribution of the major compounds amino acids (%AA-OC), carbohydrates (% CHO-OC), and fatty acids (%FA-OC) relative to total organic carbon pool in suspended particulate material (SPM) above (a) and below (b) the pycnocline, sediment trap (c) and sediment (d) samples from LY1 over 2016

‰. There was a statistically significant difference in yearly median δ^{13}C value between sample types; the most negative yearly median δ^{13}C value was -22.9 ‰ $\pm$ 0.6 SE in SPM from below the pycnocline, followed by -22.6 ‰ $\pm$ 0.6 SE in SPM from above the pycnocline, -21.3 ‰ $\pm$ 0.1 SE in sediment samples, and was the least negative in sediment trap material (-21.1 ‰ $\pm$ 0.4 SE; Kruskall Wallis H= 7.77, df= 3, P=0.051).

Seasonal SPM molar carbon-to-nitrogen (C:N) ratios were generally higher above the pycnocline and ranged from 6.5 to 7.6 above, and 5.5 to 7.6 below the pycnocline. There was a significant difference between yearly averaged SPM C:N ratios with lower C:N ratios below the pycnocline (median 6.4 $\pm$ 0.1 SE) than above (median 6.8 $\pm$ 0.2 SE; Mann-Whitney U-test, U=501.0, $n_{above,below}$= 20, P<0.01). Nitrate concentrations were higher below the pycnocline than above for the majority of the year which suggested there was higher nitrate availability to be assimilated into phytoplankton biomass (nitrate concentrations ranged from 0.5 to 6.2 μM below and 0.02 to 4.0 μM above the pycnocline; Chapter 2, Section 2.3.1.2). Sediment trap and sediment material typically had higher C:N ratios than SPM ranging from 7.5 to 10.1 and 9.1 to 9.8 respectively.

Table 4.4: Biochemical characterisations of suspended particulate material (SPM) samples collected above and below the pycnocline over the sampling season at LY1. Mean ± SD concentrations of TOC, total organic carbon; TN, total nitrogen; AA, amino acids; TFA, total fatty acids; CHO, total carbohydrates; %AA-N, percentage of total nitrogen present as amino acids; %AA-OC, percentage of organic carbon present as amino acids; %TFA-OC, percentage of organic carbon present as total fatty acids; %CHO-OC percentage of organic carbon present as total carbohydrates; C:N carbon-to-nitrogen molar ratio; -, no measurement

Date	DIY	TOC μg ml^{-1}	TN μg ml^{-1}	AA μg ml^{-1}	TFA μg ml^{-1}	CHO μg ml^{-1}	% AA-N	% AA-OC	% TFA-OC	% CHO-OC	C:N (molar)
SPM above											
30/03/2016	90	0.4 ± 0.0	0.06 ± 0.0	0.3	0.04 ± 0.0	0.2 ± 0.0	55.6	32.4	8.3 ± 3.2	17.9 ± 0.4	6.7 ± 0.1
06/04/2016	97	0.2 ± 0.0	0.04 ± 0.0	0.2	0.01 ± 0.0	0.1 ± 0.00	68.1	36.0	4.3 ± 0.4	18.4 ± 0.0	6.9 ± 0.2
16/05/2016	137	0.3 ± 0.0	0.1 ± 0.0	0.2 ± 0.0	0.02 ± 0.0	0.08 ± 0.0	55.3 ± 13.5	32.3 ± 5.6	4.9 ± 0.9	12.9 ± 0.4	6.6 ± 0.5
01/06/2016	153	0.3 ± 0.0	0.1 ± 0.0	0.2	0.02 ± 0.0	0.1 ± 0.0	60.2	33.3	5.3 ± 0.04	16.6 ± 0.3	6.6 ± 0.0
05/07/2016	187	-	-	0.1	0.01 ± 0.0	0.1 ± 0.0	-	-	-	-	-
18/07/2016	200	0.47 ± 0.1	0.1 ± 0.0	0.3	0.03 ± 0.0	0.2 ± 0.0	57.7	31.2	4.8 ± 0.3	15.2 ± 0.3	6.7 ± 0.6
01/08/2016	214	0.4± 0.0	0.06 ± 0.0	0.2 ± 0.0	0.03 ± 0.0	0.2 ± 0.0	51.4 ± 3.6	24.4 ± 1.8	5.6 ± 0.4	22.0 ± 2.1	7.6 ± 0.0
15/08/2016	228	0.3 ± 0.0	0.06 ± 0.0	0.2 ± 0.0	0.03 ± 0.0	0.1 ± 0.0	35.4 ± 0.3	21.9 ± 0.2	6.5 ± 0.5	11.3 ± 1.2	6.5 ± 0.3
13/09/2016	257	0.3 ± 0.1	0.05 ± 0.0	0.1 ± 0.0	0.02 ± 0.0	0.1 ± 0.0	44.5 ± 2.5	21.5 ± 1.1	5.2 ± 1.0	9.4 ± 0.2	7.3 ± 0.8
10/10/2016	284	0.3 ± 0.1	0.1 ± 0.0	0.2 ± 0.01	0.02 ± 0.0	0.1 ± 0.0	45.9 ± 2.5	21.9 ± 1.3	5.4 ± 0.4	9.4 ± 0.1	7.6 ± 1.7
07/11/2016	312	0.2 ± 0.0	0.03 ± 0.0	-	0.01 ± 0.0	0.1 ± 0.0	-	-	4.0 ± 0.1	11.7 ± 0.2	7.3 ± 0.3
Mean ± SD		0.3 ± 0.1	0.04 ± 0.0	0.2 ± 0.06	0.02 ± 0.0	0.1 ± 0.1	53.0 ± 9.8	28.3 ± 5.8	5.4 ± 1.2	14.5 ± 4.2	7.0 ± 0.5
SPM below											
30/03/2016	90	0.2 ± 0.0	0.03 ± 0.0	0.1	0.02 ± 0.0	0.07 ± 0.0	56.6	27.2	7.9 ± 2.0	13.7 ± 0.2	7.6 ± 0.1
06/04/2016	97	0.5 ± 0.4	0.03	0.1	0.01 ± 0.0	0.07 ± 0.0	63.3	12.4	2.3 ± 0.5	6.1 ± 0.3	6.9 ± 1.5
16/05/2016	137	0.2 ± 0.0	0.04 ± 0.0	0.2	0.02 ± 0.0	0.06 ± 0.0	57.5	33.4	7.4 ± 3.8	10.2 ± 0.7	6.4 ± 0.0
01/06/2016	153	0.3 ± 0.0	0.06 ± 0.0	0.2	0.01 ± 0.01	0.1 ± 0.0	53.3	30.6	3.2 ± 1.2	13.6 ± 1.3	6.4 ± 0.3
05/07/2016	187	-	-	0.1	0.01 ± 0.0	0.1 ± 0.0	-	-	-	-	-
18/07/2016	200	0.1 ± 0.0	0.04 ± 0.0	0.1 ± 0.0	0.01 ± 0.0	0.07 ± 0.0	52.6 ± 5.3	29.4 ± 3.7	5.2 ± 0.1	13.1 ± 0.2	6.4 ± 0.7
01/08/2016	214	0.2 ± 0.0	0.04 ± 0.0	0.1 ± 0.0	0.01 ± 0.0	0.1 ± 0.0	48.3 ± 4.0	28.7 ± 2.6	4.9 ± 0.8	17.7 ± 0.6	6.3 ± 0.1
15/08/2016	228	0.2 ± 0.0	0.03 ± 0.0	0.1 ± 0.0	0.02 ± 0.0	0.05 ± 0.0	40.1 ± 8.1	26.4 ± 5.3	9.3 ± 4.0	12.3 ± 0.6	5.5 ± 0.2
13/09/2016	257	0.2 ± 0.0	0.04 ± 0.0	0.1 ± 0.0	0.02 ± 0.0	0.06 ± 0.0	47.5 ± 2.8	27.0 ± 1.4	6.1 ± 1.8	9.8 ± 0.6	6.5 ± 0.1
10/10/2016	284	0.2 ± 0.0	0.04 ± 0.0	0.1 ± 0.0	0.01 ± 0.0	0.1 ± 0.0	42.2 ± 2.5	24.8 ± 1.5	4.1 ± 0.4	9.9 ± 0.6	6.3 ± 0.3
07/11/2016	312	0.2 ± 0.0	0.02 ± 0.0	0.1	0.02 ± 0.0	0.04 ± 0.0	32.0	16.3	9.0 ± 2.6	10.5 ± 0.2	7.0 ± 0.5
Mean ± SD		0.2 ± 0.0	0.03 ± 0.0	0.1 ± 0.0	0.02 ± 0.0	0.1 ± 0.0	49.3 ± 9.3	25.6 ± 6.5	6.0 ± 2.4	11.7 ± 3.1	6.5 ± 0.5

Table 4.5: Biochemical characterisations of sediment trap and sediment samples collected over the sampling season at LY1. Mean ± SD concentrations of TOC, total organic carbon; TN, total nitrogen; AA, amino acids; TFA, total fatty acids; CHO, total carbohydrates; %AA-N, percentage of total nitrogen present as amino acids; %AA-OC, percentage of organic carbon present as amino acids; %TFA-OC, percentage of organic carbon present as total fatty acids; %CHO-OC percentage of organic carbon present as total carbohydrates; C:N carbon-to-nitrogen molar ratio; -, no measurement

Date	DIY	TOC mg g^{-1}	TN mg g^{-1}	AA mg g^{-1}	TFA mg g^{-1}	CHO mg g^{-1}	% AA-N	% AA-OC	% TFA-OC	% CHO-OC	C:N (molar)
Sediment trap											
31/03/2016	91	81.1 ± 34.3	9.5 ± 4.6	35.7	2.5 ± 0.2	22.6 ± 1.2	57.8	19.8	2.4 ± 0.2	11.2 ± 0.6	10.1 ± 0.6
07/04/2016	98	28.0 ± 13.4	3.4 ± 1.3	8.6 ± 8.8	4.3 ± 3.1	8.9 ± 0.7	51.6 ± 40.5	19.0 ± 14.9	12.0 ± 8.7	12.7 ± 1.0	9.4 ± 0.9
17/05/2016	138	38.1 ± 18.6	4.7 ± 2.3	41.2 ± 47.0	2.7 ± 0.1	9.6 ± 2.9	26.3 ± 20.0	11.2 ± 9.1	5.5 ± 0.2	10.1 ± 3.1	9.4 ± 0.0
02/06/2016	154	47.9 ± 48.6	6.6 ± 6.7	27.9 ± 12.2	2.9 ± 1.1	8.7 ± 0.7	28.3 ± 6.4	12.1 ± 2.9	4.7 ± 1.8	7.2 ± 0.6	8.4 ± 0.0
06/07/2016	188	64.1 ± 5.0	8.0 ± 0.6	23.0 ± 3.1	1.0 ± 0.1	19.8 ± 1.4	13.8 ± 3.1	5.2 ± 1.1	1.2 ± 0.1	12.3 ± 0.9	9.4 ± 0.1
02/08/2016	215	39.9 ± 1.8	4.8 ± 0.0	13.9 ± 2.0	1.0 ± 0.2	15.0 ± 0.4	15.0 ± 2.5	5.5 ± 0.9	2.0 ± 0.3	15.0 ± 0.4	9.7 ± 0.5
16/08/2016	229	33.6 ± 1.6	3.8 ± 0.2	12.6 ± 2.9	2.7 ± 1.4	12.2 ± 1.5	10.3 ± 0.1	3.5 ± 0.0	6.3 ± 3.2	14.5 ± 1.7	10.3 ± 1.0
14/09/2016	258	42.4 ± 9.5	4.9 ± 0.7	16.4 ± 2.8	1.1 ± 0.0	13.9 ± 0.2	17.9 ± 1.6	5.3 ± 0.5	2.0±0.6	13.1 ± 0.2	10.0 ± 0.9
11/10/2016	285	53.1 ± 11.7	7.5 ± 1.3	15.7 ± 1.6	1.1	10.8 ± 8.1	7.7 ± 0.1	3.4 ± 0.1	1.6	8.1 ±6.1	8.3 ± 0.4
08/11/2016	313	13.4 ± 1.1	2.1 ± 0.1	18.2 ± 5.0	1.0 ± 0.1	16.8 ± 2.8	26.5 ± 2.4	13.5 ± 1.1	3.6±2.8	50.2± 8.4	7.5
Mean ± SD		44.2 ± 19.0	5.5 ± 2.3	21.3 ± 10.6	2.0 ± 1.2	13.8 ± 4.8	25.5 ± 17.0	9.3 ± 5.5	4.4 ± 3.3	15.5 ± 12.5	9.4 ± 0.4
Sediment											
30/03/2016	90	6.9 ± 1.1	0.8 ± 0.2	2.8 ± 0.2	0.01	3.5 ± 0.3	49.6 ± 2.5	16.7 ± 1.0	0.1	20.3 ± 1.6	9.7 ± 0.2
06/04/2016	97	8.5± 0.6	1.1 ±0.1	2.6 ± 0.2	0.03	3.4 ± 1.0	35.9 ± 2.7	12.3 ± 0.9	0.3	15.9 ± 4.5	9.5 ± 0.0
16/05/2016	137	17.2 ± 3.2	2.2 ± 0.4	6.4 ± 0.7	0.03	7.8 ± 0.9	42.0 ± 3.9	14.9 ± 1.4	0.2	18.2 ± 2.0	9.1 ± 0.0
01/06/2016	153	11.6 ± 4.5	1.4 ± 0.6	4.9 ± 1.5	0.05	5.6 ± 1.8	44.3 ± 13.7	17.1 ± 4.4	0.3	19.5± 6.2	9.4 ± 0.1
05/07/2016	187	13.3 ± 1.0	1.7 ± 0.1	5.3 ± 0.9	0.03	6.0 ± 1.0	46.1 ± 9.4	16.0 ± 3.3	0.2	18.0 ± 3.1	9.2 ± 0.1
18/07/2016	200	21.5 ± 4.4	2.8 ± 0.6	6.2 ± 0.4	0.04	8.5 ± 0.4	31.6 ± 2.2	11.3 ± 0.9	0.1	15.7 ± 0.7	9.1 ± 0.1
01/08/2016	214	20.8 ± 0.5	2.7 ± 0.1	6.1 ± 0.2	0.02	8.5 ± 0.5	32.2 ± 0.8	11.5 ± 0.3	0.1	16.3 ± 1.0	9.0 ± 0.1
15/08/2016	228	14.0 ± 1.3	1.8 ± 0.2	5.4 ± 0.2	0.04	6.1 ± 1.1	42.3 ± 1.3	15.1 ± 0.6	0.3	17.3 ± 3.2	9.1 ± 0.1
13/09/2016	257	12.7 ± 3.8	1.6± 0.5	4.3 ± 1.2	0.02	5.7 ± 0.8	38.6 ± 10.5	13.5 ± 3.4	0.1	17.9 ± 2.4	9.3 ± 0.0
10/10/2016	284	12.3 ± 0.1	1.5 ± 0.0	4.6 ± 0.3	0.02	5.7 ± 0.8	43.2 ± 2.5	14.8 ± 0.9	0.1	18.6 ± 2.7	9.3 ± 0.0
07/11/2016	312	18.8 ± 1.1	2.3 ± 0.1	5.6 ± 0.1	0.02	7.4 ± 0.6	33.6 ± 0.7	11.5 ± 0.1	0.1	15.8 ± 1.2	9.4 ± 0.3
Mean ± SD		14.3 ± 4.7	1.8 ± 0.6	4.9 ± 1.3	0.03 ± 0.0	6.2 ± 1.8	40.0 ± 6.0	14.1 ± 2.2	0.2 ± 0.1	17.59 ± 1.6	9.3 ± 0.1

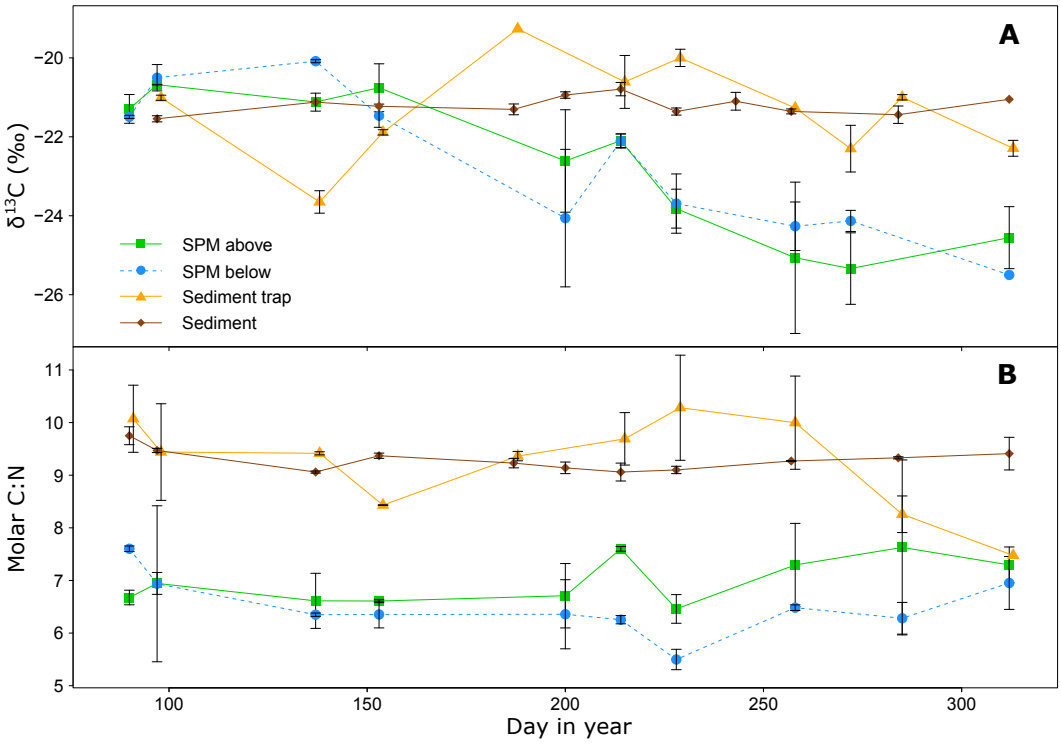

Figure 4.9: (A) Mean ± SD δ^{13}C (‰), and (B) mean ± SD molar carbon-to-nitrogen ratios (C:N) for suspended particulate material (SPM) above and below the pycnocline, sediment trap material, and sediment samples collected from LY1 over 2016

4.3.2 Amino acid composition

4.3.2.1 Suspended particulate material amino acid composition

Amino acid concentrations varied considerably over the sampling season in SPM above and below the pycnocline (Figure 4.10a, Table 4.4). There was a significant strong positive correlation between amino acid concentration and phytoplankton cell abundance (Pearson's Correlation Coefficient, r=0.9, df=8, P=0.003). The initial peak in SPM amino acid concentrations above the pycnocline on day 90 (0.3 μg ml^{-1}) corresponded to peak phytoplankton cell abundance (Chapter 2, Figure 2.13). Concentrations then decreased until a secondary peak around day 200 (0.3 μg ml^{-1}). For the majority of the year, amino acid concentrations were higher in SPM above the pycnocline than below.

Neutral amino acids (GLY: glycine, ALA: alanine, VAL: valine, ILEU: isoleucine, LEU: leucine) dominated SPM above and below the pycnocline over the sample year (Figure 4.11). Mole percentage contribution of each amino acid group followed similar trends at the two depths with neutral amino acids dominating followed by acidic (ASP: aspartic acid, GLU: glutamic acid), hydroxylic (SER: serine, THR: threonine), aromatic (TYR: tyrosine, PHE: phenylalanine), basic (HIS: histidine, ARG: arginine), non-protein (BALA: β-alanine, GABA: γ-aminobutyric acid, ORN: ornithine), and sulfidic (MET: methionine) which accounted for 45.8, 19.5, 9.8, 6.7, 5.8,

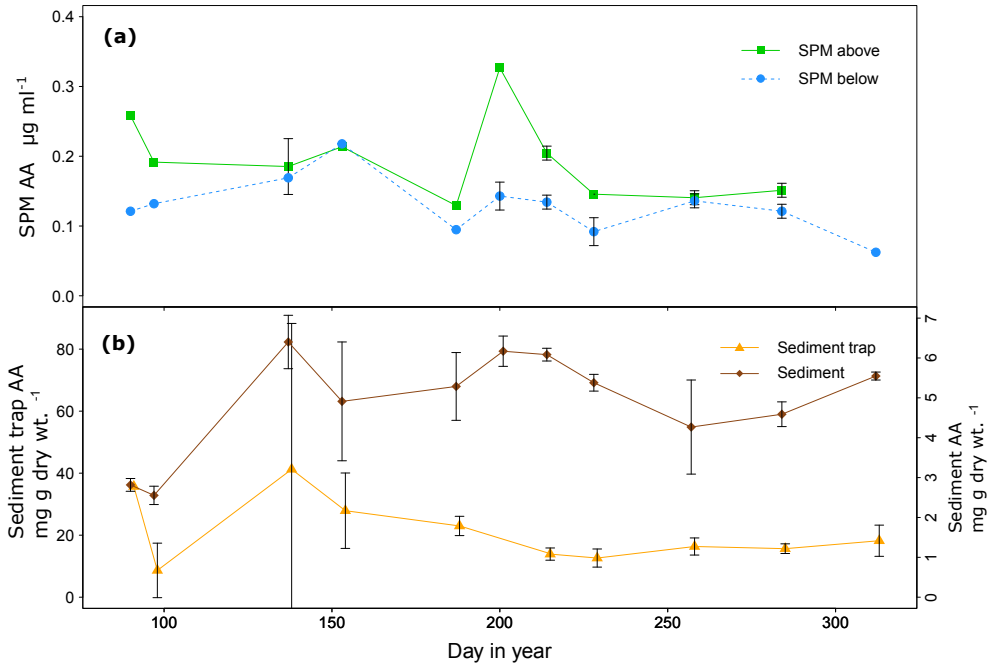

Figure 4.10: Mean ± SD seasonal amino acid concentrations in suspended particulate material (SPM) above and below the pycnocline (a; μg ml^{-1}), sediment trap and sediment material (b; mg g dry weight $^{-1}$)

0.8, 0.8 % above and 46.2, 19.5, 11.5, 6.3, 6.1, 0.7, 0.8% below the pycnocline respectively (Table C.8).

Investigating the dominant amino acid in each sample type averaged over the sampling year showed that glycine, glutamic acid, lysine, and alanine dominated SPM above the pycnocline accounting for 13.05, 13.66, 11.10, and 10.97 mole percent respectively (Figure 4.12). Similarly, SPM below the pycnocline was dominated by glycine, glutamic acid, alanine, and lysine which contributed 15.16, 13.14, 11.19, and 9.27 mole percent respectively. Non-protein amino acids β-alanine and γ-aminobutyric acid, recognised indicators of degradation, were minor components of amino acid in SPM accounting for less than one mole percent.

There was a large degree of seasonal variability in mole percentages of amino acid in all of the sample types. Intracellular amino acids in diatoms such as leucine, phenylalanine, and isoleucine, were generally higher in SPM above the pycnocline over the sampling season (Figure 4.13A, B, and C). Peaks in mole percent values of leucine, phenylalanine, and isoleucine in SPM above the pycnocline corresponded to higher degradation indices (day 228; Figures 4.13A, B, and C and Figure 4.15A) indicating fresh, labile material. Higher DI values are associated with fresher, less degraded material (Dauwe and Middelburg, 1998; Dauwe et al., 1999). Mole percentages of tyrosine were similar above and below the pycnocline, and gradually increased over the year with higher mole percentages in SPM below the pycnocline later in the year (Figure 4.13D).

Seasonal trends of diatom cell wall associated glycine, serine, and threonine (Dauwe et al., 1999)

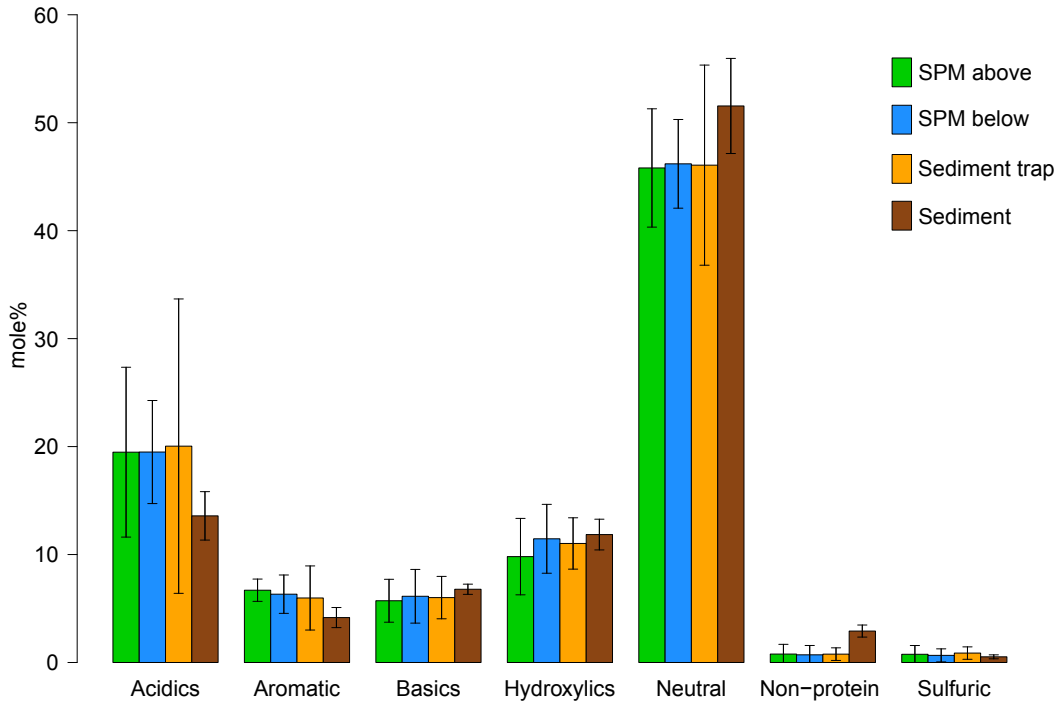

Figure 4.11: Mole percentage contribution of amino acid groups from suspended particulate material (SPM) above and below the pycnocline, sediment trap and sediment samples (mean over annual sampling ± SD). Acidics: aspartic acid, glutamic acid. Aromatic: tyrosine, phenylalanine. Basics: histidine, arginine. Hydroxylics: serine, threonine. Neutral: glycine, alanine, valine, isoleucine, leucine. Non-protein: β-alanine, γ-aminobutyric acid, ornithine. Sulfidic: methionine.

showed a relatively constant mole percent value from spring into summer, and subsequently a gradual increase in mole percent value towards the end of the year (Figure 4.14A to C). Decreased mole percent contributions of glycine, serine, and threonine in SPM above and below the pycnocline corresponded to higher DI values (Figure 4.15A). This relationship was especially evident on day 228 above the pycnocline; when mole percent of glycine, serine, and threonine was at a yearly minimum, DI was at a yearly maximum of 2.89. There were seasonal differences in mole percentages of non-protein amino acids as they progressively increased over the season (Figure 4.15B). Percentage of total nitrogen as amino acids mirrored the trend of non-protein amino acids as it was highest in spring, and then gradually decreased in SPM over the year (Figure 4.15C).

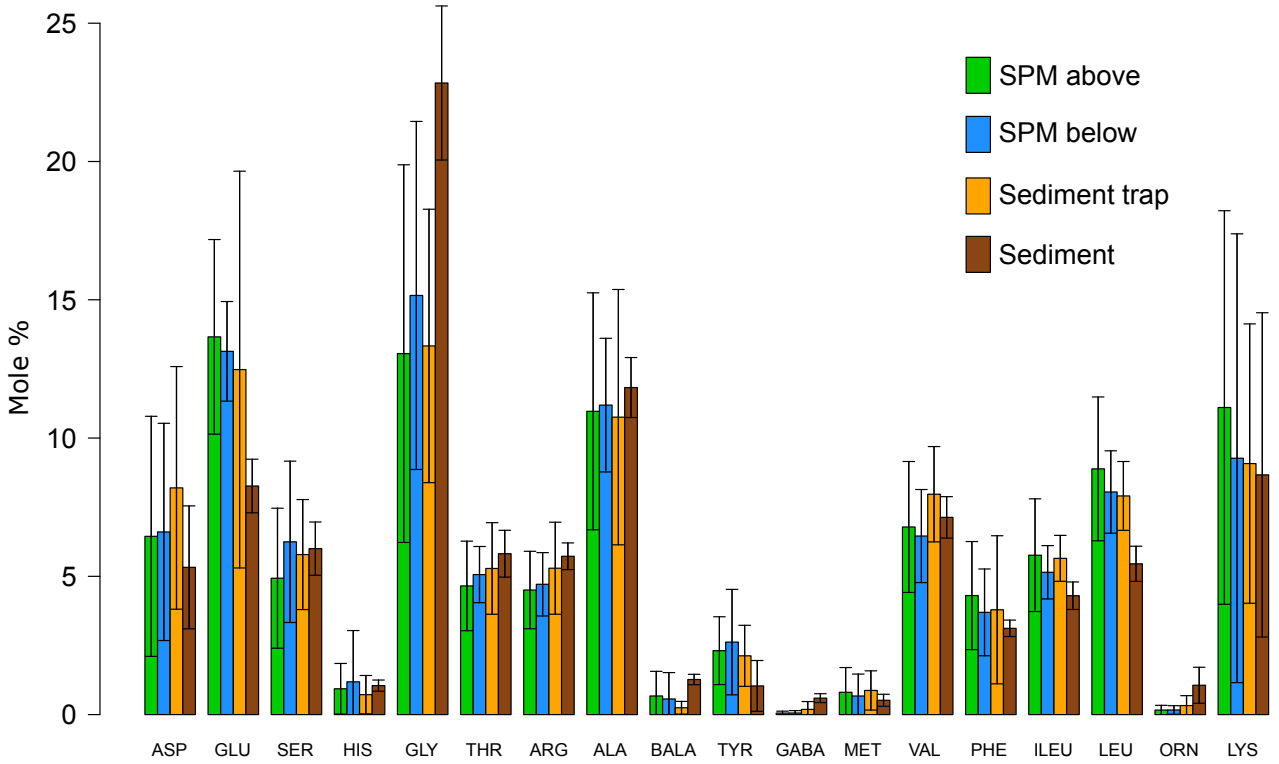

Figure 4.12: Mole percent contributions of individual protein and non-protein amino acids to AA in suspended particulate material (SPM) above and below the pycnocline, sediment trap and sediment samples. (Mean mole % $\pm$ SD averaged over annual sampling period). Aspartic acid (ASP), glutamic acid (GLU), serine (SER), histidine (HIS), glycine (GLY), threonine (THR), arginine (ARG), alanine (ALA), β-alanine (BALA), tyrosine (TYR), γ-aminobutyric acid, methonine (MET), valine (VAL), phenylalanine (PHE), isoleucine (ILEU), leucine (LEU), ornithine (ORN), and lysine (LYS).

Trends of ASP/BALA ratios above versus below the pycnocline were variable over the year with wide ranging values from 4.3 to 74.1 (Table 4.6). Ratios of GLU/GABA were high in SPM samples, relative to sediment trap and sediment material, as a result of lower mole percentages of GABA in SPM compared to sediment trap and sediment material. The sum of mole percent values of BALA and GABA (% BALA+GABA) is an additional diagenetic indicator, which is not reliant on the relationship of ASP/BALA and GLU/GABA (Cowie and Hedges, 1994). Higher % BALA+GABA was observed in sediments, with low seasonal variation, indicating a increased diagenetic state relative to sediment traps and SPM (Table 4.6). The relationship between % BALA+GABA in SPM and sediment trap material varied seasonally, with similar values in the two sample types during spring and early summer. After which % BALA+GABA values tended to be lower in sediment trap samples relative to SPM.

4.3.2.2 Sediment trap amino acid composition

Concentrations of amino acids in sediment trap material followed the same initial trend as SPM (Table 4.5). Initial concentrations of amino acids were high (35.7 mg g dry wt.$^{-1}$), and subsequently decreased in line with SPM amino acid concentrations. A secondary peak, with high standard deviation, in sediment trap amino acid concentration was reached on day 138 (41.2 mg g^{-1} $\pm$ 47.0 SD; Figure 4.10b). Following this initial variation in amino acid concentrations, concentrations showed little seasonal variation for the remainder of the year (Figure 4.10b).

Mole percentage contribution of each amino acid group in sediment trap material mirrored those of SPM (Figure 4.11; neutral 46.1, acidic 20.0, hydroxylic 11.0, aromatic 6.0, basic 6.0, sulfuric 0.8, non-protein 0.9 % mole percentage contribution). Dominant amino acids in sediment trap material included glycine, glutamic acid, and alanine (Figure 4.12, Table C.10).

Generally, seasonal trends in mole percent values of key intracellular amino acids in SPM were reflected in sediment trap material (Figure 4.13A to E). Mole percentage of leucine was similar to SPM below the pycnocline for the majority of the year. Additionally, the seasonal variation of leucine and phenylalanine corresponded to the trend in the degradation index with lower DI when there was a lower mole percent values of leucine and phenylalanine. Mole percentage of isoleucine was lower in sediment trap material when compared to SPM during spring and summer until day 215 where mole percent values of isoleucine were highest in sediment trap material. Tyrosine in sediment trap material mirrored SPM with increasing mole percentage over the year (Figure 4.13D). The range of mole percent values of glutamic acid was highest in sediment trap material, ranging from 2.62 to 19.97 mole % (Figure 4.13E).

Seasonal trends in percentages of cell wall associated amino acids glycine, serine, and threonine in sediment trap material were similar to those in SPM during spring and summer (Figure 4.14A to C). Around day 258 mole percent of glycine and serine decreased, leaving higher mole percentages in SPM relative to sediment trap material. During periods of minimum mole percent of glycine, serine and threonine on days 138 and 258, sediment trap DI values were at a maximum of 1.57 and 1.50. Sediment trap %AA-N was of a similar percent as SPM for the first sample date. However, later in the year despite higher %AA-N in the overlying water column, there was significantly

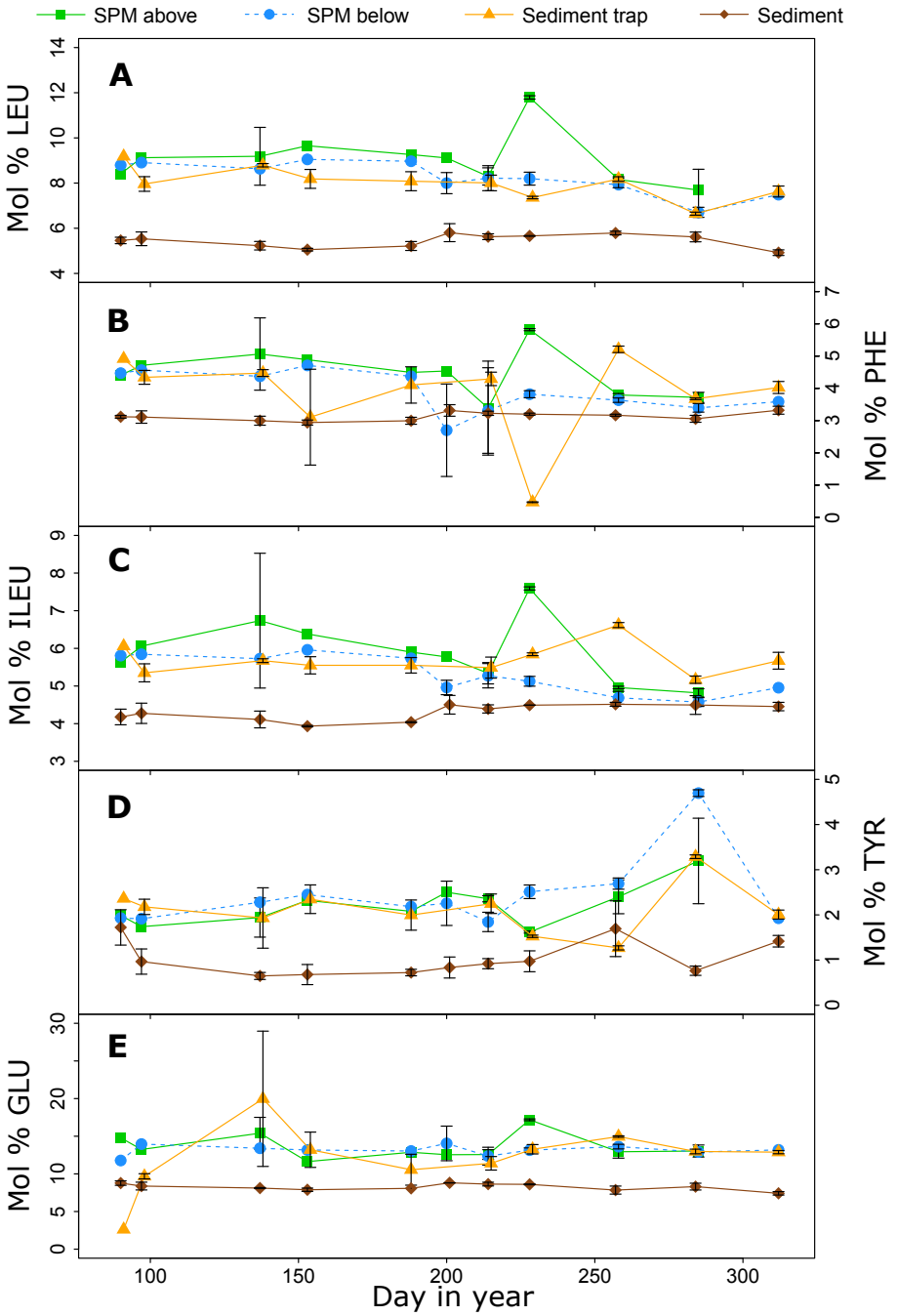

Figure 4.13: Mean ± SD mole percent contributions of diatom intracellular amino acids (A) leucine (LEU), (B) phenylalanine (PHE), (C) isoleucine (ILEU), (D) tyrosine (TYR), and (E) glutamic acid (GLU) in suspended particulate material (SPM) above and below the pycnocline, sediment trap and sediment samples.

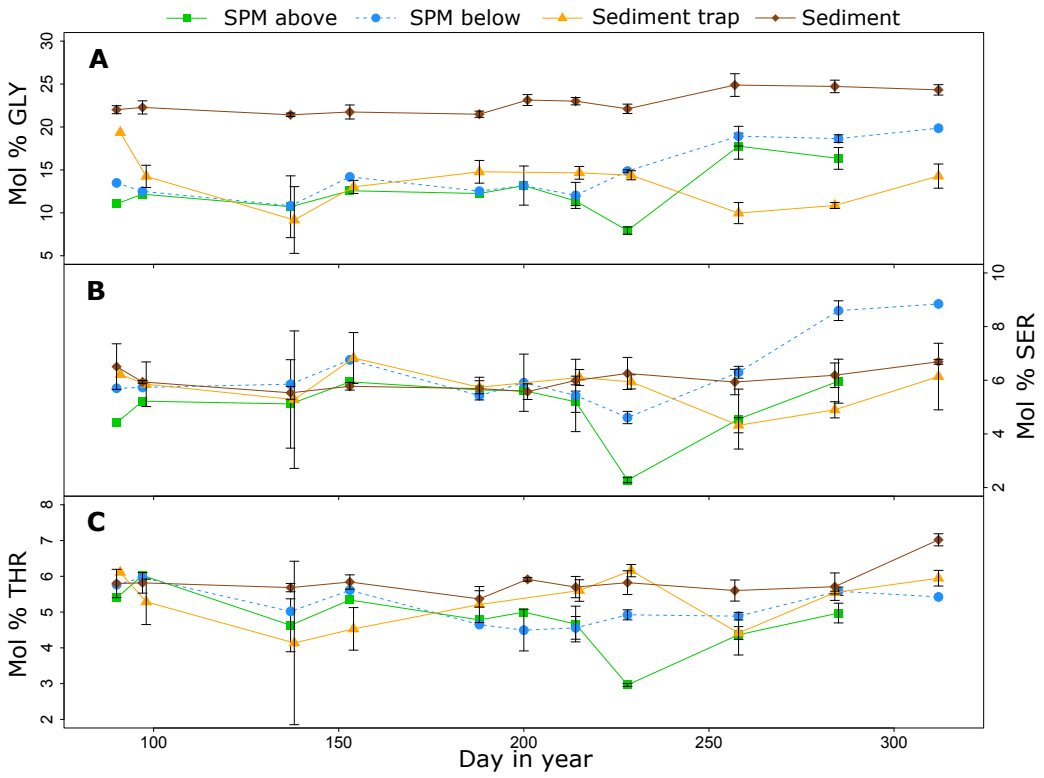

Figure 4.14: Mean ± SD mole percent contributions of diatom cell wall associated amino acids (A) glycine (GLY), (B) serine (SER), and (C) threonine (THR) in suspended particulate material (SPM) above and below the pycnocline, sediment trap and sediment samples.

lower %AA-N in sediment trap material which suggests selective loss of amino acids relative to bulk nitrogen. Ratios of ASP/BALA in sediment trap material were occasionally higher than in SPM, and always higher than sediment (Table 4.6). In contrast GLU/GABA ratios were lower in sediment trap material than SPM, and lowest values were observed in sediments.

4.3.2.3 Sediment material amino acids

Sediment amino acid concentrations were lower than that in the sediment traps, reaching a maximum of 6.4 mg g dry wt.$^{-1}$ ± 0.7 SD (Figure 4.10B, Table 4.5). Neutral amino acids dominated sediment material followed by acidics, hydroxylics, basics, aromatics, non-protein, and sulfuric which accounted for 51.6, 13.6, 11.9, 6.8, 4.2, 2.9, 0.5 % respectively (Figure 4.11). A decrease in acidic and an increase of non-protein amino acid groups in sediment samples, relative to SPM and sediment trap material, was observed.

Glycine dominated sediment amino acids accounting for 22.84 mole percent, and was responsible for the increase of neutral amino acids relative to lower mole percentages found in SPM and sediment trap material (Figure 4.12). Mole percentages of aspartic acid and glutamic acid, precusors of degradational products BALA and GABA, were lower in sediment relative to sediment trap and SPM (Figure 4.12). Ratios of ASP to BALA were often found to be higher in sediment trap material than SPM and always lowest in sediment samples (Table 4.6). GLU to GABA ratios were found to decrease from SPM, to sediment trap material with lowest ratios observed in sediments

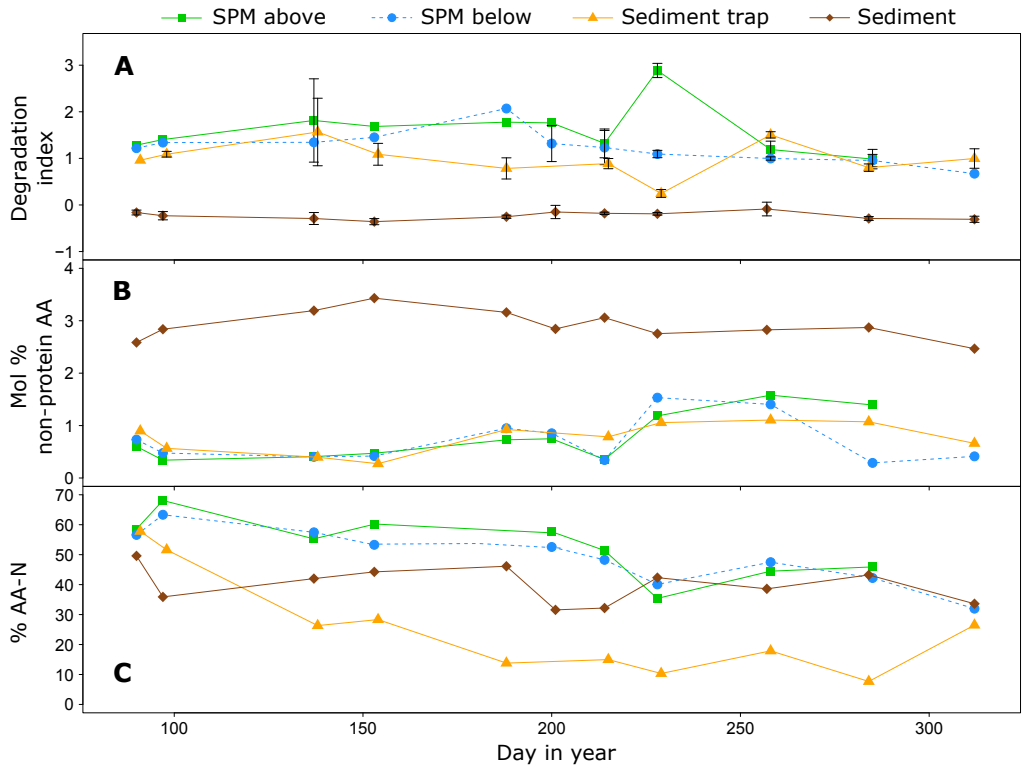

Figure 4.15: (A) Amino acid-derived degradation indices (DI), (B) mole percent contribution of non-protein amino acids, and (C) percentage of total nitrogen represented as amino acids (% AA-N) in suspended particulate material above (SPM A) and below (SPM B) the pycnocline, sediment trap and sediment samples collected from LY1 over 2016. (Mean mole% ± SD averaged over annual sampling period for A)

(Table 4.6).

Generally, mole percentages of key diatom intracellular amino acids were lowest in sediments when compared to the other sample types (Figure 4.13A to E). Additionally, there was less seasonal variation in mole percent of these amino acids in sediments in contrast to the seasonal variation in SPM and sediment trap material. During 2016, sediment samples contained a relatively constant low mole percentage of intracellular amino acids, which was reflected in the low DI value that was also relatively constant over the year (Figure 4.15A). Similarly, there was little seasonal variation in cell wall associated glycine, that was found to have a much higher mole percent contribution in sediment in contrast to the other sample types (Figure 4.14A). The seasonal range of serine and threonine in sediment was similar to SPM and sediment trap material (Figure 4.14B and C). Sediments had higher mole percent of non-protein amino acids than SPM and sediment trap samples for the entire year. Sediment %AA-N was highest on day 90 (49.60 %) and subsequently showed little seasonal variation in comparison to SPM and sediment trap samples (Figure 4.15C). For the majority of the year %AA-N was higher in sediment than sediment trap samples.

Table 4.6: Amino acid degradation indicators from suspended particulate material above (SPM A) and below (SPM B) the pycnocline, sediment trap (ST), and sediment (S) samples from dates in 2016. ASP/BALA: aspartic acid to β-alanine ratio, GLU/GABA: glutamic acid to γ-aminobutyric acid ratio, % BALA + GABA: sum of BALA and GABA mole percentages, DI: degradation index derived from Dauwe et al. (1999)

Sample	Depth (m)	Date	Day in year	ASP/ BALA	GLU/ GABA	% BALA +GABA	DI
SPM A	4	30/03/16	90	22.3	1281.3	0.4	1.3
SPM B	10	30/03/16	90	15.7	464.7	0.4	1.2
ST	20	31/03/16	91	4.9	20.3	0.5	1.0
S	50	30/03/16	90	5.5	17.4	1.8	-0.2
SPM A	5	06/04/16	97	24.7	-	0.2	1.4
SPM B	10	06/04/16	97	17.3	1675.0	0.3	1.3
ST	20	07/04/16	98	30.1	204.5	0.2	1.1
S	50	06/04/16	97	3.9	15.8	1.9	-0.2
SPM A	5	16/05/16	137	74.1	784.4	0.3	1.8
SPM B	10	16/05/16	137	32.1	453.6	0.3	1.3
ST	20	17/05/16	138	61.3	151.3	0.1	1.6
S	50	16/05/16	137	4.1	14.5	1.8	-0.3
SPM A	3	01/06/16	153	6.8	494.7	0.4	1.7
SPM B	10	01/06/16	153	9.87	526.30	0.3	1.5
ST	20	02/06/16	154	54.0	430.6	0.2	1.1
S	50	01/06/16	153	3.9	14.2	1.9	-0.4
SPM A	3	05/07/16	187	4.3	351.6	0.6	1.8
SPM B	10	05/07/16	187	3.7	546.8	0.7	2.1
ST	20	06/07/16	188	19.4	41.6	0.7	0.8
S	50	05/07/16	187	4.5	13.8	1.8	-0.3
SPM A	3	18/07/16	200	4.0	493.9	0.7	1.8
SPM B	10	18/07/16	200	20.4	1204.2	0.7	1.3
ST	20	-	-	-	-	-	-
S	50	19/07/16	201	3.9	12.1	2.0	-0.2
SPM A	3	01/08/16	214	58.5	310.8	0.2	1.3
SPM B	10	01/08/16	214	66.1	307.7	0.2	1.2
ST	20	02/08/16	215	25.1	67.9	0.5	0.9
S	50	01/08/16	214	4.3	12.4	2.0	-0.2

Table 4.6: continued

Sample	Depth (m)	Date	Day in year	ASP/ BALA	GLU/ GABA	% BALA +GABA	DI
SPM A	3	15/08/16	228	11.0	228.0	0.9	2.9
SPM B	10	15/08/16	228	5.9	106.5	1.4	1.1
ST	20	16/08/16	229	44.9	31.2	0.6	0.3
S	50	15/08/16	228	5.5	13.3	1.8	-0.2
SPM A	5	13/09/16	257	5.1	133.4	1.4	1.2
SPM B	10	13/09/16	257	6.4	145.6	1.2	1.0
ST	20	14/09/16	258	35.2	60.5	0.6	1.5
S	50	13/09/16	257	3.4	13.1	1.9	-0.1
SPM A	3	10/10/16	284	5.3	153.9	1.2	1.0
SPM B	10	10/10/16	284	79.9	185.8	0.1	1.0
ST	20	11/10/16	285	20.7	33.0	0.7	0.8
S	50	10/10/16	284	4.3	14.1	1.9	-0.3
SPM A	3	07/11/16	312	-	-	-	-
SPM B	10	07/11/16	312	68.6	-	0.1	0.7
ST	20	08/11/16	313	44.2	197.3	0.2	1.0
S	50	07/11/16	312	3.5	13.5	1.8	-0.3

4.3.3 Fatty acid composition

4.3.3.1 Suspended particulate material FA composition

Total fatty acid (TFA) concentrations varied considerably over the sampling season in SPM above and below the pycnocline (Figure 4.16a, Table C.11 and Table C.13). There was an initial peak in SPM TFA concentration above the pycnocline on day 90 (38.0 μg L^{-1}; Figure 2.13). Concentrations then decreased until a secondary peak around day 200 (29.0 μg L^{-1}). For the majority of the year TFA concentrations were higher in SPM above the pycnocline than below.

Percentage composition of polyunsaturated fatty acid (PUFA), monounsaturated fatty acid (MUFA), and saturated fatty acid (SFA) in SPM showed seasonal variation (Figure 4.17, Table C.12 and Table C.14). The SPM samples from above and below the pycnocline were relatively similar in percentage composition of PUFA, MUFA, and SFA when compared to sediment trap and sediment composition. PUFAs had a significantly higher percentage composition in SPM samples above (median 24.0 %), and below (median 23.1 %) the pycnocline compared to sediment trap (median 16.7 %), and sediment samples (median 17.9 %; Kruskall Wallis H= 18.41, df= 3, P=0.000). Percentage composition of PUFA in SPM above the pycnocline ranged from 18.70 to 40.20 % of TFA, and 16.90 to 33.00 % below the pycnocline. Percentage contribution of PUFA

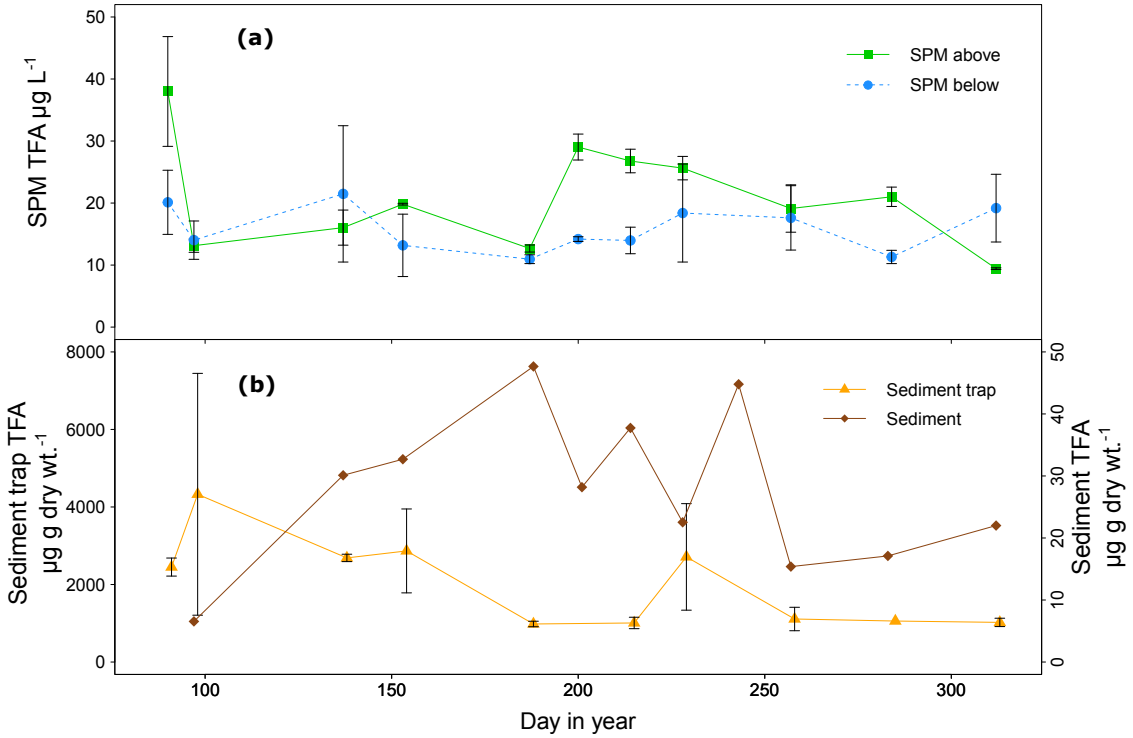

Figure 4.16: Mean ± SD seasonal total fatty acid concentrations in suspended particulate material (SPM) above and below the pycnocline (a; μg L^{-1}), sediment trap and sediment material (b; μg g dry weight $^{-1}$)

to total fatty acids in SPM was highest during spring and summer sample dates. SFA percentage contribution to TFA gradually decreased from the first sample date, until day 257 after which it increased. SFA ranged from 31.3 to 65.5 % and 38.9 to 63.5 % in SPM above and below the pycnocline respectively. MUFA generally had the lowest percentage contribution to TFA in SPM (15.8 to 36.3 % above, and 13.4 to 26.4 % below the pycnocline).

Diatoms dominated the phytoplankton community at LY1, and fatty acid biomarker 16:4(n-1) was used as a diatom indicator (Chapter 2, Figure 2.13). There was a significant positive correlation between diatom cell abundance and percentage contribution (and concentration) of 16:4(n-1) to TFA in SPM samples from above the pycnocline (Pearson's Correlation Coefficient, r=0.8, df=8, P= 0.008). Peaks in percent 16:4(n-1) contribution corresponded to peaks in diatom abundance (Figure 4.18A). Highest percent contribution of 16:4(n-1) was found in SPM during spring and summer, coinciding with peaks in microphytoplankton cell abundances, with lowest contributions occurring in winter. Other fatty acids identified as diatom biomarkers (16:1(n-7) and 20:5(n-3)) had high percentage contributions to total fatty acids which varied seasonally in SPM samples (Table C.12 and C.14).

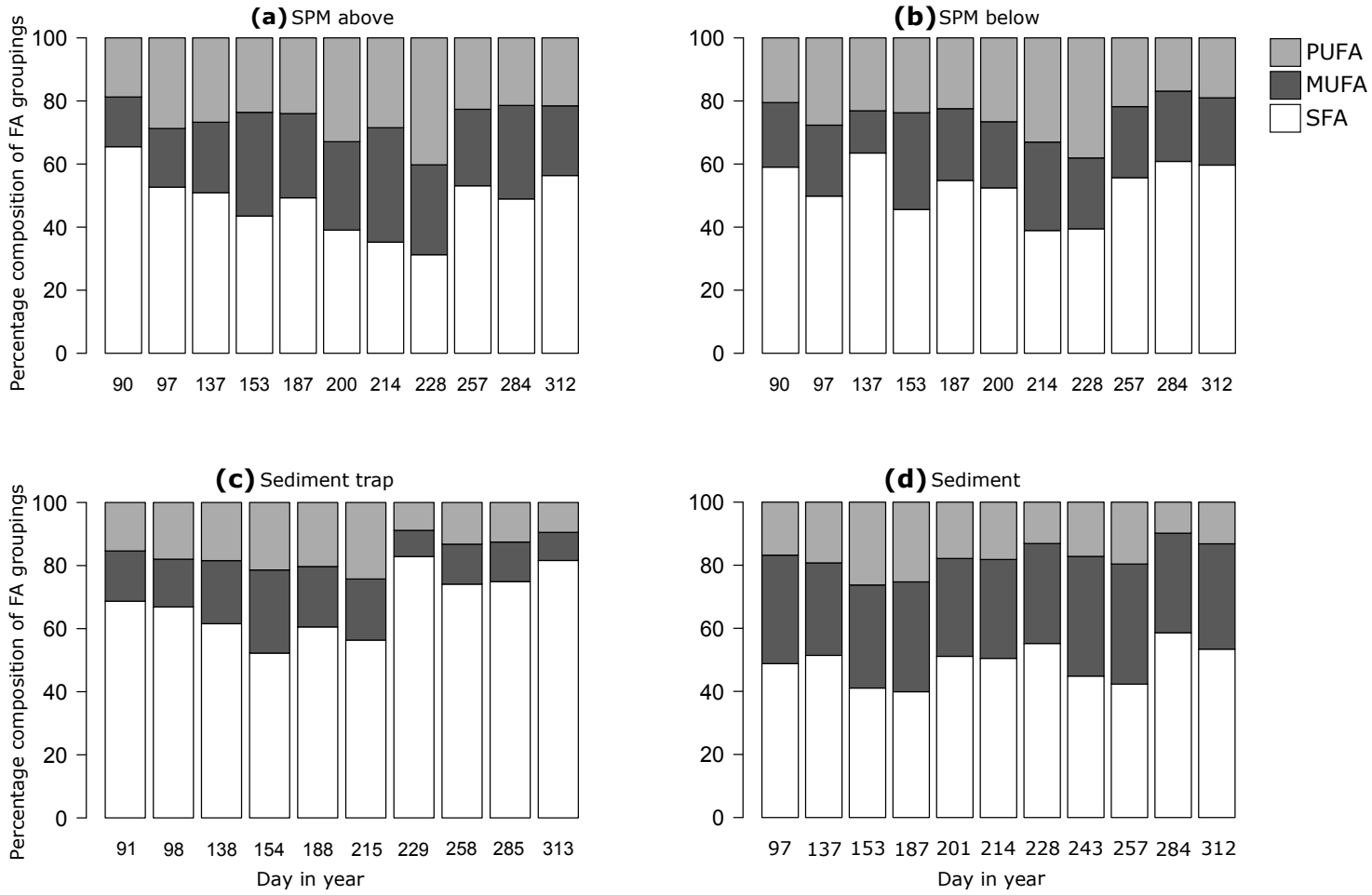

Figure 4.17: Percentage composition of polyunsaturated (PUFA), monounsaturated (MUFA), and saturated (SFA) fatty acids in suspended particulate material above (a; SPM A) and below (b; SPM B) the pycnocline, sediment trap material (c) and sediment (d) sampled over 2016

The dinoflagellate biomarker 22:6(n-3) had the highest percent contribution to total fatty acids in SPM collected above followed by SPM below the pycnocline for all of the sampling dates (Figure 4.18B). There was a significant positive correlation between dinoflagellate cell abundance, and percentage contribution of 22:6(n-3) to total fatty acids (Pearson's Correlation Coefficient, r=0.76, df=8, P=0.02; excluding anomaly of 11.01% 22:6(n-3) on day 228 Figure 4.18B). Elevated contributions of 22:6(n-3) corresponded to high cell abundances of dinoflagellates in summer.

4.3.3.2 Sediment trap FA composition

Sediment trap material had higher concentrations of TFA during the spring with a maximum of 4327.3 μg g dry wt.$^{-1}$, and lower concentrations of TFA during winter (Figure 4.16b, Table C.15). The initial peak in sediment trap material TFA concentration on day 98 and subsequently day 229 (2712.1 μg g dry wt.$^{-1}$), occurred following peaks in SPM TFA concentration.

Percentage contribution of PUFA to TFA had a lower contribution in sediment trap material relative to SPM, and contributed between 8.8 to 24.3 % of TFA (Figure 4.17, Table C.16). PUFA in sediment trap material was lowest in winter. SFAs dominated the composition of sediment trap material (median 67.8 %), and sediment (median 50.5 %), and contributed to a significantly lower percentage composition in SPM samples above (median 49.3 %), and below the pycnocline (median 54.8 %; Kruskall Wallis H= 17.93, df= 3, P= 0.000). SFA in sediment trap material followed similar trends to SPM above the pycnocline, with percentage contribution to TFA gradually decreasing over spring/ summer, and reached a maximum during winter (ranged from 61.6 to 82.9 %). MUFA were responsible for the lowest contribution to TFA in sediment trap samples accounting for 8.3 to 26.4 %.

Percentage composition of 16:4(n-1) to TFA in sediment trap material, was highest during spring similarly to SPM (Figure 4.18A). Later in the year percentage contribution of 16:4(n-1) was low in sediment trap material, but of a similar percentage composition as in SPM and sediment samples. Dinoflagellate biomarker 22:6(n-3) accounted for a similar percent composition to TFA as in SPM during the spring (Figure 4.18B). As dinoflagellate cell abundance increased, percentage contribution of 22:6(n-3) of TFA in sediment trap material increased, but not to the same extent as observed in SPM.

4.3.3.3 Sediment material FA composition

Concentrations of TFAs in sediment were considerably lower when compared to sediment trap material (Figure 4.16b, Table C.17). Sediment TFA concentrations gradually increased from day 97 to a maximum on day 188 (47.7 μg g dry wt.$^{-1}$) after which concentrations were variable until they finally decreased at the end of the year.

MUFAs had the highest contribution to TFA composition in sediments (median 32.67 %), which was significantly higher than sediment trap material (median 15.6 %), SPM above (median 26.7 %), and below (median 22.5 %) the pycnocline compositions (Kruskall Wallis H= 27.92, df= 3, P= 0.000; Table C.18). The range PUFA percentage contribution to TFA was similar in sediments

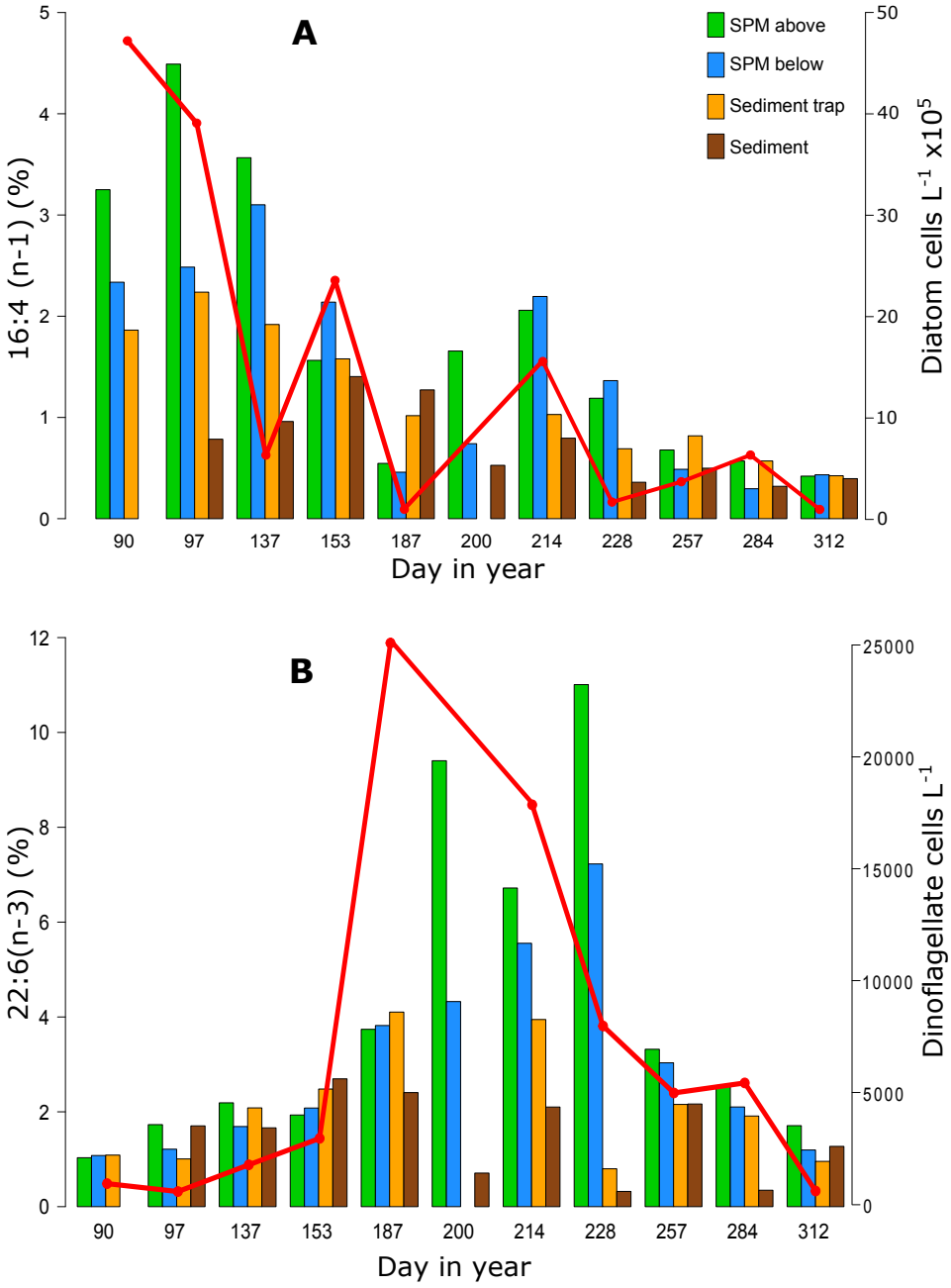

Figure 4.18: (A) Diatom biomarker 16:4(n-1) with seasonal diatom abundance (cells L^{-1}) sampled from above the pycnocline (red line and circles) and (B) Dinoflagellate biomarker 22:6(n-3) with seasonal dinoflagellate abundance (cells L^{-1}) sampled from above the pycnocline (red line and circles). Samples as a percentage of total fatty acid from suspended particulate material above (SPM A) and below (SPM B) the pycnocline, sediment trap and sediment samples collected during 2016 at site LY1.

(9.8 to 26.3 %) relative to sediment trap material (8.8 to 24.3 %; Figure 4.17).

The percent contribution of 16:4(n-1) in sediments gradually increased from day 90 to 153 during the period of high productivity and subsequently decreased. Dinoflagellate fatty acid biomarker (22:6(n-3)) contributions in the sediments were relatively constant over the first few sampling days when cell abundance was low (Figure 4.18B). The period of highest percent contribution of 22:6(n-3) in SPM was also the period for the lowest percent contribution of dinoflagellate biomarkers in sediment samples (days 200, 228, and 284).

4.3.4 Carbohydrate

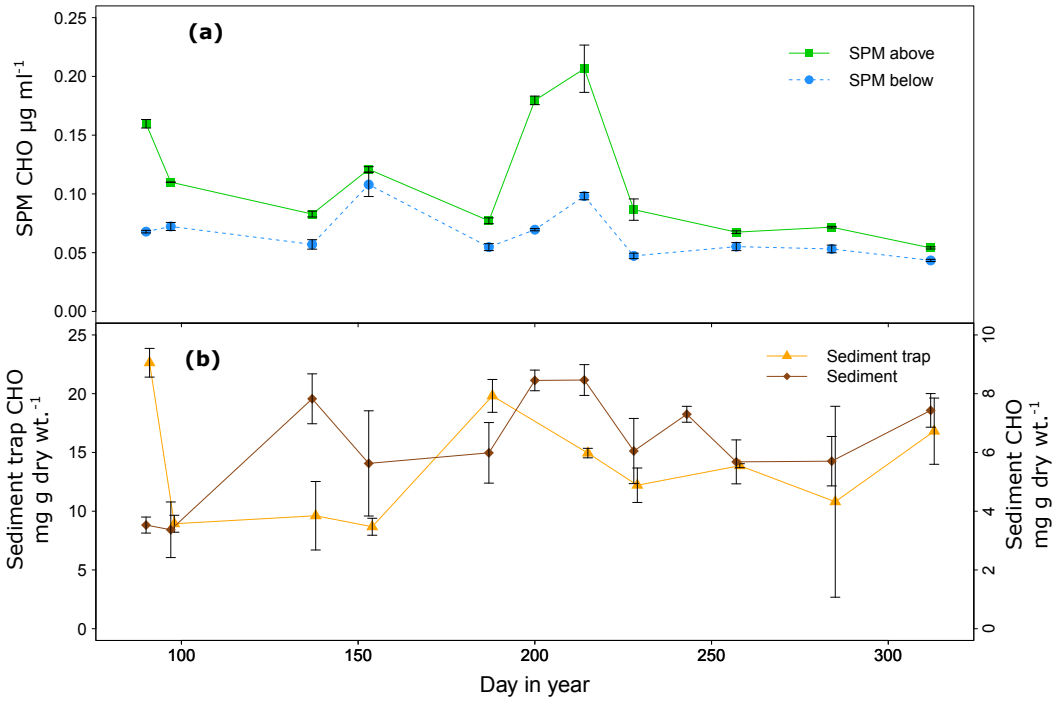

Figure 4.19: Mean ± SD seasonal carbohydrate (CHO) concentrations in suspended particulate material (SPM) above and below the pycnocline (a; μg ml^{-1}), sediment trap and sediment material (b; mg g dry weight $^{-1}$)

Carbohydrate concentrations varied considerably over the sampling season in SPM above and below the pycnocline (Figure 4.19a). There was a significant positive correlation between carbohydrate concentration and phytoplankton cell abundance (Pearson's Correlation Coefficient, r=0.62, df=8, P=0.05). The initial peak in SPM carbohydrate concentrations above the pycnocline on day 90 (0.16 μg ml^{-1}) corresponded to peak phytoplankton cell abundance (Chapter 2, Figure 2.13). Concentrations then decreased until a secondary peak around day 200 (0.21 μg ml^{-1}). For the majority of the year, carbohydrate concentrations were higher in SPM above the pycnocline than below.

Concentrations of carbohydrate in sediment trap material followed the same initial trend as SPM.

Initial concentrations of carbohydrates were high (22.6 mg g dry wt. $^{-1}$), and subsequently decreased in line with SPM carbohydrate concentrations. A secondary peak in sediment trap carbohydrate concentration, which occurred earlier than the SPM secondary peak, was reached on day 188 (19.8 mg g dry wt.$^{-1}$; Figure 4.19b). Following this peak, carbohydrate concentrations fluctuated for the remaining sample dates.

Sediment carbohydrate concentrations were lower than that in the sediment traps, reaching a maximum of 8.5 mg g dry wt.$^{-1}$ (Figure 4.19b). Sediment concentrations displayed opposing trends from day 90 to 187 compared to sediment trap material. After which carbohydrate concentration in sediment trap material and sediments followed similar trends.

4.3.5 Lithogenic tracer elements

Concentrations of particulate Al and Mn are good indicators of lithogenic elements derived from riverine inputs, atmospheric fall out, and sediment resuspension (Price et al., 1999). Seasonal trends of Al and Mn were similar and concentrations generally increased from SPM above the pycnocline, to 20 m sediment traps, and finally SPM at 45 m (Figure 4.20A & B). Both Al and Mn concentrations in SPM sampled at 45 m decreased on day 152 to concentrations lower than SPM above the pycnocline and sediment trap samples. There was a general increase in Al and Mn concentrations from spring to a maximum during late summer in SPM above the pycnocline (Al 0.06, Mn 0.003 mg L^{-1}), sediment trap (Al 0.08, Mn 0.003 mg L^{-1}), and SPM at 45 m samples (Al 0.13, Mn 0.004 mg L^{-1}).

4.3.6 Principle component analysis of particulate material at sequential stages of transport

PCA was used as a tool to quantitatively assess the biochemical composition variation between water column, sediment trap, and sediment samples. Each point on Figure 4.21A represents different sampling dates for the four sample types. PC1 explained 29.9 % of the variance of the data, and component 2 accounted for 15.2 % giving a total of 45.1 % explained from these two axes. PCA results show sediment material was compositionally different to SPM and sediment trap material. Additionally, Figure 4.21A shows the composition of all sample types varied over the sampling dates. Composition of sediment trap material was most similar to SPM below and then above the pycnocline.

PC1 was responsible for the separation of sediment from SPM and sediment trap samples. Key drivers of this separation include the percentage of fatty acid contribution to total organic carbon (%FA-OC) which was higher in SPM and sediment trap samples relative to sediments. Additionally diatom biomarkers (16:4(n-1)) and diatom intracellular amino acids (PHE, ILEU, LEU, GLU) were more associated with SPM and sediment trap material (positive PC1 values) than sediment (Figure 4.21B). Conversely, amino acid degradation indicators (GABA, BALA, GLY, ORN) had a higher percentage composition in sediment samples, resulting in the separation of sediments to the other sample types. Both ASP and GLU had higher percent compositions in SPM and sediment trap material relative to their degradational products BALA and GABA, which where more

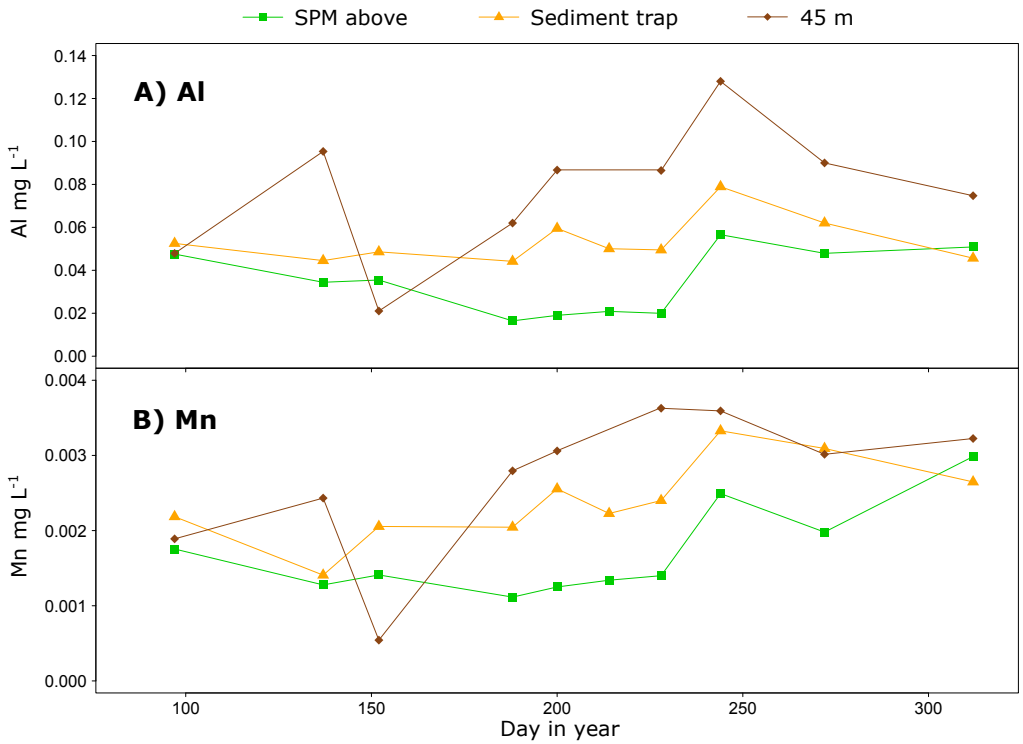

Figure 4.20: (A) Seasonal particulate Al concentrations (mg L^{-1}), and (B) seasonal particulate Mn concentrations (mg L^{-1}) in suspended particulate material above the pycnocline (SPM above), sediment trap, and suspended particulate material at near sea floor depth (45 m) samples

enriched in sediments. Additionally, the bacterial fatty acid indicator 18:1(n-7) had the highest percent composition in sediment samples. Refractory amino acids associated with diatom cell wall material (THR, GLY, SER) had higher percent composition in sediment samples. The percentage of organic carbon represented as carbohydrates (%CHO-OC) was not a key parameter in explaining the compositional differences between sample types.

PC2 was the main driver of differences between SPM above, SPM below the pycnocline, and sediment trap samples. The principle cause for this separation is fatty acid compositional differences between sediment trap material and SPM from above and below the pycnocline. PUFAs (e.g. 20:5(n-3), 20:4(n-6), 22:6(n-3), 18:4(n-3)) were more associated with SPM, and decreased in relative abundance from SPM above, to SPM below the pycnocline, to lowest relative abundances in sediment trap material. Additionally, SFA (16:0 and 18:0) had a higher relative contribution to sediment trap material when compared to SPM. There was also a transitional decrease in the percentage contribution of amino acids to organic carbon (%AA-OC) from higher relative contributions in SPM above, to SPM below the pycnocline, to lowest percent contributions in sediment trap samples.

Overall, PCA analysis highlights the compositional differences between SPM and sediment trap material compared to sediments. SPM and sediment trap material were more associated with diatom fatty acid biomarkers and diatom intracellular amino acids when compared to sediments.

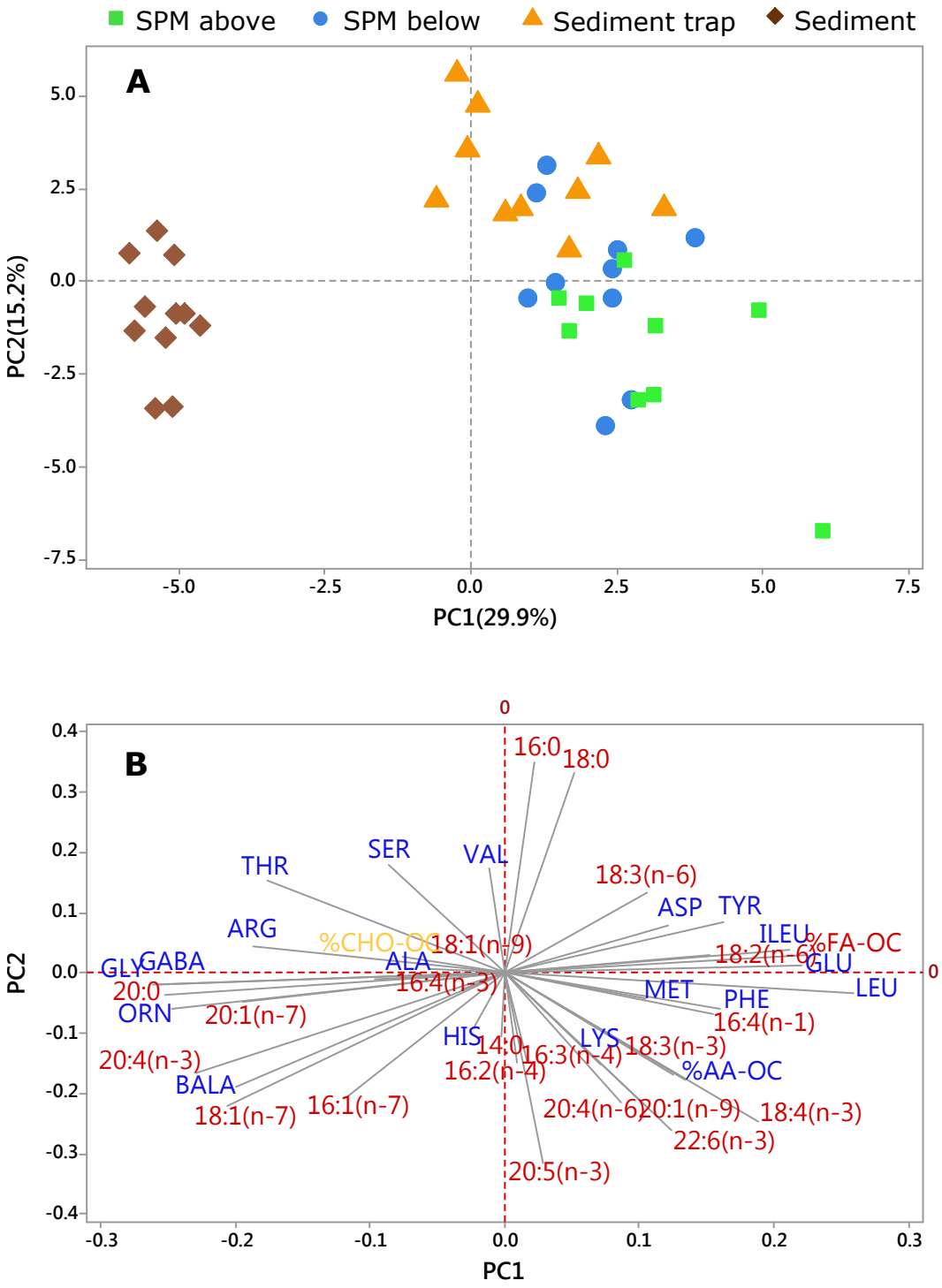

Figure 4.21: (A) PCA ordination of standardised mole percentage amino acids and percentage contribution of individual fatty acid to suspended particulate material (SPM) above and below the pycnocline, sediment trap and sediment samples. (B) PCA loading plot of amino acids (blue) and individual fatty acids (red). Percentage contribution of carbohydrate (yellow, %CHO-OC), amino acids (%AA-OC), and fatty acids (%FA-OC) to total organic carbon is also shown

Degradation, diatom cell wall, and bacterial indicators were most associated with sediments relative to SPM and sediment trap samples. The differences observed in SPM above, SPM below the pycnocline, and sediment trap material was driven by different fatty acid compositions, and proportion of organic carbon accounted for as amino acids.

4.3.7 Fluxes of particulate material

Bulk PM, organic carbon (OC), and nitrogen (N) fluxes followed similar seasonal trends with high fluxes on the first two sample dates (Figure 4.22A), which corresponded to peak phytoplankton abundance (Chapter 2, Figure 2.13). Low fluxes were observed on day 138, that coincided with low phytoplankton abundance. Subsequently bulk, OC, and N fluxes increased over the remainder of spring and summer months, with lower flux observed in winter. High bulk flux observed from June (day 188) to September (day 258; Figure 4.22A) coincided with the period of highest monthly rainfall (Figure 4.23). Fluxes of bulk PM ranged from a high of 13.7 to a low of 1.7 g m^2 d^{-1}. Organic carbon and nitrogen fluxes into sediment traps ranged from 0.04 to 1.3 and 0.01 to 0.2 g m^2 d^{-1} respectively. The secondary peak of OC flux (0.7 g OC m^2 d^{-1} $\pm$ 0.05 SD) did not reach levels observed during the phytoplankton spring bloom (1.0 g OC m^2 d^{-1} $\pm$ 0.4 SD) unlike bulk flux, in which primary (12.2 g m^2 d^{-1}) and secondary (13.7 g m^2 d^{-1}) flux peaks were of similar levels.

Concentrations of amino acids, carbohydrates, and fatty acids measured in sediment trap samples were used to calculate total fluxes of each biochemical (Figure 4.22B). Amino acids had the highest initial flux of 435.9 mg m^2 d^{-1}, which subsequently decreased for the remainder of the year with a minimum of 69.5 mg m^2 d^{-1} $\pm$ 79.2 SD (Figure 4.22B). Fluxes of carbohydrates were initially high, decreased until late spring, and after which increased to values similar to those of amino acids and fatty acids (flux range 27.4 to 276.4 mg m^2 d^{-1}). Fluxes of fatty acids were substantially lower than those of amino acids or carbohydrates, ranging from 4.5 to 31.9 mg m^2 d^{-1} (Figure 4.22B).

Microscopic analysis of sediment trap material was used to further identify the seasonal differences in composition (Figure 4.24). A large proportion of the aggregated PM was unidentifiable. In addition, long chain lengths of chain forming diatoms such as *Skeletonema* spp. (day 258 B), *Thalassiosira* spp. (day 229 A), *Pseudo-nitzschia* spp. (day 188 B), and *Guardinia* spp. (day 229 C) were found. It was also observed that solitary cells of *Pleurosigma* spp. (e.g. day 98 A, day 138 B, day 229 B, day 258 A) were common in sediment trap samples throughout the sampling year. Images also show changes in density and size of particles throughout the year with larger particles (day 98 A to C) found during high flux periods early in the year (Figure 4.22A). Particle sizes tended to be smaller but in higher densities during high flux periods later in the year (e.g. days 188, 229, 258 A to C). There was a lower density of particles found during the last two sample days (days 285 and 313 A to C) when fluxes were lower.

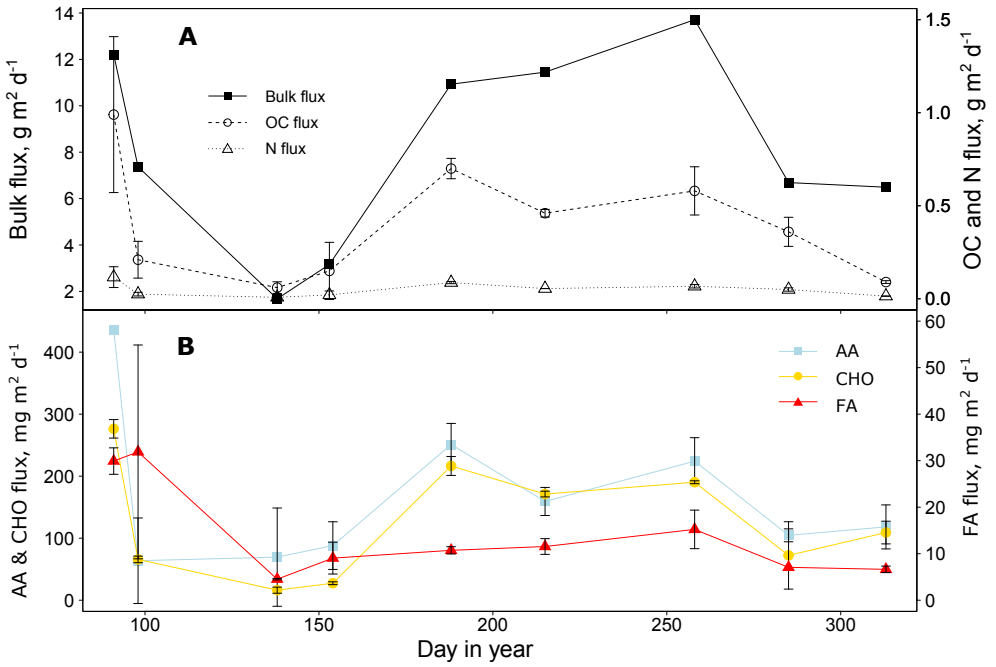

Figure 4.22: Mean ± SD of (A) seasonal fluxes (g m^2 d^{-1}) of bulk particulate material, organic carbon (OC), and nitrogen (N), and (B) Seasonal fluxes (mg m^2 d^{-1}) of amino acids (AA), carbohydrates (CHO), and fatty acids (FA) collected from sediment trap deployed at LY1 for 24 hours

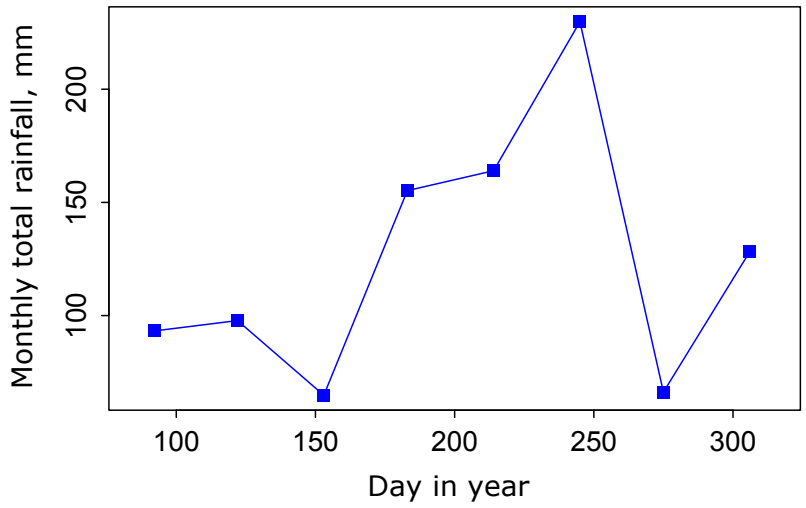

Figure 4.23: Monthly total rainfall (mm) at Dunstaffnage weather station 2016

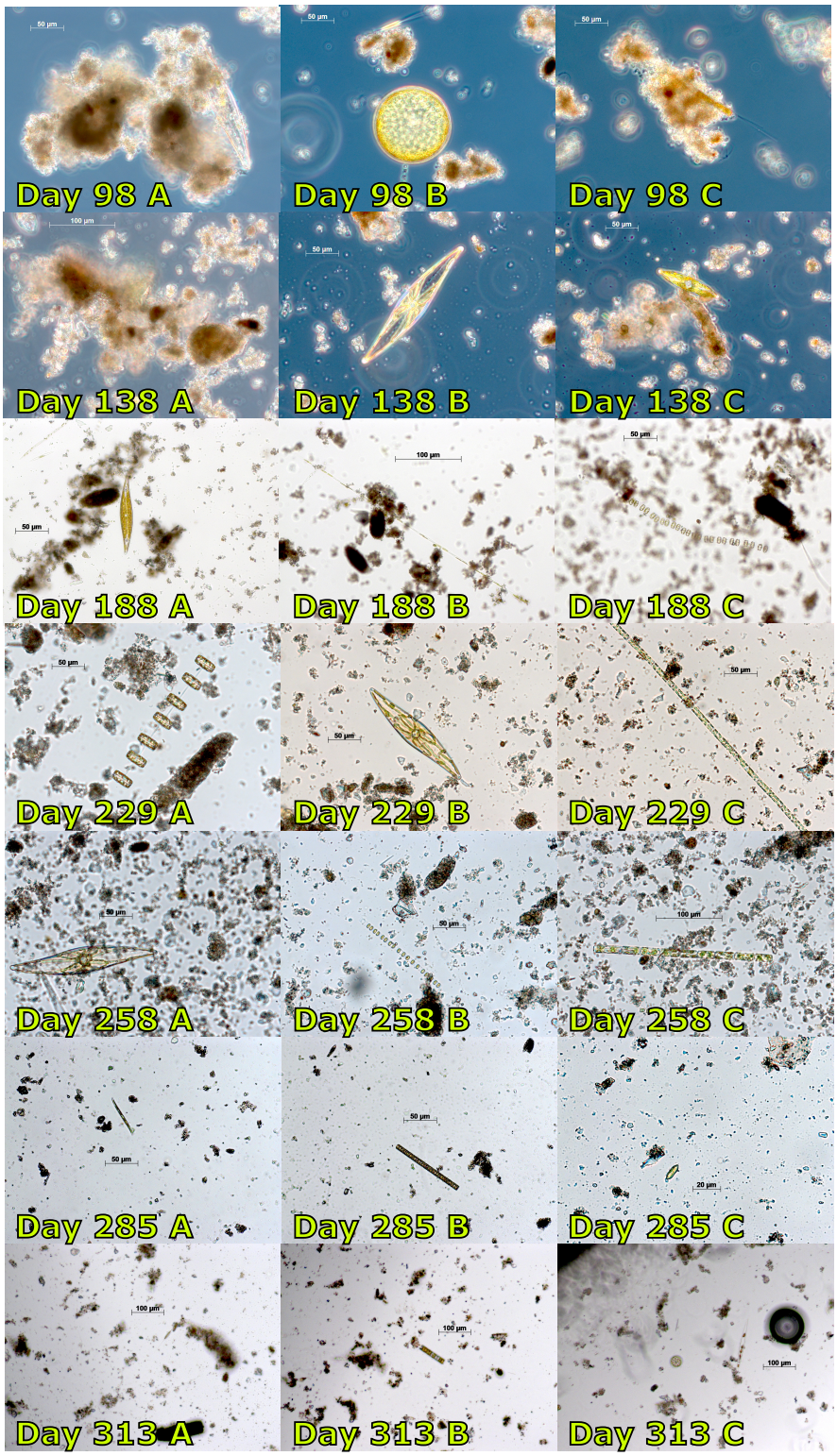

Figure 4.24: Pictures of sediment trap material containing aggregates and individual phytoplankton cells. Day 98 A to C (07/04/16) , day 138 A to C (17/05/16), day 188 A to C (06/07/16), day 229 A to C (16/08/16), day 258 A to C (14/09/16), day 285 A to C (11/10/16), day 313 A to C (08/11/16)

4.4 Discussion

4.4.1 Sources of organic material

The δ^{13}C values of SPM show a transition from more positive to more negative values over the March to November study period suggesting a progressional change in the source of SPM. During the phytoplankton bloom a higher proportion of marine organic material was observed switching to a greater relative proportion of terrestrial derived organic material during winter post-bloom periods. The seasonal range of δ^{13}C values in the four sample types varied from -20.8 to -25.4 ‰ in SPM from above the pycnocline, -20.1 to -25.5 ‰ in SPM from below the pycnocline, -19.3 to -23.7 ‰ in sediment trap samples, and -20.8 to -21.5 ‰ in sediments. Carbon isotope measurements are useful organic matter source indicators and have been suggested to be unaffected by the decomposition of organic matter (Gearing et al., 1984). Hedges et al. (1997) found that the use of δ^{13}C as a source indicator can be confounded by the molecular composition of the organic material. For example, lipids can be classed as being isotopically light in contrast to amino acids, in which the majority are isotopically heavy (Hedges et al., 1997). Therefore, the preferential utilisation or accumulation of refractory compounds can affect δ^{13}C values (Hedges et al., 1997). In addition to this, phytoplankton δ^{13}C has been shown to vary over space, time and a number of other factors such as community composition, carbon dioxide concentration, and nutrient availability (Hedges et al., 1988b, 1997; Hansman and Sessions, 2016). Therefore, without taking seasonal endmember measurements for marine and terrestrial sources specific to the Firth of Lorne, the use of δ^{13}C as a source indicator is speculative, as discussed below.

Generally, terrestrial plants have δ^{13}C values that range from -25 to -28 ‰ and marine phytoplankton average -20 ‰ (e.g. Emerson and Hedges, 1988; Hedges et al., 1997; Kandasamy and Nath, 2016). However, Hedges et al. (1988b) observed net plankton δ^{13}C values of -26.0 ‰ when microphytoplankton community composition was dominated by *Chaetoceros concavicornis* during summer to early autumn. In contrast, δ^{13}C values of -19.5 ‰ were observed when *Cerataulina bergonii* dominated in April. This highlights how the seasonally changing microphytoplankton composition can affect δ^{13}C values. Microphytoplankton community composition at LY1 shifted between two key diatoms *Skeletonema* spp. and *Chaetoceros* (coastal) spp. which dominated the community composition. The dominant source of terrigenous material into Loch Linnhe (north of LY1) is peat, which has δ^{13}C values of approximately -28 ‰ (Overnell and Young, 1995). This value is more negative than the most negative value observed at LY1. Winter SPM samples had δ^{13}C values closest to the cited range of terrestrial organic material. The transition of SPM to more negative values indicated a change in source material, in which the combination of a changing microphytoplankton community structure, and an increase in the relative proportions of terrestrial derived material, could be responsible. Other studies have found a progressive increase in terrestrial material contribution to sediment trap organic carbon from 10 % during non-winter months, to 35 % during winter months (Hedges et al., 1988b). For a large proportion of the year, from summer onwards (day 188), sediment trap material had more positive δ^{13}C values relative to more negative values in SPM (Figure 4.15A). This suggests SPM composition had a higher influence of terrestrial derived material than underlying sediment traps which had a stronger marine

organic signal. This difference could be due to two reasons; firstly, the lag in time for phytoplankton to sink from 3 m to 20 m, or secondly, due to a difference in sedimentation mechanisms for organic matter of different sources. Studies have found terrestrial organic material containing highly degraded lignin material to be less dense than seawater and remain in suspension in near surface waters (Reeves and Preston, 1991; Loh et al., 2008b). Site LY1 receives freshwater outflow from sea lochs Linnhe, Creran, and Etive, which all have large river catchment areas. Terrestrial material sourced from these three lochs could converge at site LY1 before being laterally advected elsewhere and not accounted for in sediment trap material.

Previous studies have found similar SPM δ^{13}C values in the Firth of Lorne to this study (-24.5 ‰ April 2014, -21.4 ‰ August 2014; Tierney et al., 2017). Sediment trap δ^{13}C values during spring were either similar to, or more positive compared to those of SPM. From summer onwards, sediment trap δ^{13}C values become more positive with a maximum δ^{13}C value of -19.3 ‰, indicating the presence of marine organic material. A sediment trap deployed at the head of Loch Creran had a yearly mean (December 2001 to December 2002) δ^{13}C of -21.3 ‰ $\pm$ 0.5 SD, and a stronger marine signal than underlying sediments (LC0 -24.7 ‰ $\pm$ 0.5, LC1 -23.8 ‰ $\pm$ 0.7; Loh et al., 2008b). One possibility for the different δ^{13}C values could be preferential consumption of marine POM during transition from sediment trap material to sediments. The increase in relative proportions of terrestrially derived organic matter, relative to the preferential loss of marine organic matter with increasing diagenetic state through the water column to sediments, is thought to be a typical dynamic of coastal systems (Hedges et al., 1988a). However, marine POM signals are still typically found in sediment trap material and sediment samples. A study found sediment samples (Saanich Inlet) δ^{13}C values to fall within a typical range of plankton and soil, with a higher occurrence of values being more similar to plankton (Brown et al., 1972). A further study found δ^{13}C values of sediment trap material to be more positive than net plankton values collected (Hedges et al., 1988b). However, these sediment traps were sampling for one month as opposed to "snap-shot" phytoplankton samples. In comparison to this, sediments underlying the sediment trap at LY1 showed little seasonal variation with a yearly average of -21.2 ‰ $\pm$ 0.2 SD, which was relatively similar to sediment trap yearly average of -21.3 ‰ $\pm$ 1.3 SD (Figure 4.9A). A conclusion from the Hedges et al. (1988b) study, which is consistent with this study, is that plankton influence but do not entirely control isotopic composition of sediment trap samples. This is evident from the more positive δ^{13}C values typical of a phytoplankton source, yet high C:N ratios which indicates the presence of terrestrial material and/ or degradation. Sediment δ^{13}C values over the season are similar to the yearly average of sediment trap values. It has been suggested that the lack of a seasonal record in sediments is driven by low accumulation rates due to lateral advection of PM, and bioturbation (Sancetta and Calvert, 1988). However, other sediment studies at shallow (10 to 33 m) sites in Chesapeake Bay observed no seasonal variation in the amount of POM in sediments, but observed seasonal differences in POM lipid composition (Zimmerman and Canuel, 2001). Resuspension and lateral advection processes can dominate PM distributions at a shallow, well-mixed coastal site (Hedges et al., 1988a). Differences in the hydrography between sites could result in whether seasonality is observed in sediment POM measures. These processes could lead

to sediment focusing, which could explain similarities between sediment trap material and sediment samples. This was observed at another coastal site in which a major proportion of sediment trap material was from resuspended or laterally advected PM (Hedges et al., 1988a). Additionally, a study in Loch Linnhe found that approximately 80 % of sedimentation at the sediment surface was composed of resuspended material (Overnell and Young, 1995). The dynamic conditions of LY1 are problematic for representatively sampling PM. However, using a suite of indices to determine the source and degradative state of POM will give an insight into the processes governing POM distribution at LY1.

Carbon-to-nitrogen ratios are a further indicator of organic matter source and fate in the water column (e.g. Cowie and Hedges, 1994; Hedges et al., 1997; Loh et al., 2008a). These ratios can be used as a source indicator to distinguish between marine plankton (C:N ratio 6 to 7), terrestrial derived vascular plants (C:N ratio >20), soils (C:N ratio 7 to 20), and riverine particulate organic matter (C:N ratio between 8 to 10; Meybeck, 1982; Emerson and Hedges, 1988; Goñi and Hedges, 1995; Hedges et al., 1997; Hedges and Oades, 1997). The variation in C:N ratio values arise from compositional differences with vascular plants being characteristically carbon rich, in contrast to protein rich phytoplankton (Emerson and Hedges, 1988). Preferential utilisation of nitrogen relative to carbon has the potential to modify C:N ratios, which means that the effects of degradation can limit their use as source indicators. C:N ratio was on average lowest in SPM below the pycnocline (mean 6.5 $\pm$ 0.6 SD) in comparison to slightly higher values in SPM above the pycnocline (mean 7.0 $\pm$ 0.5 SD). Generally, SPM C:N ratios were lowest in spring during highly productive periods when δ^{13}C was most positive, and higher towards late summer and winter when δ^{13}C was most negative. When δ^{13}C was most depleted in SPM during winter, SPM C:N ratios reached a maximum (mean 7.6 $\pm$ 1.7 SD) which is in the range of marine plankton, soil and riverine particulate organic material. The C:N ratios observed in sediment trap material were higher than SPM (mean 9.4 $\pm$ 0.4 SD). During the period of more positive δ^{13}C values in sediment trap material (-19.3 to -21.3 ‰) relative to previous and subsequent dates, C:N ratios were also higher (9.3 to 10.3), which could indicate the presence of partially degraded phytodetritus. On the other hand, given the similar ranges of C:N ratios indicating source, it could also suggest the presence of terrestrially derived material. There was little seasonal variation in sediment C:N ratio (mean 9.3 $\pm$ 0.1 SD), which was similar to sediment trap yearly average. Sediment δ^{13}C values were also relatively constant throughout the year (mean -21.2 $\pm$ 0.3 SD) and indicated a greater relative proportion of marine organic material. The lack of seasonal variation in sediment C:N, which were higher relative to SPM, and more positive δ^{13}C values, indicated the presence of marine derived organic material, which was subjected to continuous bioturbation and modification processes resulting in higher C:N ratios. A further explanation is that there were different terrigenous inputs to SPM, relative to traps and sediments, with the latter having a more positive δ^{13}C signature. Different sedimentation mechanisms of differently sourced material, coupled with lateral advection and resuspension processes could explain the differences between SPM with sediment trap material and sediments, and the similarities between sediment trap material and sediment.

Investigating δ^{13}C values in relation to other source indicators provides further information on the sources of organic matter at LY1. Positive correlations between amino acid concentration and

phytoplankton cell abundance, diatom fatty acid biomarker 16:4 (n-1) and diatom cell abundance, dinoflagellate fatty acid biomarker 22:6 (n-3) and dinoflagellate cell abundance indicate the importance of marine derived organic material to the SPM fraction (SPM from above the pycnocline). Concentrations of lithogenic tracer elements Al and Mn where highest throughout the entire water column during late summer and winter (Figure 4.20A & B), which corresponded to the period when SPM δ^{13}C values were the most negative. There was a negative correlation found between δ^{13}C values and Mn concentrations in SPM from above the pycnocline. Relationships between terrigenous indicators, coupled with high rainfall during the period of high Al and Mn concentrations (Figure 4.23), suggests higher proportions of terrestrially derived material towards the end of the year, which may have dominated SPM relative to sinking sediment trap material samples. There was no correlation found between sediment trap source parameters (δ^{13}C, C:N ratios, and lithogenic tracer elements). Additionally, higher C:N ratios were related to lower concentrations of Al and Mn. The lack of correlation found between sediment trap and sediments and source indicators suggests degradation processes could be important in explaining seasonal compositional variation. Additionally, the lack of correlation between source indicators with sediment trap material and sediments could be due to resuspension and lateral advection. These processes could result in the PM sampled originating from different sources and having a high residence time in the water column for degradation to alter the biochemical composition.

Isotopic, elemental, and biochemical compositions of organic matter at LY1 suggest that it was predominantly of mixed marine and terrestrial origin. However the relative contributions of marine and terrestrial organic matter varied seasonally and with particulate organic material fraction. A seasonal progression from a greater relative proportion of marine organic material to terrigenous material was observed in SPM (shown by transition to more negative δ^{13}C values). More positive δ^{13}C values relative to SPM (and lack of correlation between terrigenous indicators) suggest sediment trap material had a high relative proportion of marine derived organic matter. However, sediment trap material C:N ratio mean of 9.4 ± 0.4 SD, suggest this material could be a mixture of phytodetritus and PM from a riverine source. Without marine and terrestrial endmembers specific to sampling location and period, it is difficult to determine the definite predominance of source material. Given the relatively high concentrations of lithogenic trace elements in sediment trap material, and the fact that PM is predominantly composed of inorganic material, it is likely that sediment trap material is composed mainly of resuspended sediments. Further to seasonal and fraction type source variations, differences in the elemental, and biochemical compositions of the different sample types over the season indicate evidence of diagenetic alteration.

4.4.2 Seasonal diagenesis in suspended, sinking, and benthic fractions

In addition to shifts in PM source between fractions and over the sampling season, degradation of the PM is also important for explaining changes in biochemical composition. The extent of seasonal changes in organic matter biochemical composition varied between the four sample types. However, seasonal trends between SPM above and below the pycnocline were relatively similar. The SPM fraction transitioned from fresh, labile organic material to more refractory material during the sampling period from March to November. A range of biochemical parameters were used

to indicate this transition including C:N ratio, DI, %AA-N, individual amino acid and fatty acid biomarkers. C:N ratios of SPM were lower during spring and early summer (during the period of high microphytoplankton abundance) relative to later in the year. This could either indicate an increased degradation state between spring and winter or a shift in source material. A shift in source material is likely, as changes to the relative proportion of marine versus terrestrial material (indicated with δ^{13}C values) was observed in SPM. Fatty acid biomarker analysis indicated a higher relative proportion of diatom derived organic material during the spring and summer relative to the winter (Figure 4.18). Despite this shift in source, there is also evidence for increasing degradation state as indicated by the negative correlation between SPM above the pycnocline DI values and C:N ratio. The proportion of nitrogen represented by amino acids (% AA-N) and non-protein amino acids are further indicators of diagenetic alteration (Dauwe and Middelburg, 1998; Carr et al., 2016). The % AA-N in SPM reached a maximum in spring (68.1 %) and subsequently decreased for the rest of the year (Figure 4.15C). Non-protein amino acids are generally less reactive than protein amino acids resulting in their net accumulation during degradation (Dauwe and Middelburg, 1998). Mole percentages of non-protein amino acids in SPM increased as the year progressed (Figure 4.15B). Varying seasonal trends were observed with ASP/BALA and GLU/GABA ratios. However, these ratios are argued to be unreliable as diagenetic indicators due to breakdown of ASP and GLU not always resulting in production of BALA and GABA, and variability in source composition can effect the ratios (Cowie and Hedges, 1994; Dauwe and Middelburg, 1998). The sum of persistent diagenetic by-products BALA and GABA are unambiguous indicators of degradation (Cowie and Hedges, 1994). An increase in % BALA+GABA was observed over the course of the year into later summer and winter maximums (Table 4.6), and the positive correlation between % BALA+GABA and C:N ratio indicated more degraded material towards the end of the year. Given the trends observed from a suite of degradation measures, it seems evident SPM in the spring is fresher and labile relative to SPM collected during late summer to winter. Degradation processes and a shift in the relative proportions of source material are suggested to be responsible for this.

Seasonal variation in sediment trap biochemical composition was observed. Positive δ^{13}C values during post-bloom periods suggest the predominance of microphytoplankton sedimenting into traps after a time delay during transition from surface waters to 20 m (Figure 4.9A). Decrease in % AA-N was observed in parallel with high C:N ratios and low DI values during the period from day 187 to day 229. In addition to this, % BALA+GABA was high from day 188 to 284 relative to previous and subsequent dates, which coincided with the period of high C:N ratios. There was a progressive increase in the relative proportion of SFA, and decrease in PUFA from spring to winter (Figure 4.17). This trend of increasing SFA relative to decreasing PUFA is a typical indication of degradation (Najdek et al., 2002). Higher C:N ratios coupled with more positive δ^{13}C values, lower DI, and high % BALA+GABA indicated the presence of phytodetritus in sediment traps (day 187 to 229). The lack of correlation between terrigenous parameters and without definitive terrestrial endmembers, it is hard to determine the contribution of terrigenous organic material to sediment trap organic matter. It is likely that terrigenous material, in addition to phytodetritus, formed a substantial component of sediment trap PM at LY1, and further analysis of

other parameters is needed. The presence of sediments in trap material is evident on the cellulose nitrate filters, microscopic pictures of the samples, and high concentrations of lithogenic trace elements (Figure 4.7 and Figure 4.24). Other studies have found large seasonal variability in the relative proportions of marine and terrestrial derived organic material in sediment trap samples deployed in Dabob Bay using a range of parameters including lignin biomarkers (Hedges et al., 1988b).

In comparison to SPM and sediment trap material, there was little seasonal variation observed in all of the measured biochemical parameters from sediment samples. Other studies have found a lack in seasonal changes in biochemical parameters (including protein, carbohydrate, and lipid analysis) which is suggested to be a result of the dynamic "pulsing" environment (Pusceddu et al., 1999). The relatively uniform seasonal trends of high C:N, low DI, high % BALA+GABA, low relative proportions of terrigenous, diatom and dinoflagellate fatty acid biomarkers are consistent with continuous bioturbation of the surface sediment. The frequency of sampling in this study could have missed the deposition of fresh material which could have been quickly reworked by benthic fauna. Additionally, lateral advection of PM between sediment trap and sea floor depths could also be responsible for the lack of seasonality in the measured parameters. This could be because SPM, which displays seasonal trends in composition, is not efficiently transferred and incorporated into the underlying sediments. DI values of less than -0.30 are said to be representative of refractory material (Carr et al., 2016) however this is dependent on location and source input. LY1 sediments yearly DI average was -0.23 $\pm$ 0.08 SD and only on two occasions was DI greater than -0.30. There was a greater relative proportion of PUFA in sediments during the spring in contrast to summer and winter, which could be sourced from the high phytoplankton abundance in overlying water column during spring. A study found an increase in oxygen consumption rates in surface sediment samples during and after the phytoplankton bloom (Hicks et al., 2017). This suggests high remineralisation and grazing rates of reactive organic matter (e.g. PUFAs) that reaches the sea floor during the bloom period.

This study further indicates that seasonality is significant in affecting the biochemical composition of organic matter, which ultimately determines its reactivity, and subsequent cycling in the water column or benthic interface. High seasonal variability in biochemical composition was observed in SPM and sediment trap material as shown in other studies (e.g. Hedges et al., 1988b; Cripps and Clarke, 1998). In contrast, the lack of seasonal variability of biochemical parameters observed in sediments at LY1, has also been reported in other shallow coastal sites (Pusceddu et al., 1999). Finally, this lack of seasonal variation in all of the source parameters in sediment samples, suggests continuously re-worked surface sediments, and/or inefficient transport of SPM vertically to the seafloor.

4.4.3 Diagenesis at sequential stages of transport

Clear differences in the biochemical composition of each of the sample types at different stages of transport was observed. Overall TOC, TN, AA, TFA, and CHO concentrations generally decreased during transition from SPM to sediments (Table 4.4 and 4.5). This follows the trend of

decreasing POM availability during its transition through the water column to the seafloor, as a result of remineralisation (e.g. Lampitt, 1992; Buesseler and Boyd, 2009; Sanders et al., 2014). Percentage contributions of the biochemical classes AA, TFA, CHO to TOC also follow this trend and decreased from SPM to sediment trap material (except anomaly on day 313; Figure 4.17). The contribution of the three biochemical classes to TOC displayed different trends dependent on class between sediment trap and sediment samples (Figure 4.17). Sediments contained less TOC (yearly average 14.3 mg g^{-1} $\pm$ 4.7 SD) than sediment trap material (yearly average 44.2 mg g^{-1} $\pm$ 19.0 SD), yet the proportion of amino acid carbon that contributed to TOC was slightly higher (sediment trap yearly average % AA-OC 9.3 % $\pm$ 5.5 SD, sediment yearly average % AA-OC 14.1 & $\pm$ 2.2 SD). The higher proportion of amino acids could be a result of meiofauna present in the sediment samples. Typically, % AA-OC has been observed to decrease with depth and sedimentation due to the labile nature of AA (Lee and Cronin, 1984; Cowie and Hedges, 1992b). However, other studies have found a higher contribution of % AA-OC in sediments relative to overlying traps (Lee et al., 2000). The yearly average of carbohydrate carbon contribution to TOC (% CHO-OC) in sediment trap material (11.6 % CHO-OC $\pm$ 2.7 SD) was lower relative to sediments (17.6 % CHO-OC $\pm$ 1.6 SD). The only biochemical class to show a substantial reduction in its contribution to TOC between sediment traps and sediments was fatty acids (sediment trap 4.6 % TFA-OC $\pm$ 3.3 SD, sediment 0.2 % TFA-OC $\pm$ 0.1 SD). Fatty acid concentrations in sediments were between 0.2 to 2.9 % of the concentration of sinking sediment trap material, which is similar reduction found in other studies (Budge and Parrish, 1998).

The biochemical composition of organic material at sequential stages of transport was different as shown by PCA analysis (Figure 4.21). Other studies have used PCA for comparison of multiple biochemical classes (e.g. Sheridan et al., 2002; Ingalls et al., 2006), or with only amino acids and defined the first principle component as a degradation indicator (Dauwe and Middelburg, 1998; Dauwe et al., 1999). In this study, a clear separation of sediments relative to SPM and sediment trap material was observed and driven by PC1. Specific amino acids (ILEU, GLU, LEU) had large positive loadings on PC1 (Figure 4.21B). These intracellular amino acids are among the most labile compounds in plankton (Wakeham and Lee, 1993), and were most associated with fresh SPM. Generally, intracellular amino acids were higher in SPM and sediment trap material compared to sediments (Figure 4.13A to D). This is also seen in the PCA analysis, as loadings of ILEU, GLU, LEU decrease as samples transition from SPM, to sediment trap material, and then finally sediments. Low proportions of GLU and LEU were observed in sediments in comparison to sediment trap material as shown in other studies (Cowie and Hedges, 1992b). GLY, SER, and THR are protein-silica complexes in diatom cell walls and tend to accumulate during degradation as more reactive amino acids are preferentially consumed (Lee et al., 2000; Ingalls et al., 2003). GLY and non-protein amino acids (GABA, ORN, and BALA) had large negative loadings on PC1 (Figure 4.21B), which were associated with degraded sediment samples relative to more labile sediment trap and SPM. This trend of increasing GLY and non-protein amino acids in sediment, relative to sediment trap material, has been observed in other coastal study sites (Cowie and Hedges, 1992b). Mole percentages of GLY were relatively similar in SPM and sediment trap samples when compared to the much higher relative abundances found in sediments (Figure 4.14A).

Another study observed high values of GLY in sediments relative to other selectively degraded amino acids (Cowie and Hedges, 1992b). Further studies at deeper study sites (approximately 5000 m), have seen clear increases of GLY with increasing depth and maximum relative abundances found in sediments (Lee and Cronin, 1984; Lee et al., 2000). Generally SPM, and to a lesser extent sediment trap material, had positive scores associated with high positive loadings of biochemical compounds indicative of freshness (e.g. intracellular amino acids and PUFAs). The PCA analysis provided good visual representation of how biochemical composition changed with POM fraction, and which key compounds were responsible for differences between sample type.

Fatty acids are well known as degradation indicators due to their selective removal relative to other biochemical compounds (e.g. Reemtsma et al., 1990; Fileman et al., 1998; Parrish et al., 2005). Fatty acid compositions in sediment samples were vastly different to SPM and sediment trap samples. MUFAs (20:1(n-7), 18:1(n-7), and 16:1(n-7)) and SFA (20:0) dominated the total fatty acid composition of sediments (Figures 4.17 & 4.21B). Dominance of MUFA and SFA over PUFA has been recognised in highly degraded aggregates and sediment material (e.g. Fileman et al., 1998; Budge et al., 2001; Najdek et al., 2002; Parrish et al., 2005). A positive correlation between DI and PUFA in SPM from above the pycnocline was found, with higher PUFA percent composition corresponding to higher DI values. PUFAs were present in sediment however their composition was dominated by 20:4(n-3), which was different to the mixed assemblage of PUFAs dominating SPM fraction. A further study found sedimentary lipid compositions to be different from water column SPM which were enriched in branched and SFA (Wakeham et al., 1997a). The surprising lack of branched and long chain fatty acids observed in this study could be a result of the small sample quantities available for analysis. Despite a substantially lower %FA-OC found in sediments relative to sediment trap material, percent composition of PUFA in sediments was often similar to or higher than percentage composition in sediment trap material. This deviates from the expected trend of lower relative proportion of PUFAs to total fatty acids in sediments, relative to water column samples due to their reactivity (Wakeham et al., 1997a; Fileman et al., 1998; Budge et al., 2001). This could be a result of the presence of meiofauna contributing to the sediment fatty acid budget. However, other studies at relatively shallow coastal sites have found higher concentrations of PUFA in sediments relative to deeper sites (Budge et al., 2001). The shallow water column, and potentially short residence time of the lipid material in the shallow water column, could be predicted to enable the transfer of a higher proportion of PUFA to the sediment intact. Niggemann and Schubert (2006) found that water column depth was important in determining the concentrations of total fatty acids in sediments. Highest concentrations were found at shallow sites and were attributed to a reduced water column degradation period. On the other hand, sediment resuspension and lateral advection could be responsible for the similarities in the PUFA relative proportions observed between trap material and sediments. However, PCA analysis shows despite the similar relative proportions of PUFA in sediment and sediment trap material, the composition was vastly different. This could be a result of differences in grazing or remineralisation processes in the water column versus the benthos.

There were also clear biochemical differences observed between SPM and sediment trap material

which was driven by PC2 and predominantly fatty acid composition (Figure 4.21). For the majority of the year, PUFA percent composition of total fatty acids was highest in SPM from above the pycnocline, followed by SPM below the pycnocline, and lowest in sediment trap material (Figure 4.17). This is also shown in the PCA analysis where SPM has the highest loadings of PUFA (e.g. 20:5(n-3), 22:6(n-3), 18:4(n-3), 16:4(n-1)). In contrast to SPM, sediment trap material total fatty acid composition was primarily composed of SFA (Figure 4.17), in which 16:0 and 18:0 predominated (Figure 4.21B). The dominance of SFA to total fatty acids in sediment trap material is typical of more degraded material as previously discussed. This trend is also observed in other studies with proportions of PUFA decreasing from SPM to trap samples, and differences in composition between SPM versus sediments, with MUFA and SFA predominating in sediments (Budge et al., 2001; Parrish et al., 2005).

Further indices not included in the PCA analysis that suggest increasing diagenetic alteration with depth include %AA-N and DI. There was no correlation between %AA-N and DI in any of the sample types. However, the relationship between %AA-N and degradation state is recognised (e.g. Cowie and Hedges, 1994; Carr et al., 2016). Sediment trap %AA-N was similar to SPM on the first and last sample date but otherwise much lower (Figure 4.15C). The converse relationship between SPM and sediment trap material of lower %AA-N coupled with higher C:N ratios, higher proportion of SFA relative to PUFA in sediment trap material, indicates a more degraded state of organic material in sediment traps in comparison to SPM. Excluding the first two sample dates, %AA-N was higher in sediments relative sediment trap material. In contrast to SPM and sediment trap material, there was little seasonal variation in sediment % AA-N which could be a result of continuous bioturbation of the surface sediment and physical water column processes such as resuspension. As a result of the seasonal decrease in %AA-N observed in SPM and sediment trap material, and the relatively yearly constant of %AA-N in sediments, toward the end of summer (post day 228) percentage compositions of %AA-N became similar in SPM and sediment samples (Figure 4.15C).

Other degradation indicators such as GLU/GABA and ASP/BALA ratios showed varying trends down the water column (Table 4.6). ASP/BALA ratios were higher in SPM than sediments for the majority of sample dates, however sediment trap material values were often higher than those for SPM. GLU/GABA ratios generally followed expected trend of decreasing ratios down the water column. However, as previously discussed, GLU/GABA and ASP/BALA ratios may not be the best indices of degradation. Studies in the Peruvian upwelling region found increasing BALA concentrations with depth but ASP/BALA ratios to vary seasonally and not necessarily increasing with depth (Ittekkot et al., 1984). SPM and sediment trap % BALA + GABA followed similar seasonal trends with low mole percentages in spring, increasing into summer (Figure 4.6). Mid-summer % BALA + GABA in SPM was higher than in sediment trap material. This suggests SPM was more degraded than sediment trap material during this period, however this is not shown in any of the other degradation indices (e.g. DI, %AA-N, C:N). Sediment % BALA + GABA was substantially higher than the other sample types for the whole sampling period. Additionally, sediment samples were more enriched in non-protein amino acids relative to the other sample types with an yearly average of 2.91 mole % $\pm$ 0.27 SD (Figure 4.15B).

Analysis of the suite of biochemical indicators demonstrated that there were diagenetic differences between POM at sequential stages of transport. However, predicting the fate of organic material can be difficult due to its chemical complexity, range of sources, varying reactivities, and the fact that degradation processes of one organic matter type is likely to be different to others (Goñi and Hedges, 1995). The results show clear diagenetic differences between the SPM, sinking sediment trap, and sediment fractions. These differences are driven by the relative proportions of reactive fatty acids and amino acids which generally decrease in relative abundance with depth (except %AA-N between sediment trap to sediments). PCA analysis highlights the complex interaction between individual amino acids and fatty acids which explain the compositional variation between the different POM fractions. These biochemical differences between sample types have implications for determining the quality of POM at different stages of transport in the water column.

4.4.4 Flux

Bulk, OC, and N flux measured in the nine individual sediment trap deployments during 2016 displayed similar temporal trends with an initial maximum during spring coinciding with the phytoplankton spring bloom, and a secondary maximum in September (day 258; Figure 4.22A).

The seasonally averaged particulate material bulk flux at LY1 was 8.19 g m^2 d^{-1} $\pm$ 4.16 SD. The same sediment traps used in this study had previously been placed at the head of Loch Creran (trap at 10 m in 37 m water column), and recorded averaged bulk flux of particulate material from monthly deployments of 11.11 g m^2 d^{-1} $\pm$ 8.66 SD (Loh et al., 2010). The environmental conditions of this study's coastal site and the Loh et al. (2010) loch site were vastly different (dynamic, well mixed coastal site of LY1 versus semi-enclosed head of Loch Creran site), and bulk fluxes determined in this study were at the lower end of the range of the Loch Creran study (Loh et al., 2010). Other studies in Loch Linnhe recorded bulk fluxes of 12.40 g m^2 d^{-1} from sediment traps at 20 m depth in a 120 m water column (Overnell and Young, 1995). Comparisons to other studies in locations relatively near to LY1 show higher fluxes were observed in semi-enclosed environments (Loch Creran and Linnhe), relative to the open and dynamic LY1 study site. Lateral advection of PM could be responsible for the lower fluxes observed in LY1 traps.

Seasonal trends of bulk flux were, in general, closely related to monthly total rainfall measured at Dunstaffnage weather station (Figures 4.22A and 4.23). Bulk flux was high on the initial two sampling dates (12.21 and 7.37 g m^2 d^{-1} respectively) when rainfall was low (93.2 mm), suggesting that flux in this period was driven by phytoplankton biomass (which was at a seasonal maximum). Bulk flux then reached a yearly minimum (day 138, 1.68 g m^2 d^{-1}) when phytoplankton cell abundance had also decreased and rainfall was low (64.8 mm). Subsequently, bulk flux increased over summer and winter in line with increased rainfall and Al and Mn concentrations, which indicated an increase in terrigenous inputs during this period (Figure 4.20).

During the initial peak of bulk flux, OC and N flux was also at a maximum (0.99 g OC m^2 d^{-1}, 1.16 g N m^2 d^{-1}) coinciding with the spring bloom. The secondary peak of bulk flux reached similar levels to the first in contrast to OC flux, where secondary peaks were not as high as peak fluxes observed during the bloom. Secondary peaks of bulk fluxes during summer and winter were

sustained by high rainfall and terrestrial run off. High densities of material were collected during high flux periods on days 91, 98, 188, 215, and 258 (Figure 4.7). Secondary peaks of OC flux on days 188 and 258 follow late spring and summer increases in diatom and dinoflagellate cell abundances. At site LY1 the yearly average OC flux was 0.40 g OC m^2 d^{-1} $\pm$ 0.31 SD, which is comparable to nearby studies at the head of Loch Creran 0.67 g OC m^2 d^{-1} (Loh et al., 2010), Loch Linnhe 0.44 g OC m^2 d^{-1} (Overnell and Young, 1995), and higher than Loch Etive 0.025 g OC m^2 d^{-1} (Ansell, 1974). Determining PM flux, and its biochemical composition is key for determining the quantity and quality of organic matter that fuels benthic food webs.

Fluxes of AA, CHO, TFA followed similar seasonal trends to bulk, OC, and N fluxes (Figure 4.22). Yearly averaged AA fluxes were highest 168.28 mg AA m^2 d^{-1} $\pm$ 120.10 SD when compared to CHO and TFA which averaged 127.22 mg CHO m^2 d^{-1} $\pm$ 90.50 SD, and 14.06 mg TFA m^2 d^{-1} $\pm$ 10.05 SD respectively. These fluxes were comparable to other studies which found mean TFA fluxes of 8.8 mg TFA m^2 d^{-1} $\pm$ 7.4 SD (Budge and Parrish, 1998), and the maximum AA flux at site LY1 during the spring bloom (435 mg AA m^2 d^{-1}) was similar to fluxes found in productive surface waters of the central equatorial Pacific (approximately 400 mg AA m^2 d^{-1}; Lee et al., 2000).

In summary, the initial peak in flux was driven by microphytoplankton abundance due to maximum fluxes occurring at the same time as the bloom and high OC fluxes. Secondary periods of high flux were driven by rainfall and terrestrial run off. This suggests the relative abundance of terrigenous material that is incorporated with marine PM, predominates during periods of high rainfall. Further evidence of this is shown with other indicators e.g. Al and Mn concentrations and δ^{13}C values.

4.5 Conclusions

The results from this study demonstrate the difference in biogeochemical composition of PM fractions at sequential stages of transport in the water column. Key conclusions include:

1. The source of POM in the surface waters of LY1 is likely to be mixture of marine and terrestrial derived organic matter. A seasonal progression from a greater relative proportion of marine to terrigenous organic material was observed in SPM fractions (indicated by transition to more negative δ^{13}C values, and correlation with lithogenic tracer elements and terrigenous fatty acid biomarkers). More positive δ^{13}C values observed in sediment traps, coupled with high C:N ratios and other degradation indicators, and the lack of correlation with terrigenous organic matter indicators, suggests the presence of phytodetritus. However, the reported range of sediment trap material C:N ratio (mean 9.4 $\pm$ 0.4 SD) falls within values typical of a riverine source (C:N ratio 8 to 10; Meybeck, 1982). Additionally, seasonal flux patterns indicate the importance of rainfall and terrestrial inputs into sediment traps, which drive high fluxes between July to September. Therefore δ^{13}C and C:N values indicate sediment trap material is likely to be a mix of marine and terrestrially derived POM. Sediment samples δ^{13}C values did not vary seasonally and were similar to the yearly average of sediment trap δ^{13}C values. The similarity observed between trap material and

sediments suggests resuspension plays an important role in POM dynamics at LY1.

2. Compositional differences were observed between POM at sequential stages of transport. SPM was the most labile fraction in comparison to sediment trap and sediments at LY1. Higher concentrations of molecular biomarkers (AA, TFA, CHO), lower C:N ratios, higher DI, high percentage composition of PUFAs, and high % AA-N were evidence of this. Sediment trap material was compositionally more similar to SPM than sediments as shown by the PCA analysis. Compositional differences between SPM and sediment trap material were driven by fatty acid composition. There was a higher relative proportion of PUFAs in SPM compared to sediment trap material, which was dominated by SFA. At a molecular-level, sediments were compositionally distinct from SPM and sediment trap material. They were more degraded relative to the other fractions with higher DI, non-protein amino acids, cell wall associated amino acids, and fatty acid bacterial indicators. Labile, intracellular amino acids were more associated with SPM and sediment trap material when compared to sediments as shown by the PCA analysis. Although sediments still contained labile PUFAs, TFA concentrations were between 0.2 to 2.9 % of sediment trap material.

3. More positive δ^{13}C values in sediment trap material relative to SPM, further suggest a higher proportion of terrigenous organic material in suspended rather than sinking fractions. This difference could be a result of different sedimentation mechanisms of different source materials. Slow sinking, suspended particles have a higher terrestrial organic material signal, when compared to faster sinking PM collected in sediment traps. Inorganic terrestrial material was shown to be an important component of the faster sinking sediment trap material (as shown by the lithogenic tracer element analysis). This inorganic component can act as a ballast to enhance sedimentation rates, and as sorptive protection of organic material from degradation.

4. The absence of seasonality observed in all of the sediment parameters could be due a range of factors. Firstly, low accumulation rates as a result of laterally advected PM between sediment trap depths and the seafloor. Secondly, bioturbation processes could quickly rework freshly sedimented material and further change its biochemical composition. Thirdly, resuspension of sediment in a shallow, coastal environment could be responsible for the lack of seasonal variation observed in sediments. Sediments provide time-averaged samples in which short-term variability of source and composition can be lost.

5. Biogeochemical compositional changes over time and depth demonstrate the range of reactivities among individual biomarker compounds. This study demonstrates that seasonal investigations are essential to aid understanding of the complex and continuously changing biochemistry of POM. In a shallow coastal environment, it is unlikely that POM will be vertically transported to the seafloor. The high energy environment encourages lateral advection and resuspension on PM, which can affect the representative sampling of PM fraction. Finally, a suite of specific molecular-level and biomarker analyses are essential to help fathom POM sources and degradation processes.

Chapter 5

Determining the reactivity of the suspended versus sinking fraction of particulate organic material

5.1 Introduction

Remineralisation depth of particulate organic material (POM) is dependent on the balance between POM sinking velocities and their remineralisation rate (Ploug et al., 2008a; Kwon et al., 2009). In turn, this is dependent on POM reactivity and numerous other factors including heterotrophic consumption, microbial colonisation, and physical environment conditions. As mentioned previously, POM is heterogeneous in nature originating from marine and terrestrial sources, in which an inorganic component is associated with the organic fraction of the particulate material (PM). The reactivity of POM is important in predicting its fate in the water column. In this study reactivity is defined as the rate at which POM is respired and broken down into organic and inorganic material. During this degradation, oxygen (O_2) is consumed directly or indirectly, and can be used to trace biological activity (Glud, 2008). Fresh, labile, and biologically reactive POM is more likely to be readily respired into inorganic material (remineralisation), when compared to degraded, refractory material, which is more likely to be preserved to depth (Giering et al., 2014). The depth at which POM is remineralised is significant as it affects global air-sea carbon dioxide balance, global oceanic distribution of many elements, and food supply to the benthos (Kwon et al., 2009; McDonnell et al., 2015). Additionally, the export of POM drives the biological carbon pump (BCP), in which approximately 1 to 40 % of photosynthetically fixed carbon is exported to depth, where remineralisation rates are considerably slower than in surface waters (Herndl and Reinthaler, 2013; Iversen and Ploug, 2013).

Size, shape, and density of PM are key determinants of whether PM is classified into the suspended particulate material (SPM), or sinking fraction. These factors affect the sinking velocity of PM, and residence time in the water column, which play a significant role in particulate remineralisation efficiency. Further factors that affect PM sinking velocity and therefore water column residence time include biogeochemical composition, addition of ballast material, aggregation and

disaggregation (Smayda, 1970; Goutx et al., 2007; Bach et al., 2016). Additionally, the composition of PM in a coastal setting will vary seasonally, with typically higher relative inputs of terrigenous material towards the end of summer and winter (Hedges et al., 1988b). This material can include lithogenic elements which will affect PM sinking velocities and reactivity. Particles with higher residence times in surface waters, i.e. SPM, are subjected to higher remineralisation rates as a result of longer exposure to bacterial and heterotrophic grazers (Goutx et al., 2007). There is a wide spectrum of PM present in the water column having different compositions and contributions to carbon export. Enhancing the understanding of the reactivity of suspended versus sinking classes of PM, would provide valuable information on their fate in the water column.

Biochemical composition is a key determinant of POM reactivity, and numerous biochemical indicators have been used as relative estimates of reactivity including C:N ratio, selected lipid, pigments, lignins, proteins, and carbohydrates (e.g. Cowie et al., 1992; Cowie and Hedges, 1994; Niggemann and Schubert, 2006; Goutx et al., 2007). The composition of PM can change substantially over a season in response to changing microphytoplankton community composition, and seasonally dependent terrigenous inputs. The organic-rich nature of POM in coastal environments, means that the majority is remineralised in the water column and suspended sediments (De Haas et al., 2002). Selective consumption of labile carbohydrates, lipids, and proteins in fresh POM results in the accumulation of refractory material (Ingalls et al., 2003). This selective consumption and preservation allows the relative abundances of these compounds to be used to determine the degradation state of POM (e.g. Wakeham et al., 1997a; Cowie and Hedges, 1992b; Lee et al., 2000; Ingalls et al., 2003). However, the use of some degradative state indicators in comparison studies is questionable due to non-uniform distributions, specific degradation pathways, and multiple sources of compounds (Dauwe and Middelburg, 1998). The use of compounds that are universal in distribution, and form the majority of POM in marine and terrestrial systems, serve as representative degradation indices (Cowie and Hedges, 1994; Dauwe and Middelburg, 1998; Niggemann and Schubert, 2006). The coupling of well-established biogeochemical lability indicators with O_2 consumption rates, will determine how organic matter composition affects remineralisation.

Oxygen uptake rates as a tracer for biological activity and organic matter degradation is well established. Sediment studies have focused on using the rate of total O_2 consumption as a proxy for the rate of carbon degradation (or reactivity) as O_2 is consumed through aerobic respiration (e.g. Glud, 2008; Hargrave, 1972; Li et al., 2012; Glud et al., 2016; Hicks et al., 2017). These studies have investigated benthic carbon remineralisation in a range of dynamic settings and over seasonal cycles. A few studies have investigated carbon-specific respiration rates of suspended and sediment trap POM (e.g. Iversen et al., 2010; Iversen and Ploug, 2013; Boyd et al., 2015; McDonnell et al., 2015; Cavan et al., 2017). However, fewer studies have simultaneously measured biogeochemical composition, and more specifically at a molecular-level (Goutx et al., 2007). No other studies have investigated seasonal changes between SPM and sediment trap material reactivity, in relation to molecular-level biogeochemical composition in a coastal environment. This study addresses this knowledge gap, and investigates how the seasonally varying composition of suspended versus sinking fractions of PM affects its reactivity. The focus of this study is a coastal

environment which are significant areas for marine, estuarine, and terrestrial carbon cycling. Additionally, PM created in nutrient-rich coastal waters can affect biogeochemical cycles at a global scale, as PM can be laterally advected to open-ocean systems. The unique coupling of seasonal reactivity measurements of SPM and sinking PM fractions with molecular-level compositional analysis, will enhance understanding of organic material cycling in a coastal environment. It will provide information on compositional changes of PM down the water column from the suspended and sinking fractions, and associated reactivity. From this information, it is possible to estimate how the composition of PM, in terms of molecular-level analysis of key components and the relative proportions of marine and terrigenous material, determines its fate in the water column.

5.1.1 Research objectives

The aim of this study was to examine the difference of PM reactivity between suspended (water column samples) and sinking (sediment trap material) fractions. An additional aim included sampling SPM from above and below the pycnocline in order to address compositional and reactivity differences in material across a physical environment gradient. A further aim was to investigate the seasonal variation in reactivity of PM in the two fraction types. Lastly, a comparison between the reactivity of sediment trap material collected from a coastal site, to a restricted exchange environment was aimed to contrast PM reactivity with the physical environment. Specific objectives included using O_2 consumption rates, coupled with other biogeochemical measures of organic material lability (e.g. carbohydrate concentration, fatty acids, amino acids, and lithogenic tracer elements), to estimate the reactivity of different fractions of PM. Research questions specific to this Chapter include:

1. What is the relationship between biogeochemical measures of organic material lability and reactivity?
2. How does the reactivity of suspended versus sinking particulate material change seasonally?
3. What is the difference in reactivity of material collected from site LY1 in the Firth of Lorne versus RE5 in Loch Etive?

5.2 Methods

Oxygen consumption rates were used as a proxy to determine the reactivity of SPM and sediment trap material. SPM was collected from depths from above and below the pycnocline at site LY1. CTD data were used to determine these depths and Niskin bottles were used to collect seawater. SPM was stored in Nalgene containers in the dark inside a cool box until they were returned to the laboratory. Sediment traps were deployed ten times during 2016 at site LY1 (as described in Chapter 4, Table 4.1), and on eight of these deployments sediment trap material was used for reactivity determination. Sample dates were split into their respective season for statistical analyses (Table 5.1). Aliquots of sediment trap material (Chapter 4, Section 4.2.2.2) were used for incubation experiments within four hours of sediment trap recovery. For both SPM and sediment trap

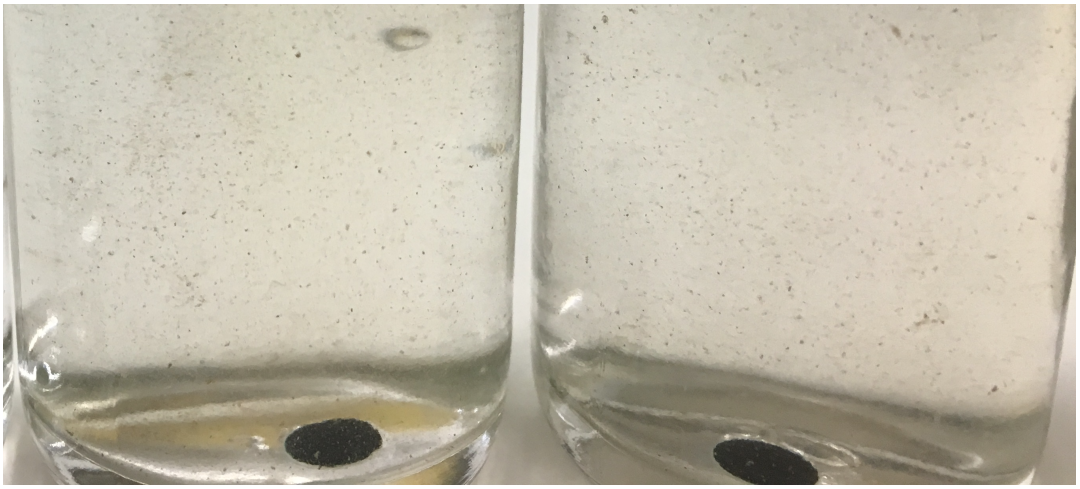

Figure 5.1: Glass vials containing sediment trap material and PyroScience oxygen optode sensor spots

samples, the fraction was homogenised and poured into air-tight glass vials (32.39 ml) leaving no head space. Samples of SPM and sediment trap material were incubated in at least duplicate vials (and most often five replicates of each sample was used). Glass vials contained pre-calibrated O_2 optode sensor spots which were adhered to the vial with silicone based-glue (PyroScience Sensor Technology; Figure 5.1). Prior to each incubation, sensor spots were calibrated using Pyro Oxygen Logger one-point calibration (100 % air saturation), and filtered seawater from site LY1 (20 m). Bare fiber-optic O_2 sensors were connected to a multi-purpose O_2 meter (FireStingO_2) which was connected to a laptop containing Pyro Oxygen Logger software. Samples were incubated in the dark for up to 5 hours (dependent on rate of O_2 concentration decrease) in a CT room (8°C) on a roller table (to ensure constant mixing). An additional vial was used to measure seawater temperature with an external temperature sensor during each O_2 measurement. Oxygen concentrations (mg L^{-1}) were measured at time zero and then approximately every 15 minutes for the first 45 minutes, and then at less regular intervals (due to logistical restraints). Oxygen consumption rate was calculated as the difference in O_2 concentration at time zero and the time point where there was a 10 % decrease in concentration, divided by time. Rate calculations have focused on this initial decrease, as is it the most representative period for rate calculations in enclosed settings, where prolonged incubations can approach anoxia. Studies using sediment have found the initial decrease in O_2 concentration was linear (Glud, 2008; Hicks et al., 2017). The initial 10 % decrease observed in this study often fell in between the first two sampling time points, which was not ideal. Sediment dry weight calculations from other sediment trap fractions on respective dates were used to calculate the amount of sediment in each of the incubation vials. Additional organic carbon (OC) concentration measurements from respective sediment trap fractions were used to calculate the amount of OC in each incubation vial.

Samples from a one-time deployment of sediment traps (100 m) at site RE5 in Loch Etive (15/06/16) were incubated following the same method as above. The purpose of this was to use sediment trap O_2 consumption rates in a restricted exchange environment, as a comparison to those observed at LY1.

Table 5.1: Suspended particulate material (SPM) and sediment trap material collected from LY1 sampling dates used for reactivity experiments

SPM collection	Sediment trap recovery date	Day in year	Season
-	17/05/2016	138	Spring
-	02/06/2016	154	Spring
05/07/2016	06/07/2016	187/ 188	Summer
01/08/2016	02/08/2016	214/ 215	Summer
16/08/2016	16/08/2016	229	Summer
14/09/2016	14/09/2016	258	Summer
11/10/2016	11/10/2016	285	Winter
08/11/2016	08/11/2016	313	Winter

Methods for the analyses of amino acid (AA) concentration, carbohydrate (CHO) concentration, total fatty acid (TFA) concentration, degradation index (DI; Dauwe and Middelburg, 1998), bulk flux, individual amino acids and fatty acids, and lithogenic tracer elements are described in Chapter 4, Section 4.2.3. Data was used from Chapter 4 to investigate the relationship between reactivity and biochemical composition of PM.

5.2.1 Statistical analysis

Simple linear regression was used to estimate the time point where initial O_2 concentrations had fallen by 10 %. This was then used in O_2 consumption rate calculations. Correlation (Pearson's Correlation Coefficient) and regression analysis were used to determine the relationship between reactivity of sediment trap material with other lability parameters. All analyses were carried out using the statistical programme R and Minitab 17.

5.3 Results

Oxygen concentration decreased with increasing incubation period for all of the SPM and sediment trap material incubation dates (Figure 5.2, 5.3, & 5.4). The time taken for initial O_2 concentrations in SPM incubations at time zero to decrease by approximately 10 %, was faster between July to August (<60 minutes), compared to September to November sample dates (between 200 to 1400 minutes). Similarly, the first five sample dates (May to August between 10 to 27 minutes) of the sediment trap material incubations were faster relative to September, October, and November (between 132 to 415 minutes). Linear regression best described the relationship between O_2 concentration and time when compared to other regression techniques (polynomial regression). The relationship between the initial 10 % O_2 concentration decrease and incubation period was linear when compared to later measurements which often plateaued. It was this initial linear decrease, where R^2 was >0.61 for all sample dates (except 11/10/16 SPM below the pycnocline R^2=0.46), that was used for reactivity calculations (e.g. Glud, 2008; Hicks et al., 2017).

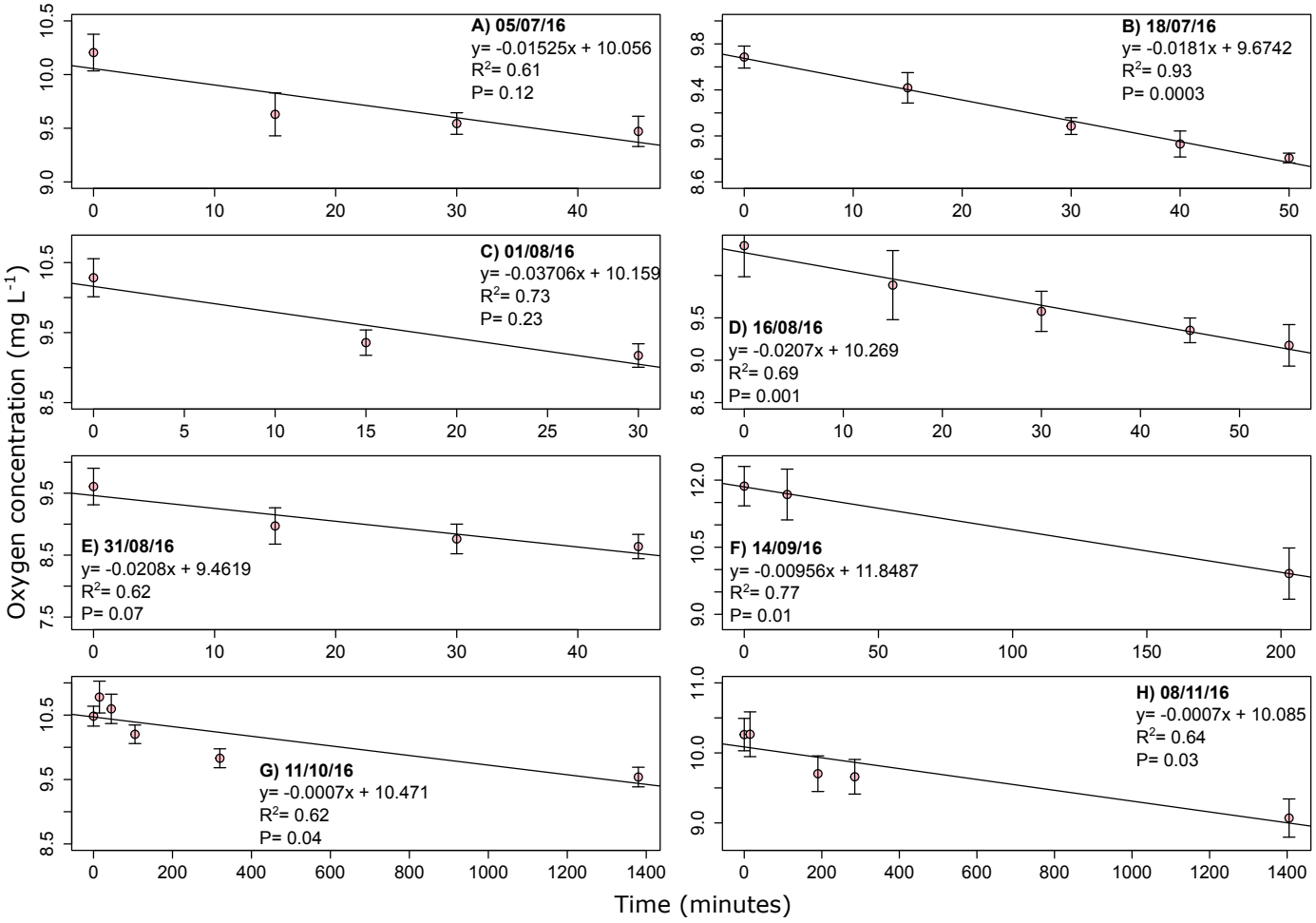

Figure 5.2: Mean oxygen concentrations (mg L^{-1}) $\pm$ SD during incubation experiments with suspended particulate material (SPM) sampled from above the pycnocline and from sample dates A) 05/07/16, B) 18/07/16, C) 01/08/16, D) 16/08/16, E) 31/08/16, F) 14/09/16, G) 11/10/16, and H) 08/11/16. Linear regression fit data is shown for each sample date.

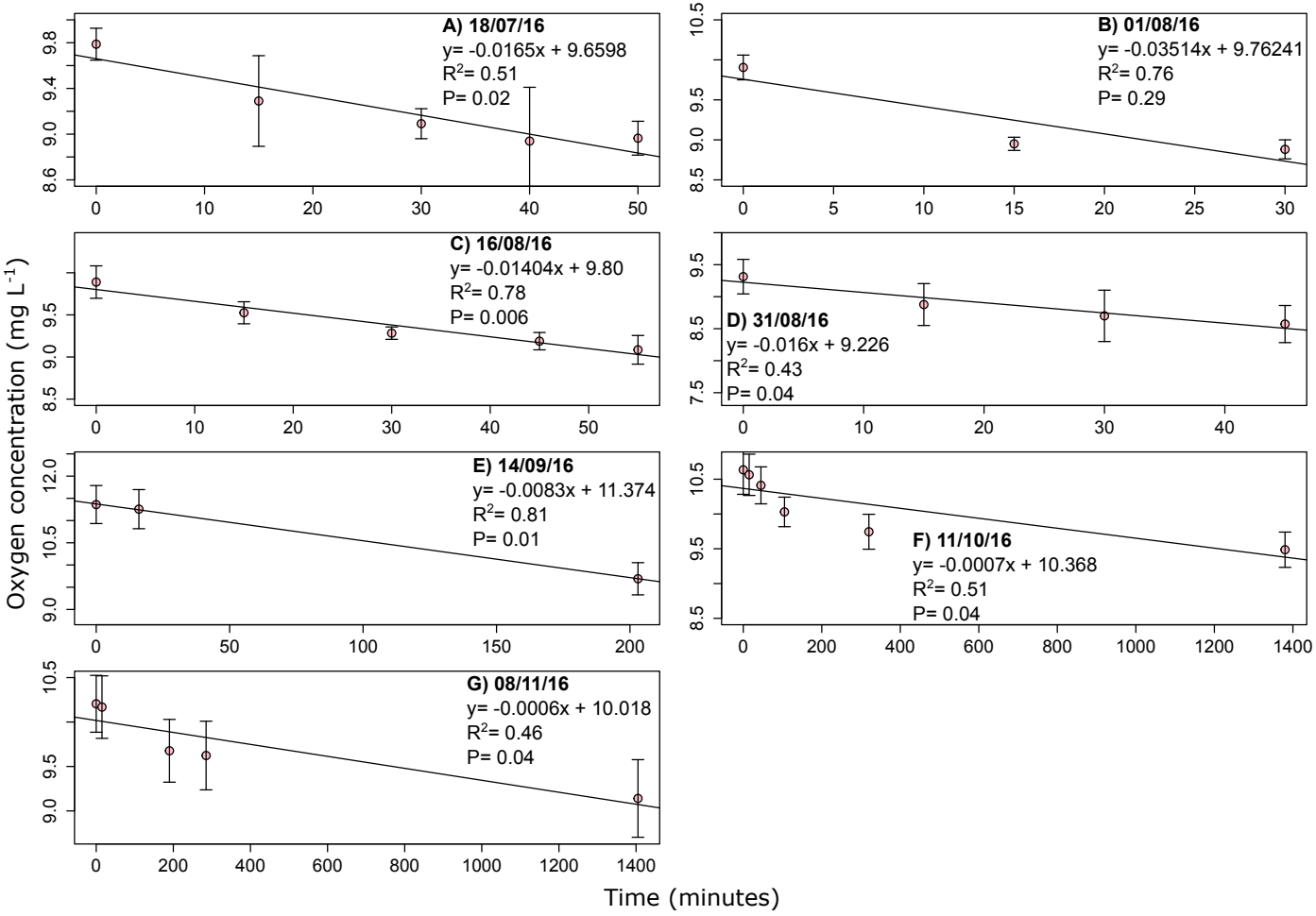

Figure 5.3: Mean oxygen concentrations (mg L^{-1}) $\pm$ SD during incubation experiments with suspended particulate material (SPM) sampled from below the pycnocline and from sample dates A) 18/07/16, B) 01/08/16, C) 16/08/16, D) 31/08/16, E) 14/09/16, F) 11/10/16, and G) 08/11/16. Linear regression fit data is shown for each sample date.

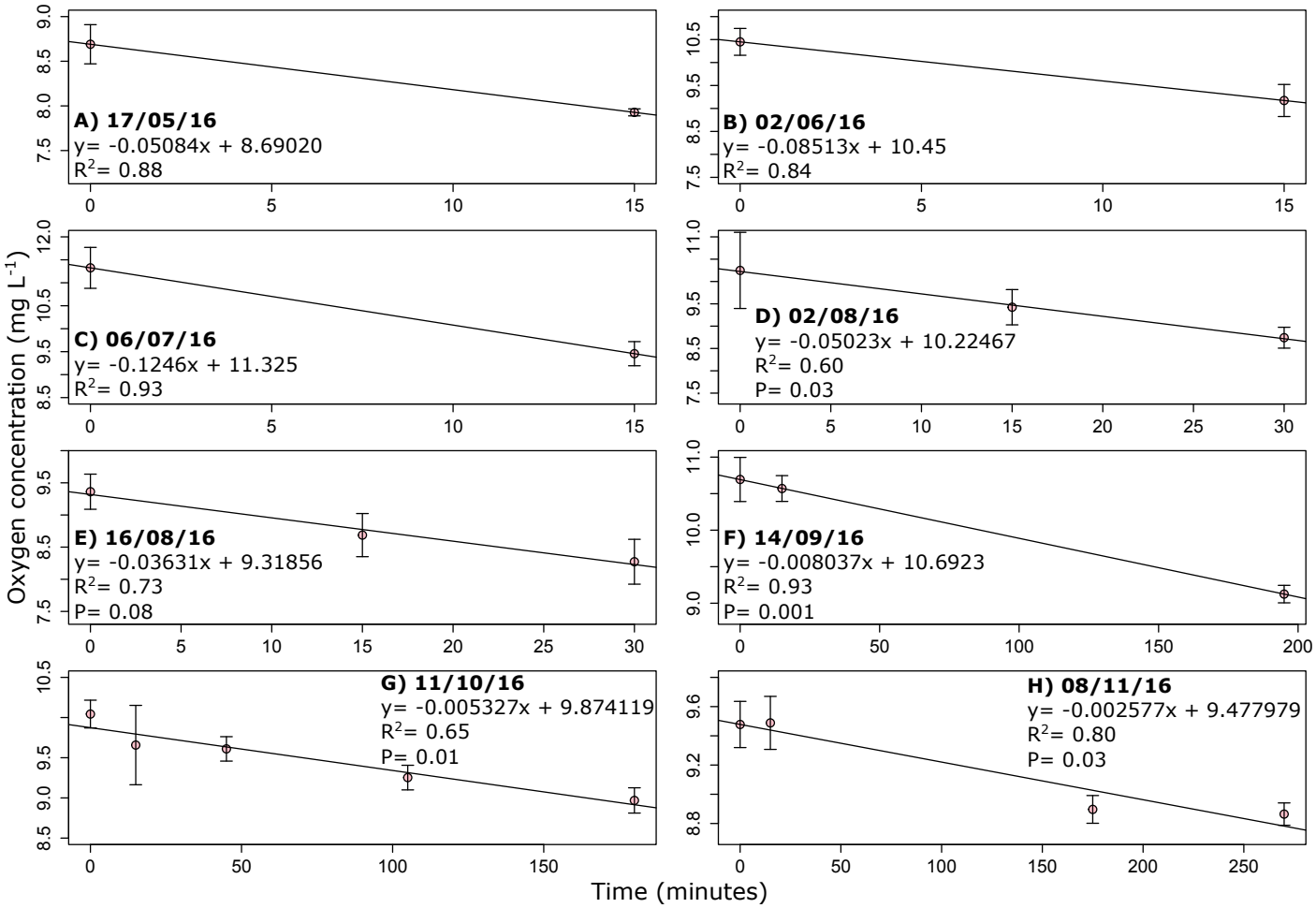

Figure 5.4: Mean oxygen concentrations (mg L^{-1}) $\pm$ SD during incubation experiments with sediment trap material from sample dates A) 17/05/16, B) 02/06/16, C) 06/07/16, D) 02/08/16, E) 16/08/16, F) 14/09/16, G) 11/10/16, and H) 08/11/16. Linear regression fit data is shown for each sample date.

O_2 consumption rates of SPM from above and below the pycnocline, and sediment trap material collected from LY1 during 2016 were compared (Figure 5.5). Sediment trap material O_2 consumption rate was highest in May (day 138 maximum 2.1 mg O_2 mg OC^{-1} min^{-1} $\pm$ 0.6 SD) and subsequently decreased for the remainder of the year. The minimum O_2 consumption rates of sediment trap material occurred at the end of summer and during winter reaching minimum values of 0.03 mg O_2 mg OC^{-1} min^{-1} $\pm$ 0.0 SD. Seasonal O_2 consumption rates were not statistically different between SPM collected from above versus below the pycnocline (Mann-Whitney U-test, U=1155.0, $n_{SPMabove}$= 35, $n_{SPMbelow}$= 36, P= 0.23). The maximum O_2 consumption rate of the suspended fraction occurred below the pycnocline in August (day 214 5.4 mg O_2 mg OC^{-1} min^{-1} $\pm$ 0.9 SD). Minimum O_2 consumption rates of SPM occurred during winter, with a low of 0.09 mg O_2 mg OC^{-1} min^{-1} $\pm$ 0.0 SD observed on day 285. The SPM fraction O_2 consumption rates were significantly higher during summer sample dates in comparison to sediment trap (ST) material (Figure 5.6; Mann-Whitney U-test, U=1786.0, $n_{SPMsummer}$= 47, $n_{STsummer}$= 17, P= 0.00). In contrast, there was no significant difference between O_2 consumption rates of SPM and sediment trap material sampled in winter (Mann-Whitney U-test, U=412.0, $n_{SPMwinter}$= 24, $n_{STwinter}$= 10, P= 0.78).

Between spring, summer, and winter sampling dates, O_2 consumption rates varied. The SPM fraction O_2 consumption rates were significantly higher in summer (median 2.3 mg O_2 mg OC^{-1} min^{-1} $\pm$ 0.2 SD), when compared to winter (median 0.04 mg O_2 mg OC^{-1} min^{-1} $\pm$ 0.01 SD; Mann-Whitney U-test, U=2256.0, $n_{SPMsummer}$= 47, $n_{SPMwinter}$= 24, P= 0.00). Additionally, there was a statistically significant difference in sediment trap material O_2 consumption rates between seasons (Figure 5.6), with values being the highest in spring (median 1.7 mg O_2 mg OC^{-1} min^{-1} $\pm$ 0.2 SE), followed by summer (median 0.2 mg O_2 mg OC^{-1} min^{-1} $\pm$ 0.0 SE), and lowest in winter (median 0.1 mg O_2 mg OC^{-1} min^{-1} $\pm$ 0.0 SE; Kruskal-Wallis, H= 18.76, df= 2, n_{spring}= 8, n_{summer}= 15, n_{winter}= 10, P= 0.00). Additionally, peaks in SPM O_2 consumption rates corresponded to a peak in microphytoplankton cell abundance, and a positive correlation between microphytoplankton cell abundance and O_2 consumption rates was observed (Pearson's Correlation Coefficient, r=0.87, P= 0.02).

In order to put O_2 consumption rates at LY1 in context with other environments, a reactivity rate of 0.04 mg O_2 mg OC^{-1} min^{-1} $\pm$ 0.00 SD was measured in sediment trap material collected from 100 m in Loch Etive (site RE5). This was a one-time deployment on 15/6/2016, and when compared to O_2 consumption rates found at 20 m at LY1 on a similar date (02/06/2016, 0.09 mg O_2 mg OC^{-1} min^{-1} $\pm$ 0.03 SD), reactivity was approximately 2.3 times lower in Loch Etive relative to LY1.

Correlation analyses were used to identify relationships between O_2 consumption rates and biochemical composition (Table 5.2). Additionally, well-known diagenetic indicators were included in the correlation analysis. Concentrations of the three major biochemical classes were found to have varying relationships between PM fraction and O_2 consumption rates. Positive correlations were observed between CHO concentration and O_2 consumption rates in SPM samples (SPM Above r=0.70, P= 0.00, SPM Below r=0.61, P= 0.00), compared to negative relationships

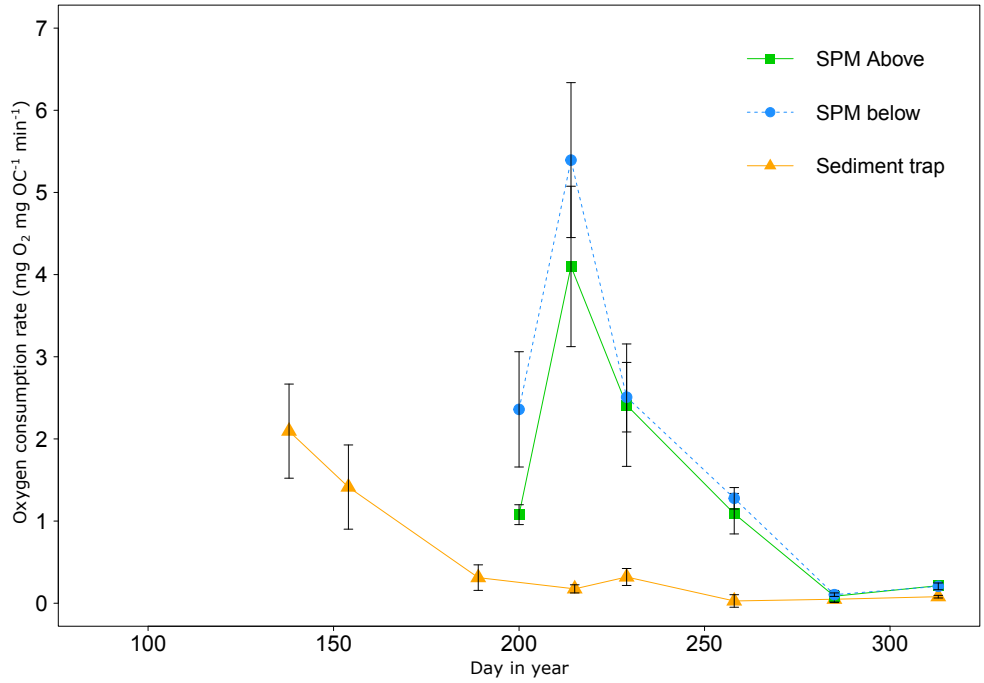

Figure 5.5: Seasonal mean ± SD oxygen consumption rates (mg O_2 per mg organic carbon (OC) min^{-1}) of suspended particulate material (SPM) above (n= 6) and below (n= 6) the pycnocline, and sediment trap material ($n_{day138,154}$= 4, n_{day189}= 2, $n_{day215,258,285,313}$= 5, n_{day229}= 3), sampled from LY1 during 2016

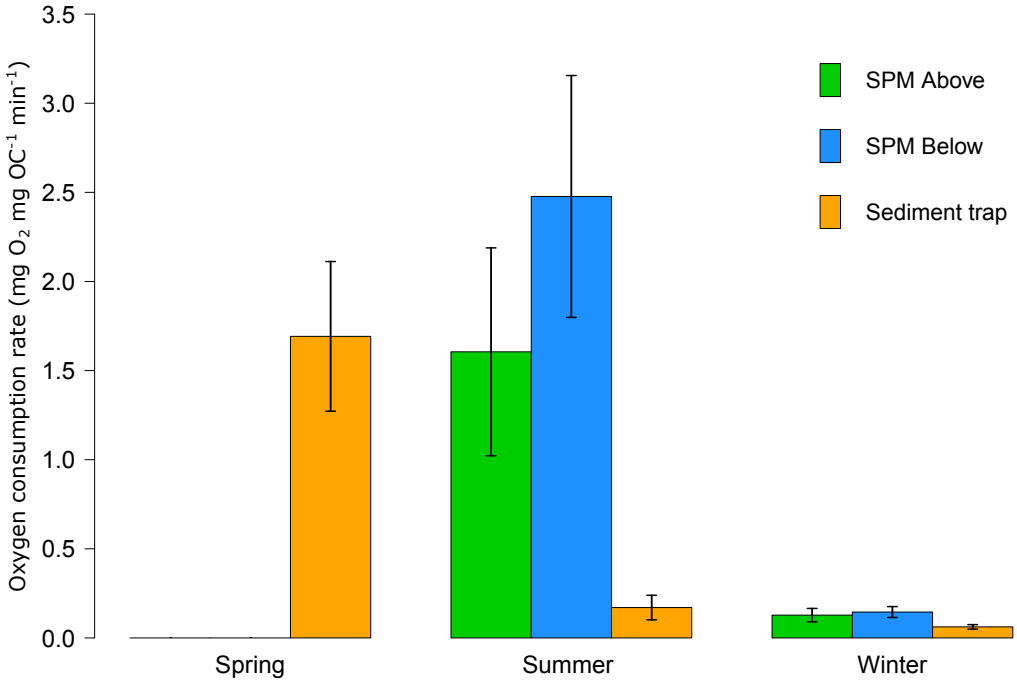

Figure 5.6: Median ± SE oxygen consumption rates (mg O_2 per mg organic carbon (OC) min^{-1}) of suspended particulate material (SPM) above (n= 6) and below (n= 6) the pycnocline, and sediment trap material ($n_{day138,154}$= 4, n_{day189}= 2, $n_{day215,258,285,313}$= 5, n_{day229}= 3), sampled from LY1 during spring, summer, and winter seasons in 2016

in sediment trap material (r=-0.60, P= 0.00). Similar relationships between the percentage of organic carbon represented as carbohydrates (%CHO-OC) and O_2 consumption rates were found as CHO concentration and O_2 consumption rates. In all of the sample types, positive correlations were found between TFA concentration and O_2 consumption rates (SPM Above r=0.58, P= 0.00, SPM Below r=0.87, P= 0.00, sediment trap material r=0.78, P= 0.00). Weaker correlations were observed between the percentage of organic carbon represented as fatty acids (%TFA-OC) and O_2 consumption rates of SPM above the pycnocline and sediment trap material. A weak inverse relationship between %TFA-OC and O_2 consumption rates was found in SPM from below the pycnocline. Conversely, a weak negative correlation was found between %TFA-OC and SPM below the pycnocline O_2 consumption rates. A weak and stronger positive correlation was observed between O_2 consumption rates and AA concentration in SPM from below the pycnocline and sediment trap material respectively.

Further analyses were carried out to identify relationships between POM reactivity with individual amino acids and fatty acids. Saturated fatty acids (SFA) were found to have negative relationships with O_2 consumption rates across all the sample types (Table 5.2). Both monounsaturated (MUFA) and polyunsaturated fatty acids (PUFA) were positively correlated with O_2 consumption rates in SPM and sediment trap material. Diatom fatty acid biomarkers (16:4(n-1) and 20:5(n-3)) had positive relationships with O_2 consumption rates and all sample types.

Negative relationships between specific amino acids such as percentage β-alanine (BALA) plus γ-aminobutyric acid (%BALA+GABA), glycine (GLY), alanine (ALA), BALA, and tyrosine (TYR), and O_2 consumption rate was found in SPM above the pycnocline. Lysine (LYS) was the only amino acid where there was a positive correlation with SPM above the pycnocline O_2 consumption rates. For SPM from below the pycnocline, negative correlations were found between serine (SER), GLY, threonine (THR), and TYR, and O_2 consumption rates. Degradation index (DI), valine (VAL), isoleucine (ILEU), leucine (LEU), and LYS were related to positive correlations with O_2 consumption rates in SPM from below the pycnocline. Sediment trap material O_2 consumption rates were negatively correlated to %BALA+GABA, THR, BALA, GABA, and LYS. Conversely, aspartic acid (ASP), glutamic acid (GLU), methonine (MET), and LEU all had positive correlations with sediment trap material O_2 consumption rates.

There was a negative relationship between sediment trap material O_2 consumption rates and bulk flux (r=-0.73, P= 0.00). Lithogenic tracer elements (Al and Mn) had negative relationships with SPM from above the pycnocline O_2 consumption rates. Stronger negative correlations were observed with Mn and O_2 consumption rates of SPM from below the pycnocline and sediment trap material.

Table 5.2: Correlation (Pearson's Correlation Coefficient r value) analysis between suspended particulate material (SPM) above and below the pycnocline, and sediment trap material reactivity and a range of parameters (samples collected from site LY1 during 2016) versus oxygen consumption rates

	SPM Above		SPM Below		Sediment trap	
	r	P	r	P	r	P
Bulk flux	-	-	-	-	-0.73	0.00
CHO	0.70	0.00	0.61	0.00	-0.60	0.00
%CHO-OC	0.76	0.00	0.92	0.00	-0.32	0.07
Fatty acids						
TFA	0.58	0.00	0.87	0.00	0.78	0.00
%TFA-OC	0.53	0.001	-0.19	0.27	0.44	0.01
SFA	-0.73	0.00	-0.84	0.00	-0.53	0.002
MUFA	0.73	0.00	0.79	0.00	0.63	0.00
PUFA	0.51	0.002	0.74	0.00	0.38	0.03
16:4(n-1)	0.81	0.00	0.93	0.00	0.88	0.00
20:5(n-3)	0.51	0.002	0.57	0.00	0.58	0.00
22:6(n-3)	0.55	0.001	0.72	0.00	0.03	0.86
Amino acids						
AA	0.04	0.85	0.36	0.03	0.90	0.00
%AA-OC	0.02	0.91	0.61	0.00	0.50	0.003
%BALA+GABA	-0.71	0.00	0.01	0.69	-0.77	0.00
DI	0.28	0.14	0.70	0.00	0.41	0.02
ASP	0.46	0.01	0.29	0.08	0.59	0.00
GLU	0.15	0.45	-0.39	0.02	0.68	0.00
SER	-0.31	0.10	-0.73	0.00	0.24	0.16
HIS	-0.34	0.06	0.39	0.03	0.24	0.16
GLY	-0.62	0.00	-0.86	0.00	-0.35	0.04
THR	-0.29	0.13	-0.78	0.00	-0.62	0.00
ARG	0.10	0.59	0.69	0.00	-0.10	0.57
ALA	-0.61	0.00	-0.18	0.29	-0.15	0.40
BALA	-0.79	0.00	0.07	0.67	-0.63	0.00
TYR	-0.54	0.002	-0.52	0.001	-0.04	0.83
GABA	-0.39	0.04	0.04	0.81	-0.57	0.00
MET	0.49	0.01	0.03	0.88	0.61	0.00
VAL	0.12	0.54	0.73	0.00	-0.22	0.20
PHE	0.00	0.97	-0.21	0.22	-0.03	0.87
ILEU	0.31	0.10	0.78	0.00	-0.12	0.50
LEU	0.27	0.16	0.72	0.00	0.61	0.00
ORN	-0.03	0.87	-0.51	0.001	-0.64	0.00
LYS	0.88	0.00	0.91	0.00	-0.64	0.00
Lithogenic tracer elements						
Al	-0.66	0.001	-0.25	0.14	-0.43	0.01
Mn	-0.61	0.004	-0.68	0.00	-0.78	0.00

Table 5.3: Comparison of sediment trap biogeochemcial composition collected from sites LY1 (Firth of Lorne) and RE5 (Loch Etive) on two sample dates in 2016. Individual fatty acids are percentage contribution to total fatty acids. Individual amino acids are reported as mole percentages.

Sample site	LY1	RE5
Date	02/06/2016	15/06/2016
Depth (m)	20	100
Bulk flux (g m^2 d^{-1})	3.2	0.1 ± 0.0
%CHO-OC	7.2	53.8
Fatty acids		
%TFA-OC	4.7 ± 1.8	9.0 ± 2.0
SFA	52.2	79.8
MUFA	26.4	9.7
PUFA	21.4	10.5
16:4(n-1)	1.6	0.2
20:5(n-3)	6.4	5.6
22:6(n-3)	2.5	0.6
Amino acids		
%AA-N	28.3	54.4
%AA-OC	12.1	19.0
%BALA+GALA	0.15	0.8
DI	1.1 ± 0.2	0.8
ASP	9.4 ± 0.6	13.3
GLU	13.2 ± 2.3	13.5
SER	6.8 ± 0.9	7.8
HIS	0.9 ± 0.2	0.7
GLY	13 ± 0.8	16.8
THR	4.5 ± 0.6	4.6
ARG	5.3 ± 0.5	7.5
ALA	10.9 ± 0.4	4.4
BALA	0.1 ± 0.1	0.2
TYR	2.4 ± 0.3	1.5
GABA	0.03 ± 0.0	0.6
MET	1.2 ± 0.5	1.3
VAL	7.4 ± 0.2	7.4
PHE	3.1 ± 1.5	4.1
ILEU	5.5 ± 0.2	4.8
LEU	8.2 ± 0.4	7.0
ORN	0.12 ± 0.0	0.2
LYS	7.8 ± 0.7	4.4
Lithogenic tracer elements		
Al (mg L^{-1})	0.34	0.33
Mn (mg L^{-1})	0.01	0.08

5.4 Discussion

5.4.1 Seasonal differences between the reactivity of suspended versus sinking fractions

Differences between the reactivity of suspended versus sinking particulate material was investigated between May and November 2016 at site LY1. The reactivity of POM depended on whether the PM was in the suspended or sinking fraction (Figure 5.6). Largest differences in reactivity between POM fraction type occurred during the summer, in contrast to winter, when similar reactivities were observed between SPM and sediment trap material. There was no significant difference in O_2 consumption rates between SPM sampled from above versus below the pycnocline. This is likely to be a result of their relatively similar chemical composition (Chapter 4). Peaks in SPM O_2 consumption rates corresponded to a peak in microphytoplankton cell abundance, and a positive correlation between microphytoplankton cell abundance and O_2 consumption rates was observed. Incubation experiments with SPM were not carried out for sampling dates earlier than day 187, and therefore missed the spring microphytoplankton bloom which reached maximum cell abundances of the period sampled. It is intuitive to think that reactivity of SPM would be highest during the spring bloom and maximum cell abundances, and therefore a relatively high proportion of fresh labile POM. Sediment trap material collected from LY1 was most reactive during the spring bloom when microphytoplankton abundances were highest (Figure 5.5). Sedimentation of the highly abundant microphytoplankton during spring and early summer into the sediment traps could have driven this higher reactivity. Reactivity was lowest during the winter, which was also the period of lowest microphytoplankton abundance. This is consistent with surface sediment studies which have shown maximum O_2 consumption rates during and after the phytoplankton bloom (Hicks et al., 2017). PM was more reactive during spring when microphytoplankton were most abundant, as shown by the positive relationship between diatom fatty acid biomarkers (16:4(n-1) and 20:5(n-3)) and reactivity. The seasonally varying reactivities of both fractions of PM are likely to be driven by a change in source material, and resulting degradation processes. Chapter 4 results showed a progressive increase of relative proportions of terrigenous organic material in SPM through to winter. This was in comparison to a higher relative proportion of marine derived organic material contribution to total PM in early spring (Chapter 4). Seasonally increasing C:N ratios (marine C:N ratio 6 to 7 (Emerson and Hedges, 1988)), more negative δ^{13}C values, and negative correlations with lithogenic tracer elements (Mn), were indicators of this seasonal shift in SPM source. Additionally, sediment trap material was also shown to vary in composition throughout the sampling season. High C:N ratios (yearly average 9.4 $\pm$ 0.4 SD), enriched δ^{13}C values (yearly average -21.3 ‰ $\pm$ 1.3 SD), and the lack of a correlation between δ^{13}C values and terrigenous indicators such as lithogenic tracer elements, suggest the presence of phytodetritus in the export flux at LY1. However, sediment trap material C:N ratios (yearly average 9.4 $\pm$ 0.4 SD) can also be interpreted as PM derived from a riverine source, which is typically in the range of between 8 to 10 (Meybeck, 1982). Without δ^{13}C marine and terrestrial endmembers specific to LY1, it is difficult to definitively identify PM source. Additionally, lateral advection and resuspension are likely to be important processes influencing the PM present at this coastal site. In this dynamic environment, vertical transport of SPM is likely to be accompanied

by lateral transport. Therefore, PM may have been suspended in the water column due to advective processes, which will ultimately affect its composition and reactivity. The extent to which remineralisation has already occurred will have a strong effect on the biochemical composition of PM. Despite this, it is clear there are seasonal changes to the composition of SPM and sediment trap material collected at LY1. Seasonal shifts in sediment trap PM composition have been found in other coastal settings where the contribution of terrestrial derived organic material increased from 10 % in non-winter months, to 35 % in winter months (Hedges et al., 1988b). This study has highlighted the importance of seasonal shifts in the source of PM, and fractions of PM at different diagenetic stages affect remineralisation rate.

5.4.2 Linking reactivity of particulate material to biogeochemical composition

The reactivity of the suspended and sinking fraction of PM was shown to be related to a number of key biochemical components. Oxygen consumption rates were highest when concentrations of labile compounds such as AA and TFA were highest in both POM fractions (Table 5.2). Particulate amino acids in POM have been found to be more labile relative to bulk OC, and degraded rapidly, in 0.2 to 2.1 days, when compared to timescales of months to years for bulk OC consumption (Smith et al., 1992). Phytoplankton abundance, AA, and TFA concentrations were lowest in winter which suggests there was less labile material available. This, coupled with a shift to greater relative proportions of terrigenous material, resulted in lower oxygen consumption rates in SPM and sediment trap material during winter sampling dates. The relationship between CHO and O_2 consumption rates varied between POM fraction. Both SPM sampled from above and below the pycnocline had a positive correlation between CHO concentration and O_2 consumption rates. By contrast, CHO concentration in sediment trap material had an inverse relationship to reactivity. A study investigating biochemical composition changes between plankton and sediment trap material collected at 955 m and 3459 m, found increasing relative abundances of CHO with increasing depth (Hedges et al., 2001). This suggests either preservation of CHO by the physical protection of minerals (Hedges et al., 2001), or preferential consumption of AA and TFA over CHO. However, further studies have found decreases in CHO relative abundance between plankton and underlying sediment traps (Hernes et al., 1996; Wakeham et al., 1997b). Additionally, CHO compositional differences were observed between plankton and sediment trap samples (Hernes et al., 1996). Ribose and storage CHO rich in glucose were preferentially lost, and structural carbohydrates rich in rhamnose, xylose, fucose, and mannose were preserved in sediment trap material, relative to plankton sources. These differences could explain the differing relationships between CHO concentration and O_2 consumption rates in SPM versus sediment trap material sampled from LY1. High reactivities were associated with higher CHO concentrations in the suspended fraction, where organic material was more labile and could have contained more storage CHO. In contrast, lower reactivities were associated with higher CHO concentrations in sediment trap material, which could have been dominated by structural CHO, due to preferential consumption of storage CHO during its transition to 20 m. Additionally, there was a higher relative proportion of terrestrial derived organic material during late summer and winter (indicated by more negative δ^{13}C values), in which CHO associated with this terrigenous input in winter, was likely to be

much less reactive due to degradation on land and during its transition into the marine environment. Molecular-level analysis of CHO in this study would have provided more information on the source and degradation of carbohydrates in SPM and sediment trap material. In summary, higher reactivities of SPM and sediment trap material occurred when there was higher relative abundances of labile materials such as AA and TFA, and the relationship with CHO depended on fraction type.

The relationship between individual amino acids and fatty acids with O_2 consumption rates varied between SPM and sediment trap material. A negative correlation between SFA and O_2 consumption rates was observed in all sample types. Conversely, positive relationships were observed between PUFA and MUFA, and O_2 consumption rates, in all sample types. These relationships coincide with higher relative abundances of PUFA associated with more labile POM, and higher relative abundances of SFA correspond to degraded material (e.g. Fileman et al., 1998; Budge et al., 2001; Najdek et al., 2002; Parrish et al., 2005). The reactivity of all sample types was highest when there was a higher relative abundance of diatom fatty acid biomarker 16:4(n-1) (and to a lesser extent 20:5(n-3)). These labile PUFAs have been shown to decrease in relative abundance with depth in the water column as they are selectively consumed (Fileman et al., 1998). This coincides with the results of this study, where higher relative abundances of 16:4(n-1) were found in SPM relative to sediment trap material (Table C.12 & C.16), and POM was more reactive when 16:4(n-1) abundances were high. A number of labile intracellular amino acids were also positively correlated to POM reactivity. Out of all the amino acids, LYS had the strongest positive relationship with O_2 consumption rates in SPM. Other amino acids associated with higher POM reactivity when relative abundances were higher include ASP, ILEU, GLU, and LEU. The extent of this relationship varied with sample type. For example, GLU had a positive relationship with O_2 consumption rates in sediment trap material, in contrast to a weak negative relationship with SPM from below the pycnocline, and no correlation with SPM from above the pycnocline. Conversely, LYS had the strongest positive relationship out of all the AA with O_2 consumption rates with SPM, in contrast to a negative relationship with sediment trap material. Positive relationships between intracellular amino acids (e.g. ILEU, GLU, and LEU) and reactivity, are expected due to their labile nature, and associated decrease in relative abundances with degradation (e.g Dauwe et al., 1999; Lee et al., 2000; Wakeham and Lee, 1993; Wakeham et al., 2009). The differences observed in this study between POM fraction and reactivity linked to key biochemicals (e.g. LYS and GLU) could be due to the small sample set used. Data were often clumped, and despite high r values, there are still uncertainties between the relationship of reactivity and certain biochemical components (Figures D.1 to D.6).

In addition to correlations between key labile biochemical compounds and reactivity, relationships between known degradation indicators and oxygen consumption rates were also observed (Table 5.2). Non-protein amino acids GABA and BALA are well known indicators of degradation, and are preserved relative to preferentially consumed protein amino acids (e.g. Cowie and Hedges, 1994; Dauwe and Middelburg, 1998; Dauwe et al., 1999; Ingalls et al., 2003; Goutx et al., 2007; Wakeham et al., 2009). With increasing relative proportions of BALA, GABA, and % BALA+GABA, the reactivity of SPM from above the pycnocline and sediment trap decreased.

There was no correlation found between BALA, GABA, or % BALA+GABA in SPM from below the pycnocline. A further non-protein amino acid, ORN, had a negative correlation with O_2 consumption rates in SPM from below the pycnocline, and sediment trap material. Additional indicators of degradation include GLY and THR, which are associated with diatom cell walls and refractory organic material (e.g. Ingalls et al., 2003; Cowie and Hedges, 1996; Carr et al., 2016). Reactivity of POM was lower at higher relative abundances of GLY and THR in SPM and sediment trap material. Degradation index (DI) is a measure which analyses complex amino acid compositions into a single value which is representative of POM degradation (Dauwe and Middelburg, 1998; Dauwe et al., 1999). Higher DI values are indicative of fresher POM, and lower DI values suggests more degraded material (Dauwe and Middelburg, 1998; Ingalls et al., 2003; Wakeham et al., 2009). There was a weak positive correlation between increasing DI values and increasing SPM reactivity sampled from above the pycnocline, and sediment trap material reactivity. A stronger positive correlation was observed in SPM from below the pycnocline. Generally, individual amino acids (which are used in the DI index calculation) in SPM sampled from below the pycnocline had stronger correlations with reactivity in comparison to SPM from above the pycnocline and sediment trap material (Table 5.2). This explains why SPM sampled from below the pycnocline had stronger positive relationships with DI. The differences observed between SPM from above versus below the pycnocline, and the relationship between individual amino acids and reactivity, could be a result of the small sample size and clumping of data. Despite these differences between sample types, the majority of amino acids used as lability or degradation indicators, followed the expected trend.

Sediment trap material was less reactive when PM flux was higher. However, this correlation analysis of sediment trap material bulk flux and O_2 consumption rates begins on day 138 when bulk flux is low, and subsequently increases over the summer and winter, which also coincides with lower PM reactivities (Chapter 4, Figure 4.22). It excludes the period of high flux in spring, which is likely to be more reactive given the high microphytoplankton cell abundances during the spring bloom. Therefore this relationship of high flux and low reactivity is driven by late summer to winter source shift to increasing terrigenous inputs. Corresponding negative correlations of CHO concentration and lithogenic tracer elements (Al and Mn), and O_2 consumption rates of sediment trap material, further support this trend. Other explanations for the lower reactivities of sinking PM relative to SPM include residence time of PM in the water column and the fact that the PM may have already undergone extensive remineralisation. A reduction in the residence time of PM in the water column, reduces the time available for microbial colonisation, and modification processes down the water column to the seafloor (de Jesus Mendes and Thomsen, 2012). Additionally, sinking particles can contain lower abundances, or less metabolically active bacteria than slow-sinking, suspended particles (Goutx et al., 2007), which suggests lower remineralisation rates due to lower microbial abundances. A further explanation for the lower reactivities of sinking PM relative to SPM, include temperature and water column depth, which have been shown to effect the rate of PM degradation. Carbon-specific respiration rates of POM were shown to decrease by 3.5 times when temperature was lowered from 15 to 4°C (Iversen and Ploug, 2013). Microbial communities attached to sinking PM in the surface ocean may not be able to function at colder

depths (Iversen and Ploug, 2013). However, site LY1 in this study was relatively shallow, and there was never more than a 1.5 °C temperature change observed from surface waters to the seafloor (approximately 50 m) during 2016. Therefore, in this study temperature may not have been an important parameter in determining PM reactivity at different depths. Lastly, the incorporation of ballast material could explain lower PM reactivity during high flux periods. Ballast material includes calcium carbonate, opal, and lithogenic material, and PM fluxes are strongly associated to mineral fluxes (Klaas and Archer, 2002). The presence of ballast material stabilises PM through sorption onto mineral surfaces, and acts as physical protection from microbial degradation (Keil et al., 1994). Ballast material increases sinking rates through adding density and reducing porosity of PM (De La Rocha and Passow, 2007; Ploug et al., 2008b). The addition of clay material to aggregates was found to physically protect POM from degradation (Arnarson and Keil, 2005), in contrast to biogenic minerals, which were found to provide no protection from degradation (Ploug et al., 2008b, 1999; Iversen et al., 2010). In this study sediment trap reactivity was lower with higher relative abundances of lithogenic tracer elements (Al and Mn). This ballast material could be responsible for reducing the reactivity of POM via four mechanisms. Firstly, increased sinking rate relative to SPM, which reduces residence time in the water column for microbial colonisation. Secondly, regardless of residence time in the water column, progressive loss of the labile portion of POM with increasing depth would result in lower reactivity. Thirdly, ballast minerals could provide sorptive protection to labile organic matter, protecting it from degradation and reducing reactivity. Lastly, a change in source material to increasing proportions of terrigenous material, which contains lithogenic elements and heavily degraded organic material, would explain the lower reactivity of PM observed in winter. Different water column processes affecting SPM versus sinking PM, and the presence of ballast material, have the potential to drive the differences in reactivity observed between the two PM fractions.

A study using novel particle interceptors (RESPIRE: REspiration of Sinking Particles In the subsuRface ocEan) determined remineralisation rates of PM *in situ* using O_2 optodes (Boyd et al., 2015). Deployments of RESPIRE traps were for 72 hours with 36 hours of particle collection and the following 36 hours for incubation experiments (Boyd et al., 2015). Remineralisation rate increased over time which was attributed to altered substrate quality or microbial community dynamics (Boyd et al., 2015). A further study using RESPIRE particle interceptors with shorter incubation periods (4 hours), found flux-normalised respiration rates to greatly vary between sites and to exponentially decrease with depth (McDonnell et al., 2015). Data from this experiment indicated a decrease in remineralisation rates after a 4 hour incubation period (Boyd et al., 2015). These different results highlight how variable the BCP and remineralisation rates can be spatially and temporally. This is also shown by the contrasting reactivities found between LY1 and RE5 in this study. Although sample date was similar, reactivities of POM were 2.3 time higher in sediment trap material collected from LY1 in comparison to RE5. Sediment traps were deployed at 20 m at site LY1, a coastal site situated in the Firth of Lorne, and 100 m in Loch Etive. The low numbers of replicates at RE5 mean that correlation analysis between biochemicals and reactivity was not possible. Table 5.3 provides a comparison between the biogeochemical composition of

sediment trap material sampled from LY1 and RE5. The biogeochemical composition varied between the two sites with substantially higher %CHO-OC in RE5 sediment trap material relative to LY1 samples. There was approximately double %TFA-OC in RE5 sediment trap material in comparison to LY1 material, and the composition of the TFA varied between sites. Sediment trap samples from LY1 contained double the amount of PUFA compared to RE5, which was dominated by SFA. Higher proportions of PUFA is indicative of more labile, fresh material, in contrast to higher proportions of SFA, which is an indication of degradation (Najdek et al., 2002; Wolff et al., 2011). Additionally, RE5 contained lower relative proportions of key diatom, dinoflagellate, and terrigenous fatty acid biomarkers in comparison to LY1. Lower proportions of diatom and dinoflagellate biomarkers is expected given the substantially lower microphytoplankton cell abundances at RE5 relative to LY1 (Chapter 2, Section 2.3.5). Site RE5 had higher relative proportions of %AA-N and %AA-OC than LY1, which suggests RE5 sediment trap material was less degraded than LY1. However, RE5 sediment trap material also had higher %BALA+GABA, and slightly lower DI values, both of which indicate higher degradation state in RE5 material in comparison to LY1. Key diatom intracellular amino acids, indicative of labile material, in RE5 sediment trap material were either lower (ILEU, LEU, LYS), similar to (GLU), or higher (ASP) than LY1 sediment trap material. In contrast, key diatom cell wall associated amino acids (SER, GLY, THR) and non-protein amino acids (GABA, BALA, ORN), indicative of a more degraded state, were all higher in RE5 sediment trap material relative to LY1. In terms of terrigenous inputs, both sites had similar concentrations of Al in sediment trap material, however, concentrations of Mn were substantially higher at RE5. Given the land locked site of RE5 with a high river catchment area, high concentrations of CHO, and lithogenic tracer elements, heavily altered terrigenous material is likely to make up a substantial proportion of sediment trap PM. Additionally, RE5 is an example of a restricted exchange environment in which infrequent deep water renewal events can lead to oxygen depletion (Edwards and Edelsten, 1977; Austin and Inall, 2002). Numerous studies have highlighted cases where a relatively large proportion of the PM formed in the surface ocean, is transported to depth and sediments in oxygen minimum zones (e.g. Van Mooy et al., 2002; Keil et al., 2016; Cavan et al., 2017; Le Moigne et al., 2017). During this study period, RE5 was undergoing a deep-water renewal event in which dissolved oxygen concentrations went from pre-sediment trap deployment concentrations of 59.6 μM (03/05/2016), to 186.8 μM one day post-sediment trap recovery (16/05/2016), to 248.3 μM which was considered to be fully flushed (24/05/2016; data supplied by Tim Brand). Suboxic conditions during the sediment trap deployment at RE5 could be responsible for lower reactivities, and the preservation of relatively labile PM to 100 m.

5.5 Conclusions

This study highlighted that O_2 consumption rates of SPM and sediment trap material showed a large degree of seasonal variation, and differences were observed between suspended versus sinking fractions. The suite of biochemical classes used in this study (that are well established indicators of material source and diagenetic state) coupled with PM reactivity estimates, are a valuable interpretive tool for predicting the fate of organic carbon in the water column. The key

findings of this study suggest:

1. The reactivity of POM was different between suspended and sinking fractions. Generally, SPM was more reactive than sinking PM which was driven by biogeochemical compositional differences. The difference in reactivity between the two fractions is significant, as it suggest SPM is more likely to be remineralised in the water column, and will therefore have a lower contribution to carbon export in contrast to faster sinking PM.

2. The reactivity of POM has a strong dependence on season, with higher reactivities occurring during spring and summer, and lowest in winter. Large differences in SPM versus sediment trap material reactivities were observed in summer, in contrast to winter when reactivities were relatively similar. This difference was driven by a shift in source material and degradation processes.

3. Molecular-level analyses of SPM from above and below the pycnocline, and sediment trap material showed varying correlations between reactivity and selected biochemical components. Higher relative abundances of labile fatty acids 16:4(n-1) and 20:5(n-3) were related to higher reactivity in all sample types. The relationship between individual amino acids and reactivity depended on POM fraction. The strongest positive relationships observed in all fractions was between LYS and reactivity. Selected degradation indicators (%BALA+GABA, GLY) showed negative correlations with reactivity.

4. The reactivity of sediment trap material at LY1 was 2.3 times more reactive than sediment trap samples collected from 100 m in Loch Etive. There could be a number of factors driving this observed difference. Firstly, depth differences of the sediment trap deployments (20 m at LY1 and 100 m at RE5) resulting in longer residence time of PM in the water column at RE5, could be responsible for a higher state of degradation and lower reactivities relative to LY1. Secondly, a difference in source material and associated biogeochemical composition between the two sites could influence POM reactivity. Lastly, a very different water column structure and suboxic conditions at the restricted exchange environment RE5, could be responsible for lower remineralisation rates of POM.

These observations provide valuable insights to how biogeochemical compositional variability impacts the reactivity of suspended and sinking PM. Understanding these dynamic relationships is essential as they are likely to be affected as a result of climate change. These changes which could affect PM composition, sedimentation rate and reactivity include alterations to the physical structure of water column, shifts in phytoplankton community composition, and precipitation events affecting amount of terrestrial material entering the water column.

Chapter 6

Discussion

Understanding how the biogeochemical characteristics of particulate matter (PM) at sequential stages of transport varies with PM fraction and season, is crucial as it plays a part in determining remineralisation of the organic component of PM (POM), and ultimately how much carbon is released back to the atmosphere. Additionally, the depth at which POM is recycled determines elemental distributions in the water column and drives globally important biogeochemical cycles. The loosely categorised suspended and sinking fractions of PM can be morphologically and biochemically distinct, which influences their buoyancy and sedimentation rates. This thesis aims to address fundamental questions regarding the origin of different fractions of POM, and how composition and reactivity of POM changes seasonally.

The fundamental questions addressed in this thesis include:

1. What is the role of biochemical and environmental parameters in determining microphytoplankton sedimentation rate?

2. How does the biogeochemical composition of particulate material vary at sequential stages of transport from the surface to the seafloor?

3. What is the relationship between the biogeochemical composition and reactivity of suspended and sinking fractions of particulate material?

To address these questions, three studies were carried out. These included investigating key microphytoplankton community structure that form an important part of the BCP, characterising the biogeochemical composition of different fractions of PM which are likely to have different contributions to carbon export, and lastly coupling PM biogeochemical composition to particle reactivity to predict its fate in the water column. This thesis addresses key questions surrounding the characterisation of PM, determining its origin, reactivity, and ultimate fate. The combination of microphytoplankton community composition analysis, biochemical classification of POM, and reactivity measures across a seasonal cycle is unprecedented.

6.1 Key findings

Key findings that have been generated from this thesis include:

1. The contribution of marine versus terrestrial POM varied seasonally and with POM fraction. There was a seasonal shift in the source of SPM, which had higher relative proportions of marine derived POM in the spring (microphytoplankton bloom), and transitioned to terrestrially derived material in winter. The seasonal progression was less distinct in sediment trap material and sediments, which suggests that terrestrially derived POM could have different sedimentation mechanisms, in comparison to marine POM, which favours terrigenous POM residence in the suspended fraction. Despite differences in the seasonal source change between POM fraction, the inorganic component of all fraction types is likely to dominate over the organic component, and originate from terrestrially derived mineral material. Additionally, the lack of seasonal change in sediment trap material and sediments is due to processes such as lateral advection and resuspension of sediments.

2. Microphytoplankton were highly abundant at LY1 during spring and less so during winter. Community composition shifts were observed in response to environmental changes which impacted sedimentation rates. Dinoflagellates had significantly faster sedimentation rates relative to diatoms and ciliates, yet they made up a small proportion of the total community composition (which was dominated by diatoms). Species-specific sedimentation rates were likely to be a result of morphological and physiological differences between species. Additionally, both physical environment parameters (particularly wind speed and pycnocline depth) and biochemical composition were shown to influence sedimentation rates of community composition. Total lipid was significantly inversely correlated to community sedimentation rates in samples from both above and below the pycnocline. This study highlights a number of important controls on the sedimentation rate of microphytoplankton, which ultimately will affect carbon export and cycling.

3. Biogeochemical analysis of PM provided information on the source and degradative state of PM. The biogeochemical composition of SPM, sediment trap material, and sediments was distinct. Generally, SPM was composed of more labile compounds (e.g. polyunsaturated fatty acids such as 16:4(n-1), diatom intracellular amino acids such as glutamic acid, leucine, isoleucine) in comparison to sediment trap material and sediments, which were composed of less labile, more refractory compounds (e.g. saturated fatty acids, monounsaturated fatty acids, diatom cell wall associated amino acids such as serine, threonine, and non-protein amino acids such as γ-aminobutyric acid, β-alanine).

4. Biogeochemical differences observed between SPM and sediment trap material were reflected in their reactivity. There was a clear seasonal shift in both the source material and reactivity of SPM from higher relative proportions of marine POM and higher reactivities, to higher relative proportions of terrigenous POM and lower reactivities. Generally, SPM was more reactive than sediment trap material until winter where similar reactivities were observed.

5. Site LY1 is situated in the Firth of Lorn and is a relatively shallow, high energy site. Similarities between sediment trap material and sediments in the majority of the parameters (and a dissimilarly with SPM) sampled suggest lateral advection and sediment focusing are key processes at LY1. This suggests that vertical sedimentation of PM does not dominate at LY1. As a result, sediment trap material could largely be composed of resuspended sediment. This is reflected in the biogeochemical compositional differences between the sample types, and the lower reactivity of sediment trap material relative to SPM.

6. Carbon flux was 5 to 70 times lower in SPM (calculated using SETCOLs) relative to faster sinking material collected in sediment traps. Lower carbon flux and higher reactivity of SPM, relative to sediment trap material, suggests that the labile components of SPM were utilised in the surface layers, and the material exported had a different chemical composition compared to the original source. This suggests that there is inefficient transfer of POM from the surface to greater depths in a highly dynamic coastal site.

6.2 Marine versus terrestrial sources of particulate organic material

Determining the origin of POM in the marine environment is important for predicting the fate of POM in the water column; whether is it likely to be remineralised or exported to depth. It is also important for estimating of global carbon budgets and predicting past productivity from sedimentary records (Volk and Hoffert, 1985; Hedges et al., 1997). Molecular-level analysis of POM can provide a suit of information on the source and degradative state of POM (e.g. Ittekkot et al., 1982; Cowie and Hedges, 1992b, 1994; Dauwe and Middelburg, 1998; Lee et al., 2000; Parrish et al., 2005; Ingalls et al., 2006). The data presented in Chapter 4 focused on the biogeochemical characterisation of different fractions of POM. A suite of indicators were used to distinguish between POM source, and to determine how this changed seasonally, and with POM fraction. These indicators included δ^{13}C values, C:N ratio, lithogenic tracer elements (Al and Mn), and fatty acid biomarkers.

In order to quantitatively estimate the relative proportions of marine versus terrestrial contribution to POM, marine and terrestrial δ^{13}C endmembers were selected from the literature. These calculations are based on assumptions that there are only two sources of POM and they are the same for all sample fractions. Additionally, it is acknowledged that δ^{13}C values of POM can change in response to season, biochemical changes, phytoplankton community structure, and in response to a range of environmental factors (e.g. Hedges et al., 1988b; Hansman and Sessions, 2016). It is also recognised that estimated relative proportions of marine versus terrestrial contribution to organic matter will obviously change depending on the endmember values selected. Appropriate endmembers were selected from the literature in order to derived estimates of the relative proportions of marine versus terrestrial POM. The marine endmember selected was -20.5 ‰, which was the average between laboratory cultured *Skeletonema costatum* (-20.9 ‰; Wong and Sackett, 1978), cultured *Chaetoceros calcitrans* (-20.4 ‰; Korb et al., 1998), and natural temperate phytoplankton community dominated by diatoms and primarily *Skeletonema costatum* (-20.3 ‰;

Gearing et al., 1984). These values seemed appropriate as *Skeletonema* and *Chaetoceros* spp. dominated the microphytoplankton community composition at LY1 (Chapter 2, Figure 2.15). The terrestrial endmember selected was -26.2 ‰, which is the average between peat δ^{13}C values (and topsoil) in Loch Linnhe (-28 ‰) and was suggested as a probable component of terrigenous OM (Overnell and Young, 1995). Additionally, topsoil values on the peninsular between Lochs Etive and Creran that is the nearest mainland to site LY1 (-24.5 ‰) were selected (Thornton et al., 2015). The relative proportions of marine and terrestrial POM inputs to SPM, sediment trap material, and sediments can be estimated using the methods described in Mitchell et al. (1997) and Loh (2005).

Let, a + b = 1, hence b = 1 -a

where a= proportion of marine POM , and b= proportion of terrestrial POM

Marine endmember (a)= -20.5 ‰, terrestrial endmember (b)= -26.2 ‰

E.g. Mean δ^{13}C SPM A in spring= -21.1 ‰

-20.5a + (-26.2b)= -21.1 ‰

Substitute b = 1 - a, to solve for a:

20.5a + 26.2(1 - a) = 21.1

20.5a + 26.2 - 26.2a = 21.1

-5.7a = 21.1 - 26.3

a= 0.9

The estimated seasonal progression of increasing relative proportions of terrestrial POM and decreasing relative proportions of marine POM in the SPM fraction was calculated (Table 6.1). Obviously the estimated relative proportions of source material has its limitations and calculated values are dependent on the endmembers selected. Despite this, the estimates show a strong seasonal shift in source material of the SPM fraction (which would be the case regardless of endmembers selected) which is not found in sediment trap material and sediments to the same extent. This decreasing seasonal trend of marine input into SPM coincides with the seasonal trends observed in microphytoplankton cell abundance (Chapter 2, Figure 2.13c & d). The gradual decrease in microphytoplankton cell abundance from spring, to summer, to winter, was reflected in seasonal progressive decrease in the relative proportion of marine POM to SPM above and below the pycnocline. Generally, there were higher amounts of rainfall during summer and winter months, facilitating the transport of terrestrial POM into the coastal zone (Chapter 2, Figure 2.9). This is reflected in the higher concentrations of the lithogenic tracer elements (Al and Mn) in summer and winter relative to spring (Chapter 4, Figure 4.20).

Table 6.1: Estimates of the relative proportions (%) of marine and terrestrial POM in suspended particulate material (SPM) sampled from above (A) and below (B) the pycnocline, sediment trap material (ST), and sediments (S). Values are split in to spring, summer and winter.

	Spring		Summer		Winter	
	% marine	% terrestrial	% marine	% terrestrial	% marine	% terrestrial
SPM A	91	9	50	50	23	77
SPM B	94	6	60	40	36	64
ST	84	16	91	9	80	20
S	86	14	89	11	88	12

In contrast to SPM, the organic component of sediment trap material appeared to be dominated by marine derived POM for the majority of the year (Table 6.1). However, the estimated relative proportion of terrigenous POM inputs of sediment trap material approximately doubled from summer (9 %) to winter (20 %). Another study in a coastal setting also observed seasonal shifts to higher terrigenous inputs of sediment trap material in winter (35 %), relative to non-winter months (10 %; Hedges et al., 1988b). The relatively similar percentage composition of sediment trap terrestrial input in spring (16 %) and winter (20 %), could be due to slow sinking rates, and/or the un-reactive nature of the material lingering in the water column after winter. Sediment trap material had the highest marine signature in summer, which could be a result of the time lag for the microphytoplankton bloom to sink from 3 m (depth at which SPM was sampled) to 20 m (sediment trap depth). According to settlement column (SETCOL) results in Chapter 3, this would have taken approximately 15.8 days. Therefore, it is plausible that the higher marine signature observed in sediment trap material in summer is due to this time lag, which would vary with microphytoplankton community composition and the physical environment. Despite δ^{13}C values indicating the presence of marine POM in sediment trap material, other source indicators, such as C:N ratio, are within the range typical of riverine inputs (9.4 $\pm$ 0.4 SD C:N ratio). However, a C:N ratio within this range could also indicate the presence of highly degraded material. The higher concentration of lithogenic tracer elements Al and Mn in sediment trap material compared to SPM indicates that terrestrially derived material, especially inorganic mineral material, was a substantial component of sediment trap and sediment samples (Chapter 4, Figure 4.20).

Unlike SPM, there was little seasonal variation observed in sediments, which had a high relative proportion of marine derived POM based on δ^{13}C values (Table 6.1). The lack of a seasonal trend in sediments (and to a lesser extent sediment trap material) was observed in all of the measured parameters, and is likely to be a result of sediments representing a time-averaged composition of POM, which has undergone resuspension, lateral advection, and bioturbation processes. These processes are likely to have resulted in the modification of POM composition, removing the most labile components. Resuspension and lateral advection are key processes determining the distribution of PM in the high energy environment of the Firth of Lorne (Chapter 2). Relative proportions of marine and terrestrial POM in sediment samples at LY1 are similar to those previously estimated for sites LC6 (11 % terrestrial and 89 % marine), and Camas Nathais (13 % terrestrial and

87 % marine) which are both located in the Firth of Lorne (Loh, 2005). This agreement between δ^{13}C values between LC6, Camas Nathais and LY1, supports higher relative proportions of marine POM in sediments. It further suggests that terrigenous POM material has a longer residence time in the suspended fraction, which would favour lateral advection and inefficient transfer of terrestrial POM to sediments. However this is not universally found, as higher relative proportions of terrestrially derived POM relative to marine derived POM are also found in sediments (e.g. Cowie and Hedges, 1992b; Loh, 2005). This is a result of preferential consumption of marine POM, which results in higher relative proportions of less labile terrestrially derived POM. These studies were in sea lochs (Etive and Creran) and a coastal site (Saanich Inlet), which were either in a restricted environment (sea lochs) or deeper (Saanich Inlet) than LY1, LC6, and Camas Nathais. The shallower, dynamic environment in the Firth of Lorne encourages resuspension and lateral advection of PM. This could explain the difference observed in the higher relative proportions of marine POM versus terrestrial POM at LY1, when compared to the reverse trends observed at restricted exchange and deeper sites where vertical processes predominate.

However, other indicators such as C:N ratio and lithogenic tracers elements (Al and Mn) both indicate terrigenous inputs formed an important component in sediment trap material and sediments. Furthermore, as previously stated, sediment samples are likely to be composed mainly of inorganic mineral material, with POM representing a small fraction of total composition. Similar to sediment trap material, the mean C:N ratio of sediments (9.3 $\pm$ 0.1 SD C:N ratio) was within the range of riverine inputs (which are typically between 8 and 10; Meybeck, 1982)), and the concentration of lithogenic tracer elements Al and Mn was highest close to the sea floor (45 m) in comparison to sediment trap and SPM sample depths. Results from a previous coastal study (Hedges et al., 1988a) showed marine POM that reached the sea floor was five times more reactive than the accompanying terrigenous POM, despite undergoing >80 % remineralisation in the upper water column. This means that despite high proportions of marine inputs into sediments, the biogeochemical composition was vastly different to the marine source at the surface (see later discussion). It is intuitive to think that terrestrial organic matter proportions would be higher in sediments than in water column samples (SPM and sediment trap materials), due to their generally lower reactivity and more refractory nature, which favours preservation. However, the higher terrestrial proportions observed in SPM when compared to sediment trap and sediment samples is logical, as it is likely to have travelled in the suspended fraction from Lochs Etive, Creran and Linnhe which have large watersheds. Terrestrial PM sourced from these sea lochs could converge at LY1 before being laterally advected elsewhere, and leave a small proportion accounted for in sediment trap material and sediment. Marine and terrestrial PM could have different settling mechanisms which could explain the higher marine contribution to the export flux. For example, highly degraded lignin material is less dense than seawater, and remains in suspension in near surface waters (Reeves and Preston, 1991; Loh et al., 2008b). Therefore, compositional differences between SPM with sediment trap material and sediments could be a result of different sedimentation mechanisms of source materials, and physical processes (resuspension and sediment focusing) affecting the distribution of PM.

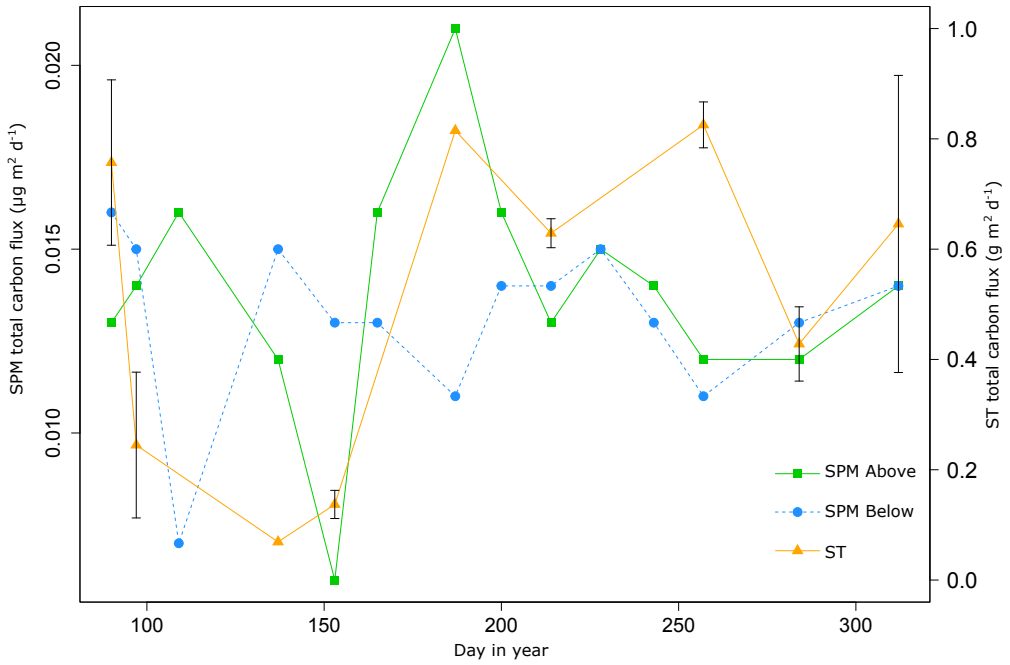

Figure 6.1: Suspended particulate material (SPM) particulate carbon flux (μg m^{-2} d^{-1}) calculated from SPM from above and below the pycnocline in SETCOL experiments during 2016. Sediment trap (ST) carbon flux (g m^{-2} d^{-1}) calculated from simultaneous sediment trap deployments is also plotted. Note the different scales for SPM versus sediment trap material

6.3 Fluxes of suspended water column versus sediment trap particulate material

Suspended versus sinking fractions of PM are likely to have different contributions to carbon export as a result of differences in their properties and associated sedimentation rates. Historically, slow-sinking, suspended particles are generally under-sampled by sediment trap deployments as a result of hydrodynamic bias (Buesseler et al., 2007). Additionally, flux calculations of this slow-sinking PM fraction have used average sinking speeds or size-based assumptions, which are not ideal (Riley et al., 2012; Durkin et al., 2015; Baker et al., 2017). Therefore better characterisation and sampling methods are needed to accurately represent the slow sinking fraction. In this study SPM was collected from above and below the pycnocline using Niskin bottles. At the time of sampling this PM was suspended in the water column, but was likely to contain both suspended material and sinking material. Placing the SPM samples into settlement columns (SETCOL) for a set period of time, enabled the PM to fractionate based on particle buoyancy, and from this the carbon flux was calculated (Chapter 3). Combined analysis of microphytoplankton community composition in the SPM, can also provide information on which key species, or combination, contributed to carbon flux. The carbon flux of SPM was then compared to the sinking PM flux collected via sediment trap deployments. The flux of carbon captured in the sediment traps was 5 to 70 times greater (depending on sampling dates) than in the flux of slow-sinking SPM (sampled above and below the pycnocline).

Carbon fluxes associated with slow-sinking SPM above and below the pycnocline, and material

captured in sediment traps between March and November 2016 were compared (Figure 6.1). During spring and summer, the carbon flux of SPM from above versus below the pycnocline followed different trends. Later in the year, from day 214, fluxes were more similar in SPM from above and below the pycnocline relative to earlier dates. This seasonal difference could be a result of the shift in source material from predominantly marine in spring, to an increased terrestrial influence in winter. The large variation in carbon flux observed in SPM from above versus below the pycnocline in spring and early summer could be a result of the large degree of variation in microphytoplankton cell abundance and composition (Chapter 2, Figure 2.13, Table A.1, & Table A.2). In comparison to later summer/ winter, where cell abundance was relatively low and terrestrial PM dominated SPM, carbon fluxes were relatively similar above and below the pycnocline. This similarity between carbon flux observed could be due to the shift in source material and similar composition of PM both above and below the pycnocline. There was a poor relationship observed between microphytoplankton community sedimentation rates and SPM carbon flux. Microphytoplankton community sedimentation rate below the pycnocline was relatively similar over 2016 (Chapter 3, Figure 3.3b). Sedimentation rates of microphytoplankton from above the pycnocline were similar to those below, except from two sample dates where sedimentation rates were substantially higher above the pycnocline (days 153 and 284). These peaks in microphytoplankton community sedimentation did not coincide with higher carbon fluxes of SPM. This suggests higher sedimentation rates of microphytoplankton community does not necessarily translate into higher carbon flux, which could be due to the presence of other carbon sources not accounted for (i.e. plankton taxa other than those counted in this experiment such as other flagellates, transparent exopolymer particles (TEP), faecal pellets, other detrital material, terrestrial organic material). Differences in the particle types collected in the SPM and sediment trap material fractions was observed (Figure 6.2). The images show higher cell abundances of microphytoplankton on days 97 and 214 in the SPM fraction, when compared to day 284 where there are long strands of other plant material present (indicating a transition from higher relative proportions of marine POM to terrestrially derived POM). Lower cell numbers of microphytoplankton are observed in sediment trap material, which transitions from larger "fluffy" aggregates to a higher abundance of smaller, more compact particles. This transition into smaller compact particles, and potentially more dense, will affect sedimentation rate and therefore carbon flux. These images show the range of particles involved in the carbon flux at LY1, which is not just microphytoplankton cells. Therefore, the lack of relationship observed between microphytoplankton community sedimentation and carbon fluxes is because measured cell sedimentation rates are not reflective of what is actually sinking out.

There were some similarities between SPM and sediment trap material carbon flux seasonal trends (Figure 6.1). Initial high fluxes of carbon in SPM and sediment trap material coincided with the microphytoplankton spring bloom. Sediment trap material flux then decreased to a minimum, whilst during the same period high fluxes of SPM from above the pycnocline were found, relative to low fluxes of SPM from below the pycnocline (days 98 to 154). The peak in carbon flux of SPM from above the pycnocline coincided with sediment trap material carbon flux (day 187). After this sampling date, there were similar carbon flux trends observed for both SPM and sediment trap

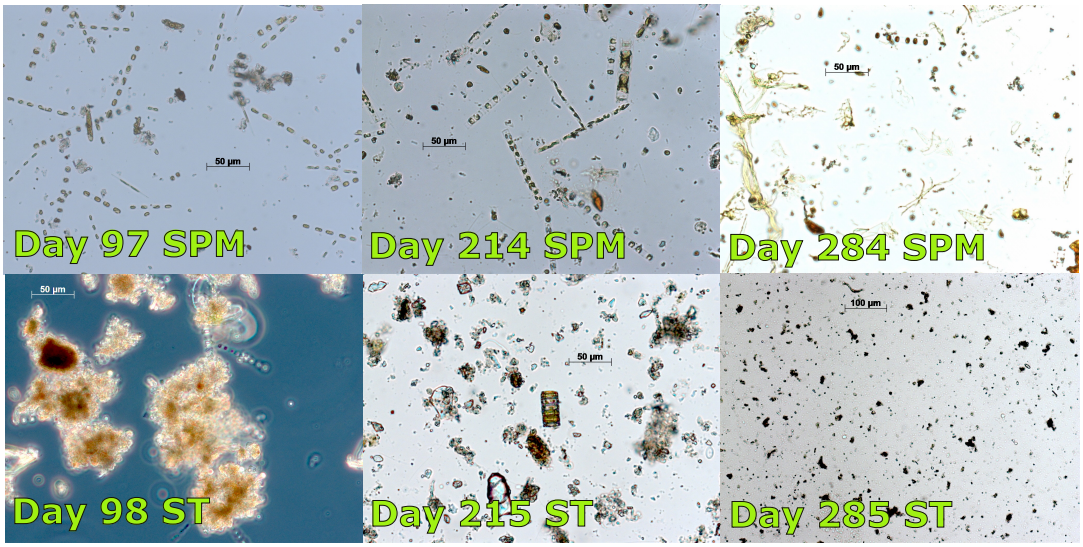

Figure 6.2: Comparison between particles in suspended particulate material (SPM) and sediment trap material (ST) samples collected on days 97 (06/04/2016), 98 (07/04/2016), 214 (01/08/2016), 215 (02/08/2016), 284 (10/10/2016), and 285 (11/10/2016)

material. It is possible a large fraction of sediment trap material originated from resuspended and/or laterally transported sediment, and this is likely to vary strongly with season. Under these circumstances, it is not surprising that SPM fluxes are minor and often do not follow the same trends as trap fluxes.

Composition of the microphytoplankton community can play a substantial role in determining the carbon flux (e.g. Herndl and Reinthaler, 2013; Turner, 2015; Durkin et al., 2016). This is a result of the diversity of morphologies and cell densities of microphytoplankton which affect aggregation and sedimentation rates. SETCOL experiments highlighted microphytoplankton sedimentation was significantly different between groups, with dinoflagellates sedimenting significantly faster (median 1.25 m d^{-1} $\pm$ 0.03 SE) than diatoms (median 0.83 m d^{-1} $\pm$ 0.03 SE), or ciliates (median 0.74 m d^{-1} $\pm$ 0.04 SE; Chapter 3, Figure 3.4). Additionally, sedimentation rates were highly species-specific, which in turn has the potential to influence community sedimentation rates depending on the species present. Microscopic observations of the composition of sediment trap material, revealed the presence of aggregates, individual microphytoplankton cells, and diatom chains (Chapter 4, Figure 4.24). These chains present in sediment trap material were generally greater than six cells in length, and SETCOL experiments showed longer chains typically had higher sedimentation rates than shorter chains. Additionally, solitary cell *Pleurosigma* spp. had high sedimentation rates relative to other solitary cells, and were frequently observed in sediment trap material (Chapter 4, Figure 4.24). Individual microphytoplankton cells and chains, despite slower sedimentation rates than aggregated cells with other material, are an important component of the BCP (e.g. Dall'Olmo and Mork, 2014; Puigcorbé et al., 2015; Durkin et al., 2016). For slow sinking cells to be exported past the surface layer, physical transport could aid their relocation to depth, or they could have been part of an aggregate which fragmented with depth (Durkin et al., 2016). However this study also found the transport of individual cells to 125 m and they were distinctly separate from other particles (Durkin et al., 2016). These studies, and the results from

this study highlight that microphytoplankton form an important part of carbon export, whether it be as individual cells, aggregated material, or repackaged into zooplankton faecal pellets. This is shown in the microscopic analysis of sediment trap material and source indicators (e.g. δ^{13}C values, fatty acid biomarkers).

There are some limitations with this comparison between SETCOL and sediment trap material carbon flux. Firstly, microphytoplankton community sedimentation was calculated based on the number of individual cells. Therefore, this excluded the interaction between cells/ chains and other PM present. The extent of interaction between cells/ chains was likely to be dependent on cell densities and the morphology of species present. For example, interactions between cells that have chitin spines and various spatial orientations including spirals (e.g. *Chaetoceros* spp.) are more likely to aggregate than single cells. Secondly, the interaction with other particle types (e.g. TEP, inorganic ballast material, repackaging of POM into faecal pellets) is not considered, and will likely affect carbon flux. Thirdly, all experiments and calculations based in SETCOL excludes turbulence, which in the natural environment will affect transport of PM and sedimentation rates. The carbon flux of SPM calculated in SETCOL was in the absence of turbulence, whereas sediment trap fluxes were calculated from samples affected by turbulence over a 24 hour deployment period. Despite these limitations, SETCOL is a recognised method which is widely used to investigate processes that are difficult to study in their natural environment (e.g. Bienfang et al., 1982; Peperzak et al., 2003; Guo et al., 2016; Cavan et al., 2017). Additionally, regardless of limitations on interactions between particles and their composition for understanding carbon flux, the key message is that SPM has a lower contribution to carbon flux than sinking material.

6.4 Linking the biogeochemical composition to reactivity of particulate material

A key aim of this thesis was to determine the relationship between biogeochemical composition of PM with reactivity since there are knowledge gaps between the form and composition of PM, sedimentation rates, and reactivity. Many studies have investigated molecular-level biogeochemical composition of PM in a range of environments (e.g. Hedges et al., 1988b; Wakeham and Lee, 1989; Cowie and Hedges, 1992b; Lee et al., 2000; Ingalls et al., 2003; Wakeham et al., 2009; Cavan et al., 2018). Additionally, many studies have investigated the reactivity of POM collected via sediment traps (e.g. Iversen et al., 2010; Iversen and Ploug, 2013; Boyd et al., 2015; McDonnell et al., 2015; Cavan et al., 2017). However, Goutx et al. (2007) is the only known study which links biogeochemical composition of marine particulate material to experimental determinations of reactivity. The coupling of detailed biogeochemical composition and reactivity experiments in this study provides invaluable information on how the seasonal shift in source material affects the reactivity of different fractions of POM.

Chapter 4 highlights the biogeochemical differences observed between the sample types. Analysis showed SPM from above and below the pycnocline were compositionally similar and dominated

by labile compounds, including diatom associated intracellular amino acids (e.g. leucine, glutamic acid, isoleucine) and polyunsaturated fatty acids (PUFA, e.g. 16:4(n-1), 18:2(n-6), 22:6(n-3)). This depended on sampling date, as relative proportions of labile compounds decreased after spring when the abundance of microphytoplankton also decreased and the relative proportion of terrestrially derived material increased. Sediment trap material contained lower relative proportions of labile material in comparison to SPM. Fatty acid composition was a key driver in determining compositional differences between SPM and sediment trap material, as trap material had higher relative proportions of saturated fatty acids in contrast to SPM (SFA e.g. 16:0 and 18:0; as shown in the PCA analysis). The lower relative proportions of labile compounds in sediment trap material could be a result of its residence time in the water column as a result of resuspension and sediment focusing. Due to the high energy environment at LY1, PM collected in sediment traps could have undergone extensive degradation in the water column before its collection in traps. Sediments were the most biogeochemically distinct out of all the sample types with higher relative proportions of cell wall associated amino acids (e.g. threonine, serine), monounsaturated fatty acids (MUFA e.g. 20:1(n-7), 18:1(n-7)) and SFA. Bioturbation processes and resuspension events are likely to have resulted in the biochemical differences between SPM, and to a lesser extent sediment trap material. Additionally, the repackaging of sinking POM into faecal pellets could created these biochemical differences. These differences were reflected in the reactivity of POM in which experiments were carried out on SPM and sediment trap material. Generally, there were statistical relationships with biogeochemical composition and reactivity of SPM and sediment trap material (Chapter 5, Table 5.2). In agreement with biogeochemical compositional analysis, SPM was more reactive than sediment trap material, except in winter. The similar reactivities of the two PM fractions in winter was driven by the shift in source material to terrestrially dominated in the SPM fraction. Other degradation indicators such as non-protein amino acids, and percentage of total nitrogen represented as amino acids, indicated SPM and sediment trap material was less labile during winter relative to earlier in the year. High rainfall and concentrations of lithogenic tracer elements, coupled with low relative proportions of marine and terrestrially derived organic material, further explain the refractory nature of POM at LY1 during winter.

Processes in the water column can affect particle dynamics, which in turn can affect PM fate in the water column. For example, degradation will alter PM chemical composition and potentially density, which in turn could affect sedimentation rate. This is especially true for highly reactive PM, such as the suspended fraction at LY1. Additionally, fragmentation of particles occurs as a result of degradation or consumption by zooplankton, which would affect subsequent sedimentation rates and particle export. These processes can affect the size and density of PM which are important factors in determining PM sedimentation rates (Sanders et al., 2014). Slow-sinking particles (0.7 to 11 m d^{-1}) comprise a major proportion of PM export as identified in open-ocean studies (e.g. Riley et al., 2012; Baker et al., 2017; Cavan et al., 2017, 2018). However, SETCOL carbon flux calculations suggest that slow-sinking SPM contributed little to the vertical flux at LY1 relative to the amount of material that was captured in the traps. As previously mentioned, resuspension and lateral advection of sediment is likely to constitute a major proportion of sediment trap material. Furthermore, the slow-sinking, suspended PM at LY1 was the most reactive, meaning it is

likely to undergo extensive chemical changes before it reaches greater depths. The particle types between the suspended and sinking fraction were visually different, with high abundances of microphytoplankton in SPM and a higher proportion of aggregated material collected in sediment traps (Figure 6.2). Additionally, there was a shift in sediment trap PM shape and size over the sampling season from larger "fluffy" to small, compact aggregates. These changes could potentially affect reactivity due to surface area available for bacterial colonisation, and more compact, dense aggregates having a lower residence time in the water column. There was still evidence of microphytoplankton present in sediment trap material. Aggregation with other slow-sinking PM or ballast material could encourage the export of labile, slow-sinking PM to depth. The particle dynamics at LY1 suggest vertical transport of labile SPM to the seafloor is inefficient. In turn this will affect elemental distributions in the water column, and quantity and quality of food source that reaches the benthos.

Site RE5 in Loch Etive provided a comparison of PM from an alternative location to compare the biogeochemistry and reactivity to samples from LY1. Reactivity experiments highlighted that sediment trap POM was 2.3 times more reactive at LY1 compared to RE5. This highlights the large degree of spatial variablitity in carbon flux and reactivity, and there are many factors which could explain the difference in reactivity between the two sites. Firstly, there were differences in the environmental conditions between the sites with LY1 being an open, dynamic coastal system in contrast to RE5 which is a sea loch with restricted exchange to the sea. Site LY1 is subject to frequent mixing as a result of the strong currents and tidal environment. In contrast, site RE5 is a deep site which undergoes infrequent mixing, leading to stagnant deep water which is overturned approximately every 16 months (Edwards and Edelsten, 1977). These differences will result in different water column structures and nutrient dynamics, which will ultimately affect the microphytoplankton community composition. For example, during similar sampling dates in June 2016, microphytoplankton cell abundance was approximately 12 times higher than the abundance at RE5. Additionally, dynamic conditions at LY1 favours resuspension of sediments, in contrast to the stagnant isolated deep waters at RE5 which favours deposition. Secondly, the sediment traps deployed at both sites were at different depths with LY1 deployed at 20 m and RE5 at 100 m. This depth difference means that PM collected at RE5 had a longer residence time in the water column and subsequently could be more degraded. However, as previously discussed, PM collected in sediment traps at LY1 could also have a high residence time in the water column as a result of resuspension and lateral advection. Thirdly, the biogeochemical composition of PM sampled from RE5 was distinctly different to LY1. Carbohydrates dominated the organic fraction of PM, and SFA dominated the fatty acid fraction at RE5 (Chapter 5, Table 5.3). Lower relative proportions of labile material when compared to LY1 (e.g. PUFA, intracellular amino acids) and higher concentrations of lithogenic tracer element Mn, indicated that RE5 sediment trap material was more refractory than LY1. Given, the lower microphytoplankton abundances observed at RE5 in comparison to LY1 (Chapter 2, Table 2.4), and the land-locked nature of the site, terrestrial inputs could predominate over marine at RE5. Increasing relative proportions of terrestrially derived material and decreasing relative proportions of more reactive marine derived material with increasing depth, is a typical trend found at RE5 and other coastal sites (e.g. Cowie and Hedges,

1992b; Loh, 2005). However, as previously discussed, LY1 does not follow this trend which is likely to be a result of the dynamic environment which favours resuspension and lateral advection processes. Fourthly, there were suboxic conditions at the restricted exchange environment site during sample collection which could be responsible for the lower remineralisation rates of PM. This could be a result of microbial respiration using alternative electron acceptors which are less efficient in comparison to oxygenated waters, or low abundances of zooplankton which repackage or fragment PM (Le Moigne et al., 2017). Differences between these study sites highlight how PM composition and reactivity can change depending on environment. Additionally, it also shows that despite cited trends that are typical for coastal settings, physical processes can dominate and determine both the composition and distribution of PM.

6.5 Recommendations for future research

Further work which would complement the work carried out in this thesis includes:

- Microphytoplankton community sedimentation SETCOL experiments which are carried out in parallel to roller table experiments using the same parcel of water to form aggregates. This would enhance understanding of how seasonally changing microphytoplankton community dynamics affects aggregate formation and composition. Sedimentation rates of the formed aggregates could also be measured in the SETCOL system to compare to original microphytoplankton community bulk sedimentation rates.

- Cultured key microphytoplankton species (which would include *Skeletonema* and *Chaetoceros* (coastal) spp. at LY1) grown under different conditions (e.g. nutrient, light, and temperature) with the aim of investigating sedimentation rates in SETCOL. Biochemical analysis (total protein, carbohydrate, and lipids) in relation to growth conditions, and their influence on sedimentation rates could be studied. Different growth phases of the cultures, which will have varying biochemical compositions, could be placed into SETCOLs to calculate sedimentation rates. This would compliment the present study, and help with explaining the complex interactions found in the natural environment.

- Bacterial modification of POM is known to result in attenuation of POM with depth (Herndl and Reinthaler, 2013). Coupling PM biogeochemical composition analysis and reactivity experiments to the colonisation and growth of particle-attached and free-living bacteria, would provide valuable information on POM degradation and cycling. It would also determine how bacteria abundances change over a seasonal cycle, which will influence oxygen consumption rates and therefore reactivity estimations.

- This study coupled with larger SETCOLs or Marine Snow Catchers to explicitly link PM characteristics to biogeochemical composition and remineralisation rates. This apparatus would allow me to carry out molecular-level analysis of POM samples that have been exclusively split into suspended and sinking fractions. Access to larger quantities of sinking material would allow the investigation of the role of faecal pellets in modifying the biochemcial composition of POM and influence on flux. Additionally, designing a larger SETCOL,

which would have larger volumes per fraction, would have enabled me to take additional measurements, to further understanding of mechanisms affecting sedimentation rates.

- Additional measures for future experimental set-ups would include understanding local current regimes which can play a significant role in PM sedimentation. Deployment of current meters would allow the comparison of fluxes, biogeochemical composition changes, and determine the impact of lateral advection of PM. Additionally, including measurements of sediment accumulation rates would also further understanding regarding the efficiency of PM sedimentation from sediment trap 20 m deployments to the seafloor. Access to a higher quantities of POM through utilisation of larger SETCOLs or Marine Snow Catchers would enable analysis of other parameters such as compound-specific isotopes and further lipid (n-alkanes, sterols) analysis. Other measurements I think would be key in determining terrestrial influence on PM would be the analysis of lignin. Given the large difference in the relative proportions of terrestrial inputs into SPM versus sediment trap material based on δ^{13}C values, lignin analysis could be used to corroborate the proportions of marine versus terrestrially derived material.

This thesis has furthered understanding on key areas of the BCP; microphytoplankton community sedimentation rates which form an important component of the sinking POM flux, the biogeochemical characterisation of different fractions of PM, and linking POM composition to reactivity to help determine the fate of POM in the water column. Achieving a holistic understanding of the BCP is essential but difficult given the numerous and interrelated processes affecting its functioning. However, studying these small components of the BCP is critical in order to build up a holistic understanding from which future changes can be assessed.

Appendix A

Environmental characterisation of a western Scotland coastal site

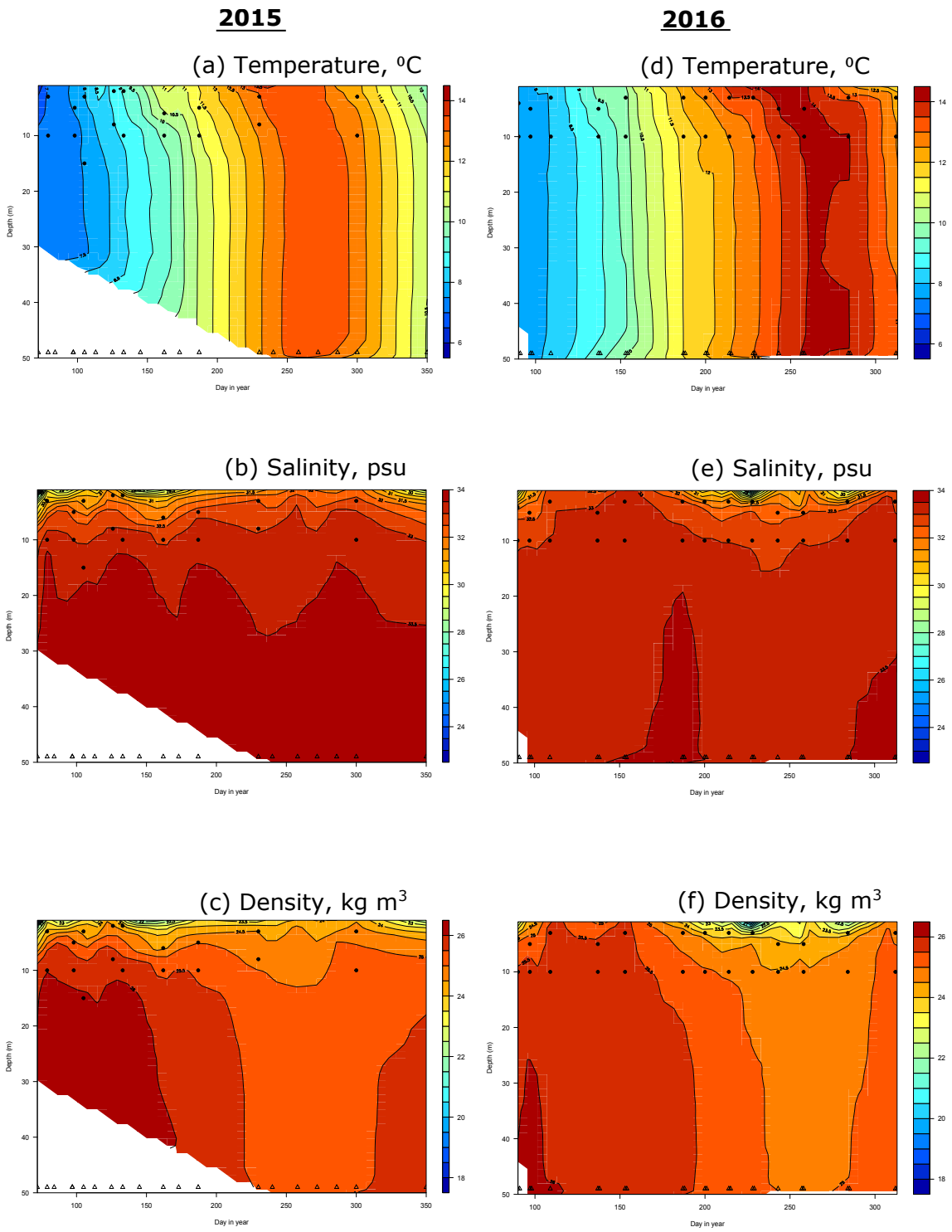

Figure A.1: Full water column profiles of temperature (°C), salinity (psu), and density (kg m^3) at LY1 during 2015 and 2016. Circle = SETCOL experiment depths, triangles = CTD sampling events

Table A.1: Seasonal distribution of key microphytoplankton taxa sampled from above (A) and below (B) the pycnocline during 2015. X indicates presence and black triangles (▲) peaks in abundance. The predominant taxa per date and depth, and maximum number of cells L^{-1} are recorded. S: *Skeletonema* spp., C: *Chaetoceros* spp. (coastal), Pd: *Pseudo-nitzschia delicatissima*, K: *Katodinium* spp., Gm: *Gymnodinium* spp., Sc: *Scrippsiella* spp., Pt: *Protoperidinium* spp., Pr: *Prorocentrum* spp., Gr: *Gyrodinium* spp.

	20/3/15		7/4/15		15/4/15		5/5/15		13/5/15		11/6/15		6/7/15		18/8/15		15/9/15		27/10/15		Max. cells x 10^5 L^{-1}	
	A	B	A	B	A	B	A	B	A	B	A	B	A	B	A	B	A	B	A	B	A	B
Diatoms																						
Skeletonema spp.	X	X	▲	▲	X	X	X	X	X	X	X	X	X	X	X	X	X	X	X	X	41.5	19.9
Chaetoceros spp. (Coast)	X	X	X	X	X	X	X	X	X	X	▲	▲	X	X	X	X	X	X	X	X	42.7	19.8
Thalassiosira spp.	X	X	X	X	▲	▲	X	X	X	X	X	X	X	X	X	X	X	X	X	X	3.3	1.8
P. delictissima	X	X	X	X	X	X	X	X	X	X	X	X	▲	X	X	X	X	▲	X	X	1.2	1.1
Chaetoceros spp. (Ocean)	X	X	X	X					X	X	▲	▲		X	X	X	X	X	X	X	0.3	0.03
L. minimus					X	X	X	X	X	X	X	X	▲	▲	X	X	X	X	X		0.4	0.2
L. danicus		X	X	X	X	X		X	X	X	X	X	▲	X	X	X	X	▲	X	X	0.2	0.05
Dactyliosolen spp.			X		X	X	X	X	X	▲	▲	X	X	X	X	X	X	X			0.03	0.03
Guardinia spp.	X		X	X	X	X	X	X	X	X	▲	▲	X		X	X	X	X	X	X	0.3	0.4
P.seriata							X	X							X	X	▲	▲	X	X	0.05	0.09
Paralia spp.	X	X	X	X			X	X	X	X	X	X	X	X	X	X	X	X	▲	▲	0.005	0.006
Navicula spp.	X	X	X	X	X	X	X	X	X	X	X	X	X	X	X	X	X	X	▲	▲	0.007	0.003
Lauderia spp.	X	X	X	X	▲	X	X	X	X	X						X	X	X	X	▲	0.02	0.02
Pleurosigma spp.	X	X	X	▲	▲	X	X	X	X	X	X	X	X	X	X	X	X	X	X	X	0.03	0.001
Asterionellopsis spp.	X		X	X	▲	▲	X	X	X	X	X								X		0.2	0.07
Thallassionema spp.	X	X				X			X		X		X		X	X	X	X	▲	▲	0.005	0.006
Predominant diatom	S	S	S	S	S	S	S	S	S	C	C	C	S	S	S	S	S	Pd	S	S		
Dinoflagellate																						
Katodinum spp.	X	X	X	X	▲	▲	X	X	X	X	X	X	X	X	X	X	X	X	X	X	0.1	0.07
Scripsiella spp.	X	X	X	X	X	X	X	X	X	▲	X	X	X	X	▲	X	X	X	X	X	0.03	0.01
Gyrodinium spp.	X	X	X	X	▲	▲	X	X	X	X	X	X	X	X	X	X	X	X	X	X	0.01	0.02
Prorocentrum spp.	X	X	X	X	X	X	X	X	X	X	▲	▲	X	X	X	X	X	X	X	X	0.007	0.006
Gymnodinium spp.	X	X	X	X	X	X	X	X	X	X	X	▲	X		X	X	X	X	▲	X	0.006	0.009
Heterocapsa spp.	X	X	X	▲	X	X	▲	X	X	X	X	X	X	X	X	X	X	X	X	X	0.004	0.004
Ceratium spp.		X	X	X		X				X	X	X	X	X	▲	▲	X	X	X	X	0.0004	0.004
Protoperidinium spp.	X	X	X	X	▲	X	X	X	X	X	X	▲	X	X	X	X	X	X	X	X	0.009	0.005
Predominant dinoflag.	K	Gm	K	K	K	K	Sc	K	Pt	Sc	Pr	Gm	Sc	Gr	K	K	K	Gr	K	Gm		

Table A.2: Seasonal distribution of key microphytoplankton taxa sampled from above (A) and below (B) the pycnocline during 2016. X indicates presence and black triangles (▲) peaks in abundance. The predominant taxa per date and depth, and maximum number of cells L^{-1} are recorded. S: *Skeletonema* spp., C: *Chaetoceros* spp. (coastal), Ps: *Pseudo-nitzschia seriata*, Pr: *Prorocentrum* spp., Gr: *Gyrodinium* spp., Pt: *Protoperidinium* spp., K: *Katodinium* spp., Sc: *Scrippsiella* spp., He: *Heterocapsa* spp.

	30/3/16		6/4/16		16/5/16		1/6/16		5/7/16		1/8/16		15/8/16		13/9/16		10/10/16		7/11/16		Max. cells L^{-1}	
	A	B	A	B	A	B	A	B	A	B	A	B	A	B	A	B	A	B	A	B	A	B
Diatoms																						
Skeletonema spp.	▲	X	X	▲	X	X	X	X	X	X	X	X	X	X	X	X	X	X	X	X	48.2	29.7
Chaetoceros spp. (Coast)	X	X	X	X	X	X	▲	▲	X	X	X	X	X	X	X	X	X	X	X	X	23.5	15.0
Thalassiosira spp.	▲	▲	X	X	X	X	X	X	X	X	X	X	X	X	X	X	X	X	X	X	1.1	0.5
P. delictissima	▲	X	X	▲	X	X	X	X	X	X	X	X	X	X	X	X	X	X	X	X	0.3	0.2
Chaetoceros spp. (Ocean)	X	X	X	X					▲	X		▲	X	X	X	X					0.005	0.003
L. minimus	X		X		X	X	▲	▲	X	X	X	X		X	X	X	X	X	X	X	0.9	0.7
L. danicus					X	X	X	X	X	X	▲	▲	X	X	X	X	X	X	X	X	1.2	0.5
Dactyliosolen spp.	X	X			X	X	▲	▲					X	X	X	X	X	X	X	X	0.008	0.03
Guardinia spp.	X		X		X	X	X	X	X	X	▲	X	X	▲	X	X	X		X	X	0.08	0.06
P.seriata	X	X	X	X	X	X	X	X	▲	▲	X	X	X	X	X	X	X	X	X	X	0.8	0.4
Paralia spp.	X	X		X	X	X	X	X	X	X	X	X	X	X	X	X	X	▲	▲	X	0.01	0.007
Navicula spp.	X	X	X	X	X	X	X	▲	X	X	X	X	X	X	▲	X	X	X	X	X	0.006	0.003
Lauderia spp.	▲	X	X	X			X	X	X	▲											0.02	0.01
Pleurosigma spp.	X	X	X	X	X	X	X	X	X	X	▲	▲	X	X	X	X	X	X	X	X	0.0007	0.001
Asterionellopsis spp.	X	X	▲	▲	X	X	X	X				X									0.02	0.02
Thallassionema spp.	X	X	X						X								▲	▲			0.02	0.005
Predominant diatom	S	S	S	S	C	C	C	C	Ps	Ps	S	S	C	C	S	S	S	S	S	S		
Dinoflagellate																						
Katodinum spp.	X	X	X	X	▲	▲	X	X	X	X	X	X	X	X	X	X	X	X	X	X	0.01	0.02
Scripsiella spp.	X	X	X	X	X	X	X	X	X	▲	X	X	X	X	▲	X	X	X	X	X	0.2	0.04
Gyrodinium spp.	X	X	X	X	▲	▲	X	X	X	X	X	X	X	X	X	X	X	X	X	X	0.02	0.005
Prorocentrum spp.	X	X	X	X	X	X	X	X	X	X	▲	▲	X	X	X	X	X	X	X	X	0.01	0.02
Gymnodinium spp.	X	X	X	X	X	X	X	X	X	X	X	▲	X		X	X	X	X	▲	X	0.02	0.01
Heterocapsa spp.	X	X	X	▲	X	X	▲	X	X	X	X	X	X	X	X	X	X	X	X	X	0.02	0.009
Ceratium spp.		X	X	X		X				X	X	X	X	X	▲	▲	X	X	X	X	0.002	0.0003
Protoperidinium spp.	X	X	X	X	▲	X	X	X	X	X	X	▲	X	X	X	X	X	X	X	X	0.01	0.01
Predominant dinoflag.	Pr	Gr	Pt	Pr	K	K	Pt	K	Sc	Sc	Sc	Sc	Sc	K	Sc	K	Sc	Sc	He	He		

Appendix B

Seasonal microplankton community sedimentation linked to environmental and biochemical drivers

Figure B.1: Settlement column (SETCOL) built at SAMS by Alistair James following the design by Bienfang (1981a)

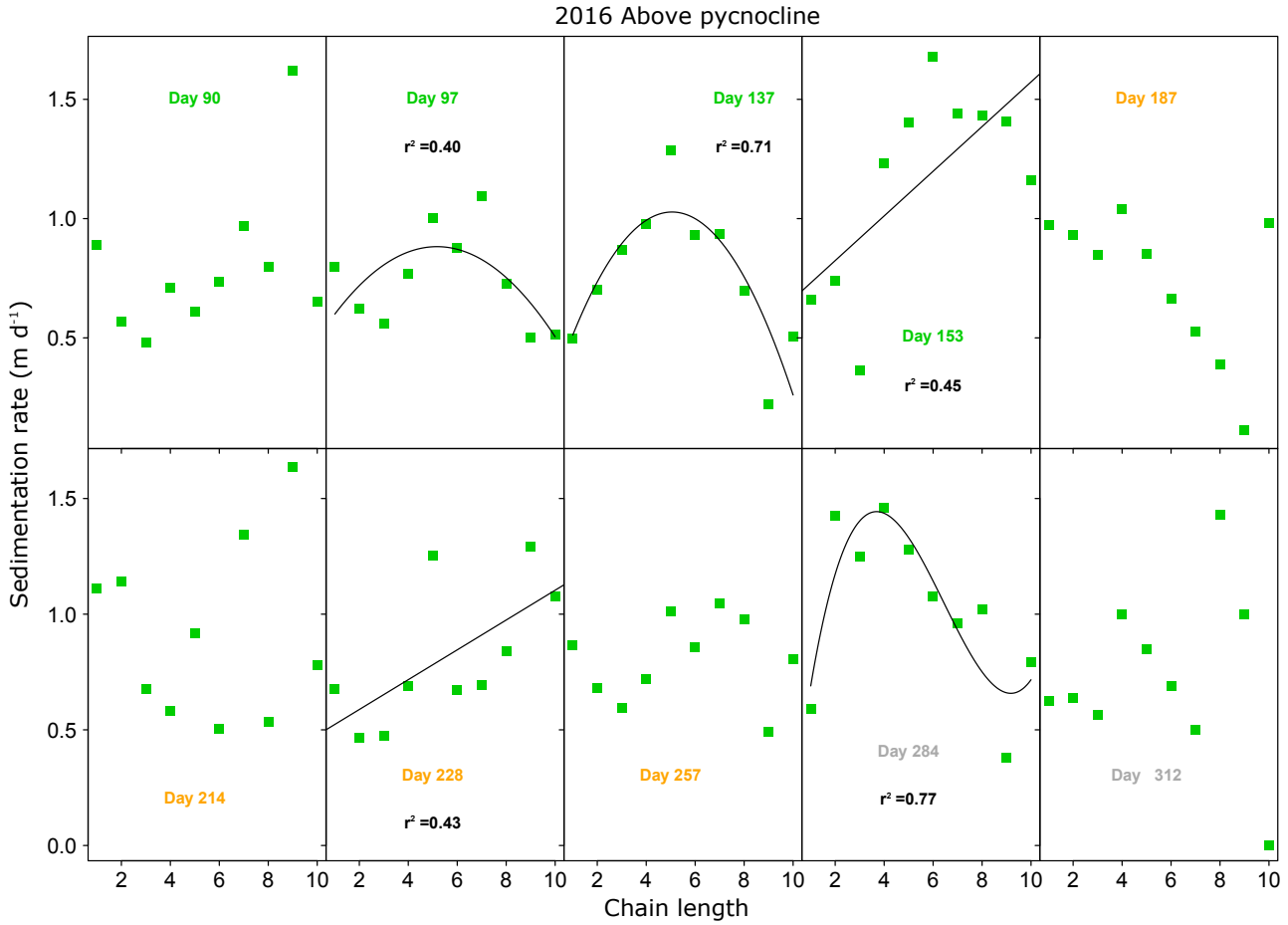

Figure B.2: Chain length and sedimentation rate (m d^{-1}) over each sampling date in spring (green; days 90, 97, 137, 153), summer (orange; days 187, 214, 228, 257), and winter (grey; day 284, 312) 2016 from samples taken above the pycnocline. On each plot are lines of best fit (quadratic, linear and cubic) and regression statistics (r^2)

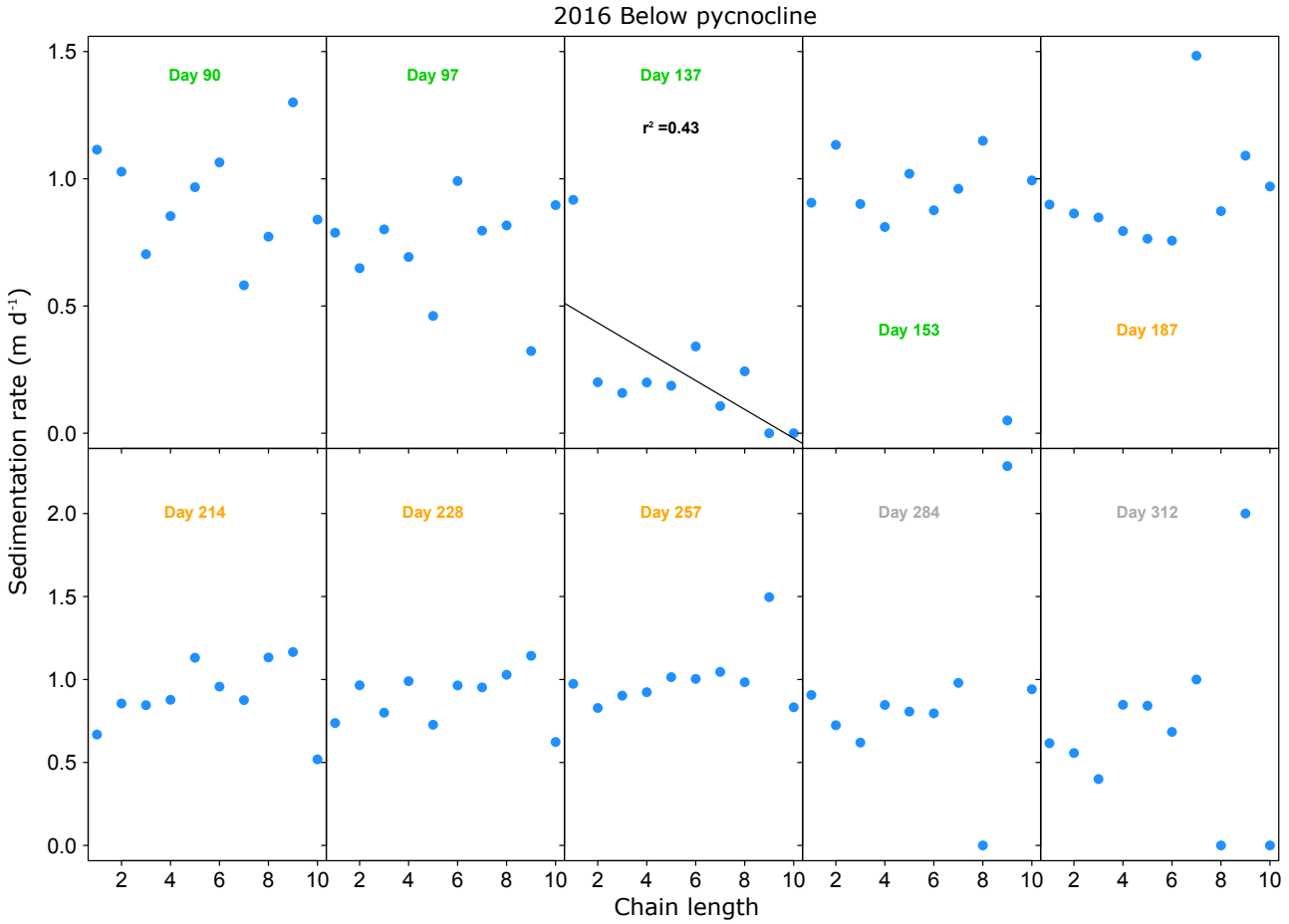

Figure B.3: Chain length and sedimentation rate (m d^{-1}) over each sampling date in spring (green; days 90, 97, 137, 153), summer (orange; days 187, 214, 228, 257), and winter (grey; day 284, 312) 2016 from samples taken below the pycnocline. On each plot are lines of best fit (linear) and regression statistics (r^2)

Appendix C

Seasonal biogeochemical composition of marine particulate material at sequential stages of transport

Table C.1: Precision information for particulate organic carbon and nitrogen analysis on suspended particulate material (SPM) from above and below the pycnocline

	TN μg ml^{-1}	Mean μg ml^{-1}	SD	Precision %	TOC μg ml^{-1}	Mean μg ml^{-1}	SD	Precision %	13C ‰	Mean ‰	SD	Precision %
SPM above												
30/03/16	0.06	0.06	0.00	4.97	0.35	0.36	0.01	2.89	-21.55	-21.29	0.36	-1.71
30/03/16	0.06				0.36				-21.04			
06/04/16	0.04	0.04	0.00	6.29	0.24	0.24	0.01	3.30	-20.67	-20.68	0.01	-0.03
06/04/16	0.04				0.23				-20.68			
16/05/16	0.04	0.05	0.01	22.59	0.23	0.26	0.04	14.80	-21.12	-21.12	0.00	-0.01
16/05/16	0.05				0.28				-21.12			
01/06/16	0.05	0.05	0.00	2.61	0.29	0.29	0.01	2.15	-20.33	-20.76	0.61	-2.92
01/06/16	0.05				0.29				-21.19			
18/07/16	0.08	0.08	0.00	0.69	0.44	0.47	0.05	9.80	-21.69	-22.61	1.30	-5.74
18/07/16	0.08				0.51				-23.53			
01/08/16	0.06	0.06	0.00	0.67	0.37	0.38	0.00	1.25	-21.98	-22.10	0.17	-0.78
01/08/16	0.06				0.38				-22.22			
15/08/16	0.06	0.06	0.00	5.26	0.33	0.31	0.03	9.47	-23.47	-23.82	0.49	-2.07
15/08/16	0.05				0.29				-24.17			
14/09/16	0.04	0.05	0.01	20.46	0.22	0.29	0.09	30.94	-23.71	-25.07	1.92	-7.65
14/09/16	0.05				0.35				-26.42			
11/10/16	0.05	0.05	0.00	0.12	0.35	0.30	0.07	21.91	-25.98	-25.34	0.91	-3.57
11/10/16	0.05				0.26				-24.70			
07/11/16	0.03	0.03	0.00	2.28	0.18	0.18	0.00	2.41	-25.11	-24.55	0.79	-3.20
07/11/16	0.03				0.19				-24.00			
SPM below												
30/03/16	0.03	0.03	0.00	3.09	0.20	0.20	0.00	2.40	-21.52	-21.50	0.04	-0.19
30/03/16	0.03				0.20				-21.47			
06/04/16	0.03	0.09	0.08	94.37	0.20	0.47	0.39	81.19	-20.74	-20.50	0.33	-1.63
06/04/16	0.15				0.75				-20.27			
16/05/16	0.04	0.04	0.00	4.90	0.23	0.22	0.01	4.40	-20.11	-20.08	0.04	-0.19
16/05/16	0.04				0.22				-20.06			
01/06/16	0.06	0.06	0.00	2.15	0.30	0.32	0.02	6.15	-21.67	-21.47	0.29	-1.37
01/06/16	0.06				0.33				-21.26			
18/07/16	0.04	0.04	0.00	11.30	0.21	0.21	0.00	0.98	-22.83	-24.06	1.74	-7.24
18/07/16	0.04				0.21				-25.29			
01/08/16	0.04	0.04	0.00	0.14	0.22	0.22	0.00	1.39	-21.98	-22.11	0.18	-0.81
01/08/16	0.04				0.22				-22.23			
15/08/16	0.03	0.03	0.00	9.46	0.17	0.15	0.02	12.95	-23.16	-23.69	0.75	-3.17
15/08/16	0.03				0.14				-24.22			
14/09/16	0.04	0.04	0.00	7.41	0.21	0.22	0.01	6.59	-24.70	-24.27	0.61	-2.53
14/09/16	0.04				0.23				-23.83			
11/10/16	0.04	0.04	0.00	9.15	0.21	0.21	0.01	4.37	-24.32	-24.13	0.27	-1.11
11/10/16	0.04				0.22				-23.94			
07/11/16	0.03	0.03	0.00	3.14	0.17	0.17	0.01	4.08	-25.50	-	-	-
07/11/16	0.03				0.16				-	-	-	

Table C.2: Precision information for particulate organic carbon and nitrogen analysis on sediment trap and sediment material

	TN mg g^{-1}	Mean mg g^{-1}	SD	Precision %	OC mg g^{-1}	Mean mg g^{-1}	SD	Precision %	13C ‰	Mean ‰	SD	Precision %
Sediment trap												
31/03/16	12.78	9.54	4.58	47.99	105.4	81.12	34.32	42.30	-	-	-	-
31/03/16	6.30				56.9				-	-	-	-
07/04/16	4.34	3.40	1.33	39.04	37.5	28.04	13.42	47.86	-21.06	-21.01	0.07	-0.31
07/04/16	2.46				18.6				-20.96			
17/05/16	6.37	4.73	2.32	49.10	51.3	38.12	18.61	48.82	-23.45	-23.65	0.28	-1.20
17/05/16	3.09				25.0				-23.85			
02/06/16	1.87	6.63	6.73	101.49	13.5	47.93	48.62	101.45	-21.84	-21.89	0.07	-0.31
02/06/16	11.40				82.3				-21.93			
06/07/16	8.38	7.99	0.55	6.85	67.7	64.14	5.00	7.80	-19.27	-	-	-
06/07/16	7.60				60.6				-	-	-	-
02/08/16	4.83	4.80	0.03	0.66	38.6	39.89	1.79	4.48	-20.14	-20.61	0.67	-3.25
02/08/16	4.78				41.2				-21.08			
16/08/16	3.69	3.82	0.19	4.84	34.8	33.61	1.64	4.88	-20.16	-20.00	0.22	-1.09
16/08/16	3.95				32.4				-19.85			
14/09/16	5.39	4.92	0.67	13.57	49.1	42.39	9.45	22.30	-22.72	-	-	-
14/09/16	4.44				35.7				-	-	-	-
11/10/16	6.53	7.47	1.34	17.87	44.8	53.11	11.68	22.00	-21.05	-21.00	0.07	-0.32
11/10/16	8.42				61.4				-20.95			
08/11/16	2.21	2.13	0.12	5.87	14.2	13.37	1.14	8.55	-22.15	-22.29	0.20	-0.90
08/11/16	2.04				12.6				-22.43			
Sediment												
30/03/16	0.73	0.83	0.15	17.60	6.16	6.94	1.10	15.85	-	-	-	-
30/03/16	0.94				7.71				-	-	-	-
06/04/16	0.99	1.05	0.08	7.46	8.07	8.49	0.59	6.99	-21.60	-21.54	0.08	-0.36
06/04/16	1.10				8.91				-21.49			
16/05/16	1.92	2.21	0.42	18.77	14.93	17.20	3.20	18.60	-21.28	-21.12	0.23	-1.08
16/05/16	2.51				19.46				-20.96			
01/06/16	1.04	1.44	0.56	39.05	8.41	11.56	4.46	38.58	-21.23	-	-	-
01/06/16	1.84				14.72				-	-	-	-
05/07/16	1.76	1.68	0.11	6.78	14.03	13.29	1.03	7.78	-21.21	-21.31	0.14	-0.64
05/07/16	1.60				12.56				-21.40			
18/07/16	2.32	2.75	0.59	21.66	18.36	21.48	4.41	20.54	-21.00	-20.94	0.08	-0.39
18/07/16	3.17				24.59				-20.88			
01/08/16	2.75	2.68	0.11	4.05	21.10	20.78	0.45	2.17	-20.67	-20.79	0.17	-0.81
01/08/16	2.60				20.46				-20.91			
15/08/16	1.67	1.79	0.17	9.73	13.11	13.99	1.26	8.98	-21.30	-21.36	0.09	-0.42
15/08/16	1.92				14.88				-21.42			
30/08/16	2.00	2.20	0.28	12.73	15.87	17.39	2.15	12.36	-21.26	-21.10	0.23	-1.07
30/08/16	2.40				18.91				-20.94			
13/09/16	1.93	1.59	0.48	30.16	15.38	12.66	3.84	30.30	-21.40	-21.36	0.06	-0.29
13/09/16	1.25				9.95				-21.31			
10/10/16	1.55	1.54	0.01	0.90	12.34	12.28	0.09	0.73	-21.60	-21.44	0.22	-1.03
10/10/16	1.53				12.22				-21.28			
07/11/16	2.29	2.32	0.05	2.30	18.00	18.75	1.06	5.64	-21.05	-	-	-
07/11/16	2.36				19.50				-	-	-	-

Table C.3: Precision information for amino acids (AA) analysis on suspended particulate material (SPM) from above and below the pycnocline

	AA ng ml^{-1}	Mean ng ml^{-1}	SD	Precision %
SPM above				
30/03/16	258.15	-	-	-
06/04/16	191.58	-	-	-
16/05/16	210.87	185.23	36.25	19.57
16/05/16	159.60			
01/06/16	213.62	-	-	-
06/07/16	129.31	-	-	-
18/07/16	326.69	-	-	-
01/08/16	196.37	204.50	12.81	6.26
01/08/16	197.87			
01/08/16	219.27			
15/08/16	146.43	145.62	1.15	0.79
15/08/16	144.80			
14/09/16	136.08	140.54	5.45	3.88
14/09/16	138.94			
14/09/16	146.62			
11/10/16	158.21	151.24	8.93	5.90
11/10/16	141.18			
11/10/16	154.34			
SPM below				
30/03/16	121.16	-	-	-
06/04/16	131.98	-	-	-
16/05/16	169.06	-	-	-
01/06/16	217.76	-	-	-
06/07/16	94.75	-	-	-
18/07/16	130.82	142.91	17.10	11.96
18/07/16	155.00			
01/08/16	138.98	134.25	9.72	7.24
01/08/16	140.70			
01/08/16	123.07			
15/08/16	113.29	91.90	18.68	20.32
15/08/16	83.56			
15/08/16	78.84			
14/09/16	144.52	136.07	7.36	5.41
14/09/16	132.62			
14/09/16	131.07			
11/10/16	113.01	121.19	7.30	6.03

Table C.3: continued

	AA ng ml^{-1}	Mean ng ml^{-1}	SD	Precision %
11/10/16	123.48			
11/10/16	127.07			
07/11/16	62.35	-	-	-

Table C.4: Precision information for amino acids (AA) analysis on sediment trap and sediment samples

	AA mg g^{-1}	Mean mg g^{-1}	SD	Precision %
Sediment trap				
31/03/16	35.70	-	-	-
07/04/16	1.97	8.64	8.79	101.69
07/04/16	5.36			
07/04/16	18.60			
17/05/16	7.98	41.24	47.04	114.06
17/05/16	74.50			
02/06/16	25.24	27.89	12.16	43.59
02/06/16	44.50			
02/06/16	26.54			
02/06/16	15.29			
06/07/16	26.56	22.98	3.11	13.54
06/07/16	21.39			
06/07/16	20.98			
02/08/16	14.68	13.90	1.97	14.21
02/08/16	12.57			
02/08/16	11.27			
02/08/16	14.37			
02/08/16	17.03			
02/08/16	13.49			
16/08/16	9.31	12.63	2.92	23.14
16/08/16	14.83			
16/08/16	13.74			
14/09/16	14.94	16.35	2.76	16.88
14/09/16	19.53			
14/09/16	14.58			
10/10/16	13.89	15.65	1.56	9.96
10/10/16	16.23			
10/10/16	16.84			
07/11/16	12.49	18.21	5.03	27.63

Table C.4: continued

	AA mg g^{-1}	Mean mg g^{-1}	SD	Precision %
07/11/16	20.22			
07/11/16	21.93			
Sediment				
30/03/16	2.64	2.82	0.16	5.82
30/03/16	2.96			
30/03/16	2.86			
06/04/16	2.54	2.55	0.23	8.96
06/04/16	2.79			
06/04/16	2.33			
16/05/16	5.63	6.40	0.67	10.50
16/05/16	6.83			
16/05/16	6.75			
01/06/16	3.30	4.91	1.49	30.27
01/06/16	5.20			
01/06/16	6.23			
06/07/16	6.08	5.29	1.13	21.36
06/07/16	4.49			
19/07/16	5.79	6.17	0.54	8.73
19/07/16	6.55			
01/08/16	6.25	6.08	0.16	2.69
01/08/16	6.07			
01/08/16	5.93			
15/08/16	5.20	5.38	0.25	4.74
15/08/16	5.56			
13/09/16	5.19	4.27	1.18	27.58
13/09/16	2.94			
13/09/16	4.68			
10/10/16	4.73	4.59	0.31	6.66
10/10/16	4.24			
10/10/16	4.80			
07/11/16	5.48	5.55	0.10	1.79
07/11/16	5.62			

Table C.5: Precision information for total fatty acids (TFA) analysis on suspended particulate material (SPM) from above and below the pycnocline

	TFA μg ml^{-1}	Mean μg ml^{-1}	SD	Precision %
SPM above				
30/03/16	0.03	0.04	0.01	38.84
30/03/16	0.05			
06/04/16	0.01	0.01	0.00	8.15
06/04/16	0.01			
16/05/16	0.02	0.02	0.00	17.66
16/05/16	0.01			
01/06/16	0.02	0.02	0.00	0.70
01/06/16	0.02			
05/07/16	0.01	0.01	0.00	4.50
05/07/16	0.01			
18/07/16	0.03	0.03	0.00	7.19
18/07/16	0.03			
01/08/16	0.03	0.03	0.00	7.11
01/08/16	0.03			
15/08/16	0.02	0.03	0.00	7.38
15/08/16	0.03			
13/09/16	0.02	0.02	0.00	19.96
13/09/16	0.02			
10/10/16	0.02	0.02	0.00	7.42
10/10/16	0.02			
07/11/16	0.01	0.01	0.00	1.36
07/11/16	0.01			
SPM below				
30/03/16	0.02	0.02	0.01	25.70
30/03/16	0.02			
06/04/16	0.02	0.01	0.00	22.05
06/04/16	0.01			
16/05/16	0.01	0.02	0.01	51.15
16/05/16	0.03			
01/06/16	0.02	0.01	0.01	38.14
01/06/16	0.01			
05/07/16	0.01	0.01	0.00	6.46
05/07/16	0.01			
18/07/16	0.01	0.01	0.00	2.70
18/07/16	0.01			
01/08/16	0.02	0.01	0.00	15.34
01/08/16	0.01			
15/08/16	0.01	0.02	0.01	42.97
15/08/16	0.02			
13/09/16	0.01	0.02	0.01	29.46
13/09/16	0.02			
10/10/16	0.01	0.01	0.00	9.45
10/10/16	0.01			
07/11/16	0.02	0.02	0.01	28.45
07/11/16	0.02			

Table C.6: Precision information for total fatty acids (TFA) analysis on sediment trap samples

	TFA mg g^{-1}	Mean mg g^{-1}	SD	Precision %
Sediment trap				
31/03/16	2.29	2.45	0.23	9.50
31/03/16	2.61			
07/04/16	6.53	4.33	3.12	72.08
07/04/16	2.12			
17/05/16	2.62	2.69	0.09	3.53
17/05/16	2.75			
02/06/16	3.63	2.87	1.08	37.76
02/06/16	2.10			
06/07/16	1.03	0.98	0.07	7.26
06/07/16	0.93			
02/08/16	0.90	1.01	0.15	14.63
02/08/16	1.11			
16/08/16	3.68	2.71	1.37	50.67
16/08/16	1.74			
14/09/16	1.32	1.11	0.30	27.23
14/09/16	0.90			
11/10/16	1.06			
08/11/16	1.10	1.02	0.11	10.51
08/11/16	0.95			

Table C.7: Concentration (ng ml^{-1}) ± SD composition of amino acids in suspended particulate material (SPM) samples collected from above and below the pycnocline from site LY1 during 2016. ASP, aspartic acid; GLU, glutamic acid; SER, serine; HIS, histidine; GLY, glycine; THR, threonine; ARG, arginine; ALA, alanine; BALA, β-alanine; TYR, tyrosine; GABA, γ-aminobutyric acid; MET, methionine; VAL, valine; PHE, phenylalanine; ILEU, isoleucine; LEU, leucine; ORN, ornithine; LYS, lysine

	SPM above and below the pycnocline individual amino acid concentrations (ng ml^{-1})																															
	ASP		GLU		SER		HIS		GLY		THR		ARG		ALA		BALA		TYR		GABA		MET		VAL		PHE		ILEU		LEU		ORN		LYS	
	Av.	SD	Av.	SD	Av.	SD	Av.	SD	Av.	SD	Av.	SD	Av.	SD	Av.	SD	Av.	SD	Av.	SD	Av.	SD	Av.	SD	Av.	SD	Av.	SD	Av.	SD	Av.	SD	Av.	SD	Av.	SD
SPM above																																		
30/03/2016	22.0	-	44.5	-	9.5	-	4.4	-	17.0	-	13.2	-	15.9	-	21.3	-	0.7	-	7.4	-	0.0	-	0.2	-	16.6	-	14.9	-	15.1	-	22.6	-	0.8	-	32.0	-
06/04/2016	11.7	-	29.9	-	8.4	-	3.7	-	14.0	-	11.0	-	12.9	-	16.4	-	0.3	-	4.8	-	0.0	-	0.6	-	13.3	-	12.0	-	12.2	-	18.4	-	0.3	-	21.6	-
16/05/2016	16.1	1.6	32.5	3.0	8.1	4.3	1.2	0.9	12.2	6.6	8.2	3.1	11.3	5.7	11.6	7.0	0.3	0.4	5.3	2.3	0.0	0.0	1.9	0.6	13.9	0.4	11.9	0.1	12.5	0.5	17.3	1.5	0.3	0.0	20.5	0.0
01/06/2016	5.5	-	29.4	-	10.7	-	2.4	-	16.2	-	10.9	-	16.3	-	19.4	-	0.5	-	7.2	-	0.0	-	2.8	-	16.4	-	13.9	-	14.4	-	21.8	-	0.3	-	25.5	-
05/07/2016	3.5	-	19.6	-	6.1	-	3.1	-	9.5	-	5.9	-	9.6	-	11.4	-	0.5	-	3.9	-	0.0	-	0.9	-	9.4	-	7.7	-	8.0	-	12.6	-	0.2	-	17.3	-
18/07/2016	8.8	-	48.4	-	15.5	-	6.4	-	26.0	-	15.6	-	23.4	-	29.0	-	1.5	-	11.9	-	0.1	-	4.7	-	23.4	-	19.7	-	19.9	-	31.4	-	0.4	-	40.6	-
01/08/2016	16.2	3.1	29.8	2.4	8.8	0.9	1.8	0.8	13.8	0.1	9.0	0.9	14.0	0.5	14.8	2.1	0.3	0.2	6.9	0.6	0.1	0.0	3.1	0.8	13.3	0.9	9.0	4.0	11.3	0.6	17.6	0.9	0.3	0.1	34.5	11.2
15/08/2016	13.2	0.6	28.2	0.5	2.7	0.1	0.8	0.0	6.6	0.4	3.9	0.0	6.7	0.2	9.2	0.5	0.8	0.1	3.3	0.0	0.1	0.0	1.5	0.9	6.6	0.1	10.7	0.2	11.1	0.2	17.3	0.3	0.6	0.2	22.3	0.9
14/09/2016	9.8	1.2	21.8	1.1	5.5	1.3	1.9	0.2	15.3	0.9	6.0	0.7	8.0	1.1	10.4	0.4	1.3	0.2	5.0	0.7	0.1	0.0	0.7	0.2	8.2	0.1	7.2	0.3	7.5	0.2	12.3	0.2	0.4	0.3	19.1	10.9
10/10/2016	10.2	1.3	23.9	2.0	7.8	1.5	1.4	0.4	15.3	1.2	7.4	0.8	9.7	0.7	14.5	3.6	1.3	0.1	7.2	2.4	0.1	0.0	1.6	0.8	8.8	0.3	7.6	0.4	7.9	0.4	12.5	1.4	0.3	0.0	13.8	0.7
SPM below																																		
30/03/2016	8.3	-	17.0	-	5.9	-	1.5	-	9.9	-	6.7	-	7.8	-	10.2	-	0.4	-	3.4	-	0.0	-	1.0	-	8.3	-	7.2	-	7.5	-	11.3	-	0.5	-	14.3	-
06/04/2016	7.8	-	21.8	-	6.4	-	1.8	-	9.9	-	7.5	-	9.1	-	11.1	-	0.3	-	3.7	-	0.0	-	1.1	-	9.0	-	8.0	-	8.1	-	12.4	-	0.3	-	13.7	-
16/05/2016	16.7	-	26.5	-	8.3	-	2.5	-	10.9	-	8.0	-	12.3	-	13.7	-	0.3	-	5.5	-	0.0	-	2.1	-	11.5	-	9.7	-	10.1	-	15.2	-	0.2	-	15.5	-
01/06/2016	7.5	-	34.2	-	12.5	-	2.0	-	18.8	-	11.8	-	17.1	-	18.6	-	0.5	-	7.8	-	0.0	-	2.4	-	15.5	-	13.7	-	13.8	-	20.9	-	0.2	-	20.4	-
05/07/2016	2.6	-	14.5	-	4.3	-	4.3	-	7.1	-	4.2	-	7.0	-	8.1	-	0.5	-	3.0	-	0.0	-	0.4	-	6.9	-	5.5	-	5.7	-	8.9	-	0.3	-	11.6	-
18/07/2016	14.5	6.5	23.8	6.2	7.0	0.6	4.9	3.3	11.2	0.9	6.1	0.2	9.5	0.6	10.7	0.1	0.7	0.4	4.6	0.6	0.0	0.0	1.0	1.0	8.8	0.4	5.2	3.2	7.4	0.4	12.0	0.5	0.3	0.2	15.1	0.9
01/08/2016	9.7	0.5	19.2	1.0	6.0	1.2	1.9	0.4	9.5	0.7	5.7	0.1	9.3	0.8	9.4	1.1	0.2	0.1	3.6	0.6	0.0	0.0	0.5	0.6	8.5	0.2	5.9	2.5	7.3	0.1	11.4	0.2	0.2	0.1	25.8	12.3
15/08/2016	7.2	2.3	14.5	3.2	3.6	0.8	1.0	0.3	8.3	1.7	4.4	1.0	6.4	1.3	8.0	1.5	0.8	0.1	3.4	0.8	0.1	0.0	1.3	0.3	5.8	1.0	4.7	0.8	5.0	0.9	8.0	1.3	0.2	0.1	9.2	1.6
14/09/2016	10.8	0.2	22.5	0.9	7.5	0.6	1.6	0.4	16.0	1.9	6.6	0.5	8.5	0.6	10.4	0.6	1.1	0.0	5.5	0.3	0.1	0.0	1.2	0.8	7.4	0.2	6.8	0.3	6.9	0.2	11.7	0.5	0.3	0.1	11.1	0.6
11/10/2016	7.0	0.7	19.1	1.1	9.1	0.7	0.7	0.2	14.1	1.1	6.7	0.5	6.7	0.4	11.2	0.4	0.1	0.0	8.6	0.6	0.1	0.0	0.8	0.2	6.1	0.4	5.7	0.5	6.0	0.5	8.9	0.8	0.2	0.0	10.1	0.5
07/11/2016	4.8	-	10.1	-	4.8	-	0.4	-	7.7	-	3.4	-	4.3	-	4.3	-	0.0	-	1.8	-	0.0	-	0.2	-	3.8	-	3.1	-	3.4	-	5.1	-	0.3	-	5.0	-

Table C.8: Mole percentages ± SD composition of amino acids in suspended particulate material (SPM) above and below the pycnocline from site LY1 during 2016. ASP, aspartic acid; GLU, glutamic acid; SER, serine; HIS, histidine; GLY, glycine; THR, threonine; ARG, arginine; ALA, alanine; BALA, β-alanine; TYR, tyrosine; GABA, γ-aminobutyric acid; MET, methionine; VAL, valine; PHE, phenylalanine; ILEU, isoleucine; LEU, leucine; ORN, ornithine; LYS, lysine; DI, degradation index

Date	mole %																		DI
	ASP	GLU	SER	HIS	GLY	THR	ARG	ALA	BALA	TYR	GABA	MET	VAL	PHE	ILEU	LEU	ORN	LYS	
SPM above																			
30/03/2016	8.1	14.8	4.4	1.4	11.1	5.4	4.5	11.7	0.4	2.0	0.01	0.08	6.9	4.4	5.6	8.4	0.2	10.7	1.3
06/04/2016	5.7	13.2	5.2	1.5	12.2	6.0	4.8	12.0	0.2	1.7	0.0	0.3	7.4	4.7	6.1	9.1	0.1	9.6	1.4
16/05/2016	8.4 ± 1.1	15.4 ± 2.1	5.1 ± 1.7	0.5 ± 0.3	10.7 ± 3.6	4.6 ± 0.7	4.3 ± 1.3	8.5 ± 3.5	0.2 ± 0.2	1.9 ± 0.4	0.02 ± 0.0	0.9 ± 0.1	8.4 ± 2.1	5.1 ± 1.1	6.7 ± 1.8	9.2 ± 1.3	0.1 ± 0.1	9.9 ± 2.2	1.8 ± 0.9
01/06/2016	2.4	11.6	5.9	0.9	12.6	5.3	5.4	12.7	0.4	2.3	0.02	1.1	8.1	4.9	6.4	9.7	0.1	10.2	1.7
05/07/2016	2.6	12.9	5.6	1.9	12.3	4.8	5.3	12.4	0.6	2.1	0.04	0.6	7.8	4.5	5.9	9.3	0.1	11.4	1.8
18/07/2016	2.5	12.5	5.6	1.6	13.2	5.0	5.1	12.4	0.6	2.5	0.03	1.2	7.6	4.5	5.8	9.1	0.1	10.6	1.8
01/08/2016	7.5 ± 1.3	12.6 ± 0.6	5.2 ± 0.4	0.7 ± 0.3	11.4 ± 0.5	4.7 ± 0.5	5.0 ± 0.2	10.3 ± 1.6	0.2 ± 0.2	2.4 ± 0.1	0.1 ± 0.0	1.3 ± 0.4	7.0 ± 0.5	3.4 ± 1.5	5.3 ± 0.3	8.3 ± 0.4	0.1 ± 0.1	14.6 ± 4.5	1.3 ± 0.3
15/08/2016	8.9 ± 0.3	17.2± 0.1	2.3 ± 0.1	0.5 ± 0.0	7.9 ± 0.4	3.0 ± 0.0	3.5 ± 0.1	9.2 ± 0.4	0.8 ± 0.1	1.6 ± 0.0	0.1 ± 0.0	0.9 ± 0.6	5.0 ± 0.0	5.8 ± 0.0	7.6 ± 0.0	11.8 ± 0.1	0.3 ± 0.1	13.7 ± 0.8	2.9 ± 0.2
14/09/2016	6.4 ± 0.9	12.9 ± 0.9	4.6 ± 1.1	1.1 ± 0.1	17.8 ± 1.5	4.4 ± 0.6	4.0 ± 0.6	10.2 ± 0.6	1.3 ± 0.1	2.4 ± 0.4	0.1 ± 0.0	0.4 ± 0.1	6.1 ± 0.1	3.8 ± 0.0	5.0 ± 0.0	8.2 ± 0.1	0.2 ± 0.1	11.3 ± 6.2	1.2 ± 0.2
10/10/2016	6.2 ± 0.7	13.0 ± 0.8	6.0 ± 0.8	0.7 ± 0.3	16.3 ± 1.3	5.0 ± 0.3	4.5 ± 0.2	13.0 ± 3.0	1.2 ± 0.1	3.2 ± 1.0	0.1 ± 0.0	0.9 ± 0.4	6.0 ± 0.1	3.7 ± 0.2	4.8 ± 0.1	7.7 ± 0.9	0.2 ± 0.0	7.6 ± 0.1	1.0 ± 0.2
SPM below																			
30/03/2016	6.4	11.8	5.7	1.0	13.5	5.8	4.6	11.7	0.4	1.93	0.03	0.7	7.2	4.5	5.8	8.8	0.3	10.0	1.2
06/04/2016	5.6	14.0	5.7	1.1	12.5	6.0	4.9	11.8	0.3	1.9	0.01	0.7	7.3	4.6	5.8	8.9	0.2	8.8	1.3
16/05/2016	9.4	13.4	5.9	1.2	10.8	5.0	5.3	11.4	0.3	2.3	0.03	1.0	7.3	4.4	5.7	8.6	0.1	7.9	1.3
01/06/2016	3.2	13.2	6.8	0.7	14.2	5.6	5.6	11.9	0.3	2.5	0.03	0.9	7.5	4.7	6.0	9.1	0.1	7.9	1.5
05/07/2016	2.6	13.0	5.4	3.6	12.5	4.7	5.3	12.0	0.7	2.2	0.02	0.4	7.8	4.4	5.7	9.0	0.2	10.5	2.1
18/07/2016	9.3 ± 3.3	14.1 ± 2.3	5.9 ± 1.1	2.7 ± 1.6	13.2 ± 2.3	4.5 ± 0.6	4.8 ± 0.8	10.6 ± 0.9	0.7 ± 0.5	2.3 ± 0.5	0.02 ± 0.0	0.6 ± 0.6	6.5 ± 0.4	2.7 ± 1.4	5.0 ± 0.2	8.0 ± 0.5	0.2 ± 0.1	9.1 ± 0.3	1.3 ± 0.4
01/08/2016	6.9 ± 0.7	12.4 ± 1.2	5.4 ± 1.4	1.2 ± 0.3	12.0 ± 1.5	4.6 ± 0.3	5.0 ± 0.7	10.0 ± 1.7	0.2 ± 0.2	1.8 ± 0.2	0.04 ± 0.0	0.3 ± 0.4	6.8 ± 0.5	3.3 ± 1.3	5.3 ± 0.3	8.2 ± 0.6	0.1 ± 0.0	16.4 ± 7.3	1.2 ± 0.4
15/08/2016	7.1 ± 0.8	13.2 ± 0.3	4.6 ± 0.2	0.9 ± 0.1	14.9 ± 0.1	4.9 ± 0.1	4.9 ± 0.1	12.0 ± 0.2	1.2 ± 0.2	2.5 ± 0.2	0.1 ± 0.0	1.2 ± 0.1	6.7 ± 0.2	3.8 ± 0.1	5.1 ± 0.1	8.2 ± 0.3	0.2 ± 0.1	8.5 ± 0.8	1.1 ± 0.1
14/09/2016	7.2 ± 0.3	13.6 ± 0.3	6.3 ± 0.2	0.9 ± 0.2	18.9 ± 1.2	4.9 ± 0.1	4.3 ± 0.1	10.4 ± 0.3	1.1 ± 0.1	2.7 ± 0.1	0.1 ± 0.0	0.7 ± 0.5	5.6 ± 0.2	3.6 ± 0.1	4.7 ± 0.2	7.9 ± 0.1	0.2 ± 0.1	6.8 ± 0.6	1.0 ± 0.0
10/10/2016	5.2 ± 0.5	12.9 ± 0.1	8.6 ± 0.4	0.5 ± 0.1	18.6 ± 0.5	5.6 ± 0.1	3.8 ± 0.1	12.5 ± 0.7	0.1 ± 0.0	4.7 ± 0.1	0.1 ± 0.00	0.5 ± 0.1	5.1 ± 0.1	3.4 ± 0.1	4.6 ± 0.1	6.7 ± 0.2	0.2 ± 0.0	6.9 ± 0.1	1.0 ± 0.1
07/11/2016	7.0	13.2	8.8	0.5	19.9	5.4	4.7	9.2	0.1	1.9	0.0	0.2	6.2	3.6	5.0	7.5	0.3	6.6	0.7

Table C.9: Concentration (mg g^{-1}) $\pm$ SD composition of amino acids in sediment trap and sediment samples from site LY1 during 2016. ASP, aspartic acid; GLU, glutamic acid; SER, serine; HIS, histidine; GLY, glycine; THR, threonine; ARG, arginine; ALA, alanine; BALA, β-alanine; TYR, tyrosine; GABA, γ-aminobutyric acid; MET, methionine; VAL, valine; PHE, phenylalanine; ILEU, isoleucine; LEU, leucine; ORN, ornithine; LYS, lysine

	Sediment trap and sediment individual amino acid concentrations (mg g^{-1})																																	
	ASP		GLU		SER		HIS		GLY		THR		ARG		ALA		BALA		TYR		GABA		MET		VAL		PHE		ILEU		LEU		ORN		LYS	
	Av.	SD	Av.	SD	Av.	SD	Av.	SD	Av.	SD	Av.	SD	Av.	SD	Av.	SD	Av.	SD	Av.	SD	Av.	SD	Av.	SD	Av.	SD	Av.	SD	Av.	SD	Av.	SD	Av.	SD	Av.	SD
Sediment trap																																				
31/03/2016	0.8	-	1.2	-	2.0	-	0.6	-	4.4	-	2.2	-	3.4	-	3.7	-	0.1	-	1.3	-	0.0	-	0.5	-	3.1	-	2.4	-	2.4	-	3.6	-	0.2	-	3.9	-
07/04/2016	0.9	1.0	1.0	1.0	0.4	0.3	0.2	0.2	0.7	0.7	0.4	0.4	0.6	0.6	0.7	0.7	0.0	0.0	0.3	0.3	0.0	0.0	0.1	0.1	0.6	0.6	0.5	0.5	0.5	0.5	0.7	0.7	0.0	0.0	1.1	1.3
17/05/2016	5.6	6.8	11.5	14.5	1.3	1.1	0.3	0.4	1.6	1.5	1.1	0.9	1.8	1.5	1.9	1.7	0.0	0.0	0.9	0.9	0.0	0.0	0.5	0.5	2.9	3.2	2.3	2.6	2.3	2.6	3.6	4.0	0.1	0.1	3.6	4.5
02/06/2016	2.8	1.3	4.5	2.8	1.6	0.6	0.3	0.1	2.2	0.8	1.2	0.4	2.1	0.8	2.2	0.8	0.0	0.0	0.9	0.3	0.0	0.0	0.4	0.2	1.9	0.8	1.2	0.9	1.6	0.6	2.4	0.9	0.0	0.0	2.5	1.1
06/07/2016	2.0	0.2	2.9	0.2	1.1	0.2	0.2	0.0	2.1	0.5	1.2	0.0	1.9	0.2	2.0	0.5	0.1	0.0	0.7	0.0	0.0	0.0	0.3	0.0	1.8	0.3	1.3	0.0	1.4	0.2	2.0	0.2	0.1	0.0	2.1	1.2
02/08/2016	1.2	0.3	1.9	0.4	0.7	0.1	0.1	0.0	1.2	0.2	0.8	0.1	1.2	0.2	1.1	0.2	0.0	0.0	0.5	0.1	0.0	0.0	0.2	0.0	1.1	0.2	0.8	0.1	0.8	0.1	1.2	0.2	0.1	0.0	1.1	0.3
16/08/2016	1.1	0.3	2.0	0.5	0.6	0.1	0.1	0.0	1.1	0.2	0.8	0.2	0.9	0.2	1.0	0.2	0.0	0.0	0.3	0.1	0.0	0.0	0.1	0.0	1.0	0.2	0.1	0.0	0.8	0.2	1.0	0.2	0.1	0.1	1.7	0.3
14/09/2016	1.8	0.2	2.8	0.5	0.6	0.1	0.1	0.0	1.0	0.2	0.7	0.1	0.9	0.1	0.7	0.1	0.0	0.0	0.3	0.1	0.0	0.0	0.1	0.0	1.5	0.3	1.1	0.2	1.1	0.2	1.4	0.2	0.1	0.0	2.2	0.4
10/10/2016	1.1	0.1	2.4	0.3	0.6	0.1	0.1	0.0	1.0	0.1	0.8	0.1	1.0	0.1	1.7	0.2	0.0	0.0	0.7	0.1	0.1	0.0	0.1	0.0	1.0	0.1	0.8	0.1	0.8	0.1	1.1	0.1	0.1	0.0	2.1	0.2
07/11/2016	1.4	0.5	2.8	0.8	1.0	0.4	0.2	0.0	1.6	0.6	1.0	0.3	1.4	0.4	1.2	0.4	0.0	0.0	0.5	0.1	0.0	0.0	0.1	0.1	1.3	0.4	1.0	0.3	1.1	0.3	1.5	0.4	0.1	0.1	2.1	0.5
Sediment																																				
30/03/2016	0.2	0.0	0.3	0.0	0.2	0.0	0.0	0.0	0.4	0.0	0.2	0.0	0.2	0.0	0.2	0.0	0.0	0.0	0.1	0.0	0.0	0.0	0.0	0.0	0.2	0.0	0.1	0.0	0.1	0.0	0.2	0.0	0.0	0.0	0.2	0.0
06/04/2016	0.2	0.0	0.3	0.0	0.1	0.0	0.0	0.0	0.4	0.0	0.2	0.0	0.2	0.0	0.2	0.0	0.0	0.0	0.0	0.0	0.0	0.0	0.0	0.0	0.2	0.0	0.1	0.0	0.1	0.0	0.2	0.0	0.0	0.0	0.3	0.1
16/05/2016	0.4	0.1	0.6	0.1	0.3	0.0	0.1	0.0	0.9	0.1	0.4	0.0	0.5	0.1	0.5	0.1	0.1	0.0	0.1	0.0	0.0	0.0	0.0	0.0	0.4	0.0	0.3	0.0	0.3	0.0	0.4	0.0	0.1	0.0	1.0	0.1
01/06/2016	0.3	0.1	0.5	0.1	0.3	0.1	0.1	0.0	0.7	0.2	0.3	0.1	0.4	0.1	0.4	0.1	0.0	0.0	0.0	0.0	0.0	0.0	0.0	0.0	0.3	0.1	0.2	0.1	0.2	0.1	0.3	0.1	0.1	0.0	0.8	0.3
05/07/2016	0.3	0.0	0.5	0.1	0.3	0.1	0.1	0.0	0.7	0.1	0.3	0.1	0.4	0.1	0.5	0.1	0.0	0.0	0.1	0.0	0.0	0.0	0.0	0.0	0.4	0.1	0.2	0.1	0.2	0.1	0.3	0.1	0.1	0.0	0.8	0.1
19/07/2016	0.4	0.0	0.7	0.1	0.3	0.0	0.1	0.0	0.9	0.1	0.4	0.0	0.5	0.0	0.6	0.1	0.1	0.0	0.1	0.0	0.0	0.0	0.1	0.0	0.5	0.1	0.3	0.0	0.3	0.0	0.4	0.1	0.1	0.0	0.5	0.1
01/08/2016	0.4	0.1	0.7	0.0	0.3	0.0	0.1	0.0	0.9	0.0	0.4	0.0	0.5	0.0	0.6	0.0	0.1	0.0	0.1	0.0	0.0	0.0	0.1	0.0	0.4	0.0	0.3	0.0	0.3	0.0	0.4	0.0	0.1	0.0	0.5	0.0
15/08/2016	0.4	0.0	0.6	0.0	0.3	0.0	0.1	0.0	0.8	0.0	0.3	0.0	0.5	0.0	0.5	0.0	0.0	0.0	0.1	0.0	0.0	0.0	0.0	0.0	0.4	0.0	0.2	0.0	0.3	0.0	0.3	0.0	0.1	0.0	0.4	0.0
13/09/2016	0.2	0.0	0.4	0.1	0.2	0.1	0.1	0.0	0.7	0.2	0.2	0.1	0.4	0.1	0.4	0.1	0.0	0.0	0.1	0.0	0.0	0.0	0.0	0.0	0.3	0.1	0.2	0.1	0.2	0.1	0.3	0.1	0.1	0.0	0.3	0.1
10/10/2016	0.3	0.1	0.5	0.1	0.3	0.0	0.1	0.0	0.7	0.0	0.3	0.0	0.4	0.0	0.4	0.0	0.0	0.0	0.1	0.0	0.0	0.0	0.0	0.0	0.3	0.0	0.2	0.0	0.2	0.0	0.3	0.0	0.1	0.0	0.4	0.0
07/11/2016	0.3	0.0	0.5	0.0	0.3	0.0	0.1	0.0	0.9	0.0	0.4	0.0	0.5	0.0	0.5	0.0	0.1	0.0	0.1	0.0	0.0	0.0	0.0	0.0	0.4	0.0	0.3	0.0	0.3	0.0	0.3	0.0	0.1	0.0	0.5	0.0

Table C.10: Mole percentages ± SD composition of amino acids in sediment trap and sediment samples from site LY1 during 2016. ASP, aspartic acid; GLU, glutamic acid; SER, serine; HIS, histidine; GLY, glycine; THR, threonine; ARG, arginine; ALA, alanine; BALA, β-alanine; TYR, tyrosine; GABA, γ-aminobutyric acid; MET, methionine; VAL, valine; PHE, phenylalanine; ILEU, isoleucine; LEU, leucine; ORN, ornithine; LYS, lysine; DI, degradation index

Date	mole %																		DI
	ASP	GLU	SER	HIS	GLY	THR	ARG	ALA	BALA	TYR	GABA	MET	VAL	PHE	ILEU	LEU	ORN	LYS	
Sediment trap																			
31/03/2016	2.0	2.6	6.2	1.2	19.4	6.1	6.4	13.7	0.4	2.4	0.1	1.2	8.8	4.9	6.1	9.2	0.4	8.9	1.0
07/04/2016	7.9 ± 2.3	9.7 ± 0.3	5.9 ± 0.8	1.3 ± 0.6	14.3 ± 1.3	5.3 ± 0.6	5.3 ± 0.4	11.1 ± 0.5	0.2 ± 0.1	2.2 ± 0.2	0.1 ± 0.0	1.1 ± 0.3	7.3 ± 0.4	4.3 ± 0.2	5.4 ± 0.2	8.0 ± 0.3	0.3 ± 0.1	10.5 ± 2.1	1.1 ± 0.1
17/05/2016	11.4 ± 3.4	20.0 ± 9.0	5.3± 2.6	0.5 ± 0.2	9.2 ± 3.9	4.1 ± 2.3	4.5 ± 2.2	8.7 ± 3.7	0.1 ± 0.1	1.9 ± 0.7	0.1 ± 0.1	1.0 ± 0.1	7.7 ± 0.1	4.5 ± 0.1	5.7 ± 0.1	8.8 ± 0.1	0.3 ± 0.1	6.3 ± 2.8	1.6 ± 0.7
02/06/2016	9.4 ± 0.6	13.2 ± 2.3	6.8 ± 1.0	1.0 ± 0.2	13.0 ± 0.8	4.5 ± 0.6	5.3 ± 0.5	10.9 ± 0.4	0.1 ± 0.1	2.4 ± 0.3	0.03 ± 0.0	1.2 ± 0.5	7.4 ± 0.2	3.1 ± 1.5	5.6 ± 0.2	8.2 ± 0.4	0.1 ± 0.0	7.8 ± 0.7	1.1 ± 0.2
06/07/2016	8.0 ± 1.5	10.6 ± 2.1	5.7 ± 0.2	0.7 ± 0.2	14.8 ± 1.3	5.2 ± 0.1	6.0 ± 0.2	12.0 ± 1.2	0.4 ± 0.1	2.0 ± 0.3	0.3 ± 0.1	1.1 ± 0.1	8.1 ± 0.3	4.1 ± 0.6	5.6 ± 0.2	8.1 ± 0.4	0.3 ± 0.0	7.3 ± 2.9	0.8 ± 0.2
02/08/2016	7.8 ± 1.7	11.4 ± 0.9	6.1 ± 0.3	0.7 ± 0.1	14.7 ± 0.7	5.6 ± 0.3	6.0 ± 0.3	10.9 ± 0.9	0.3 ± 0.1	2.3 ± 0.2	0.2 ± 0.1	1.0 ± 0.2	8.0 ± 0.3	4.3 ± 0.2	5.5 ± 0.3	8.0 ± 0.4	0.3 ± 0.1	7.0 ± 2.1	0.1 ± 0.1
16/08/2016	7.9 ± 0.6	13.3 ± 0.6	5.9 ± 0.3	0.4 ± 0.1	14.4 ± 0.5	6.2 ± 0.2	5.1 ± 0.3	10.5 ± 0.2	0.2 ± 0.0	1.5 ± 0.0	0.4 ± 0.0	0.6 ± 0.2	8.4 ± 0.0	0.5 ± 0.0	5.8 ± 0.0	7.4 ± 0.1	0.5 ± 0.4	11.1 ± 0.7	0.3 ± 0.1
14/09/2016	10.9 ± 0.5	15.0 ± 0.1	4.3 ± 0.3	0.4 ± 0.1	10.0 ± 1.2	4.4 ± 0.2	4.0 ± 0.1	6.5 ± 0.1	0.3 ± 0.1	1.3 ± 0.1	0.3 ± 0.1	0.5 ± 0.1	10.1 ± 0.0	5.2 ± 0.1	6.6 ± 0.1	8.2 ± 0.1	0.5 ± 0.2	11.7 ± 1.5	1.5 ± 0.1
11/10/2016	6.5 ± 0.2	13.0 ± 0.3	4.9 ± 0.3	0.6 ± 0.1	10.9 ± 0.4	5.6 ± 0.0	4.7 ± 0.2	15.1 ± 0.4	0.3 ± 0.0	3.3 ± 0.0	0.4 ± 0.0	0.6 ± 0.1	6.9 ± 0.1	3.7 ± 0.0	5.2 ± 0.1	6.7 ± 0.1	0.4 ± 0.1	11.5 ± 1.3	0.8 ± 0.1
08/11/2016	7.1 ± 0.5	12.9 ± 0.2	6.1 ± 1.2	0.7 ± 0.1	14.3 ± 1.4	6.0 ± 0.2	5.3 ± 0.1	9.4 ± 0.1	0.1 ± 0.0	2.0 ± 0.1	0.1 ± 0.0	0.5 ± 0.4	7.5 ± 0.2	4.0 ± 0.2	5.7 ± 0.2	7.6 ± 0.2	0.5 ± 0.1	10.2 ± 1.9	1.0 ± 0.2
Sediment																			
30/03/2016	6.9 ± 0.9	8.8 ± 0.3	6.5 ± 0.9	1.1 ± 0.2	22.0 ± 0.5	5.8 ± 0.4	5.9 ± 0.1	11.7 ± 0.2	1.3 ± 0.1	1.7 ± 0.4	0.5 ± 0.1	0.4 ± 0.1	7.1 ± 0.3	3.1 ± 0.0	4.2 ± 0.2	5.5 ± 0.1	0.8 ± 0.3	6.8 ± 0.3	-0.1 ± 0.1
06/04/2016	5.2 ± 0.2	8.4 ± 0.5	5.9 ± 0.1	1.0 ± 0.1	22.3 ± 0.8	5.8 ± 0.3	5.7 ± 0.1	11.9 ± 0.8	1.3 ± 0.1	1.0 ± 0.3	0.5 ± 0.0	0.5 ± 0.0	7.2 ± 0.5	3.1 ± 0.2	4.3 ± 0.3	5.5 ± 0.3	1.0 ± 0.5	9.4 ± 2.9	-0.2 ± 0.1
16/05/2016	5.1 ± 1.0	8.1 ± 0.1	5.5 ± 0.2	0.9 ± 0.0	21.4 ± 0.2	5.7 ± 0.1	5.4 ± 0.3	11.3 ± 0.3	1.2 ± 0.0	0.7 ± 0.1	0.6 ± 0.0	0.5 ± 0.1	6.7 ± 0.2	3.0 ± 0.1	4.1 ± 0.2	5.2 ± 0.2	1.4 ± 0.0	13.1 ± 0.6	-0.3 ± 0.1
01/06/2016	5.0 ± 1.0	7.9 ± 0.2	5.8 ± 0.1	1.0 ± 0.1	21.8 ± 0.8	5.8 ± 0.2	5.5 ± 0.3	11.2 ± 0.1	1.3 ± 0.1	0.7 ± 0.2	0.6 ± 0.1	0.5 ± 0.1	6.6 ± 0.1	2.9 ± 0.1	3.9 ± 0.0	5.1 ± 0.1	1.6 ± 0.2	12.8 ± 0.3	-0.4 ± 0.1
05/07/2016	5.3 ± 0.4	8.1 ± 0.0	5.7 ± 0.4	1.0 ± 0.0	21.5 ± 0.4	5.4 ± 0.2	5.5 ± 0.4	11.4 ± 0.2	1.2 ± 0.0	0.7 ± 0.1	0.6 ± 0.1	0.5 ± 0.0	6.7 ± 0.0	3.0 ± 0.1	4.0 ± 0.0	5.2 ± 0.2	1.4 ± 0.2	12.9 ± 0.5	-0.3 ± 0.0
19/07/2016	5.1 ± 0.9	8.8 ± 0.0	5.6 ± 0.3	1.1 ± 0.1	23.1 ± 0.6	5.9 ± 0.1	5.7 ± 0.2	12.3 ± 0.7	1.3 ± 0.1	0.8 ± 0.2	0.7 ± 0.0	0.7 ± 0.0	7.4 ± 0.3	3.3 ± 0.2	4.5 ± 0.3	5.8 ± 0.4	0.8 ± 0.1	6.9 ± 0.3	-0.2 ± 0.1
01/08/2016	5.6 ± 1.2	8.6 ± 0.3	6.0 ± 0.2	1.2 ± 0.1	23.0 ± 0.4	5.7 ± 0.3	5.8 ± 0.2	12.2 ± 0.3	1.3 ± 0.1	0.9 ± 0.1	0.7 ± 0.1	0.6 ± 0.1	7.3 ± 0.2	3.2 ± 0.1	4.4 ± 0.1	5.6 ± 0.1	1.0 ± 0.1	6.7 ± 0.1	-0.2 ± 0.0
15/08/2016	6.4 ± 0.2	8.6 ± 0.1	6.3 ± 0.6	1.2 ± 0.1	22.1 ± 0.6	5.8 ± 0.3	6.0 ± 0.2	12.1 ± 0.2	1.2 ± 0.1	1.0 ± 0.2	0.7 ± 0.1	0.5 ± 0.1	7.3 ± 0.1	3.2 ± 0.0	4.5 ± 0.0	5.7 ± 0.0	0.9 ± 0.0	6.6 ± 0.4	-0.2 ± 0.0
13/09/2016	4.4 ± 1.7	7.9 ± 0.5	5.9 ± 0.5	1.1 ± 0.1	24.9 ± 1.3	5.6 ± 0.3	5.8 ± 0.3	12.3 ± 0.4	1.3 ± 0.1	1.7 ± 0.6	0.6 ± 0.1	0.5 ± 0.1	7.4 ± 0.1	3.2 ± 0.0	4.5 ± 0.1	5.8 ± 0.1	0.9 ± 0.1	6.4 ± 0.1	-0.1 ± 0.2
10/10/2016	5.2 ± 1.4	8.3 ± 0.5	6.2 ± 0.5	1.1 ± 0.1	24.7 ± 0.7	5.7 ± 0.4	5.8 ± 0.1	12.3 ± 0.3	1.3 ± 0.2	0.8 ± 0.1	0.6 ± 0.1	0.4 ± 0.1	7.2 ± 0.2	3.1 ± 0.1	4.5 ± 0.3	5.6 ± 0.2	1.0 ± 0.2	6.2 ± 0.3	-0.3 ± 0.0
07/11/2016	4.4 ± 0.0	7.4 ± 0.2	6.7 ± 0.1	1.0 ± 0.0	24.3 ± 0.6	7.0 ± 0.2	5.9 ± 0.1	11.2 ± 0.2	1.3 ± 0.0	1.4 ± 0.1	0.6 ± 0.0	0.6 ± 0.1	7.8 ± 0.1	3.3 ± 0.1	4.5 ± 0.1	4.9 ± 0.1	0.7 ± 0.0	7.1 ± 0.1	-0.3 ± 0.1

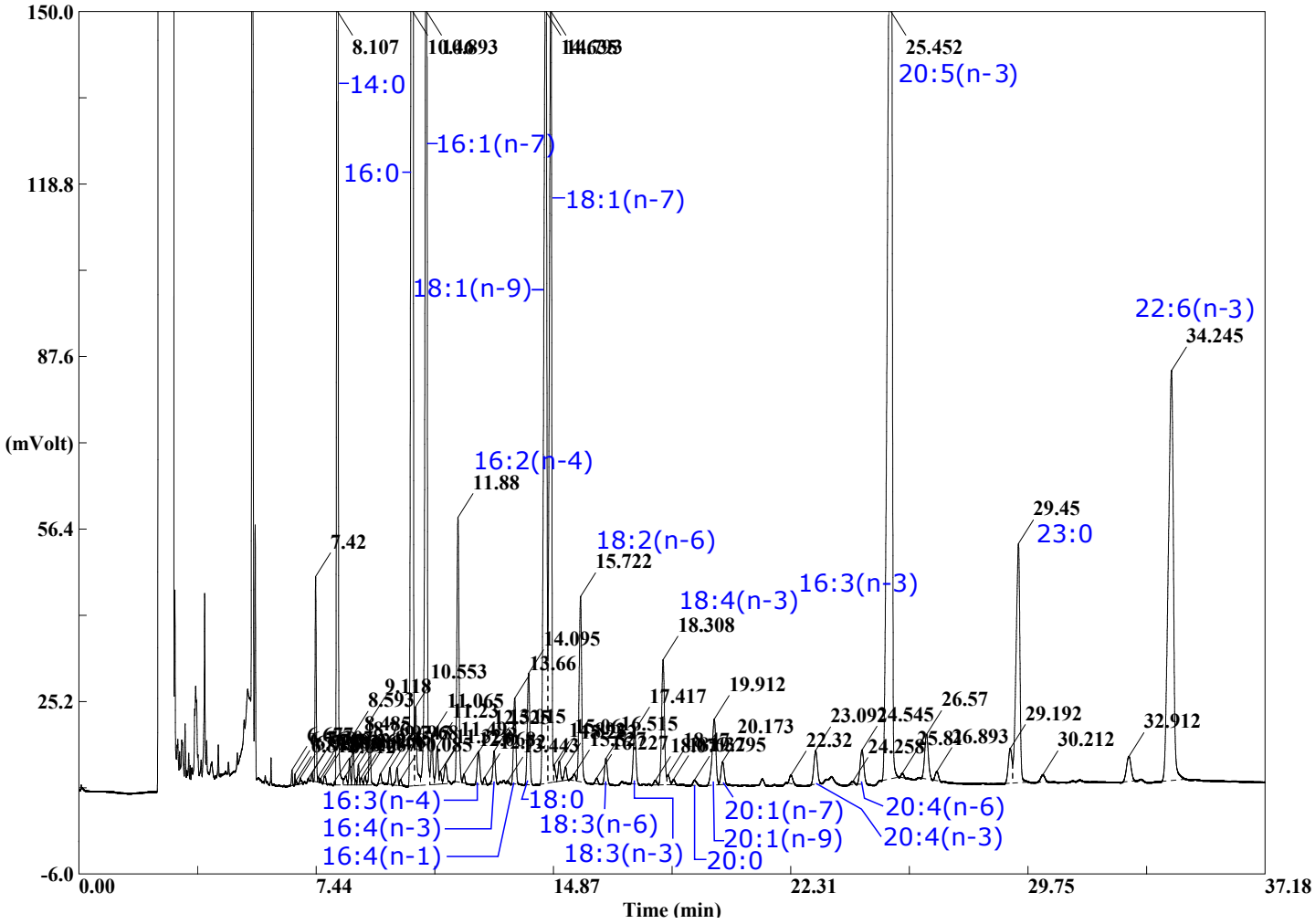

Figure C.1: Example of a fatty acid gas chromatogram extracted from suspended particulate material from site LY1

Table C.11: Concentration (μg L^{-1}) of individual fatty acids from suspended particulate material (SPM) samples collected from above the pycnocline at site LY1 during 2016

	SPM above the pycnocline fatty acid concentration (μg L^{-1})																					
	30/04/16		06/04/16		16/05/16		01/06/16		05/07/16		18/07/16		01/08/16		15/08/16		13/09/16		10/10/16		07/11/16	
	Av.	SD	Av.	SD	Av.	SD	Av.	SD	Av.	SD	Av.	SD	Av.	SD	Av.	SD	Av.	SD	Av.	SD	Av.	SD
14:0	3.2	0.6	1.2	0.1	1.7	0.2	0.8	0.1	0.2	0.1	1.1	0.2	2.5	0.1	1.2	0.1	1.0	0.0	1.0	0.1	0.6	0.0
16:0	11.6	5.5	3.4	0.3	4.1	0.6	5.1	0.1	3.6	0.2	7.3	0.9	6.1	0.3	5.4	0.4	5.9	1.0	6.9	0.2	3.3	0.1
16:1(n-7)	3.9	0.0	1.8	0.1	1.7	0.3	3.6	0.0	1.0	0.1	3.4	0.1	6.8	1.4	2.6	0.2	1.1	0.1	1.4	0.1	0.5	0.1
16:2(n-4)	0.8	0.0	0.4	0.1	0.4	0.1	0.5	0.1	0.1	0.0	0.5	0.1	0.6	0.1	0.5	0.0	0.2	0.0	0.2	0.0	0.1	0.0
16:3(n-4)	1.1	0.3	0.6	0.1	0.2	0.0	0.2	0.0	0.1	0.0	0.5	0.0	0.4	0.0	0.3	0.0	0.2	0.0	0.3	0.0	0.1	0.0
16:4(n-3)	0.1	0.0	0.0	0.0	0.0	0.0	0.0	0.0	0.0	0.0	0.0	0.0	0.0	0.0	0.3	0.0	0.0	0.0	0.1	0.0	0.1	0.0
16:4(n-1)	1.2	0.4	0.6	0.1	0.6	0.1	0.3	0.0	0.1	0.1	0.5	0.0	0.6	0.0	0.3	0.0	0.1	0.0	0.1	0.0	0.0	0.0
18:0	10.5	6.7	2.2	0.2	2.2	0.3	2.6	0.0	2.4	0.0	2.9	0.3	0.8	0.0	1.3	0.1	3.0	0.7	2.2	0.2	1.4	0.0
18:1(n-9)	0.9	0.3	0.3	0.0	1.1	0.3	1.9	0.1	1.4	0.1	1.5	0.0	0.9	0.0	1.5	0.1	1.7	0.5	3.0	0.3	1.1	0.1
18:1(n-7)	0.5	0.1	0.2	0.0	0.5	0.1	0.8	0.0	0.5	0.0	1.2	0.0	1.1	0.1	1.6	0.1	0.6	0.1	0.9	0.1	0.3	0.1
18:2(n-6)	0.8	0.2	0.6	0.2	1.1	0.6	1.2	0.1	0.9	0.1	0.9	0.0	0.7	0.0	0.6	0.0	0.6	0.2	1.0	0.1	0.5	0.1
18:3(n-6)	0.1	0.0	0.1	0.0	0.1	0.1	0.0	0.0	0.1	0.1	0.1	0.0	0.1	0.0	0.0	0.0	0.1	0.0	0.0	0.0	0.0	0.0
18:3(n-3)	0.1	0.0	0.1	0.0	0.3	0.0	0.4	0.0	0.3	0.0	0.5	0.0	0.5	0.0	0.6	0.0	0.3	0.1	0.6	0.1	0.2	0.0
18:4(n-3)	0.9	0.2	0.5	0.1	0.6	0.1	0.3	0.1	0.4	0.1	1.5	0.0	1.2	0.0	1.7	0.1	0.9	0.2	0.9	0.1	0.4	0.0
20:0	0.3	0.2	0.1	0.0	0.1	0.0	0.1	0.0	0.1	0.0	0.1	0.0	0.0	0.0	0.1	0.0	0.3	0.2	0.1	0.0	0.1	0.0
20:1(n-9)	0.1	0.0	0.0	0.0	0.3	0.0	0.2	0.0	0.4	0.0	2.0	0.0	1.0	0.0	1.6	0.1	1.3	0.5	0.9	0.1	0.2	0.0
20:1(n-7)	0.1	0.1	0.0	0.0	0.0	0.0	0.0	0.0	0.0	0.0	0.0	0.0	0.0	0.0	0.1	0.0	0.1	0.1	0.0	0.0	0.0	0.0
20:4(n-3)	0.1	0.1	0.0	0.0	0.0	0.0	0.1	0.0	0.0	0.0	0.1	0.0	0.1	0.0	0.2	0.0	0.2	0.2	0.1	0.0	0.0	0.0
20:4(n-6)	0.1	0.0	0.1	0.0	0.1	0.0	0.1	0.0	0.1	0.1	0.1	0.0	0.1	0.0	0.2	0.0	0.0	0.0	0.0	0.0	0.0	0.0
20:5(n-3)	1.1	0.4	0.6	0.1	0.6	0.1	1.0	0.1	0.4	0.0	2.0	0.1	1.6	0.0	2.8	0.2	1.0	0.1	0.7	0.1	0.4	0.0
22:6(n-3)	0.4	0.1	0.2	0.0	0.4	0.1	0.4	0.0	0.5	0.0	2.7	0.5	1.8	0.3	2.8	0.2	0.6	0.2	0.5	0.1	0.2	0.0
Total fatty acid	38.0		13.1		16.0		19.8		12.7		29.0		26.8		25.6		19.1		21.0		9.4	

Table C.12: Individual fatty acid percent composition for suspended particulate material (SPM) samples collected from above the pycnocline at site LY1 during 2016

	Percent composition of individual fatty acids in SPM from above the pycnocline (%)																					
	30/03/16		06/04/16		16/05/16		01/06/16		05/07/16		18/07/16		01/08/16		15/08/16		13/09/16		10/10/16		07/11/16	
	Av.	SD	Av.	SD	Av.	SD	Av.	SD	Av.	SD	Av.	SD	Av.	SD	Av.	SD	Av.	SD	Av.	SD	Av.	SD
14:0	8.7	1.7	9.4	0.1	11.0	1.0	3.9	0.2	1.6	0.6	3.6	0.5	9.2	1.0	4.7	0.0	5.3	0.9	4.9	0.1	5.9	0.3
16:0	29.9	3.0	26.1	0.0	25.6	0.6	25.9	0.1	28.1	0.2	25.2	1.3	22.8	0.7	21.1	0.0	31.0	1.0	33.0	1.7	35.5	1.2
16:1(n-7)	11.0	4.2	13.9	0.5	10.3	0.2	18.4	0.0	7.8	0.4	11.7	1.2	25.2	3.3	10.0	0.0	5.6	0.7	6.5	0.2	5.6	0.6
16:2(n-4)	2.1	0.8	2.9	0.3	2.6	0.0	2.7	0.3	1.0	0.0	1.9	0.1	2.1	0.1	1.8	0.0	0.9	0.2	0.8	0.0	0.9	0.1
16:3(n-4)	2.9	0.3	4.2	0.5	1.2	0.0	1.0	0.2	1.0	0.1	1.7	0.1	1.4	0.2	1.1	0.0	1.2	0.1	1.5	0.1	1.2	0.0
16:4(n-3)	0.2	0.0	0.1	0.1	0.2	0.0	0.2	0.1	0.3	0.1	0.1	0.0	0.1	0.0	1.2	0.0	0.2	0.0	0.3	0.0	0.7	0.0
16:4(n-1)	3.2	0.2	4.5	0.7	3.6	0.0	1.6	0.2	0.5	0.4	1.7	0.0	2.1	0.0	1.2	0.0	0.7	0.2	0.6	0.0	0.4	0.0
18:0	26.2	7.4	16.4	0.0	13.8	0.5	13.2	0.2	18.7	0.5	9.8	0.5	3.1	0.3	5.0	0.0	15.4	0.6	10.3	0.3	14.4	0.2
18:1(n-9)	2.5	0.2	2.6	0.4	6.7	0.4	9.4	0.3	11.3	0.0	5.2	0.5	3.4	0.2	5.9	0.0	8.6	1.0	14.4	0.3	11.4	0.4
18:1(n-7)	1.5	0.3	1.6	0.1	3.2	0.2	4.1	0.1	4.1	0.1	4.2	0.2	4.1	0.1	6.2	0.0	3.2	0.2	4.3	0.3	2.9	0.6
18:2(n-6)	2.4	1.3	4.5	1.6	6.5	2.6	6.2	0.5	7.2	0.1	3.3	0.2	2.7	0.2	2.4	0.0	3.1	0.4	4.7	0.1	5.7	0.6
18:3(n-6)	0.4	0.2	0.8	0.0	0.9	0.2	0.2	0.1	0.6	0.4	0.5	0.1	0.4	0.0	0.2	0.0	0.5	0.2	0.2	0.1	0.2	0.2
18:3(n-3)	0.3	0.1	0.4	0.1	1.7	0.1	2.2	0.0	2.1	0.0	1.6	0.1	1.7	0.1	2.4	0.0	1.8	0.1	2.8	0.1	2.2	0.1
18:4(n-3)	2.5	0.4	4.0	0.4	3.6	0.0	1.4	0.3	3.4	0.4	5.3	0.3	4.4	0.4	6.8	0.0	4.5	0.1	4.4	0.2	4.0	0.4
20:0	0.7	0.3	0.7	0.0	0.5	0.0	0.5	0.1	0.8	0.0	0.4	0.0	0.2	0.0	0.5	0.0	1.4	0.7	0.6	0.0	0.6	0.0
20:1(n-9)	0.4	0.1	0.4	0.4	2.0	0.4	0.8	0.1	3.5	0.1	6.9	0.3	3.6	0.3	6.2	0.0	6.4	1.6	4.4	0.3	2.2	0.2
20:1(n-7)	0.4	0.4	0.1	0.1	0.1	0.0	0.2	0.1	0.0	0.0	0.1	0.0	0.1	0.0	0.3	0.0	0.3	0.3	0.0	0.0	0.0	0.0
20:4(n-3)	0.3	0.3	0.1	0.0	0.1	0.0	0.7	0.0	0.3	0.0	0.3	0.0	0.4	0.1	0.7	0.0	0.9	0.8	0.3	0.0	0.3	0.1
20:4(n-6)	0.4	0.2	0.8	0.2	0.8	0.0	0.3	0.1	0.4	0.4	0.3	0.1	0.3	0.0	0.7	0.0	0.2	0.3	0.2	0.2	0.2	0.0
20:5(n-3)	2.9	0.2	4.9	0.5	3.5	0.1	5.2	0.4	3.3	0.0	6.8	0.1	6.0	0.5	10.8	0.0	5.4	1.7	3.1	0.1	3.9	0.5
22:6(n-3)	1.0	0.1	1.7	0.2	2.2	0.0	1.9	0.2	3.7	0.1	9.4	1.0	6.7	0.6	11.0	0.0	3.3	0.2	2.6	0.1	1.7	0.0
SFAs	65.5		52.7		50.9		43.5		49.3		39.0		35.2		31.3		53.1		48.9		56.4	
MUFA	15.8		18.6		22.4		32.9		26.7		28.0		36.3		28.5		24.3		29.6		22.1	
PUFA	18.7		28.7		26.7		23.6		24.0		32.9		28.5		40.2		22.6		21.4		21.5	

Table C.13: Concentration (μg L^{-1}) of individual fatty acids from suspended particulate material (SPM) samples collected from below the pycnocline at site LY1 during 2016

	SPM below the pycnocline fatty acid concentration (μg L^{-1})																					
	30/03/16		06/04/16		16/05/16		01/06/16		05/07/16		18/07/16		01/08/16		15/08/16		13/09/16		10/10/16		07/11/16	
	Av.	SD	Av.	SD	Av.	SD	Av.	SD	Av.	SD	Av.	SD	Av.	SD	Av.	SD	Av.	SD	Av.	SD	Av.	SD
14:0	1.3	0.4	1.1	0.4	1.6	0.1	0.5	0.1	0.2	0.0	0.3	0.1	0.8	0.1	0.8	0.3	0.7	0.1	0.5	0.0	0.7	0.3
16:0	5.7	1.5	3.5	0.8	7.6	5.2	3.5	1.4	3.2	0.3	4.0	0.2	3.6	0.4	4.5	1.5	5.5	1.0	4.3	0.4	7.4	2.3
16:1(n-7)	1.8	0.5	2.1	0.5	1.3	0.1	2.6	1.0	0.8	0.2	1.3	0.1	2.0	0.2	1.1	1.5	0.8	0.2	0.5	0.0	0.8	0.3
16:2(n-4)	0.3	0.1	0.3	0.2	0.4	0.0	0.4	0.2	0.1	0.0	0.2	0.0	0.3	0.0	0.4	0.3	0.3	0.3	0.1	0.0	0.1	0.1
16:3(n-4)	0.5	0.1	0.4	0.3	0.2	0.0	0.1	0.0	0.1	0.0	0.2	0.0	0.4	0.1	0.3	0.1	0.2	0.1	0.2	0.0	0.2	0.1
16:4(n-3)	0.0	0.0	0.0	0.0	0.0	0.0	0.0	0.0	0.0	0.0	0.0	0.0	0.0	0.0	0.1	0.0	0.1	0.1	0.1	0.0	0.1	0.0
16:4(n-1)	0.5	0.1	0.4	0.3	0.6	0.0	0.3	0.1	0.0	0.0	0.1	0.0	0.3	0.0	0.3	0.2	0.1	0.0	0.0	0.0	0.1	0.0
18:0	4.7	0.9	2.2	0.1	5.1	4.5	2.0	1.0	2.5	0.2	3.0	0.2	0.9	0.1	1.4	0.0	3.0	0.3	1.9	0.1	3.3	0.7
18:1(n-9)	1.4	0.4	0.6	0.2	0.6	0.0	0.8	0.3	1.0	0.1	0.8	0.1	0.7	0.1	1.5	0.9	1.8	1.0	1.6	0.2	2.6	0.9
18:1(n-7)	0.7	0.1	0.3	0.1	0.4	0.0	0.6	0.3	0.4	0.0	0.5	0.0	0.7	0.0	0.6	0.0	0.4	0.1	0.3	0.0	0.5	0.1
18:2(n-6)	1.0	0.7	1.2	0.7	1.4	1.0	0.7	0.0	0.8	0.1	1.0	0.6	0.5	0.2	0.6	0.1	0.7	0.4	0.5	0.0	1.2	0.3
18:3(n-6)	0.1	0.1	0.1	0.0	0.1	0.0	0.0	0.0	0.1	0.1	0.1	0.0	0.1	0.0	0.1	0.1	0.1	0.0	0.0	0.0	0.1	0.1
18:3(n-3)	0.2	0.0	0.1	0.0	0.2	0.0	0.1	0.0	0.2	0.0	0.2	0.0	0.3	0.1	0.3	0.0	0.5	0.4	0.1	0.0	0.4	0.1
18:4(n-3)	0.5	0.1	0.4	0.2	0.5	0.0	0.2	0.0	0.3	0.1	0.5	0.1	0.7	0.2	1.0	0.4	0.5	0.0	0.3	0.1	0.5	0.1
20:0	0.1	0.0	0.1	0.0	0.1	0.1	0.1	0.1	0.1	0.0	0.1	0.0	0.0	0.0	0.3	0.2	0.4	0.3	0.1	0.0	0.1	0.0
20:1(n-9)	0.2	0.1	0.1	0.0	0.2	0.0	0.1	0.0	0.3	0.0	0.3	0.0	0.5	0.1	1.1	0.4	0.9	0.3	0.2	0.0	0.3	0.1
20:1(n-7)	0.0	0.0	0.0	0.0	0.0	0.0	0.0	0.0	0.0	0.0	0.0	0.0	0.0	0.0	0.0	0.0	0.1	0.1	0.0	0.0	0.0	0.0
20:4(n-3)	0.0	0.0	0.0	0.0	0.0	0.0	0.1	0.1	0.0	0.0	0.0	0.0	0.1	0.0	0.4	0.4	0.3	0.3	0.0	0.0	0.1	0.0
20:4(n-6)	0.1	0.0	0.1	0.0	0.1	0.0	0.0	0.0	0.0	0.0	0.1	0.0	0.0	0.0	0.1	0.1	0.1	0.0	0.0	0.0	0.0	0.0
20:5(n-3)	0.7	0.2	0.8	0.6	0.6	0.1	0.7	0.3	0.4	0.0	0.7	0.0	1.0	0.3	2.2	1.0	0.6	0.0	0.3	0.1	0.6	0.1
22:6(n-3)	0.2	0.1	0.2	0.1	0.3	0.0	0.3	0.1	0.4	0.0	0.6	0.1	0.8	0.2	1.3	0.3	0.5	0.0	0.2	0.1	0.2	0.0
Total fatty acid	20.1		14.0		21.5		13.2		11.0		14.2		14.0		18.4		17.6		11.3		19.2	

Table C.14: Individual fatty acid percent composition for suspended particulate material (SPM) samples collected from below the pycnocline at site LY1 during 2016

	Percent composition of individual fatty acids in SPM from below the pycnocline (%)																					
	30/03/16		06/04/16		16/05/16		01/06/16		05/07/16		18/07/16		01/08/16		15/08/16		13/09/16		10/10/16		07/11/16	
	Av.	SD	Av.	SD	Av.	SD	Av.	SD	Av.	SD	Av.	SD	Av.	SD	Av.	SD	Av.	SD	Av.	SD	Av.	SD
14:0	6.5	0.2	8.0	0.8	8.1	3.5	3.9	0.5	1.4	0.1	2.0	0.5	5.8	0.2	4.1	0.1	4.0	0.5	4.5	0.1	3.6	0.4
16:0	28.5	0.1	25.2	0.1	33.6	7.1	26.2	0.9	29.3	0.7	28.5	1.9	26.2	1.3	25.3	2.8	31.9	3.8	38.3	0.3	38.3	1.1
16:1(n-7)	8.7	0.4	15.1	0.1	6.7	3.1	19.6	0.1	7.0	1.7	9.2	0.8	14.3	0.8	4.9	6.1	4.4	0.0	4.6	0.3	4.1	0.2
16:2(n-4)	1.3	0.0	2.4	0.5	2.2	1.0	3.3	0.1	0.8	0.0	1.3	0.1	2.5	0.5	2.1	0.5	1.6	1.3	0.8	0.1	0.7	0.1
16:3(n-4)	2.7	0.1	2.8	1.3	1.1	0.5	1.1	0.3	0.9	0.3	1.4	0.1	2.6	0.1	1.5	0.1	1.2	0.2	1.5	0.2	0.9	0.4
16:4(n-3)	0.2	0.0	0.2	0.0	0.2	0.1	0.3	0.1	0.3	0.0	0.3	0.1	0.3	0.0	0.5	0.0	0.4	0.3	0.6	0.0	0.7	0.1
16:4(n-1)	2.3	0.0	2.5	1.7	3.1	1.6	2.1	0.1	0.5	0.3	0.7	0.1	2.2	0.1	1.4	0.3	0.5	0.1	0.3	0.0	0.4	0.1
18:0	23.5	1.4	15.8	3.0	21.2	10.0	14.9	1.8	23.3	0.4	21.3	1.9	6.6	0.5	8.6	3.8	17.6	3.4	17.1	0.3	17.2	1.3
18:1(n-9)	7.2	0.3	4.4	0.5	3.3	1.6	5.8	0.1	9.1	0.3	5.9	0.4	5.3	0.1	7.9	1.4	9.7	3.0	13.8	0.4	13.3	0.9
18:1(n-7)	3.4	0.5	2.2	0.0	2.2	1.1	4.2	0.4	3.9	0.5	3.5	0.1	4.9	0.4	3.5	1.4	2.5	0.2	2.5	0.5	2.4	0.0
18:2(n-6)	4.8	2.3	3.8		6.3	1.5	6.1	2.0	6.9	1.8	6.7	4.0	3.7	0.6	3.2	0.7	4.0	1.4	4.1	0.2	6.4	0.4
18:3(n-6)	0.7	0.7	0.9	0.3	0.8	0.4	0.3	0.0	0.7	0.5	0.5	0.2	0.5	0.1	0.5	0.3	0.3	0.2	0.4	0.1	0.6	0.6
18:3(n-3)	0.9	0.0	0.4	0.1	1.1	0.6	1.0	0.1	1.6	0.0	1.5	0.1	2.4	0.0	1.7	0.5	2.6	1.5	1.1	0.1	1.9	0.0
18:4(n-3)	2.5	0.2	2.6	1.2	2.7	1.3	1.7	0.6	2.7	0.6	3.8	0.3	5.0	0.5	5.3	0.0	2.8	0.7	2.6	0.4	2.7	0.2
20:0	0.5	0.3	0.8	0.1	0.6	0.0	0.6	0.3	0.9	0.1	0.7	0.1	0.3	0.1	1.5	0.5	2.1	1.0	0.9	0.0	0.6	0.0
20:1(n-9)	1.0	0.1	0.6	0.1	1.2	0.6	1.0	0.0	2.7	0.2	2.3	0.0	3.5	0.1	5.9	0.3	5.2	0.1	1.4	0.1	1.5	0.0
20:1(n-7)	0.2	0.0	0.2	0.1	0.1	0.1	0.1	0.0	0.1	0.0	0.1	0.0	0.1	0.0	0.2	0.1	0.8	0.5	0.1	0.0	0.0	0.0
20:4(n-3)	0.1	0.0	0.2	0.0	0.1	0.0	0.6	0.2	0.3	0.1	0.3	0.1	0.6	0.2	2.0	1.2	1.3	1.4	0.2	0.0	0.3	0.0
20:4(n-6)	0.6	0.1	0.5	0.1	0.5	0.2	0.2	0.1	0.3	0.3	0.5	0.2	0.3	0.3	0.6	0.1	0.4	0.0	0.4	0.2	0.2	0.1
20:5(n-3)	3.3	0.1	5.0	3.5	3.3	2.0	5.0	0.1	3.7	0.3	5.2	0.3	7.4	1.1	12.1	0.5	3.7	0.9	2.9	0.6	3.0	0.4
22:6(n-3)	1.1	0.0	1.2	0.7	1.7	1.1	2.1	0.2	3.8	0.6	4.3	0.6	5.6	0.8	7.2	1.5	3.0	1.0	2.1	0.4	1.2	0.1
SFAs	59.0		49.8		63.5		45.6		54.8		52.4		38.9		39.5		55.7		60.8		59.7	
MUFA	20.5		22.5		13.4		30.7		22.7		21.0		28.0		22.5		22.5		22.3		21.3	
PUFA	20.5		22.5		23.1		23.7		22.4		26.6		33.0		38.1		21.8		16.9		19.0	

Table C.15: Concentration (μg g^{-1}) of individual fatty acids from sediment trap material collected from LY1 during 2016

	Sediment trap fatty acid concentration (μg g^{-1})																		
	31/03/16		07/04/16		17/05/16		02/06/16		06/07/16		02/08/16		16/08/16		14/09/16		11/10/16	08/11/16	
	Av.	SD	Av.	SD	Av.	SD	Av.	SD	Av.	SD	Av.	SD	Av.	SD	Av.	SD		Av.	SD
14:0	136.3	32.0	152.8	79.7	176.2	6.5	283.4	115.0	62.8	5.7	62.9	8.9	124.3	123.4	48.7	8.0	32.9	30.9	3.6
16:0	966.3	73.2	1761.8	1462.9	1015.9	99.9	887.7	0.0	370.8	23.0	350.6	55.4	1279.1	532.4	486.2	123.5	499.5	518.7	80.1
16:1(n-7)	197.6	29.7	334.8	185.1	253.0	0.2	504.1	0.2	78.3	25.8	76.5	4.4	107.4	112.2	65.1	23.2	47.6	21.6	1.1
16:2(n-4)	39.4	10.3	78.6	51.1	62.4	13.8	79.0	0.2	11.7	2.9	15.1	4.0	36.3	36.2	18.7	4.1	19.5	17.2	3.8
16:3(n-4)	49.0	10.5	92.7	55.9	44.3	3.3	28.1	0.1	9.0	1.6	8.4	0.7	9.5	8.7	9.8	5.7	9.1	1.9	0.6
16:4(n-3)	4.1	1.0	16.1	9.0	9.5	0.6	10.1	0.0	3.3	0.3	5.9	4.1	10.2	11.3	4.7	0.1	6.7	5.9	0.8
16:4(n-1)	46.2	15.8	92.4	57.5	51.2	14.1	45.4	0.0	10.0	0.0	10.3	0.1	22.5	24.3	9.2	3.0	6.0	4.2	1.5
18:0	550.2	28.9	1111.9	985.4	450.7	40.8	319.7	0.1	151.7	1.1	146.4	28.4	737.8	160.4	274.7	88.2	249.7	264.8	24.2
18:1(n-9)	125.6	23.0	173.3	8.6	222.5	3.7	167.0	0.1	63.1	3.4	87.7	6.0	112.7	112.5	48.2	9.5	51.5	39.2	1.8
18:1(n-7)	52.9	3.0	41.9	18.1	44.1	0.9	58.4	0.0	23.4	1.4	20.4	1.2	33.2	33.5	20.3	7.6	17.0	11.3	0.6
18:2(n-6)	46.7	9.2	106.3	11.6	54.1	5.7	81.2	0.3	26.8	0.5	65.9	23.5	56.9	41.7	23.1	2.0	26.4	19.1	5.1
18:3(n-6)	4.7	2.0	22.4	19.3	15.3	11.6	22.5	0.0	7.6	0.5	6.9	5.4	22.0	24.0	4.7	1.3	5.4	4.7	0.4
18:3(n-3)	16.5	3.6	10.8	8.5	18.9	5.6	20.6	0.0	12.3	0.5	20.6	3.3	10.8	9.7	4.5	0.4	3.0	1.7	0.3
18:4(n-3)	39.1	11.8	58.6	25.4	42.4	7.4	44.0	0.0	20.3	0.3	14.1	0.7	5.6	6.3	6.7	2.8	2.4	1.1	0.2
20:0	26.6	7.9	35.7	25.6	12.4	14.0	16.0	0.0	8.5	0.1	9.2	2.3	28.8	17.1	12.8	2.5	10.2	11.5	1.7
20:1(n-9)	11.9	2.3	8.9	5.6	9.8	5.3	19.9	0.1	21.4	1.2	6.7	2.8	8.1	8.7	6.2	2.1	11.9	12.9	0.1
20:1(n-7)	3.6	0.2	5.7	1.9	7.5	5.4	5.6	0.0	2.4	0.2	2.5	0.2	3.2	3.3	1.5	0.9	4.6	4.7	0.6
20:4(n-3)	6.2	0.5	7.6	2.7	5.3	0.1	20.1	0.0	5.1	0.4	4.5	0.1	11.9	12.4	3.8	1.3	7.9	6.1	0.2
20:4(n-6)	2.6	1.0	9.2	9.5	1.8	0.6	1.7	0.0	1.5	0.3	0.8	0.4	4.8	2.8	1.9	0.7	1.4	1.4	0.9
20:5(n-3)	97.8	24.0	168.6	82.0	132.9	38.5	182.4	0.1	51.3	4.9	53.1	0.3	61.3	66.2	34.9	9.4	24.7	22.1	1.4
22:6(n-3)	26.7	4.0	37.2	13.7	55.8	3.5	69.6	0.1	40.3	3.4	39.6	2.7	25.6	26.7	24.4	10.2	20.2	9.7	1.7
Total fatty acid	2449.9	232.8	4327.3	3119.2	2686.0	94.9	2866.3	0.9	981.6	71.3	1008.1	147.5	2712.1	1374.1	1110.1	302.3	1057.5	1010.5	90.4

Table C.16: Individual fatty acid percent composition for sediment trap samples collected from LY1 during 2016

	Percent composition of individual fatty acids in sediment trap samples (%)																			
	31/03/16		07/04/16		17/05/16		02/06/16		06/07/16		02/08/16		16/08/16		14/09/16		11/10/16		08/11/16	
	Av.	SD	Av.	SD	Av.	SD	Av.	SD	Av.	SD	Av.	SD	Av.	SD	Av.	SD	Av.	SD	Av.	SD
14:0	5.5	0.8	3.9	1.0	6.6	0.5	9.8	0.3	6.4	0.1	6.2	0.0	3.9	2.6	4.5	0.5	3.1	-	3.1	0.6
16:0	39.5	0.8	38.5	6.0	37.8	2.4	30.8	0.7	37.8	0.4	34.7	0.4	48.4	4.9	43.9	0.8	47.2	-	51.2	3.3
16:1(n-7)	8.0	0.4	8.4	1.8	9.4	0.3	17.6	0.1	7.9	2.1	7.6	0.7	3.3	2.4	5.8	0.5	4.5	-	2.2	0.3
16:2(n-4)	1.6	0.3	1.9	0.2	2.3	0.6	2.8	0.4	1.2	0.2	1.5	0.2	1.1	0.8	1.7	0.1	1.8	-	1.7	0.5
16:3(n-4)	2.0	0.2	2.3	0.3	1.6	0.1	1.0	0.2	0.9	0.2	0.8	0.2	0.3	0.2	0.8	0.3	0.9	-	0.2	0.0
16:4(n-3)	0.2	0.0	0.4	0.1	0.4	0.0	0.4	0.1	0.3	0.0	0.6	0.3	0.3	0.3	0.4	0.1	0.6	-	0.6	0.1
16:4(n-1)	1.9	0.5	2.2	0.3	1.9	0.6	1.6	0.6	1.0	0.1	1.0	0.2	0.7	0.5	0.8	0.0	0.6	-	0.4	0.2
18:0	22.6	3.3	23.6	5.7	16.8	0.9	11.0	0.7	15.5	1.0	14.5	0.7	29.5	9.0	24.6	1.3	23.6	-	26.2	0.0
18:1(n-9)	5.1	0.5	5.3	3.6	8.3	0.4	5.9	03	6.4	0.1	8.7	0.7	3.6	2.3	4.4	0.3	4.9	-	3.9	0.5
18:1(n-7)	2.2	0.1	1.1	0.4	1.6	0.0	2.0	0.0	2.4	0.0	2.0	0.2	1.0	0.7	1.8	0.2	1.6	-	1.1	0.2
18:2(n-6)	1.9	0.2	3.2	2.0	2.0	0.1	3.0	0.7	2.7	0.3	6.4	1.4	2.0	0.5	2.2	0.8	2.5	-	1.9	0.7
18:3(n-6)	0.2	0.1	0.5	0.1	0.6	0.4	0.8	0.1	0.8	0.1	0.7	0.4	0.7	0.5	0.4	0.0	0.5	-	0.5	0.0
18:3(n-3)	0.7	0.1	0.2	0.0	0.7	0.2	0.7	0.0	1.3	0.0	2.0	0.0	0.4	0.2	0.4	0.1	0.3	-	0.2	0.0
18:4(n-3)	1.6	0.3	1.5	0.5	1.6	0.3	1.5	0.0	2.1	0.2	1.4	0.1	0.2	0.1	0.6	0.1	0.2	-	0.1	0.0
20:0	1.1	0.2	0.8	0.0	0.5	0.5	0.6	0.0	0.9	0.1	0.9	0.1	1.0	0.1	1.2	0.1	1.0	-	1.1	0.1
20:1(n-9)	0.5	0.0	0.2	0.0	0.4	0.2	0.7	0.2	2.2	0.0	0.7	0.4	0.3	0.2	0.6	0.0	1.1	-	1.3	.01
20:1(n-7)	0.1	0.0	0.2	0.1	0.3	0.2	0.2	0.0	0.2	0.0	0.3	0.0	0.1	0.1	0.1	0.0	0.4	-	0.5	0.1
20:4(n-3)	0.3	0.0	0.2	0.1	0.2	0.0	0.7	0.1	0.5	0.0	0.4	0.1	0.4	0.3	0.3	0.0	0.7	-	0.6	0.0
20:4(n-6)	0.1	0.1	0.2	0.1	0.1	0.0	0.1	0.0	0.1	0.0	0.1	0.0	0.2	0.0	0.2	0.0	0.1	-	0.1	0.1
20:5(n-3)	4.0	0.6	4.3	1.2	5.0	1.6	6.4	0.2	5.2	0.1	5.3	0.8	1.9	1.5	3.1	0.0	2.3	-	2.2	0.1
22:6(n-3)	1.1	0.1	1.0	0.4	2.1	0.2	2.5	0.3	4.1	0.1	3.9	0.3	0.8	0.6	2.2	0.3	1.9	-	1.0	0.1
SFAs	68.7		66.9		61.6		52.2		60.5		56.4		82.9		74.1		74.9		81.6	
MUFA	15.9		15.2		20.0		26.4		19.2		19.4		8.3		12.7		12.5		8.9	
PUFA	15.4		18.0		18.4		21.4		20.3		24.3		8.8		13.2		12.5		9.5	

Table C.17: Concentration (μg g^{-1}) of individual fatty acids from sediments collected from LY1 during 2016

	Sediment fatty acid concentration (μg g^{-1})										
	06/04/16	16/05/16	01/06/16	06/07/16	19/07/16	01/08/16	15/08/16	30/08/16	13/09/16	10/10/16	07/11/16
14:0	0.4	2.1	2.5	4.2	1.5	2.9	1.1	2.9	0.9	0.8	1.2
16:0	1.7	8.5	7.6	11.0	8.8	10.4	7.2	11.8	3.8	5.5	6.3
16:1(n-7)	1.2	5.3	5.2	9.5	4.6	6.6	2.7	7.6	2.5	2.4	3.8
16:2(n-4)	0.2	0.8	0.9	1.2	0.9	0.7	0.3	0.7	0.2	0.2	0.3
16:3(n-4)	0.1	0.7	0.8	1.2	0.3	0.5	0.2	0.7	0.2	0.2	0.1
16:4(n-3)	0.0	0.1	0.2	0.2	0.1	0.2	0.1	0.3	0.1	0.1	0.1
16:4(n-1)	0.1	0.3	0.5	0.6	0.1	0.3	0.1	0.2	0.1	0.1	0.1
18:0	0.8	4.0	2.4	2.9	3.2	4.8	3.6	4.3	1.3	3.0	3.3
18:1(n-9)	0.4	1.2	2.3	3.1	1.4	2.1	2.5	5.0	1.8	1.5	1.5
18:1(n-7)	0.7	2.0	2.6	3.6	2.4	2.6	1.5	3.1	1.0	1.2	1.6
18:2(n-6)	0.1	0.5	0.5	0.7	0.7	0.8	0.6	1.0	0.3	0.4	0.3
18:3(n-6)	0.0	0.1	0.1	0.1	0.1	0.1	0.1	0.1	0.1	0.1	0.1
18:3(n-3)	0.0	0.2	0.2	0.3	0.2	0.2	0.1	0.3	0.1	0.1	0.2
18:4(n-3)	0.0	0.4	0.5	0.7	0.2	0.3	0.1	0.3	0.1	0.1	0.1
20:0	0.3	0.9	0.9	1.0	0.9	1.0	0.6	1.1	0.4	0.7	1.0
20:1(n-9)	0.0	0.2	0.3	0.2	0.2	0.2	0.3	0.6	0.3	0.1	0.3
20:1(n-7)	0.0	0.1	0.2	0.2	0.2	0.3	0.1	0.7	0.3	0.1	0.2
20:4(n-3)	0.2	0.7	1.1	1.8	0.8	0.6	0.4	1.0	0.5	0.2	0.4
20:4(n-6)	0.0	0.1	0.1	0.2	0.1	0.1	0.1	0.1	0.0	0.0	0.0
20:5(n-3)	0.2	1.6	2.8	4.0	1.3	2.3	0.8	2.1	1.0	0.2	0.8
22:6(n-3)	0.1	0.5	0.9	1.1	0.2	0.8	0.1	0.8	0.3	0.1	0.3
Total fatty acid	6.5	30.1	32.7	47.7	28.2	37.7	22.5	44.8	15.4	17.1	22.0

Table C.18: Individual fatty acid percent composition for sediment samples collected from LY1 during 2016

	Percent composition of individual fatty acids in sediments (%)									
	06/04/16	16/05/16	01/06/16	05/07/16	19/07/16	01/08/16	15/08/16	13/09/16	10/10/16	07/11/16
14:0	6.7	6.9	7.8	8.7	5.5	7.6	4.7	6.0	4.9	5.5
16:0	26.4	28.2	23.3	23.0	31.2	27.5	31.8	25.0	32.2	28.6
16:1(n-7)	17.6	17.8	16.0	19.9	16.2	17.6	12.0	16.2	14.0	17.1
16:2(n-4)	2.4	2.7	2.7	2.5	3.1	1.8	1.3	1.3	1.0	1.2
16:3(n-4)	2.0	2.3	2.6	2.6	1.2	1.3	1.0	1.6	1.4	0.7
16:4(n-3)	0.2	0.3	.5	0.4	0.4	0.4	0.4	.4	0.5	0.5
16:4(n-1)	0.8	1.0	1.4	1.3	0.5	0.8	0.4	0.5	0.3	0.4
18:0	11.7	13.3	7.2	6.1	11.3	12.6	15.9	8.6	17.5	14.9
18:1(n-9)	5.5	4.1	6.9	6.5	4.8	5.6	11.3	11.7	9.0	6.8
18:1(n-7)	10.3	6.7	7.9	7.5	8.5	6.8	6.6	6.8	7.1	7.1
18:2(n-6)	1.2	1.5	1.5	1.4	2.5	2.1	2.8	2.0	2.4	1.6
18:3(n-6)	0.5	0.3	0.4	0.3	0.4	0.3	0.3	.4	0.4	0.4
18:3(n-3)	0.7	.5	0.7	0.6	0.6	0.4	0.5	.8	0.6	0.8
18:4(n-3)	0.6	1.2	1.5	1.4	0.7	0.8	0.5	0.9	0.5	0.6
20:0	4.0	3.1	2.8	2.1	3.1	2.7	2.8	2.7	3.9	4.4
20:1(n-9)	0.7	0.5	1.1	0.5	0.8	0.5	1.2	1.7	0.9	1.5
20:1(n-7)	0.2	0.3	0.7	0.4	0.7	0.8	0.6	1.7	0.6	0.9
20:4(n-3)	2.6	2.2	3.4	3.8	2.7	1.7	1.8	3.2	0.9	2.0
20:4(n-6)	0.3	0.4	0.4	0.4	0.4	0.3	0.3	0.3	0.1	0.2
20:5(n-3)	3.7	5.2	8.5	8.3	4.7	6.0	3.4	6.2	1.4	3.5
22:6(n-3)	1.7	1.7	2.7	2.4	0.7	2.1	0.3	2.2	0.3	1.3
SFAs	48.8	51.4	41.1	39.9	51.1	50.5	55.2	42.3	58.6	53.4
MUFA	34.4	29.3	32.7	34.8	31.0	31.3	31.7	38.1	31.6	33.4
PUFA	16.8	19.3	26.3	25.3	17.9	18.2	13.1	19.6	9.8	13.2

Appendix D

Determining the reactivity of the suspended versus sinking fraction of particulate organic material

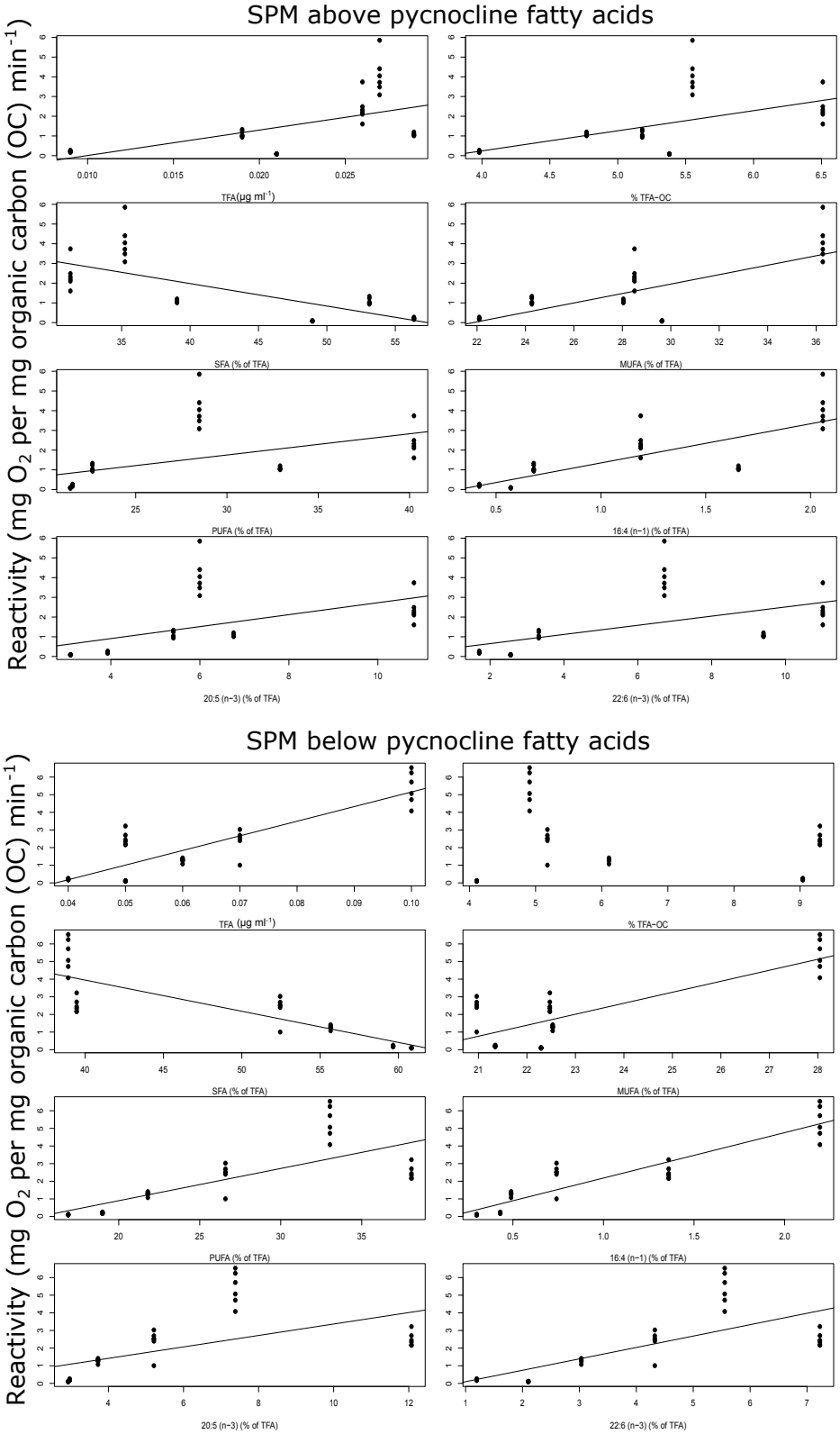

Figure D.1: Correlation analysis between reactivity and total fatty acids (TFA), percentage of organic carbon presented as TFA, saturated fatty acids (SFA), monounsaturated fatty acids (MUFA), polyunsaturated fatty acids (PUFA), and individual fatty acids from suspended particulate material (SPM) from above and below the pycnocline at LY1

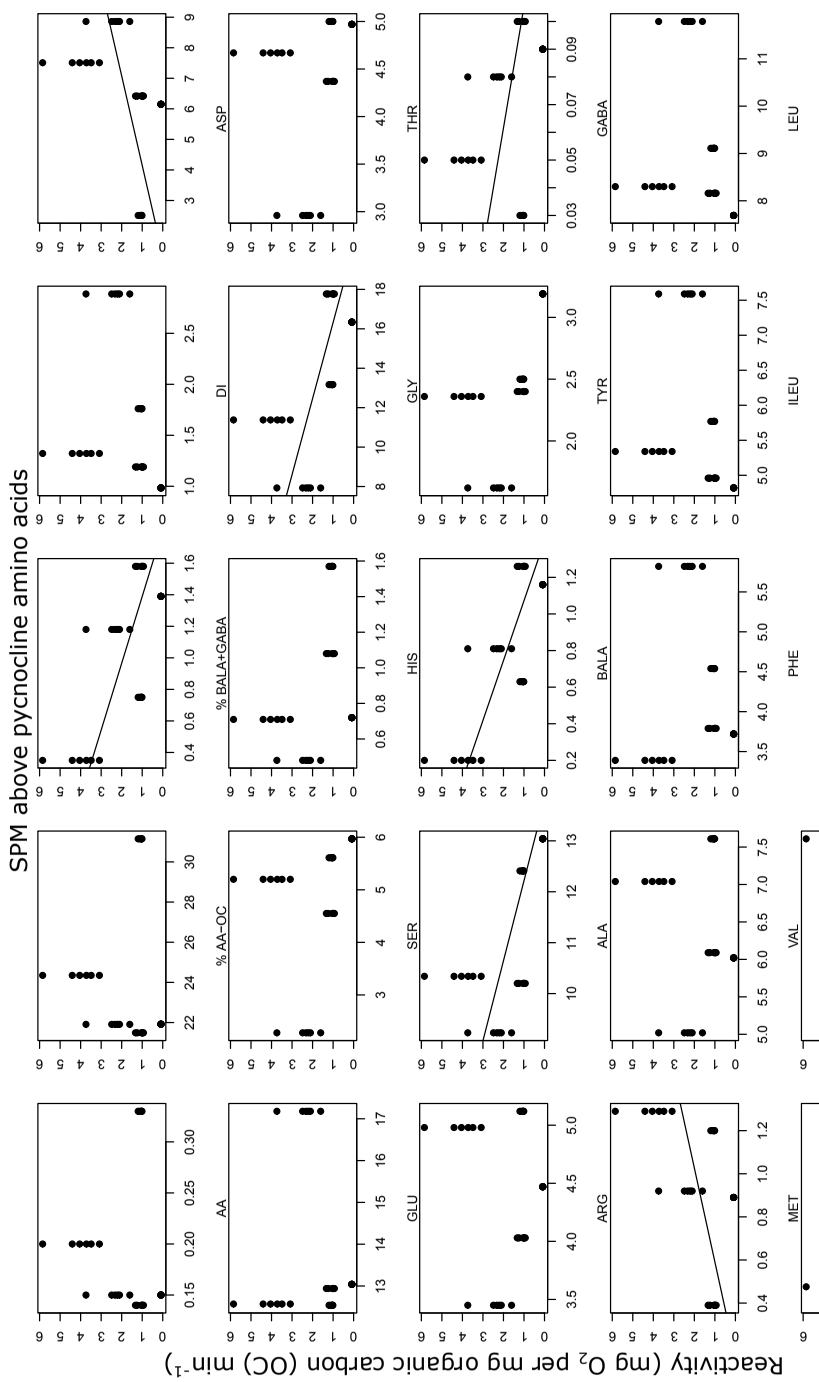

Figure D.2: Correlation analysis between reactivity and amino acids (AA), percentage of organic carbon presented as AA, percentage of BALA plus GABA, degradation index (DI), and individual amino acids from SPM from above the pycnocline at LY1

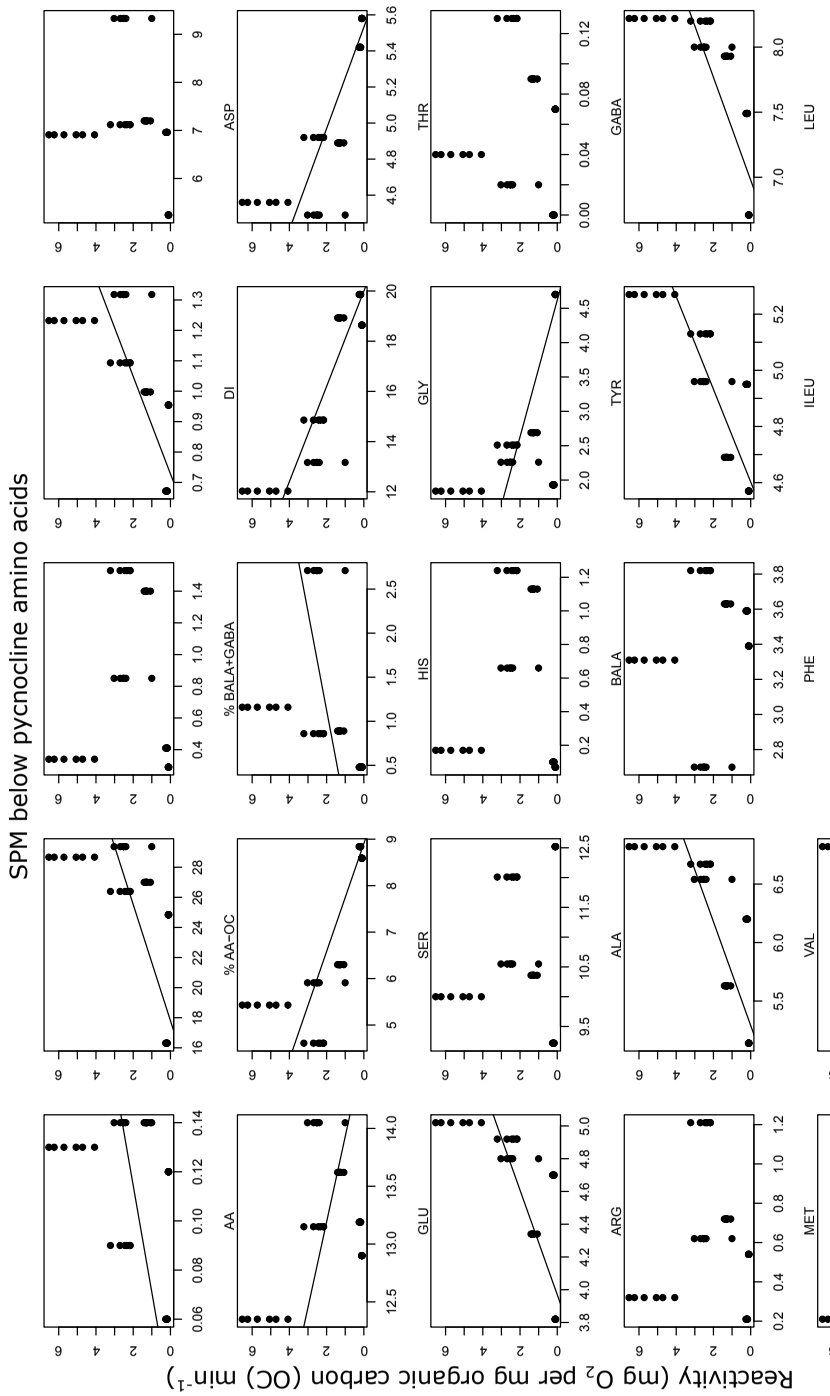

Figure D.3: Correlation analysis between reactivity and amino acids (AA), percentage of organic carbon presented as AA, percentage of BALA plus GABA, degradation index (DI), and individual amino acids from SPM from below the pycnocline at LY1

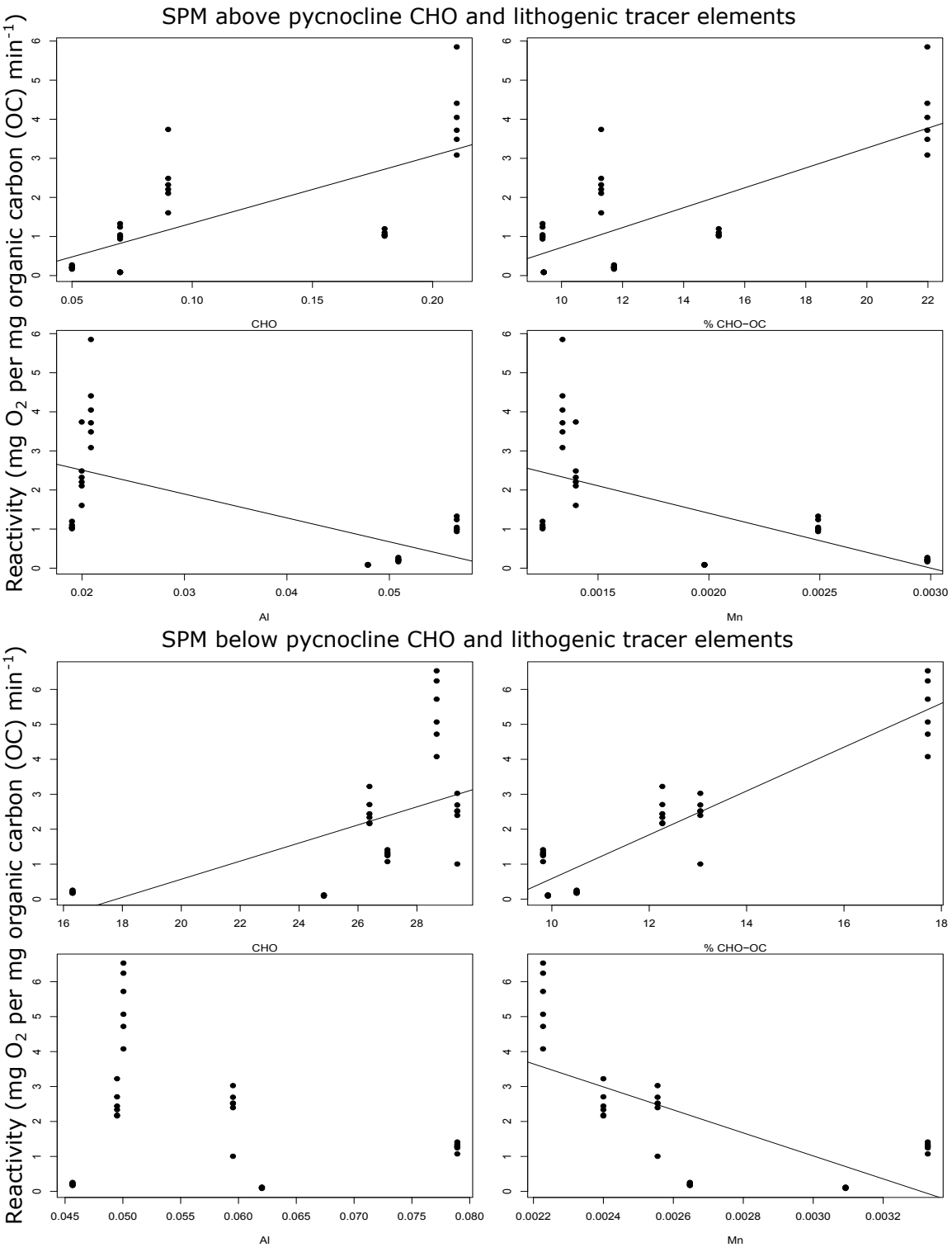

Figure D.4: Correlation analysis between reactivity and carbohydrate (CHO), percentage of organic carbon presented as CHO, and lithogenic tracer elements (Al and Mn) from SPM from below the pycnocline at LY1

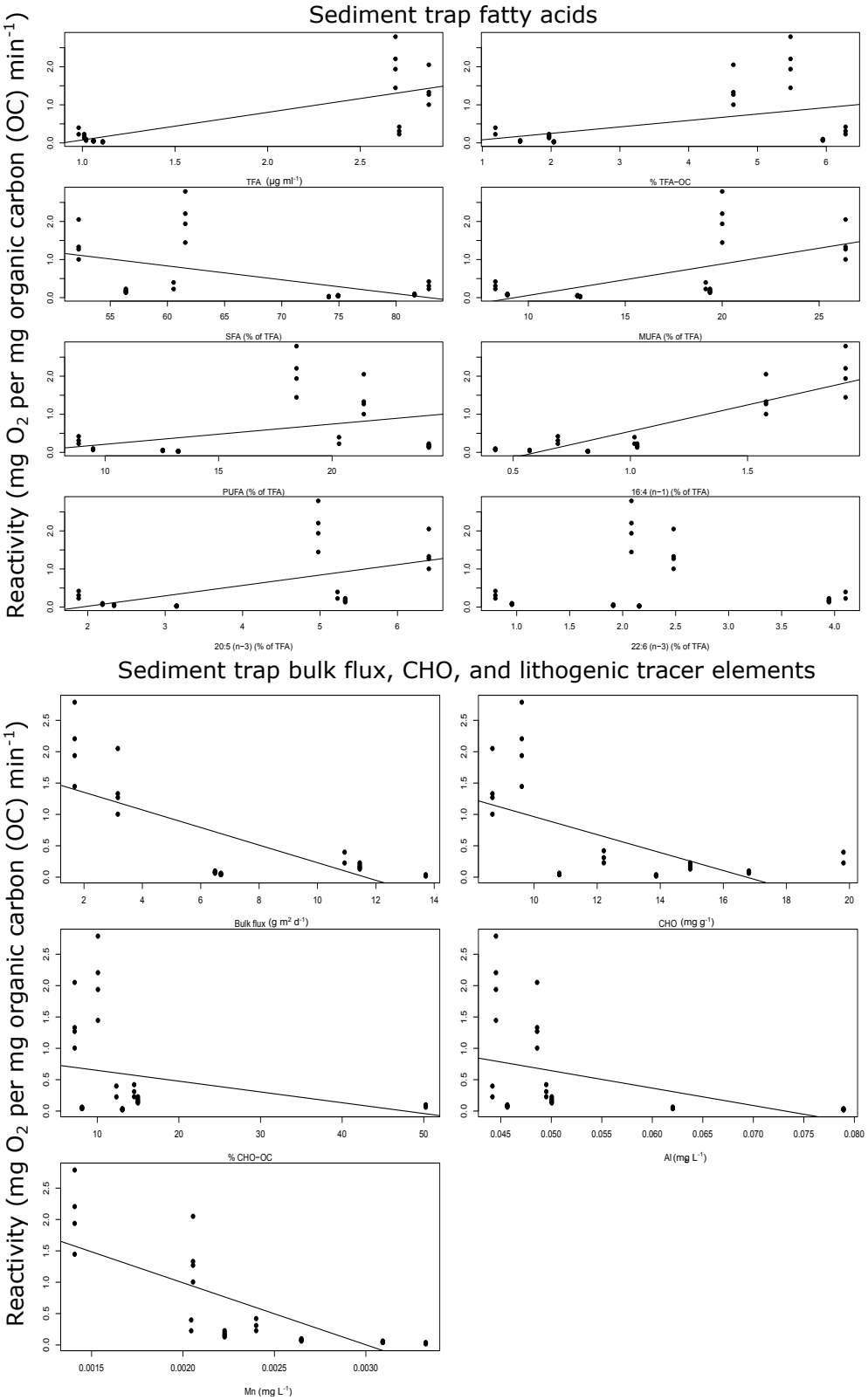

Figure D.5: Correlation analysis between reactivity and total fatty acids (TFA), percentage of organic carbon presented as TFA, saturated fatty acids (SFA), monounsaturated fatty acids (MUFA), polyunsaturated fatty acids (PUFA), individual fatty acids, bulk flux, carbohydrate (CHO), percentage of organic carbon presented as CHO, and lithogenic tracer elements (Al and Mn) from sediment trap material sampled from LY1

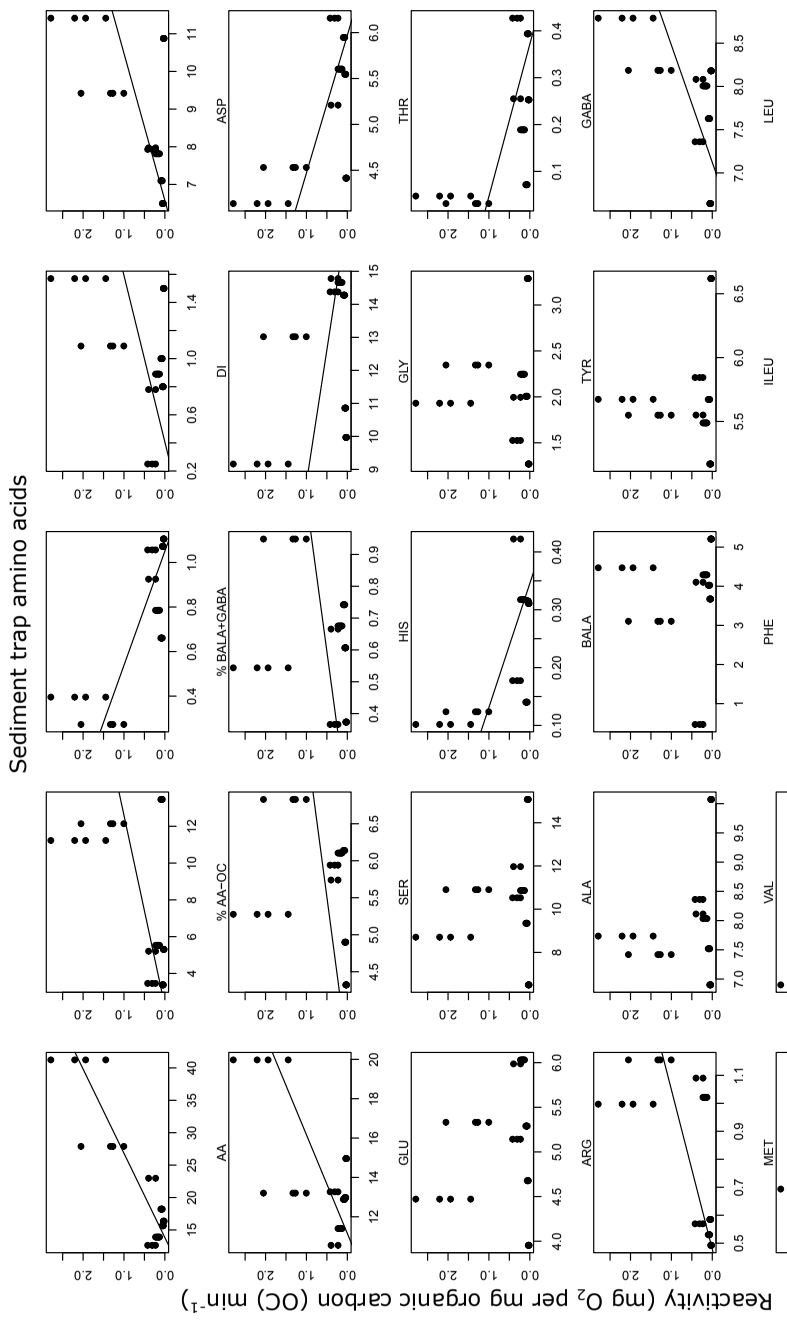

Figure D.6: Correlation analysis between reactivity and amino acids (AA), percentage of organic carbon presented as AA, percentage of BALA plus GABA, degradation index (DI), and individual amino acids from sediment trap material sampled from LY1

Bibliography

Alonso-González, I. J., Arístegui, J., Lee, C., and Calafat, A. (2010). Regional and temporal variability of sinking organic matter in the subtropical northeast Atlantic Ocean: a biomarker diagnosis. *Biogeosciences*, 7:2101–2115.

Alonso-Gonzalez, I. J., Aristegui, J., Lee, C., Sanchez-Vidal, A., Calafat, A., Fabres, J., Sangra, P., Masque, P., Hernandez-Guerra, A., and Benitez-Barrios, V. (2010). Role of slowly settling particles in the ocean carbon cycle. *Geophysical Research Letters*, 37:1–5.

Ansell, A. D. (1974). Sedimentation of organic detritus in Lochs Etive and Creran, Argyll, Scotland. *Marine Biology*, 27:263–273.

Armstrong, R. A., Lee, C., Hedges, J. I., Honjo, S., and Wakeham, S. G. (2002). A new, mechanistic model for organic carbon fluxes in the ocean based on the quantitative association of POC with ballast minerals. *Deep-Sea Research Part II: Topical Studies in Oceanography*, 49:219–236.

Arnarson, T. S. and Keil, R. G. (2005). Influence of organic-mineral aggregates on microbial degradation of the dinoflagellate *Scrippsiella trochoidea*. *Geochimica et Cosmochimica Acta*, 69(8):2111–2117.

Arnarson, T. S. and Keil, R. G. (2007). Changes in organic matter-mineral interactions for marine sediments with varying oxygen exposure times. *Geochimica et Cosmochimica Acta*, 71(14):3545–3556.

Arrigo, K. R. (2005). Marine microorgansisms and global nutrient cycles. *Nature*, 437:349–355.

Austin, W. E. N. and Inall, M. E. (2002). Deep-water renewal in a Scottish fjord: Temperature, salinity and oxygen isotopes. *Polar Research*, 21(2):251–258.

Bach, L. T., Boxhammer, T., Larsen, A., Hildebrandt, N., Schulz, K. G., and Riebesell, U. (2016). Influence of plankton community structure on the sinking velocity of marine aggregates. *Global Biogeochemical Cycles*, 30(8):1145–1165.

Baker, C. A., Henson, S. A., Cavan, E. L., Giering, S. L. C., Yool, A., Gehlen, M., Belcher, A., Riley, J. S., Smith, H. E. K., and Sanders, R. (2017). Slow-sinking particulate organic carbon in the Atlantic Ocean: Magnitude, flux, and potential controls. *Global Biogeochemical Cycles*, 31:1051–1065.

Balzano, S., Pancost, R. D., Lloyd, J. R., and Statham, P. J. (2011). Changes in fatty acid composition in degrading algal aggregates. *Marine Chemistry*, 124:2–13.

Bannon, C. C. and Campbell, D. A. (2017). Sinking towards destiny: High throughput measurement of phytoplankton sinking rates through time-resolved fluorescence plate spectroscopy. *PLoS ONE*, 12(10):1–16.

Bauer, J. E., Cai, W. J., Raymond, P. A., Bianchi, T. S., Hopkinson, C. S., and Regnier, P. A. G. (2013). The changing carbon cycle of the coastal ocean. *Nature*, 504:61–70.

Beaulieu, S. E. (2002). Accumulation and fate of phytodetritus on the seafloor. *Oceanography and Marine Biology: an Annual Review*, 40:171–232.

Benner, R. (2004). What happens to terrestrial organic matter in the ocean? *Marine Chemistry*, 92:307–310.

Bergkvist, J., Thor, P., Jakobsen, H. H., Wängberg, S. Å., and Selander, E. (2012). Grazer-induced chain length plasticity reduces grazing risk in a marine diatom. *Limnology and Oceanography*, 57(1):318–324.

Berner, R. A. (1989). Global biogeochemical cycles of carbon and sulfur and their effect on atmospheric oxygen over phanerozoic time. *Palaeogeography, Palaeoclimatology, Palaeoecology*, 75:97–122.

Berx, B., Gallego, A., Heath, M., and The MASTS Community (2015). Loch Linnhe and Firth of Lorn MASTS Case Study Workshop Report. Technical Report 1.

Bianchi, T. S. (2011). The role of terrestrially derived organic carbon in the coastal ocean: A changing paradigm and the priming effect. *Proceedings of the National Academy of Sciences*, 108(49):19473–19481.

Bienfang, P., Szyper, J., and Laws, E. (1983). Sinking rate and pigment responses to light-limitation of a marine diatom: implications to dynamics of chlorophyll maximum layers. *Oceanologica Acta*, 6(82):55–62.

Bienfang, P. K. (1980). Phytoplankton sinking rates in oligotrophic waters off Hawaii, USA. *Marine Biology*, 61:69–77.

Bienfang, P. K. (1981a). SETCOL - A technological simple and reliable method for measuring phytoplankton sinking rates. *Canadian Journal of Fisheries and Aquatic Sciences*, 38:1289–1294.

Bienfang, P. K. (1981b). Sinking rates of heterogenous, temperate phytoplankton populations. *Journal of Plankton Research*, 3(2):235–253.

Bienfang, P. K. and Harrison, P. J. (1984). Sinking-rate response of natural assemblages of temperate and subtropical phytoplankton to nutrient depletion. *Marine Biology*, 83:293–300.

Bienfang, P. K., Harrison, P. J., and Quarmby, L. M. (1982). Sinking rate response to depletion of nitrate, phosphate and silicate in four marine diatoms. *Marine biology*, 302:295–302.

Billett, D. S. M., Lampitt, R. S., Rice, A. L., and Mantoura, R. F. C. (1983). Seasonal sedimentation of phytoplankton to the deep-sea benthos. *Nature*, 302:520–522.

BjÆrke, O., Jonsson, P. R., Alam, A., and Selander, E. (2015). Is chain length in phytoplankton regulated to evade predation? *Journal of Plankton Research*, pages 1–10.

Boëchat, I. G. and Giani, A. (2000). Factors affecting biochemical composition of seston in an eutrophic reservoir (Pampulha Reservoir, Belo Horizonte, MG). *Revista Brasileira de Biologia*, 60(1):63–71.

Boyd, P. W. (2015). Toward quantifying the response of the oceans' biological pump to climate change. *Frontiers in Marine Science*, pages 1–15.

Boyd, P. W., McDonnell, A., Valdez, J., LeFevre, D., and Gall, M. P. (2015). RESPIRE: An in situ particle interceptor to conduct particle remineralization and microbial dynamics studies in the

oceans' Twilight Zone. *Limnology and Oceanography: Methods*, 13:494–508.

Bravo, I. and Figueroa, R. I. (2014). Towards an Ecological Understanding of Dinoflagellate Cyst Functions. *Microorganisms*, 2:11–32.

Brito, A. C., Sá, C., Mendes, C. R., Brand, T., Dias, A. M., Brotas, V., and Davidson, K. (2015). Structure of late summer phytoplankton community in the Firth of Lorn (Scotland) using microscopy and HPLC-CHEMTAX. *Estuarine, Coastal and Shelf Science*, 167:86–101.

Brown, F. S., Baedecker, M. J., Nissenbaum, A., and Kaplan, I. R. (1972). Early diagenesis in a reducing fjord, Saanich Inlet, British Columbia-III. Changes in organic constituents of sediments. *Geochimica et Cosmochimica Acta*, 36:1185–1203.

Budge, S. M. and Parrish, C. C. (1998). Lipid biogeochemistry of plankton, settling matter and sediments in Trinity Bay, Newfoundland: II. Fatty acids. *Organic Geochemistry*, 29(5):1547–1559.

Budge, S. M., Parrish, C. C., and Mckenzie, C. H. (2001). Fatty acid composition of phytoplankton, settling particulate matter and sediments at a bivalve culture site. *Marine Chemistry*, 76:285–303.

Buesseler, K. O. (1998). The decoupling of production and particle export in the surface ocean. *Global Biogeochemical Cycles*, 12(2):297–310.

Buesseler, K. O., Antia, A. N., Chen, M., Fowler, S. W., Gardner, W. D., Gustafsson, O., Harada, K., Michaels, A. F., van der Loeff, M. R., Sarin, M., Steinberg, D. K., and Trull, T. (2007). An assessment of the use of sediment traps for estimating upper ocean particle fluxes. *Journal of Marine Research*, 65:345–416.

Buesseler, K. O. and Boyd, P. W. (2009). Shedding light on processes that control particle export and flux attenuation in the twilight zone of the open ocean. *Limnology and Oceanography*, 54(4):1210–1232.

Burd, A. B., Buchan, A., Church, M., Landry, M., McDonnell, A., Passow, U., Steinberg, D., and Benway, H. (2016). Towards a transformative understanding of the ocean's biological pump: Priorities for future research. *Report of the NSF Biology of the Biological Pump Workshop, February 19-20, 2016*, page 67.

Burd, A. B. and Jackson, G. A. (2009). Particle aggregation. *Annual review of marine science*, 1:65–90.

Burdige, D. J. (2005). Burial of terrestrial organic matter in marine sediments: A re-assessment. *Global Biogeochemical Cycles*, 19:1–7.

Calbet, A. and Landry, M. R. (2004). Phytoplankton growth, microzooplankton grazing, and carbon cycling in marine systems. *Limnology and Oceanography*, 49(1):51–57.

Callaway, R., Shinn, A. P., Grenfell, S. E., Bron, J. E., Burnell, G., Cook, E. J., Crumlish, M., Culloty, S., Davidson, K., Ellis, R. P., Flynn, K. J., Fox, C., Green, D. M., Hays, G. C., Hughes, A. D., Johnston, E., Lowe, C. D., Lupatsch, I., Malham, S., Mendzil, A. F., Nickell, T., Pickerell, T., Rowley, A. F., Stanley, M. S., Tocher, D. R., Turnbull, J. F., Webb, G., Wootton, E., and Shields, R. J. (2012). Review of climate change impacts on marine aquaculture in the UK and Ireland. *Aquatic Conservation: Marine and Freshwater Ecosystems*, 22(3):389–421.

Carr, S. A., Mills, C. T., and Mandernack, K. W. (2016). The use of amino acid indices for assessing organic matter quality and microbial abundance in deep-sea Antarctic sediments of

IODP Expedition 318. *Marine Chemistry*, 186:72–82.

Cavan, E. L., Giering, S. L., Wolff, G. A., Trimmer, M., and Sanders, R. (2018). Alternative Particle Formation Pathways in the Eastern Tropical North Pacific's Biological Carbon Pump. *Journal of Geophysical Research: Biogeosciences*, (7):2198–2211.

Cavan, E. L., Trimmer, M., Shelley, F., and Sanders, R. (2017). Remineralization of particulate organic carbon in an ocean oxygen minimum zone. *Nature Communications*, 8:1–9.

Christie, W. W. (1982). A simple procedure for rapid transmethylation of glycerolipids and cholesteryl esters. *Journal Of Lipid Research*, 23:1072–1075.

Cohen, R. R. H. (1985). Physical processes and the ecology of a winter dinoflagellate bloom of *Katodinium rotundatum*. *Marine Ecology Progress Series*, 26:135–144.

Conte, M. H., Ralph, N., and Ross, E. H. (2001). Seasonal and interannual variability in deep ocean particle fluxes at the Oceanic Flux Program (OFP)/Bermuda Atlantic Time Series (BATS) site in the western Sargasso Sea near Bermuda. *Deep-Sea Research Part II: Topical Studies in Oceanography*, 48(8-9):1471–1505.

Cowie, G. L. and Hedges, J. I. (1984). Carbohydrate sources in a coastal marine environment. *Geochimica et Cosmochimica Acta*, 48:2075–2087.

Cowie, G. L. and Hedges, J. I. (1992a). Improved amino acid quantification in environmental samples: charge-matched recovery standards and reduced analysis time. *Marine Chemistry*, 37:223–238.

Cowie, G. L. and Hedges, J. I. (1992b). Sources and reactivities of amino acids in a coastal marine environment. *Limnology and Oceanography*, 37(4):703–724.

Cowie, G. L. and Hedges, J. I. (1994). Biochemcial indicators of diagenetic alteration in natural organic matter mixtures. *Nature*, 369:304–307.

Cowie, G. L. and Hedges, J. I. (1996). Digestion and alteration of the biochemical constituents of a diatom (*Thalassiosira weissflogii*) ingested by an herbivorous zooplankton (*Calanus pacificus*). *Limnology and Oceanography*, 41(4):581–594.

Cowie, G. L., Hedges, J. I., and Calvert, S. E. (1992). Sources and reactivities of amino acids in an intermittently anoxic marine environment. *Geochimica et Cosmochimica Acta*, 37(4):703–724.

Cripps, G. C. and Clarke, A. (1998). Seasonal variation in the biochemical composition of particulate material collected by sediment traps at Signy Island, Antarctica. *Polar Biology*, 20:414–423.

Culver, M. E. and Smith, W. O. J. (1989). Effects of environmental variation on sinking rates of marine phytoplanton. *Journal of Phycology*, 25:262–270.

Dale, A. C., Boulcott, P., and Sherwin, T. J. (2011). Sedimentation patterns caused by scallop dredging in a physically dynamic environment. *Marine Pollution Bulletin*, 62:2433–2441.

Dall'Olmo, G. and Mork, K. A. (2014). Carbon export by small particles in the Norwegian Sea. *Geophysical Research Letters*, 41:2921–2927.

Daniels, C. J., Poulton, A. J., Esposito, M., Paulsen, M. L., Bellerby, R., St John, M., and Martin, A. P. (2015). Phytoplankton dynamics in contrasting early stage North Atlantic spring blooms: composition, succession, and potential drivers. *Biogeosciences*, 12:2395–2409.

Dauwe, B. and Middelburg, J. J. (1998). Amino acids and hexosamines as indicators of organic matter degradation state in North Sea sediments. *Limnology and Oceanography*, 43(5):782–798.

Dauwe, B., Middelburg, J. J., Herman, P. J., and Heip, C. H. R. (1999). Linking diagenetic alteration of amino acids and bulk organic matter reactivity. *Limnology and Oceanography*, 44(7):1809–1814.

Davies, J. M. (1975). Energy flow through the benthos in a Scottish Sea Loch. *Marine Biology*, 31:353–362.

Davis, C. E., Blackbird, S., Wolff, G., Woodward, M., and Mahaffey, C. (2018). Seasonal organic matter dynamics in a temperate shelf sea. *Progress in Oceanography*, (In Press).

De Haas, H., Van Weering, T. C. E., and De Stigter, H. (2002). Organic carbon in shelf seas: sinks or sources, processes and products. *Continental Shelf Research*, 22:691–717.

de Jesus Mendes, P. A. and Thomsen, L. (2012). Effects of ocean acidification on the ballast of surface aggregates sinking through the twilight zone. *PloS one*, 7(12):e50865.

De La Rocha, C. L. and Passow, U. (2007). Factors influencing the sinking of POC and the efficiency of the biological carbon pump. *Deep Sea Research Part II: Topical Studies in Oceanography*, 54(5-7):639–658.

Dell'aquila, G., Ferrante, M. I., Gherardi, M., Cosentino, L. M., D'Alcalà, M. R., Iudicone, D., and Amato, A. (2017). Nutrient consumption and chain tuning in diatoms exposed to storm-like turbulence. *Scientific Reports*, 7:1–11.

Diekmann, A. B. S., Peck, M. A., Holste, L., St John, M. A., and Campbell, R. W. (2009). Variation in diatom biochemical composition during a simulated bloom and its effect on copepod production. *Journal of Plankton Research*, 31(11):1391–1405.

Dubois, M., Gilles, K. A., Hamilton, J. K., Rebers, P. A., and Smith, F. (1956). Colorimetric method for determination of sugars and related substances. *Analytical Chemistry*, 28:350–356.

Dugdale, R. C. and Wilkerson, F. P. (1998). Silicate regulation of new production in the equatorial Pacific upwelling. *Nature*, 391:270–273.

Durkin, C. A., Estapa, M. L., and Buesseler, K. O. (2015). Observations of carbon export by small sinking particles in the upper mesopelagic. *Marine Chemistry*, 175:72–81.

Durkin, C. A., Van Mooy, B. A. S., Dyhrman, S. T., and Buesseler, K. O. (2016). Sinking phytoplankton associated with carbon flux in the Atlantic Ocean. *Limnology and Oceanography*, 61:1172–1187.

Edwards, A. and Edelsten, D. J. (1977). Deep water renewal of Loch Etive: A three basin Scottish fjord. *Estuarine and Coastal Marine Science*, 5(5):575–595.

Edwards, A. and Sharples, F. (1985). Scottish Sea Lochs: A catalogue. *Scottish Marine Biological Association Special Issue*, 134:110 pp.

Ellet, D. J. and Edwards, A. (1983). Oceanography and inshore hydrography of the Inner Hebrides. *Proceedings of the Royal Society of Edinburgh*, 83B:143–160.

Emerson, S. and Hedges, J. I. (1988). Process contolling the organic carbon content of open ocean sediments. *Palaeogeography*, 3(5):621–634.

Eppley, R. W., Holmes, R. W., and Strickland, J. D. H. (1967). Sinking rates of marine phytoplankton measured with a fluorometer. *Journal of Experimental Marine Biology and Ecology*, I:191–208.

Erga, S. R., Lie, G. C., Aarø, L. H., Aursland, K., Olseng, C. D., Frette, Ø., and Hamre, B. (2010). Fine scale vertical displacement of *Phaeodactylum tricornutum* (Bacillariophyceae) in stratified

waters: Influence of halocline and day length on buoyancy control. *Journal of Experimental Marine Biology and Ecology*, 384(1-2):7–17.

Erga, S. R., Lie, G. C., Aarø, L. H., Frette, Ø., and Hamre, B. (2015). Migratory behaviour of *Skeletonema grethae* (Bacillariophyceae) in stratified waters. *Diatom Research*, 30(1):13–25.

Falkowski, P. G., Katz, M. E., Knoll, A. H., Quigg, A., Raven, J. A., Schofield, O., and Taylor, F. J. R. (2004). The Evolution of Modern Eukaryotic. *Science*, 305(July):354–360.

Falkowski, P. G., Laws, E. A., Barber, R. T., and Murray, J. W. (2003). Phytoplankton and their role in primary, new, and export production. In *Ocean Biogeochemistry*, pages 99–108. Springer-Verlag Berlin Heidelberg.

Fehling, J., Davidson, K., Bolch, C., and Tett, P. (2006). Seasonality of *Pseudo-nitzschia* spp. (Bacillariophyceae) in western Scottish waters. *Marine Ecology Progress Series*, 323:91–105.

Fenchel, T. and Jonsson, P. R. (1988). The functional biology of *Strombidium sulcatum*, a marine oligotrich ciliate (Ciliophora, Oligotrichina). *Marine Ecology Progress Series*, 48:1–15.

Field, C. B., Behrenfeld, M. J., Randerson, J. T., Falkowski, P., Field, C. B., Behrenfeld, M. J., and Randerson, J. (1998). Primary Production of the Biosphere: Integrating Terrestrial and Oceanic Components. *Science*, 281:237–240.

Fileman, T. W., Pond, D. W., Barlow, R. G., and Mantoura, R. F. C. (1998). Vertical profiles of pigments, fatty acids and amino acids: Evidence for undegraded diatomaceous material sedimenting to the deep ocean in the Bellingshausen Sea, Antarctica. *Deep Sea Research Part I: Oceanographic Research Papers*, 45:333–346.

Finkel, Z. V., Beardall, J., Flynn, K. J., Quigg, A., Rees, T. A. V., and Raven, J. A. (2010). Phytoplankton in a changing world : cell size and elemental stoichiometry. *Journal of Plankton Research*, 32:119–137.

Fisher, A. E. and Harrison, P. J. (1996). Does carbohydrate content affect the sinking rates of marine diatoms. *Journal of Phycology*, 32:360–365.

Folch, J., Lees, M., and Sloane Stanley, G. H. (1957). A simple method for the isolation and purification of total lipides from animal tissue. *Journal of Biological Chemistry*, 226:497–509.

Fortier, L. and Legget, W. C. (1982). Fickian transport and the dispersal of fish larvae in estuaries. *Canadian Journal of Fisheries and Aquatic Science*, 39:1150–1163.

Fragoso, G. M., Poulton, A. J., Yashayaev, I. M., Head, E. J., Stinchcombe, M., and Purdie, D. A. (2016). Biogeographical patterns and environmental controls of phytoplankton communities from contrasting hydrographical zones of the Labrador Sea. *Progress in Oceanography*, 141:212–226.

Gage, J. (1972). A preliminary survey of the benthic macrofauna and sediments in Lochs Etive and Creran, sea-lochs along the west coast of Scotland. *Journal of the Marine Biological Association of the UK*, 52:237–276.

Gattuso, J. P., Magnan, A., Billé, R., Cheung, W. W., Howes, E. L., Joos, F., Allemand, D., Bopp, L., Cooley, S. R., Eakin, C. M., Hoegh-Guldberg, O., Kelly, R. P., Pörtner, H. O., Rogers, A. D., Baxter, J. M., Laffoley, D., Osborn, D., Rankovic, A., Rochette, J., Sumaila, U. R., Treyer, S., and Turley, C. (2015). Contrasting futures for ocean and society from different anthropogenic CO_2 emissions scenarios. *Science*, 349(6243).

Gearing, J. N., Gearing, P. J., Rudnick, D. T., Requejo, A. G., and Hutchins, M. J. (1984). Isotopic variability of organic carbon in a phytoplankton-based temperate estuary. *Geochimica et Cosmochimica Acta*, 48:1089–1098.

Gemmell, B. J., Oh, G., Buskey, E. J., and Villareal, T. A. (2016). Dynamic sinking behaviour in marine phytoplankton: rapid changes in buoyancy may aid in nutrient uptake. *Proceedings of the Royal Society B: Biological Sciences*, 283(1840):20161126.

Giering, S. L. C., Sanders, R., Lampitt, R. S., Anderson, T. R., Tamburini, C., Boutrif, M., Zubkov, M. V., Marsay, C. M., Henson, S. A., Saw, K., Cook, K., and Mayor, D. J. (2014). Reconciliation of the carbon budget in the ocean's twilight zone. *Nature*, 507:480–483.

Glud, R. N. (2008). Oxygen dynamics of marine sediments. *Marine Biology Research*, 4(4):243–289.

Glud, R. N., Berg, P., Stahl, H., Hume, A., Larsen, M., Eyre, B. D., and Cook, P. L. (2016). Benthic Carbon Mineralization and Nutrient Turnover in a Scottish Sea Loch: An Integrative In Situ Study. *Aquatic Geochemistry*, 22:443–467.

Goñi, M. A. and Hedges, J. I. (1995). Sources and reactivities of marine-derived organic matter in coastal sediments as determined by alkaline CuO oxidation. *Geochimica et Cosmochimica Acta*, 59(14):2965–2981.

Goutx, M., Wakeham, S. G., Lee, C., Duflos, M., Guigue, C., Liu, Z., Moriceau, B., Sempéré, R., Tedetti, M., and Xue, J. (2007). Composition and degradation of marine particles with different settling velocities in the northwestern Mediterranean Sea. *Limnology and Oceanography*, 52(4):1645–1664.

Grasshoff, K., Kremling, K., and Ehrhardt, M. (2009). *Methods of seawater analysis*. John Wiley & Sons.

Guidi, L., Stemmann, L., and Jackson, G. A. (2009). Effects of phytoplankton community on production, size and export of large aggregates: A world-ocean analysis. *Limnology and Oceanography*, 54(6):1951–1963.

Guinder, V. A., López-Abbate, M. C., Berasategui, A. A., Negrin, V. L., Zapperi, G., Pratolongo, P. D., Fernández Severini, M. D., and Popovich, C. A. (2015). Influence of the winter phytoplankton bloom on the settled material in a temperate shallow estuary. *Oceanologia*, 57(1):50–60.

Guo, S., Sun, J., Zhao, Q., Feng, Y., Huang, D., and Liu, S. (2016). Sinking rates of phytoplankton in the Changjiang (Yangtze River) estuary: A comparative study between *Prorocentrum dentatum* and *Skeletonema dorhnii* bloom. *Journal of Marine Systems*, 154:5–14.

Haake, B., Ittekkot, V., Honjo, S., and Manganini, S. (1993). Amino acid, hexosamine and carbohydrate fluxes to the deep subarctic Pacific (Station P). *Deep Sea Research Part I: Oceanographic Research Papers*, 40(3):547–560.

Hamilton, S. E. and Hedges, J. I. (1988). The comparative geochemistries of lignins and carbohydrates in an anoxic fjord. *Geochimica et Cosmochimica Acta*, 52:129–142.

Hansman, R. L. and Sessions, A. L. (2016). Measuring the in situ carbon isotopic composition of distinct marine plankton populations sorted by flow cytometry. *Limnology and Oceanography: Methods*, 14:87–99.

Hargrave, B. T. (1972). Aerobic decomposition of and detritus as a function of particle surface

area and organic sediment content. *Limnology and Oceanography*, 17(4):583–586.

Hecky, R. E. and Kilham, P. (1988). Nutrient limitation of phytoplankton in freshwater and marine environments : A review of recent evidence on the effects of enrichment. *Limnology and Oceanography*, 33:796–822.

Hecky, R. E., Moever, K., Kilham, P., and Degens, E. T. (1973). The amino acid and sugar composition of diatom cell walls. *Marine Biology*, 19:323—-331.

Hedges, J. I. (1992). Global biogeochemical cycles: progress and problems. *Marine Chemistry*, 39:67–93.

Hedges, J. I., Baldock, J. A., Gélinas, Y., Lee, C., Peterson, M., and Wakeham, S. G. (2001). Evidence for non-selective preservation of organic matter in sinking marine particles. *Nature*, 409:801–804.

Hedges, J. I., Clark, W. A., and Cowie, G. L. (1988a). Fluxes and reactivities of organic matter in a coastal marine bay. *Limnology and Oceanography*, 33:1137–1152.

Hedges, J. I., Clark, W. A., and Cowie, G. L. (1988b). Organic matter sources to the water column and surficial sediments of a marine bay. *Limnology and Oceanography*, 33(5):1116–1136.

Hedges, J. I. and Keil, R. G. (1995). Sedimentary organic matter preservation. *Marine Chemistry*, 49:81–115.

Hedges, J. I. and Keil, R. G. (1999). Organic geochemical perspectives on estuarine processes: Sorption reactions and consequences. *Marine Chemistry*, 65:55–65.

Hedges, J. I., Keil, R. G., and Benner, R. (1997). What happens to terrestrial organic matter in the ocean? *Organic Geochemistry*, 27:195–212.

Hedges, J. I. and Oades, J. M. (1997). Comparartive organic geochemistries of soils and sediments. *Organic Geochemistry*, 27(7):319–361.

Henson, S., Cole, H., Beaulieu, C., and Yool, A. (2013). The impact of global warming on seasonality of ocean primary production. *Biogeosciences*, 10(6):4357–4369.

Henson, S. A., Sanders, R., and Madsen, E. (2012). Global patterns in efficiency of particulate organic carbon export and transfer to the deep ocean. *Global Biogeochemical Cycles*, 26:1–14.

Herndl, G. J. and Reinthaler, T. (2013). Microbial control of the dark end of the biological pump. *Nature Geoscience*, 6:718–724.

Hernes, P. J., Hedges, J. I., Peterson, M. L., Wakeham, S. G., and Lee, C. (1996). Neutral carbohydrate geochemistry of particulate material in the central equatorial Pacific. *Deep Sea Research Part II*, 43:1181–1204.

Hicks, N., Brand, T., and community, M. (2016). Loch Etive. MASTS Case Study Workshop Report. Technical Report August, Marine Alliance for Science and Technology for Scotland.

Hicks, N., Ubbara, G. R., Silburn, B., Smith, H. E., Kröger, S., Parker, E. R., Sivyer, D., Kitidis, V., Hatton, A., Mayor, D. J., and Stahl, H. (2017). Oxygen dynamics in shelf seas sediments incorporating seasonal variability. *Biogeochemistry*, 135(1-2):35–47.

Hoppenrath, M., Elbrächter, M., and Drebes, G. (2009). *Marine phytoplankton*. Kleine Senckenberg-Reihe 49.

Howe, J. A., Anderton, R., Arosio, R., Dove, D., Bradwell, T., Crump, P., Cooper, R., and Cocuccio, A. (2015). The seabed geomorphology and geological structure of the Firth of Lorn, western Scotland, UK, as revealed by multibeam echo-sounder survey. *Earth and Environmental*

Science Transactions of the Royal Society of Edinburgh, 105:273–284.

Howe, J. A., Shimmield, T., Austin, W., and Longva, O. (2002). Post-glacial depositional environments in a mid-high latitude glacially-overdeepened sea loch, inner Loch Etive, western Scotland. *Marine Geology*, 185:417–433.

Huisman, J., Arrayás, M., Ebert, U., and Sommeijer, B. (2002). How Do Sinking Phytoplankton Species Manage to Persist? *The American Naturalist*, 159(3):245–254.

Ichinotsuka, D., Ueno, H., and Nakano, S. I. (2006). Relative importance of nanoflagellates and ciliates as consumers of bacteria in a coastal sea area dominated by oligotrichous *Strombidium* and *Strobilidium*. *Aquatic Microbial Ecology*, 42:139–147.

Inall, M., Gillibrand, P., Griffiths, C., MacDougal, N., and Blackwell, K. (2009). On the oceanographic variability of the North-West European Shelf to the West of Scotland. *Journal of Marine Systems*, 77:210–226.

Ingalls, A. E., Lee, C., Wakeham, S. G., and Hedges, J. I. (2003). The role of biominerals in the sinking flux and preservation of amino acids in the Southern Ocean along 170°W. *Deep-Sea Research Part II: Topical Studies in Oceanography*, 50:713–738.

Ingalls, A. E., Liu, Z., and Lee, C. (2006). Seasonal trends in the pigment and amino acid compositions of sinking particles in biogenic $CaCO_3$ and SiO_2 dominated regions of the Pacific sector of the Southern Ocean along 170°W. *Deep-Sea Research Part I: Oceanographic Research Papers*, 53:836–859.

IPCC (2013). Summary for Policymakers. In *Climate Change 2013: The Physical Science Basis. Contribution of Working Group I to the Fifth Assessment Report of the Intergovernmental Panel on Climate Change*. Cambridge University Press, Cambridge, United Kingdom and New York, NY, USA.

Ittekkot, V., Degens, E. T., and Brockmann, U. (1982). Monosaccharide composition of acid-hydrolzable carbohydrates in particulate matter during a plankton bloom. *Limnology and Oceanography*, 27(4):770–776.

Ittekkot, V., Deuser, W. G., and Degens, E. (1984). Seasonality in the fluxes of sugars, amino acids, and amino sugars to the deep ocean: Sargasso Sea. *Deep-Sea Research*, 31(9):1057–1069.

Iversen, M. H., Nowald, N., Ploug, H., Jackson, G. A., and Fischer, G. (2010). High resolution profiles of vertical particulate organic matter export off Cape Blanc, Mauritania: Degradation processes and ballasting effects. *Deep Sea Research Part I: Oceanographic Research Papers*, 57:771–784.

Iversen, M. H. and Ploug, H. (2013). Temperature effects on carbon-specific respiration rate and sinking velocity of diatom aggregates - potential implications for deep ocean export processes. *Biogeosciences Discussions*, 10:371–399.

Jo, N., Kang, J. J., Park, W. G., Lee, B. R., Yun, M. S., Lee, J. H., Kim, S. M., Lee, D., Joo, H., Lee, J. H., Ahn, S. H., and Lee, S. H. (2017). Seasonal variation in the biochemical compositions of phytoplankton and zooplankton communities in the southwestern East/Japan Sea. *Deep Sea Research Part II: Topical Studies in Oceanography*, 143:82–90.

Johnson, T. O. and Smith, W. O. (1986). Sinking rates of phytoplankton assemblages in the Weddell Sea marginal ice zone. *Marine Ecology Progress Series*, 33:131–137.

Kabeya, N., Fonseca, M. M., Ferrier, D. E., Navarro, J. C., Bay, L. K., Francis, D. S., Tocher,

D. R., Castro, L. F. C., and Monroig, Ó. (2018). Genes for de novo biosynthesis of omega-3 polyunsaturated fatty acids are widespread in animals. *Science Advances*, 4(5):1–9.

Kamykowski, D., Reed, R. E., and Kirkpatrick, G. J. (1992). Comparison of sinking velocity, swimming velocity, rotation and path characteristics among six marine dinoflagellate species. *Marine Biology*, 113:319–328.

Kandasamy, S. and Nath, B. N. (2016). Perspectives on the terrestrial organic matter transport and burial along the land-deep sea continuum: caveats in our understanding of biogeochemical processes and future needs. *Frontiers in Marine Science*, 3(December):1–18.

Keil, R. G. and Hedges, J. I. (1993). Sorption of organic matter to mineral surfaces and the preservation of organic matter in coastal marine sediments. *Chemical Geology*, 107:385–388.

Keil, R. G., Montluçon, D. B., Prahl, F. G., and Hedges, J. I. (1994). Sorptive preservation of labile organic matter in marine sediments. *Nature*, 370(18):549–552.

Keil, R. G., Neibauer, J. A., Biladeau, C., Van Der Elst, K., and Devol, A. H. (2016). A multiproxy approach to understanding the "enhanced" flux of organic matter through the oxygen-deficient waters of the Arabian Sea. *Biogeosciences*, 13:2077–2092.

King County (2017). Puget Sound Marine Monitoring, http://green2.kingcounty.gov/marine/Photo/Individual/2/423?photoId=1066. Date visited 27/03/2018.

Kiørboe, T., Anderson, K. P., and Dam, H. G. (1990). Coagulation efficiency and aggregate formation in marine phytoplankton. *Marine Biology*, 107:235–245.

Kiørboe, T., Hansen, J. L. S., Alldredge, A. L., Jackson, G. A., Passow, U., Dams, H. G., Drapeaus, D. T., Waite, A., and Garcia, C. M. (1996). Sedimentation of phytoplankton during a diatom bloom: rates and mechanisms. *Journal of Marine Research*, 54:1123–1148.

Kiriakoulakis, K., Stutt, E., Rowland, S. J., Vangriesheim, A., Lampitt, R. S., and Wolff, G. A. (2001). Controls on the organic chemical composition of settling particles in the Northeast Atlantic Ocean. *Progress in Oceanography*, 50:65–87.

Klaas, C. and Archer, D. E. (2002). Association of sinking organic matter with various types of mineral ballast in the deep sea: Implications for the rain ratio. *Global Biogeochemical Cycles*, 16(4):1–14.

Korb, R. E., Raven, J. A., and Johnston, A. M. (1998). Relationship between aqueous CO_2 concentrations and stable carbon isotope discrimination in the diatoms Chaetoceros calcitrans and Dityl. *Marine Ecology Progress Series*, 171:303–305.

Kraberg, A., Baumann, M., and Durselen, C. (2010). *Coastal phytoplankton, photo guide for northern European seas*. Verlag Dr. Friedrich Pfeil.

Kwon, E. Y., Primeau, F., and Sarmiento, J. L. (2009). The impact of remineralization depth on the air-sea carbon balance. *Nature Geoscience*, 2(9):630–635.

Lampitt, R. S. (1992). The contribution of deep-sea macroplankton to organic remineralization: results from sediment trap and zooplankton studies over the Madeira Abyssal Plain. *Deep Sea Research Part A, Oceanographic Research Papers*, 39(2):221–233.

Lampitt, R. S., Boorman, B., Brown, L., Lucas, M., Salter, I., Sanders, R., Saw, K., Seeyave, S., Thomalla, S. J., and Turnewitsch, R. (2008). Particle export from the euphotic zone: Estimates using a novel drifting sediment trap, 234Th and new production. *Deep Sea Research Part I:*

Oceanographic Research Papers, 55:1484–1502.

Lampitt, R. S., Wishner, K. F., Turley, C. M., and Angel, M. V. (1993). Marine snow studies in the Northeast Atlantic Ocean: distirbution, composition and role as a food source for migrating plankton. *Marine Biology*, 116:689–702.

Landeira, J. M., Ferron, B., Lunven, M., Morin, P., Marie, L., and Sourisseau, M. (2014). Biophysical interactions control the size and abundance of large phytoplankton chains at the Ushant tidal front. *PLoS ONE*, 9(2):1–14.

Lannergren, C. (1979). Buoyancy of Natural Populations of Marine Phytoplankton. *Marine biology*, 54:1–10.

Le Moigne, F., Cisternas-Novoa, C., Piontek, J., Maßmig, M., and Engel, A. (2017). On the effect of low oxygen concentrations on bacterial degradation of sinking particles. *Scientific Reports*, 7(1):1–12.

Le Moigne, F. A. C., Sanders, R. J., Villa-Alfageme, M., Martin, A. P., Pabortsava, K., Planquette, H., Morris, P. J., and Thomalla, S. J. (2012). On the proportion of ballast versus non-ballast associated carbon export in the surface ocean. *Geophysical Research Letters*, 39(15):1–6.

Lee, C. and Cronin, C. (1982). The vertical flux of particulate organic nitrogen in the sea: decomposition of amino acids in the Peru upwelling area and the equatorial Atlantic. *Journal of Marine Research*, 40:227–251.

Lee, C. and Cronin, C. (1984). Particulate amino acids in the sea: Effects of primary productivity and biological decomposition. *Journal of Marine Research*, 42(4):1075–1097.

Lee, C., Wakeham, S. G., and Hedges, J. I. (2000). Composition and flux of particulate amino acids and chloropigments in equatorial Pacific seawater and sediments. *Deep Sea Research Part I: Oceanographic Research Papers*, 47:1535–1568.

Leftley, J. W. and MacDougal, N. (1991). The Dunstaffnage sediment trap and its moorings. *DML Internal report, Dunstaffnage Marine Lab*, 174:8.

Lewis, N. I., Xu, W., Jericho, S. K., Kreuzer, H. J., Jericho, M. H., and Cembella, A. D. (2006). Swimming speed of three species of *Alexandrium* (Dinophyceae) as determined by digital inline holography. *Phycologia*, 45(1):61–70.

Li, H., Lu, Y., Zheng, J., Yang, W., and Liu, J. (2014). Biochemical and Genetic Engineering of Diatoms for Polyunsaturated Fatty Acid Biosynthesis. *Marine Drugs*, 12(1):153–166.

Li, J., Crowe, S. A., Miklesh, D., Kistner, M., Canfield, D. E., and Katsev, S. (2012). Carbon mineralization and oxygen dynamics in sediments with deep oxygen penetration, Lake Superior. *Limnology and Oceanography*, 57(6):1634–1650.

Loh, P. S. (2005). *An assessment of the contribution of terrestrial organic matter to total organic matter in sediments in Scottish sea lochs*. PhD thesis, UHI Millennium Institute.

Loh, P. S., Miller, A. E. J., Reeves, A. D., Harvey, S. M., and Overnell, J. (2008a). Assessing the biodegradability of terrestrially-derived organic matter in Scottish sea loch sediments. *Hydrology and Earth System Sciences*, 12:811–823.

Loh, P. S., Reeves, A. D., Harvey, S. M., Overnell, J., and Miller, A. E. J. (2008b). The fate of terrestrial organic matter in two Scottish sea lochs. *Estuarine, Coastal and Shelf Science*, 76:566–579.

Loh, P. S., Reeves, A. D., Miller, A. E. J., Harvey, S. M., and Overnell, J. (2010). Sediment fluxes

and carbon budgets in Loch Creran, western Scotland. *Geological Society, London, Special Publications*, 344(1):103–124.

Loh, P. S., Reeves, A. D., Overnell, J., Harvey, S. M., and Miller, A. E. J. (2002). Assessment of terrigenous organic carbon input to the total organic carbon in sediments from Scottish transitional waters (sea lochs): methodology and preliminary results. *Hydrology and Earth System Sciences*, 6:959–970.

Lomas, M. W., Steinberg, D. K., Dickey, T., Carlson, C. A., Nelson, N. B., Condon, R. H., and Bates, N. R. (2010). Increased ocean carbon export in the Sargasso Sea linked to climate variability is countered by its enhanced mesopelagic attenuation. *Biogeosciences*, 7:57–70.

Lowry, O. H., Rosebrough, N. J., Farr, A. L., and Randall, R. J. (1951). Protein measurement with the folin phenol reagent. *The Journal of Biological Chemistry*, 193:265–275.

MacIntyre, S., Alldredge, A. L., and Gotschalk, C. C. (1995). Accumulation of marine snow at density discontinues in the water column. *Limnology and Oceanography*, 40(3):449–468.

Malviya, S., Scalco, E., Audic, S., Vincent, F., Veluchamy, A., Poulain, J., Wincker, P., Iudicone, D., de Vargas, C., Bittner, L., Zingone, A., and Bowler, C. (2016). Insights into global diatom distribution and diversity in the world's ocean. *Proceedings of the National Academy of Sciences*, 113(11):1516–1525.

Margalef, R. (1978). Life-forms of phytoplankton as survival alternatives in an unstable environment. *Oceanologica Acta*, 1:493–509.

Marsh, J. B. and Weinstein, D. B. (1966). Simple charring method for determination of lipids. *Journal of Lipid research*, 7(4):574–576.

Mayor, D. J., Sanders, R., Giering, S. L. C., and Anderson, T. R. (2014). Microbial gardening in the ocean's twilight zone: Detritivorous metazoans benefit from fragmenting, rather than ingesting, sinking detritus: Fragmentation of refractory detritus by zooplankton beneath the euphotic zone stimulates the harvestable productio. *BioEssays*, 36:1132–1137.

McDonnell, A. M. P., Boyd, P. W., and Buesseler, K. O. (2015). Effects of sinking velocities and microbial respiration rates on the attenuation of particulate carbon fluxes through the mesopelagic zone. *Global Biogeochemical Cycles*, 29:175–193.

McDonnell, A. M. P. and Buesseler, K. O. (2010). Variability in the average sinking velocity of marine particles. *Limnology and Oceanography*, 55(5):2085–2096.

Meybeck, M. (1982). Carbon, nitrogen, and phosphorus transport by world rivers. *American Journal of Science*, 282:401–450.

Mitchell, L., Harvey, S. M., Gage, J. D., and Fallick, A. E. (1997). Organic carbon dynamics in shelf edge sediments off the Hebrides: a seasonal perspective. *Internationale Revue der gesamten Hydrobiologie und Hydrographie*, 3:425–435.

Najdek, M., Debobbis, D., Miokovic, D., and Ivancic, I. (2002). Fatty acid and phytoplankton compositions of different types of mucilaginous aggregates in the northern Adriatic. *Journal of Plankton Research*, 24(5):429–441.

Neuer, S., Davenport, R., Freudenthal, T., Wefer, G., Llinás, O., Rueda, M., Steinberg, D. K., and Karl, D. M. (2002). Differences in the biological carbon pump at three subtropical ocean sites. *Geophysical Research Letters*, 29(18):1–4.

Niggemann, J. and Schubert, C. J. (2006). Fatty acid biogeochemistry of sediments from the

Chilean coastal upwelling region: Sources and diagenetic changes. *Organic Geochemistry*, 37(5):626–647.

Nørgaard-Pedersen, N., Austin, W. E., Howe, J. A., and Shimmield, T. (2006). The Holocene record of Loch Etive, western Scotland: Influence of catchment and relative sea level changes. *Marine Geology*, 228:55–71.

Overnell, J., Brand, T., Bourgeois, W., and Statham, P. J. (2002). Manganese dynamics in the water column of the upper basin of Loch Etive, a Scottish fjord. *Estuarine, Coastal and Shelf Science*, 55(3):481–492.

Overnell, J. and Young, S. (1995). Sedimentation and carbon flux in a scottish sea loch, loch linnhe. *Estuarine, Coastal and Shelf Science*, 41(3):361–376.

Parrish, C. C., Thompson, R. J., Deibel, D., and Saliot, A. (2005). Lipid classes, fatty acids, sterols and diol ethers in a cold ocean coastal food web during the spring bloom. *Marine Ecology Progress Series*, 286:57–68.

Passow, U. (1991). Species-specific sedimentation and sinking velocities of diatoms. *Marine biology*, 108:449–455.

Passow, U. (2002). Production of transparent exopolymer particles (TEP) by phyto- and bacterioplankton. *Marine Ecology Progress Series*, 236:1–12.

Passow, U. (2016). Formation of rapidly-sinking, oil-associated marine snow. *Deep Sea Research Part II: Topical Studies in Oceanography*, 129:232–240.

Passow, U. and Carlson, C. A. (2012). The biological pump in a high CO2 world. *Marine Ecology Progress Series*, 470:249–271.

Passow, U., De La Rocha, C. L., Fairfield, C., and Schmidt, K. (2014). Aggregation as a function of PCO2 and mineral particles. *Limnology and Oceanography*, 59(2):532–547.

Peperzak, L., Colijn, F., Koeman, R., Gieskes, W. W. C., and Joordens, J. C. A. (2003). Phytoplankton sinking rates in the rhine region of freshwater influence. *Journal of Plankton Research*, 25(4):365–383.

Perry, C. (2010). Sedimentation in the Firth of Lorn, Marine Special Area of Conservation. Technical Report 19, Scottish Marine and Freshwater Science.

Pitcher, G. C., Walker, D. R., and Mitchell-Innes, B. A. (1989). Phytoplankton sinking rate dynamics in the southern Benguela upwelling system. *Marine Ecology Progress Series*, 55:261–269.

Planque, B., Lazure, P., and Jegou, A. (2006). Typology of hydrological structures modelled and observed over the Bay of Biscay shelf. *Scientia Marina*, (June):43–50.

Ploug, H. and Grossart, H. (2000). Bacterial growth and grazing on diatom aggregates: Respiratory carbon turnover as a function of aggregate size and sinking velocity. *Limnology and Oceanography*, 45(7):1467–1475.

Ploug, H., Grossart, H. P., Azam, F., and Jorgensen, B. B. (1999). Photosynthesis, respiration, and carbon turnover in sinking marine snow from surface waters of Southern California Bight: implications for the carbon cycle in the ocean. *Marine Ecology Progress Series*, 179:1–11.

Ploug, H., Iversen, M. H., and Fischer, G. (2008a). Ballast, sinking velocity, and apparent diffusivity within marine snow and zooplankton fecal pellets: Implications for substrate turnover by attached bacteria. *Limnology and Oceanography*, 53(5):1878–1886.

Ploug, H., Iversen, M. H., Koski, M., and Buitenhuis, E. T. (2008b). Production, oxygen respiration rates, and sinking velocity of copepod fecal pellets: Direct measurements of ballasting by opal and calcite. *Limnology and Oceanography*, 53(2):469–476.

Pond, D., Harris, R., Head, R., and Harbour, D. (1996). Environmental and nutritional factors determining seasonal variability in the fecundity and egg viability of *Calanus helgolandicus* in coastal waters off Plymouth, UK. *Marine Ecology Progress Series*, 143(1-3):45–63.

Price, N. B., Brand, T., Pates, J. M., Mowbray, S., Theocharis, A., Civitarese, G., Miserocchi, S., Heussner, S., and Lindsay, F. (1999). Horizontal distributions of biogenic and lithogenic elements of suspended particulate matter in the Mediterranean Sea. *Progress in Oceanography*, 44:191–218.

Puigcorbé, V., Benitez-nelson, C. R., Masqué, P., Verdeny, E., White, A. E., Popp, B. N., Prahl, F. G., and Lam, P. J. (2015). Global Biogeochemical Cycles. *Global Biogeochemical Cycles*, 29:1309–1332.

Pusceddu, A., Sara, G., Armeni, M., Fabiano, M., and Mazzola, A. (1999). Seasonal and spatial changes in the sediment organic matter of a semi-enclosed marine system (W-Mediterranean Sea). *Hydrobiologia*, 397:59–70.

Redfield, A. C. (1934). On the proportions of organic derivatives in sea water and their relation to the composition of plankton. pages 176–192. James Johnstone Memorial Volume.

Reemtsma, T., Haake, B., Ittekkot, V., Nair, R. R., and Brockmann, U. H. (1990). Downward flux of particulate fatty acids in the central arabian sea. *Marine Chemistry*, 29:183–202.

Reeves, A. D. and Preston, M. R. (1991). A study of the composition and distribution of lignin in resuspended and permanently suspended particles in the river Tamar Estuary. *Estuarine, Coastal and Shelf Science*, 32:11–25.

Reynolds, C. S. (2006). *The Ecology of Phytoplankton*. Cambridge University Press.

Richardson, T. and Cullen, J. J. (1995). Changes in buoyancy and chemical composition during growth of a coastal marine diatom: ecological and biogeochemical consequences. *Marine Ecology Progress Series*, 128:77–90.

Riebesell, U. (1989). Comparison of sinking and sedimentation rate measurements in a diatom winter/spring bloom. *Marine Ecology Progress Series*, 54:109–119.

Riley, J. S., Sanders, R., Marsay, C., Le Moigne, F. A. C., Achterberg, E. P., and Poulton, A. J. (2012). The relative contribution of fast and slow sinking particles to ocean carbon export. *Global Biogeochemical Cycles*, 26:1–10.

Ríos, A. F., Fraga, F., Pérez, F. F., and Figueiras, F. G. (1998). Chemical composition of phytoplankton and Particulate Organic Matter in the Ría de Vigo (NW Spain). *Scientia Marina*, 62(3):257–271.

Rontani, J. F., Zabeti, N., and Wakeham, S. G. (2011). Degradation of particulate organic matter in the equatorial Pacific Ocean: Biotic or abiotic? *Limnology and Oceanography*, 56(1):333–349.

Sabine, C. L., Feely, R. A., Gruber, N., Key, R. M., Lee, K., Bullister, J. L., Wanninkhof, R., Wong, C. S., Wallace, D. W. R., Tilbrook, B., Millero, F. J., Peng, T., Kozyr, A., Ono, T., and Rios, A. F. (2004). The Oceanic Sink for Anthropogenic CO2. *Science*, 305(5682):367–371.

Sancetta, C. and Calvert, S. E. (1988). The Annual Cycle of Sedimentation in Saanich Inlet British Columbia Canada Implications for the Interpretation of Diatom Fossil Assemblages. *Deep-Sea*

Research Part A Oceanographic Research Papers, 35(1):71–90.

Sanders, R., Henson, S. A., Koski, M., De La Rocha, C. L., Painter, S. C., Poulton, A. J., Riley, J., Salihoglu, B., Visser, A., Yool, A., Bellerby, R., and Martin, A. P. (2014). The Biological Carbon Pump in the North Atlantic. *Progress in Oceanography*, 129:200–218.

Sanders, R., Morris, P. J., Poulton, A. J., Stinchcombe, M. C., Charalampopoulou, A., Lucas, M. I., and Thomalla, S. J. (2010). Does a ballast effect occur in the surface ocean? *Geophysical Research Letters*, 37(8):1–5.

Sargent, J. R. (1976). The Structure, Metabolism and Function of Lipids in Marine Organisms. In Malins, D. C. and Sargent, J. R., editors, *Biochemical and Biophysical Perspectives in Marine Biology*, pages 149–212.

Schmidt, K., De La Rocha, C. L., Gallinari, M., and Cortese, G. (2014). Not all calcite ballast is created equal: differing effects of foraminiferan and coccolith calcite on the formation and sinking of aggregates. *Biogeosciences*, 11(1):135–145.

Sheridan, C. C., Lee, C., Wakeham, S. G., and Bishop, J. K. (2002). Suspended particle organic composition and cycling in surface and midwaters of the equatorial Pacific Ocean. *Deep-Sea Research Part I: Oceanographic Research Papers*, 49:1983–2008.

Simon, N., Cras, A. L., Foulon, E., and Lemée, R. (2009). Diversity and evolution of marine phytoplankton. *Comptes Rendus - Biologies*, 332(2-3):159–170.

Smayda, T. J. (1970). The suspension and sinking of phytoplankton in the sea. *Oceanography Marine Biology Annual Review*, 8:353–414.

Smayda, T. J. (1997). Harmful algal blooms: Their ecophysiology and general relevance to phytoplankton blooms in the sea. *Limnology and Oceanography*, 42(5):1137–1153.

Smayda, T. J. (2000). *Ecological features of harmful algal blooms in coastal upwelling ecosystems*, volume 22.

Smayda, T. J. (2010). Adaptations and selection of harmful and other dinoflagellate species in upwelling systems. 2. Motility and migratory behaviour. *Progress in Oceanography*, 85(1-2):53–70.

Smayda, T. J. and Bienfang, P. K. (1983). Suspension properties of various phyletic groups of phytoplankton and tintinnids in an oligotrophic subtropical system. *Marine Ecology*, 4:289–300.

Smayda, T. J. and Boleyn, B. J. (1966). Experimental observations on the flotation of marine diatoms. II. *Skeletonema costatum* and *Rhizosolenia setigera*. *Limnology and Oceanography*, 11:18–34.

Smetacek, V. S. (1985). Role of sinking in diatom life-history: ecological, evolutionary and geological significance. *Marine Biology*, 84:239–251.

Smith, D. C., Simon, M., Alldredge, A. L., and Azam, F. (1992). Intense hydrolytic enzyme activity on marine aggregates and implications for rapid particle dissolution. *Nature*, 359:139–142.

Stashchuk, N., Inall, M., and Vlasenko, V. (2007). Analysis of Supercritical Stratified Tidal Flow in a Scottish Fjord. *Journal of Physical Oceanography*, 37(7):1793–1810.

Steinberg, D. K., Van Mooy, B. A. S., Buesseler, K. O., Boyd, P. W., and Karl, D. M. (2008). Bacterial vs. zooplankton control of sinking particle flux in the ocean's twilight zone. *Limnology*

and Oceanography, 53(4):1327–1338.

Stemmann, L., Eloire, D., Sciandra, A., Jackson, G., Guidi, L., Picheral, M., and Gorsky, G. (2008). Volume distribution for particles between 3.5 to 2000 μm in the upper 200 m region of the South Pacific Gyre. *Biogeosciences Discussions*, 5:299–310.

Stokes, G. G. (1851). On the Effect of the Internal Friction of Fluids on the Motion of Pendulums. *Transactions of the Cambridge Philosophical Society*, 9(2):8–14.

Swedish Meterological and Hydrological Institute (2018). Nordic Microalgae and aquatic protozoa, http://nordicmicroalgae.org/taxon/Gyrodinium spirale?media_id=Gyrodinium spirale_3.jp. Date visited 27/03/2018.

Szyper, J. P. and Karl, D. M. (1991). RACER : Sinking rates and vertical flux of phytoplankton pigments. *Antarctic Journal of the United States*, 27(5):168–170.

Tett, P., Heaney, S. I., and Droop, M. R. (1985). The redfield ratio and phytoplankton growth rate. *Journal of the Marine Biological Association of the United Kingdom*, 65:487–504.

Tett, P. B. (1987). *Plankton in Biological surveys of estuaries and coasts*. Cambridge University Press, Cambridge, UK.

The University of British Columbia (2012). Phytopedia - The Phytoplankton Encyclopedia Project, https://www.eoas.ubc.ca/research/phytoplankton/dinoflagellates/scrippsiella/s_trochoidea. Date visited 28/03/2018.

Thornton, B., Martin, G., Procee, M., Miller, D. R., Coull, M., Yao, H., Chapman, S. J., Hudson, G., and Midwood, A. J. (2015). Distributions of carbon and nitrogen isotopes in Scotland's topsoil: a national-scale study. *European Journal of Soil Science*, 66:1002–1011.

Throndsen, J., Hasle, G. R., and Tangen, K. (2007). *Phytoplankton of Norwegian coastal waters*. Almater Forlag As.

Tierney, K. M., Muir, G. K. P., Cook, G. T., MacKinnon, G., Howe, J. A., Heymans, J. J., Hughes, D. J., and Xu, S. (2017). Ecosystem uptake and transfer of Sellafield-derived radiocarbon (14C) part 2: The West of Scotland. *Marine Pollution Bulletin*, 115:57–66.

Tomas, C. R. (1997). *Identifying marine phytoplankton*. Academic Press.

Townsend, D. W., Cammen, L. M., Holligan, P. M., Campbell, D. E., and Pettigrew, N. R. (1994). Causes and consequences of variability in the timing of spring phytoplankton blooms. *Deep Sea Research Part I*, 41:747–765.

Turner, J. T. (2015). Zooplankton fecal pellets, marine snow, phytodetritus and the ocean's biological pump. *Progress in Oceanography*, 130:205–248.

UK Meterological Office (2017). Historic station data, http://www.metoffice.gov.uk/public/weather/climate-historic/#?tab=climateHistoric. Date visited 20/04/2017.

UK Meterological Office (2019). When does spring start, https://www.metoffice.gov.uk/weather/learn-about/weather/seasons/spring/when-does-spring-start. Date visited 23/02/2019.

Van De Poll, W. H., Kulk, G., Timmermans, K. R., Brussaard, C. P. D., Van Der Woerd, H. J., Kehoe, M. J., Mojica, K. D. A., Visser, R. J. W., Rozema, P. D., and Buma, A. G. J. (2013). Phytoplankton chlorophyll a biomass, composition, and productivity along a temperature and stratification gradient in the northeast Atlantic Ocean. *Biogeosciences*, 10(6):4227–4240.

Van Mooy, B. A. S., Keil, R. G., and Devol, A. H. (2002). Impact of suboxia on sinking particulate organic carbon: Enhanced carbon flux and preferential degradation of amino acids via denitrification. *Geochimica et Cosmochimica Acta*, 66(3):457–465.

Verity, P. G. and Smetacek, V. (1996). Organism life cycle, predation, and the structure of marine pelagic ecosystems. *Marine Ecology Progress Series*, 130:277–293.

Vogel, S. (1983). *Life in Moving Fluids: The Physical Biology of Flow*. Princeton University, Princeton, N.J.

Volk, T. and Hoffert, M. I. (1985). Ocean carbon pumps: analysis of relative strength and efficiencies in ocean-driven atmospheric CO2 changes. *The Carbon Cycle and Atmospheric CO2: Natural variations Archaean to present. Geophysical Monograph Series*, 32:99–110.

Waite, A., Bienfang, P. K., and Harrison, P. J. (1992a). Spring bloom sedimentation in a subarctic ecosystem. I. Nutrient sensitivity. *Marine Biology*, 114:119–129.

Waite, A., Fisher, A., Thompson, P. A., and Harrison, P. J. (1997). Sinking rate versus cell volume relationships illuminate sinking rate control mechanisms in marine diatoms. *Marine Ecology Progress Series*, 157:97–108.

Waite, A. M. and Nodder, S. D. (2001). The effect of in situ iron addition on the sinking rates and export flux of Southern Ocean diatoms. *Deep-Sea Research Part II: Topical Studies in Oceanography*, 48:2635–2654.

Waite, A. M., Thompson, P. A., and Harrison, P. J. (1992b). Does energy control the sinking rates of marine diatoms? *Limnology and Oceanography*, 37(3):468–477.

Wakeham, S. G., Hedges, J. I., Lee, C., and Pease, T. K. (1993). Effects of poisons and preservatives on the composition of organic matter in a sediment trap experiment. *Journal of Marine Research*, 51:669–696.

Wakeham, S. G., Hedges, J. I., Lee, C., Peterson, M. L., and Hernes, P. J. (1997a). Composition and transport of lipid biomarkers through the water column and surficial sediments of the equatorial Pacific Ocean. *Deep-Sea Research II*, 44(97):2131–2162.

Wakeham, S. G. and Lee, C. (1989). Organic geochemistry of particulate matter in the ocean: The role of particles in oceanic sedimentary cycles. *Organic Geochemistry*, 14(1):83–96.

Wakeham, S. G. and Lee, C. (1993). Production, transport, and alteration of particulate organic matter in the marine water column. *In: Organic Geochemistry, Plenum Press, New York*, pages 145–165.

Wakeham, S. G., Lee, C., Hedges, J. I., Hernes, P. J., and Peterson, M. L. (1997b). Molecular indicators of diagentic status in marine organic matter. *Geochimica et Cosmochimica Acta*, 61(24):5363–5369.

Wakeham, S. G., Lee, C., Peterson, M. L., Liu, Z., Szlosek, J., Putnam, I. F., and Xue, J. (2009). Organic biomarkers in the twilight zone-Time series and settling velocity sediment traps during MedFlux. *Deep-Sea Research Part II: Topical Studies in Oceanography*, 56(18):1437–1453.

Wakeham, S. G. and McNichol, A. P. (2014). Transfer of organic carbon through marine water columns to sediments - insights from stable and radiocarbon isotopes of lipid biomarkers. *Biogeosciences*, 11:6895–6914.

Walsby, A. E. and Xypolyta, A. (1977). The form resistance of chitan fibres attached to the cells of Thalassiosira fluviatilis Hustedt. *British Phycological Journal*, 12(3):215–223.

Wilson, S. E., Ruhl, H. A., and Smith, K. L. (2013). Zooplankton fecal pellet flux in the abyssal northeast Pacific: A 15 year time-series study. *Limnology and Oceanography*, 58(3):881–892.

Wilson, S. E., Steinberg, D. K., and Buesseler, K. O. (2008). Changes in fecal pellet characteristics with depth as indicators of zooplankton repackaging of particles in the mesopelagic zone of the subtropical and subarctic North Pacific Ocean. *Deep Sea Research Part II: Topical Studies in Oceanography*, 55:1636–1647.

Wolff, G. A., Billett, D., Bett, B. J., Holtvoeth, J., FitzGeorge-Balfour, T., Fisher, E., Cross, I., Shannon, R., Salter, I., Boorman, B., King, N. J., Jamieson, A., and Chaillan, F. (2011). The effects of natural iron fertilisation on deep-sea ecology: The Crozet Plateau, southern Indian ocean. *PLoS ONE*, 6:1–9.

Wong, W. W. and Sackett, W. M. (1978). Fractionation of stable carbon isotopes by marine phytoplankton. *Geochimica et Cosmochimica Acta*, 42:1809–1815.

Wood, B. J. B., Tett, P. B., and Edwards, A. (1973). An Introduction to the Phytoplankton, Primary Production and Relevant Hydrography of Loch Etive. *Journal of Ecology*, 61(2):569–585.

Zimmerman, A. R. and Canuel, E. A. (2001). Bulk organic matter and lipid biomarker composition of Chesapeake Bay surficial sediments as indicators of environmental processes. *Estuarine, Coastal and Shelf Science*, 53(3):319–341.